Final Report

Groundwater Modeling

of the Cañutillo Wellfield

Prepared for

El Paso Water Utilities Public Service Board

APRIL, 2002

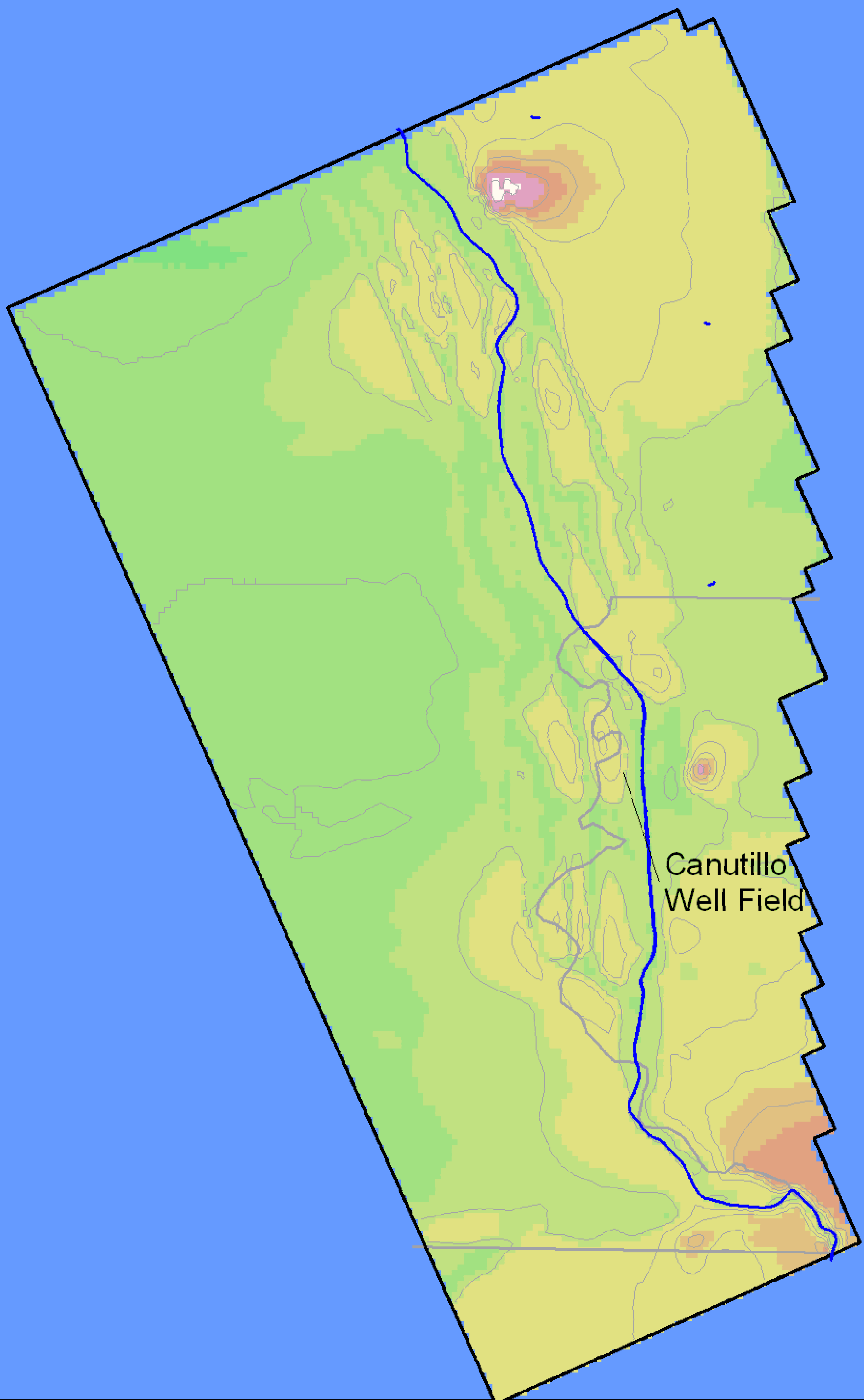

CH2MHILL

Prepared for

EPWU

April 2002

CH2MHILL
Albuquerque

Contents

Contents, continued

Contents, continued

Contents, continued

Contents, continued

Contents, continued

Contents, continued

Contents, continued

Contents, continued

Contents, continued

Figures **Page**

Contents, continued

Acronyms

ac-ft	acre-feet
ac-ft/yr	acre-feet per year
EPWU	El Paso Water Utility
ET	evapotranspiration package
ft^2/day	square feet per day
ft^3/s	cubic feet per second
FTP	File Transfer Protocol
gpcd	gallons per capita per day
GMS	Groundwater Modeling System
GWIS	USGS Groundwater Information System
LSF	Lower Santa Fe unit
mg/L	milligrams per liter
MOC	method of characteristics
MSF	Middle Santa Fe unit
NHD	National Hydrologic Dataset
NIF	Net Irrigation Flux
NMED	New Mexico Environment Department
OSE	Office of the State Engineer of New Mexico
RMS	root mean squared
SAR	Sodium Absorption Ration
TDS	total dissolved solids
TMR	Telescoping Mesh Refinement
TVD	total-variation-diminishing
TWC	Texas Water Commission
UA	University of Arizona
USF	Upper Santa Fe unit
USGS	U.S. Geological Survey
WRRI	Water Resources Research Institute

Executive Summary

Executive Summary

Introduction

The Cañutillo Wellfield Modeling Project is part of the El Paso Water Utility's (EPWU's) ongoing effort to provide a safe and sustainable water supply. The purpose of this model is to provide insight into the groundwater system of the Mesilla Bolson and as such provide information to be used in water resources planning. More specifically, EPWU would like a tool that allows them to assess various operating scenarios' effects on aquifer water quality and longevity. To achieve this goal, the Cañutillo model will evolve and be refined over time.

Data Compilation

The Mesilla Bolson has been studied extensively since the early 1900s. As such, a large volume of material exists that examines the geology and hydrogeology of the basin. Earlier studies and modeling efforts collected data related to groundwater flow. Because these efforts were generally concerned with regional groundwater flow, data were collected throughout the Mesilla Bolson. This modeling effort builds on past regional groundwater flow modeling efforts and expands these efforts to include water quality simulation. Therefore, data compilation is focused on the data required to complete this task, namely groundwater and surface water chemical data in the Cañutillo area.

The U.S. Geological Survey (USGS) routinely monitors the Rio Grande for flow and water quality. In addition, the USGS has conducted a number of seepage studies where surface water quality data have been collected for the Rio Grande and select canals and drains. These and other data were collected for use in model development.

Conceptual Model

The conceptual model used in this exercise follows largely from the conceptual models used by Weedon and Maddock (1999), Hamilton and Maddock (1993), and Frenzel (1992). Because this modeling effort includes the addition of solute transport, surface and goundwater water quality data are required over time. Water quality varies significantly within the Mesilla Bolson. The quality of excess irrigation water and the quality of river and canal seepage water affects groundwater quality. River and canal seepage are freshwater inflows into the shallow alluvium, while excess irrigation water typically is of lower quality. As such, the shallow alluvium usually has lower total dissolved solids (TDS) concentrations near the Rio Grande. TDS concentrations typically increase proportionally moving away from the river. Rio Grande water quality typically degrades downstream due to drain returns. Groundwater in the shallow alluvium is often higher in TDS than deeper groundwater. The thickness of freshwater varies significantly over the Mesilla Basin. The zone of slightly saline water in the shallow alluvium increases in thickness moving away from the Rio Grande.

In general, water quality data have primarily been collected in areas of anthropogenic activity. Therefore, very little data are available on the Eastern and Western areas of the model. While significant amounts of data have been collected in the Cañutillo area. Water quality data are regularly collected by both EPWU and the USGS. However, in part due to the model layering scheme and in part due to spatial and temporal data gaps, some level of generalization and synthesis of data is required to represent the Cañutillo area in three dimensions. As such, data collected over several years from various locations was used to produce "average" water quality profiles for "historical" and "present" conditions.

Flow Model Development

The Cañutillo model was developed from a modified version of the Weeden and Maddock (1999) model to better represent local conditions in the Cañutillo wellfield and to facilitate the eventual development of a contaminant transport model. In addition to the changes noted above, the following changes were incorporated into the Cañutillo model:

- The model area was decreased from the Rincon and Mesilla valleys. The southern and eastern boundaries remained the same, the northern boundary was moved to near Mesquite, and the western boundary moved to approximately 7.4 miles to the west of the Cañutillo wellfield.
- The grid was made uniform at a spacing of approximately 200 meters.
- Additional canals, drains, and laterals were added. Because the grid spacing is much smaller than the original model, additional canals, drains, and laterals can be represented.

The model-layering scheme used by Weedon and Maddock presents significant obstacles in the simulation of contaminant transport. There are often large differences in concentrations within individual hydrostratigraphic units. In this layering system, these differences must be averaged along with concentrations from distinct hydrostratigraphic units to produce the appropriate layer concentration. Averaging will result in incorrect simulated estimates of concentrations at individual wells. Likewise, vertical barriers to migration of elevated concentrations will not be accurately represented in the numerical model. This layering approach limits model accuracy to the representation of general water quality trends. As such, model results cannot be used to accurately predict concentrations in individual wells.

Within limitations presented by the model-layering scheme used by Weedon and Maddock, the Cañutillo model represents the local groundwater flow in the Cañutillo wellfield for the purpose of simulating generalized trends in local contaminant transport.

Flow Model Calibration

During development of a groundwater flow model, parameters such as hydraulic conductivity are input to the model based on available test data, knowledge of the aquifer hydrogeology, and extrapolation between known values. Because there are relatively few test values for a given parameter, large areas of a model grid are typically assigned values based on extrapolation with the best available information. With the knowledge that parameters are largely extrapolated, the process of model calibration adjusts these uncertain parameters to produce model results that more closely match values, such as aquifer heads that have been observed over time. Because many different combinations of parameters can result in the same overall model solution, a model solution is not unique. The process of model calibration attempts to find a model solution that matches observed data well and is realistic based on known data.

For this exercise, a baseline simulation was completed that incorporated the best available information on model parameters and starting conditions. This simulation was then compared to subsequent simulations to gage model improvement with parameter changes. Model parameters such as hydraulic conductivity, river bottom elevation, and vertical hydraulic conductivity of the riverbed were altered until the best solution was achieved with respect to select head targets. Calibration to these targets will allow for comparison to the Weeden and Maddock model. Additional time series water level data is available in the Cañutillo Wellfield area. Additional temporal calibration points would allow for the evaluation of water level trends. However, with the current model layering calibration to additional points will not likely result in additional model accuracy. Future model revisions that explore the Cañutillo area in more detail should include additional spatial and temporal calibration points.

The following conclusions can be drawn with respect to the final calibrated groundwater flow model for the Cañutillo wellfield area:

- The model represents the streamflow system in the Cañutillo area well slightly better than the Weedon and Maddock model. Improvements to the model representation of streamflow would require more information on canal return flows. These data are required to determine Rio Grande leakage explicitly. These data are not presently available.
- The model represents Rio Grande seepage in the winter reasonably well. However, observed values are of a different time scale and therefore can only act as a general guide. Likewise, Rio Grande seepage varies significantly from year to year.
- The model represents aquifer heads well, with slight improvements over Weeden and Maddock (1999).
- Based on sensitivity analysis, the model appears to be near a local optimum.

Transport Model Development

The Cañutillo wellfield flow and transport model was developed to provide more reliable estimates of changes in water quality over time than can be produced analytically. The transport model covers the same area as the Cañutillo flow model and uses the solved head distribution from the flow model as an input. The flow model solution is used along with estimates of initial concentration and potential concentration inflows over time to simulate changes in constituent concentration over time. Changes in concentration occur as constituents move by advection along flow lines. The rate at which constituents move is dependent on the aquifer porosity and the degree to which the concentration is diluted through dispersion.

At best, solute transport modeling is difficult and the results are often subject to interpretation. Any error in the flow model is often magnified in the transport model results. As noted previously, the model-layering scheme used by Weedon and Maddock (1999) presents significant obstacles in the simulation of contaminant transport. There are often large differences in concentrations within individual hydrostratigraphic units. In this layering system, these differences must be averaged along with concentrations from distinct hydrostratigraphic units to produce the appropriate layer concentration. Averaging will result in incorrect simulated estimates of concentrations at individual wells. Likewise, vertical barriers to migration of elevated concentrations will not be accurately represented in the numerical model.

Transport Model Calibration

Calibration of a groundwater transport model requires that concentrations in individual wells are matched over time through changing select parameters, boundary conditions, and initial concentrations.. Model parameters specifically associated with the transport model such as porosity and dispersivity are altered and simulations are completed until the best model fit of simulated and observed concentrations is achieved.

In part due to the model layering scheme used by Weedon and Maddock and in part due to spatial and temporal data gaps, some level of generalization and synthesis of data are required to represent water quality in the Cañutillo area in three dimensions. As such, data collected over several years from various locations was used to produce "average" water quality profiles for "historical" and "present" conditions. The generalizations in water quality representation will increase uncertainty associated with simulation results.

To calibrate the solute transport model, it is desirable to have calibration points that are well distributed over the model area, both horizontally and vertically. Because of the lack of consistent data over the calibration period, the Cañutillo Solute Transport model was calibrated to a single point in time. Calibrating to a single point in time does not allow for the analysis changes in water quality over time which could be important in examining mechanisms for degradation in EPWU wells. However, with the current model-layering calibration to additional points will not likely result in additional model accuracy. Future model revisions that explore the Cañutillo area in more detail should include additional spatial and temporal calibration points.

A baseline simulation was completed based on the best available information on model parameters and starting conditions. This simulation was then compared to subsequent simulations to gage model improvement with parameter changes. Model parameters such as porosity, mountain- and slope-front recharge concentration, and irrigation recharge concentration were altered until the best solution was achieved. The best overall model fit of simulated to observed values was achieved with effective porosities of 0.25 for layer 1 and 0.3 for layers 2 through 4 and with the initial irrigation recharge TDS concentration of 1,412 milligrams per liter (mg/L). As stated previously, the model-layering scheme from Weedon and Maddock requires that concentrations are averaged across discrete hydrostratigraphic units introducing additional uncertainty into the model results. This uncertainty was demonstrated in the calibration results at individual EPWU wells.

Within limitations presented by the model-layering scheme used by Weedon and Maddock, the Cañutillo model represents the local groundwater flow and contaminant transport in the Cañutillo wellfield for the purpose of simulating generalized trends in local contaminant transport. Because of model limitations, model results cannot be used to accurately predict concentrations in individual wells and therefore manage the wellfield on a well-by-well basis.

1. Introduction

1. Introduction

El Paso Water Utility (EPWU) is committed to providing a safe and sustainable water supply. The Cañutillo wellfield is an important part of EPWU's long-term water supply strategy. The Cañutillo wellfield model is being developed as a tool to manage this important resource. The purpose of this model is to provide insight into the groundwater system of the Mesilla Bolson and as such provide information to be used in water resources planning. More specifically, EPWU would like a tool that allows them to assess various operating scenarios' effects on aquifer water quality and longevity. Previous modeling efforts have for the most part focused on examining the regional aquifer system. These efforts evolved over time from regional research studies into tools appropriate for regional evaluations. The current modeling effort continues this evolution by building a local-scale model in the Cañutillo area for wellfield management at a local scale. As with the previous regional studies, the Cañutillo model will evolve and be refined as necessary to meet the needs of EPWU, namely, the management of its precious westside resources.

Because of potential delays in the construction and operation of the Upper Valley Water Treatment Plant, it is expected that EPWU will be forced to rely on water pumped from the Cañutillo wellfield to meet water supply demands in west El Paso. Over time, EPWU has noted brackish water intrusion into Cañutillo wells and thus the degradation of water quality in the Cañutillo wellfield. To plan for future changes in water quality as well as to estimate the potential long-term yield of the aquifer, a comprehensive groundwater flow and solute transport model is required.

For the purpose of water resource management, EPWU would like a comprehensive groundwater flow and transport model to assess:

- Migration of brackish water
- Recharge of freshwater
- Interaction of aquifer layers
- Pumping effects on water quality
- Aquifer yield
- Pumping effects on the Rio Grande

Assessments of these factors will aid in long-term planning related to EPWU water resources and help to manage groundwater withdrawals for the prevention of water quality deterioration.

In the transition from reliance solely on groundwater to a sustainable surface supply for west El Paso, EPWU would like to use its groundwater resources as effectively as possible. Effective use of these resources includes planning for the eventual degradation of this water supply and recognition that it has a definite lifetime. To properly assess water quality degradation and aquifer longevity, a comprehensive groundwater flow and solute transport model is required. This model will be developed specifically for the Cañutillo wellfield area from the existing regional model developed by Maddock.

The following sections describe in detail the process of model development and calibration. This process includes the compilation of appropriate data, development of a conceptual model, development of a groundwater flow model, calibration of the groundwater flow model, development of a solute transport model, and calibration of the solute transport model.

2. Data Compilation for the Cañutillo Wellfield Modeling Project

2. Data Compilation for the Cañutillo Wellfield Modeling Project

2.1 Introduction

The Mesilla Bolson has been studied extensively since the early 1900s. As such, a large volume of material exists examining the geology and hydrogeology of the basin. Earlier studies and modeling efforts collected extensive data related to groundwater flow. This modeling effort took the most recent regional groundwater flow model and used it to establish boundary conditions for a local-scale model of the Cañutillo wellfield area.

To construct a groundwater flow and solute transport model, various types of data are required including, but not limited to; horizontal and vertical hydraulic conductivity and or transmissivity, hydrostratigraphy, storativity, groundwater levels, porosity measurements, water budget, pumping data, surface water flows, groundwater chemical data, and surface water chemical data. Therefore, data compilation is focused on the data required to complete this task, namely groundwater and surface water chemical data. Data compiled from earlier groundwater flow-modeling efforts, such as, hydraulic conductivity and surface water flow data will not be explicitly presented. For information on other groundwater flow data, please see the forthcoming sections on the conceptual model.

This section presents a brief review of literature sources consulted during the data compilation process and a synopsis of data that have been compiled to date.

2.2 Literature Review

Large amounts of data on the Mesilla Bolson have been collected and reported on over time. This review provides a brief listing of some of the more prominent studies.

2.2.1 Hydrogeology/Geology/Water Resources

Extensive predevelopment data are available from the studies of Slichter (1905) and Lee (1907). These studies provide a wealth of data on water levels, hydraulic gradients, and aquifer properties used extensively in the steady-state groundwater models that ultimately led to Weeden and Maddock (1999). Limited data were also collected related to groundwater quality.

Conover (1954) added to the early information available with a comprehensive and often cited study. This study lists hydrogeologic properties, examines ground and surface water quality and interaction, and provides information on surface water flow and groundwater levels (including level elevation maps).

Wilson (1981) provides extensive data on water levels including an invaluable well inventory; hydrographs of observation wells; aquifer testing data; groundwater withdrawal data; and surface water flow, diversion, and depletion data. Also provided and of particular interest to this study are plots of several hydrologic cross-sections. These cross-sections display total dissolved solids (TDS) measurements and electrical resistively data defining the interface of various water quality zones throughout much of the Mesilla Bolson.

In 1983 the U.S. Geological Survey (USGS) began a formal groundwater monitoring network of 143 wells in the Mesilla Bolson. Hydrogeologic data from this network (expanded over time to 188 wells) were reported and updated in Nickerson (1986, 1989, 1993, 1995, and 1999). Data includes hydrographs, aquifer test data, groundwater quality data (in early reports), surface water quality data (1999), and seepage investigations.

Hawley and Lozinsky (1992) used data from recent borings to update the hydrostratigraphic model of the basin. This update resulted in model revisions by Frenzel (1992) and forms the basis of subsequent modeling efforts and is the current primary reference on basin hydrostratigraphy.

Creel (2000) collected groundwater level data and water quality data for New Mexico wells. These data were derived from the USGS Groundwater Information System (GWIS) and New Mexico Environment Department (NMED) databases on public drinking water quality. Creel's database is available through the Internet at the New Mexico Water Resources Research Institute (WRRI).

CH2M HILL (2000a) lists average water quality in several canals, drains, and laterals. These data were used in the Boyle BESTSM model to evaluate changes in water quality over time for various EPWU action scenarios.

2.2.2 Groundwater Modeling

Previous groundwater modeling studies consulted in this effort include Updegraff and Gelhar (1978), Khaleel et al. (1983), Gates et al. (1984), Peterson et al. (1984), Turnbull (1985), Maddock and Wright (1987), and Wilson (1989). The local-scale model developed in this study used the Weeden and Maddock (1999) regional model to establish boundary conditions. The Weeden and Maddock model evolved over time from the Frenzel and Kaehler (1990), Frenzel (1992), and Hamilton and Maddock (1993). Turnbull (1985) is the only known previous attempt at constructing a solute transport for the Mesilla Bolson.

Frenzel and Kaehler (1990) created a regional Mesilla Bolson MODFLOW model to examine the regional hydrology. This model simulated conditions from 1915 through 1975. The Frenzel (1992) model was based on Frenzel and Kaehler (1990). This model incorporated recent aquifer testing, reduced the number of model layers based on recent changes in hydrogeologic understanding from Hawley and Lozinsky (1992), included estimates of evapotranspiration, and lengthened the simulation period through 1985.

Building on the Frenzel (1992), Hamilton and Maddock (1993) added a more detailed representation of canals, drains, etc. and extended the simulation period to 1990. In addition, Hamilton and Maddock incorporated a version of the Purdic streamflow package altered to allow in segment diversions from canals and representation of diversions as percentages of total flow rather than absolute volumetric flow. Boyle Engineering Corporation (1999) coupled the Hamilton and Maddock (1993) model with the BESTSM (Boyle 2000) hydraulic model to examine water quality interaction between surface and groundwater in more detail. Lang and Maddock (1995) used the Hamilton and Maddock (1993) model to evaluate lining of canals.

Weeden and Maddock (1999) extended the Hamilton and Maddock (1993) model to include the Rincon Basin, updated the model to a two-season basis, and extended the simulation period through 1995. While these updates resulted in the expansion of the model and added detail to the stress periods, Weeden and Maddock also simplified some data from Hamilton and Maddock in order to incorporate the Hamilton and Maddock model into the Groundwater Modeling System (GMS) interface. In addition, the extension of the simulation period through 1995 was completed by repeating the 1990 stress period rather than incorporating new data. These simplifications coupled with the simplified representation of basin hydrostratigraphy with the chosen layering scheme result in significant limitations for accurately representing a local scale model and attempting solute transport. To continue the evolution of modeling studies with the most recent data, the Weeden and Maddock (1999) model will be used as a basis for this study. It is anticipated that the Cañutillo model will continue to evolve in order to address the limitations posed by previous simplifications.

Table 2-1 provides brief synopses of many of the reports and studies consulted in this effort.

2.3 Data Compiled

2.3.1 Groundwater Level Data

The efforts previously described leading up to the groundwater model presented in Weeden and Maddock (1999) examined groundwater flow parameters extensively. Figure 2-1 presents target hydraulic head locations for Weeden and Maddock (1999). Additional water level data were collected from the WRRI. The WRRI spent considerable time validating the collected data to ensure reliability (Kennedy, 2000). However, the WRRI database contains little information about the hydrostratigraphic unit associated with individual water levels. Therefore, targets used in Weeden and Maddock (1999) will be relied upon for calibration of groundwater heads. Calibration to these targets will allow for comparison to the Weeden and Maddock model. Additional time series water level data is available in the Cañutillo wellfield area. Additional temporal calibration points would allow for the evaluation of water level trends. However, with the current model layering calibration to additional points will not likely result in additional model accuracy. Future model revisions that explore the Cañutillo area in more detail should include additional spatial and temporal calibration points.

2.3.2 Water Quality Data

Surface water has long been used in the Mesilla Valley for the irrigation of agricultural crops. As such, a long record of water quality data exists for the Rio Grande and associated irrigation diversion structures.

TABLE 2-1
Select List of Reports Consulted

Author	Title	Year	Comments
Bahr, T.G.	*Water Resources and Growth of the Mesilla Valley: An Issue Paper*	1979	General Water Balance information, 1975 water withdrawals by source.
Basler, J.A., Alary, L.J	*Quality of the shallow water in the Rincon and Mesilla Valleys, New Mexico and Texas*	1968	Early USGS report examining shallow water quality in the Rincon and Mesilla Valleys. US BOR wells were sampled. Results are tabulated along with water level information.
Boyle Engineering	*Cañutillo Wellfield Master Plan*	1999	Documents model development of coupled revised Hamilton and Maddock, 1993 with BESTSM. Provides results of future scenario simulations.
Bromilow, Frank	*Flow Studies in the Mesilla Valley, WR and Their Economic Importance in NM*	1956	Not Available
CH2M HILL	*Draft Environmental Impact Statement*	2000a	EIS includes average water quality and flow data for Canals, Drains, the Rio Grande, and Wastewater Inputs.
CH2M HILL	*Draft Water Resources Technical Report*	2000b	Similar information to EIS. However, more detail is included, including mathematical relationships between TDS and Na, Cl, and SO4 for various river Reaches. Some information on agricultural practices and irrigation return flows.
CH2M HILL	*Cañutillo Wellfield Expansion, Wellfield Data Review*	2000c	Brief memorandum that examined data and reports in the vicinity of the Cañutillo wellfield with respect to expansion
CH2M HILL	*Cañutillo Wellfield Expansion, Conceptual Well Design and Construction Program*	2000d	Brief memorandum that uses a modified version of Hamilton and Maddock Model to estimate well effects. Current water quality data were plotted in the Cañutillo area.
Cliett, Tom	*Preliminary Report on EPWU Cañutillo Field Expansion for Westway*	1991	Examines data on groundwater occurrence in the vicinity of Westway and recommends a location for a test well. Indicates poor water quality near Westway.
Cliett, Tom	*Ground Water Occurrence of the Cañutillo-Anthony, Texas Area*	1990	Examines the relationship of ground water to the sedimentary units. Includes a summary of well and aquifer characteristics. Some water quality data over time.
Cliett, Tom	*Report on La Tuna Federal Correctional Institution*	1995	Test pumping and water quality results for La Tuna Well No. 9
Cliett, Tom	*Cañutillo South Test Drilling Project*	1990	Report on the drilling and testing of three test holes in the Lower Mesilla Valley. Includes sample data from study and e-logs.
Cliett, Tom and John W. Hawley	*General Geology and Groundwater Occurrence of the El*	1995	Discusses the geology, hydrogeology and water quality of the Mesilla

TABLE 2-1
Select List of Reports Consulted

Author	Title	Year	Comments
	Paso Area		Bolson. Two generalized cross-sections.
Conover, Clyde Stuart	*Ground-water conditions in the Rincon and Mesilla Valleys and adjacent areas in New Mexico*	1954	Early and often cited comprehensive study of Mesilla Bolson. Includes significant data on water levels and limited data on water quality.
Creel, B.J., Sammis T.W., Kennedy J.F., Sitze D.O., Asare D., Monger, H.C. and Z.A. Samani	*Ground-Water Aquifer Sensitivity Assessment and Management Practices Evaluation for Pesticides in the Mesilla Valley of New Mexico*	1998	Aquifer sensitivity analysis for pesticide contamination. Includes DRASTIC analysis of Mesilla Valley and modeling of pesticide application. DRASTIC analysis gives estimates of general recharge.
Frenzel, P.F., and Kaehler, C.A.	*Geohydrology and simulation of ground-water flow in the Mesilla Basin, Doña Ana County, New Mexico, and El Paso County, Texas, with a section on Water quality and geochemistry, by S.K. Anderholm*	1990	Original documentation of the Frenzel model with some information on water quality.
Frenzel, Peter F.	*Simulation of ground-water flow in the Mesilla Basin, Dona Ana County, New Mexico, and El Paso County, Texas*	1992	USGS report revising the 1990 Frenzel model. Includes a model description, water balance information, tabular data of hydraulic conductivity by well and unit., and target head information.
Gates, J. S., White, D. E. , Leggat, E. R.	*Preliminary study of the aquifers of the lower Mesilla Valley in Texas and New Mexico by model simulation*	1984	Early basic model of the Mesilla basin. Relatively coarse grid size.
Gutierrez, Melida	*Analysis of the Sediments of Well A-3 Mesilla Valley, Texas*	1990	Cuttings and geophysical logs of well A-3 were analyzed to characterize the local geology.
Hamilton, S.L., and Maddock, T., III	*Application of a Ground-Water Flow Model to the Mesilla Basin, New Mexico and Texas*	1993	First documentation of Maddock's changes to Frenzel's model. Changes included representation of the Rio Grande and diversion system as a "stream" type boundary.
Hawley, J.W.	*Introduction to hydrogeologic features of the Mesilla Bolson area, Doña Ana County, New Mexico*	1984	Basic geology of the Mesilla Bolson.
Hawley, J.W., Lozinski, R.P.	*Hydrogeologic framework of the Mesilla Basin in New Mexico and western Texas*	1992	This report was a major update to the understanding of the Basin. Changes to the Frenzel 1990 model were made based on new geologic understanding provided in this report.
Healy, Denis F.	*Water-Quality Assessment of the Rio Grande Valley, Colorado, New Mexico, and Texas - Occurrence and distribution of selected pesticides and nutrients at selected surface-water sites in the Mesilla Valley, 1994-95*	1995	NAWQA, Pesticide data in RG and irrigation drains in Mesilla
Huff, G. F.	*Water-quality data for the Rio Grande between Picacho Bridge near Las Cruces and Calle del Norte Bridge near*	1998	Rio Grande water quality data collected near Las Cruces wastewater outfall (1996), no interpretation.

TABLE 2-1
Select List of Reports Consulted

Author	Title	Year	Comments
	Mesilla, New Mexico		
Khaleel, R. et al.	*Numerical Modeling of Ground-Water Flow in the Lower Rio Grande Basin, New Mexico.*	1983	Not Available
King, W.E.,J. W. Hawley, A. M. Taylor, and R. P. Wilson	*Geology and ground-water resources of central and western Doña Ana County, New Mexico*	1971	
Lang, P.T., and Maddock, T., III	*Simulation of Groundwater Flow to Assess the Effects of Pumping and Canal Lining on the Hydrologic Regime of the Mesilla Basin, Dona Ana County, New Mexico and El Paso County, Texas*	1985	Presents similar information to other Maddock reports. Includes more information on canals and drains than other reports
Lansford, R.R., Creel, B.J., and Seipel, C.	*Demonstration of Irrigation Return Flow Water Quality Control in the Mesilla Valley, New Mexico*	1980	Linear programming model of Mesilla Valley irrigation practices. Examines alternative irrigation practices.
Murray, C.R.	*Reconnaissance survey of well sites of U.S. Grazing Service in Deming-Las Cruces area, New Mexico*	1942	Proposes well sites based on information from area wells near Deming, El Paso, etc.
Myers, Robert G. , Orr, Brennon R.	*Geohydrology of the aquifer in the Santa Fe Group, northern West Mesa of the Mesilla Basin near Las Cruces, New Mexico*	1985	USGS study of wells on the northern West Mesa near Las Cruces. Data were summarized for existing wells in this area and collected from two test wells.
Nickerson, E.L.	*Aquifer Tests in the Flood-Plain Alluvium and Santa Fe Group at the Rio Grande Near Cañutillo, El Paso County, Texas*	1989	USGS aquifer testing from specific zones in the Cañutillo wellfield. The alluvial zone was tested with by observing monitoring wells during a flood pulse. The intermediate and deep zones were tested by stressing the aquifer at a known rate.
Nickerson, E.L.	*Selected geohydrologic data for the Mesilla Basin, Dona Ana County, New Mexico, and El Paso County, Texas*	1986	Report of data compiled from their groundwater monitoring program. Includes hydrologic sections, hydrographs, resistivity logs, and tabular data of water levels and chemical data for 143 wells.
Nickerson, Edward	*U. S. Geological Survey seepage investigations of the lower Rio Grande in the Mesilla Valley*	1999	Summary of USGS seepage investigations on the Rio Grande. This report includes information on surface water quality from 6 sites
Nickerson, Edward L.	*Selected hydrologic data for the Mesilla ground-water basin, 1987 through 1992 water years, Dona Ana County, New Mexico, and El Paso County, Tex*	1995	Report of data compiled from their groundwater monitoring program. Includes hydrologic sections, hydrographs, resistivity logs, seepage data (hydrologic and chemical), and tabular data of water levels for 181 wells. Includes data from previous studies OF 86-75 (excludes chemical data)
Nickerson, Edward L. , Myers, Robert G.	*Geohydrology of the Mesilla ground-water basin, Dona Ana County, New Mexico, and El Paso County, Texas*	1993	USGS report of gw monitoring/study of USGS monitoring network. Documents gw levels, well hydrographs, k/kv (from previous study), flow direction, river/gw relations, water quality at selected sites, test

TABLE 2-1
Select List of Reports Consulted

Author	Title	Year	Comments
			holes w/ resistivity logs.
NMED	*Chemical Quality of New Mexico Community Water Supplies*	1980	Water Quality data from wells by county. Individual well data for 117 wells w/ locational information, no interval/depth information, no date of sample information.
Peterson, D.M., Khaleel, R., and Hawley, J.W.	*Quasi Three-dimensional Modeling of Groundwater Flow in the Mesilla Bolson, New Mexico and Texas*	1984	Report of a transient numerical model of the Mesilla Bolson. This model was developed to gain further understanding of the Mesilla, specifically surface and groundwater interaction.
Richardson, Gary L.	*Preliminary Groundwater Model of the Mesilla Valley*	1972	Not Available
Richardson, Jesse U.	*Underground Water Problems in the Mesilla Valley*	1956	Early report that cites lack of data. Indicates existence of US BOR wells used in Basler.
Sammis, T.W.	*Demonstration of Irrigation Return Flow Water Quality in the Mesilla Valley, New Mexico*	1980	Examines the relationship of irrigation practices to irrigation efficiency and return flow quality with a demonstration farm. Includes water quality data for La Mesa Drain. TDS maps and seepage loss calculations.
Theis, C.V.	*Ground-water supplies near Las Cruces, New Mexico*	1942	Estimates water resources in the Las Cruces area through limited testing of area wells. Examines water quality.
Turnbull, S.J.	*Numerical Modeling of Ground-Water Flow in the Cañutillo Wellfield, Cañutillo, Texas*	1985	Model report for groundwater flow and solute transport model of the Mesilla Valley. Includes contour maps of TDS concentrations based on nearest neighbor interpolation of well data. Tabulated transmissivities.
Updegraff, C.D. and Gelhar, L.W.	*Parameter Estimation for a Lumped Parameter Groundwater Model of the Mesilla Valley, New Mexico*	1978	Modeled Mesilla Valley with a lumped parameter model. They determined that the best fit of an overall water balance occurred when a disconnected steam was simulated for the Rio Grande.
USGS	*Water Resources Data New Mexico Water Year 1998*	1996	Contains tabulated surface water flow and water quality data as well as seepage investigation results.
USGS	*Water Resources Data New Mexico Water Year 1998*	1997	Contains tabulated surface water flow and water quality data as well as seepage investigation results.
USGS	*Water Resources Data New Mexico Water Year 1998*	1998	Contains tabulated surface water flow and water quality data as well as seepage investigation results.
USGS	*Water Resources Data New Mexico Water Year 1998*	1999	Contains tabulated surface water flow and water quality data as well as seepage investigation results.

TABLE 2-1
Select List of Reports Consulted

Author	Title	Year	Comments
Wade, S.C. and Reiter, M.	*A Hydrothermal Study to Estimate Vertical Groundwater Flow in the Cañutillo Wellfield, between Las Cruces and El Paso*	1994	Uses temperature profile data from USGS piezometers in the Cañutillo to estimate Kv, vertical porosities
Weeden, C., and Maddock, T., III	*Simulation of Groundwater Flow in the Rincon Valley Area and Mesilla Basin, New Mexico and Texas*	1999	Provides detailed information on groundwater flow modeling of the Mesilla Basin. Includes extensive data used for model calibration.
West, Francis	*The Mesilla Valley: A Century of Water Resource Investigations*	1996	A history of water resource studies in the Mesilla Valley. Includes graphs of Rio Grande Flow, Groundwater Levels, Drain Flows, and Salt balance over time.
Wilson, Clyde A. , White, Robert R.	*Geohydrology of the central Mesilla Valley, Dona Ana County, New Mexico*	1984	USGS report of gw monitoring/study of deep irrigation wells (EBID). Aquifer test results(k, kv, Sc), lithographic logs, and water quality data are reported. Tabular values from multiple wells over time of specific capacity/water quality.
Wilson, Clyde A. , White, Robert R. , Orr, Brennon R. , Roybal, R. Gary	*Water resources of the Rincon and Mesilla valleys and adjacent areas, New Mexico*	1981	An often cited reference with large amounts of well information, surface-water data, seepage information (2 studies), aquifer test data (53 tests), water-quality data (450 analyses), water level contours, depth to water, freshwater thickness, hydrogeologic cross-sections, well inventory of 1,530 wells.
Wilson, Lee	*Projected Impacts of Expanding the Cañutillo Wellfield*	1989	Report to EPWU on the modeled effects of three pumping scenarios.
Woodward, Dennis G., Myers, Robert G.	*Seismic investigation of the buried horst between the Jornada del Muerto and Mesilla ground-water basins near Las Cruces, Dona Ana*	1997	Seismic reflection profiles were completed near the Jornada Horst to the northeast of Las Cruces. Includes plots and cross-sections as well as generalized water table maps
Zohdy, A.R., Bisdorf, R.J. and Gates, J.S.	*Schlumberger Soundings in the Lower Mesilla Valley of the Rio Grande, Texas and New Mexico.*	1976	Includes plots of sounding results versus depth. These data can be used to examine layer interfaces.

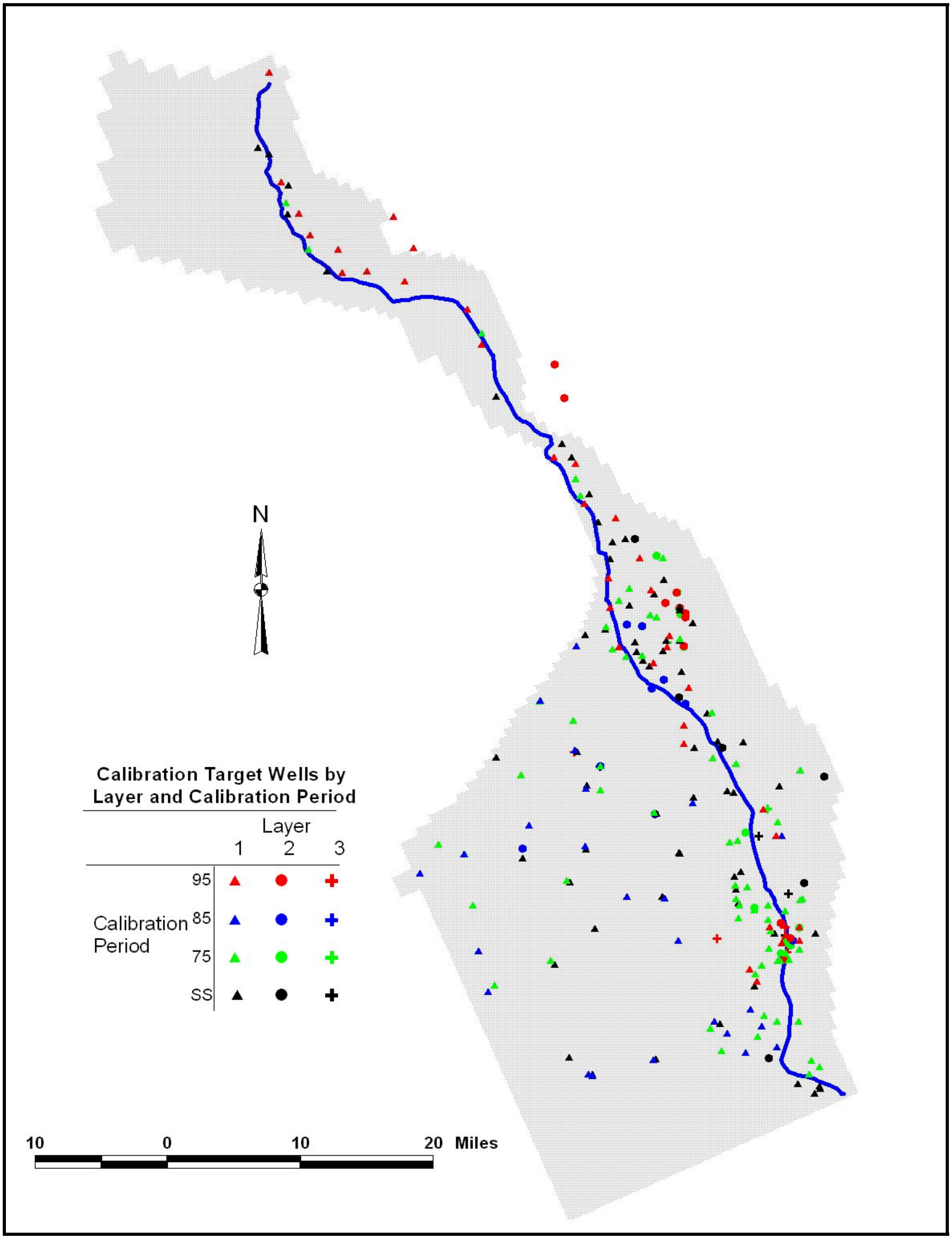

Figure 2-1. Water Level Sites for Calibration

Groundwater has only been used extensively for irrigation and public water supply since the drought of the early 1950s. Water quality data were collected at many well sites by various entities. However, irrigated areas and centers of population make up a relatively small portion of the Mesilla Basin. Therefore, groundwater data are centered on areas of anthropogenic activity and are more limited beyond the valley area. Little data are available on the Eastern and Western areas of the model. Significant amounts of data have been collected in the Cañutillo area and water quality data are regularly collected by both EPWU and the USGS. However, in part due to the model layering scheme and in part due to spatial and temporal data gaps, some level of generalization and synthesis of data is required to represent water quality in the Cañutillo area in three dimensions. As such, data collected over several years from various locations was used to produce "average" water quality profiles for "historical" and "present" conditions. In general, in areas where significant time series data are available, care was taken to represent historical or present conditions accurately. In particular, in wells where marked changes in groundwater quality occur over the time period of interest, data were used for the starting year and ending year (1970 and 1995) rather than averaging the water quality changes. The generalizations in water quality representation will increase uncertainty associated with simulation results.

As part of this project, some additional groundwater quality data will be collected in areas where model confidence is low. These data will be added to the database to enhance overall understanding of how groundwater quality varies spatially and how groundwater quality changes over time. These data will be collected after the production of this report.

2.3.2.1 Surface Water Quality Data

The USGS routinely monitors the Rio Grande for flow and water quality. These data are readily available through their annual *Water Resources Data Report Series for New Mexico* (USGS, 1996, 1997, 1998, and 1999). In addition, the USGS has conducted a number of seepage studies where surface water quality data have been collected for the Rio Grande and select canals and drains (Nickerson, 1986, 1993, 1995, and 1999). CH2M HILL (2000a and 2000b) reports average Rio Grande, canal, and drain water quality measurements used in Boyle's BESTSM model to evaluate environmental effects of changes to surface water management practices.

2.3.2.2 Groundwater Quality Data

Groundwater quality data were obtained from the EPWU, the WRRI, the Office of the State Engineer of New Mexico (OSE), the NMED and the USGS. The EPWU maintains a database of Texas and New Mexico groundwater wells in the Cañutillo area. This database includes water level and water quality information over time for this area. To estimate depth to groundwater over the Mesilla Basin, the WRRI collected large amounts of well data in New Mexico. These data include water level measurements and water quality information over time.

The OSE maintains New Mexico water well registration information. This information includes water level information and some limited water quality data. The water level information is available to the general public through the Internet at the OSE website. However, information is not readily available on well construction, elevation, water level measurement dates, or water quality measurement results. Likewise, not all registered wells are listed on the website.

The USGS currently monitors a network of wells in the Mesilla Bolson. Water level data, some aquifer testing data, and limited water quality information are collected from this network. The USGS maintains these data and other water well data in its GWIS. Historical groundwater quality data are available from Wilson et al. (1981). Figure 2-2 presents locations of water quality data.

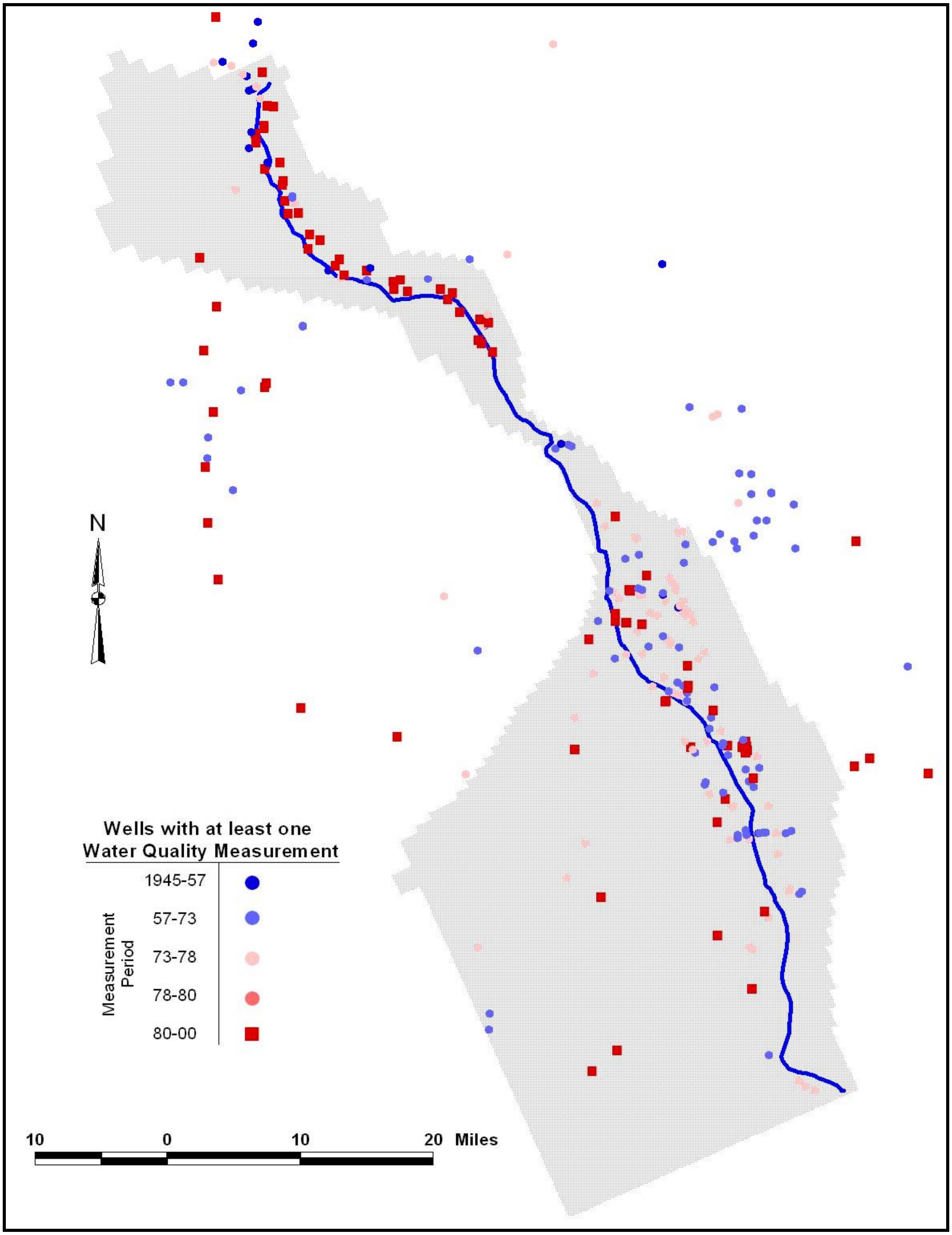

Figure 2-2. Water Quality Measurement Sites

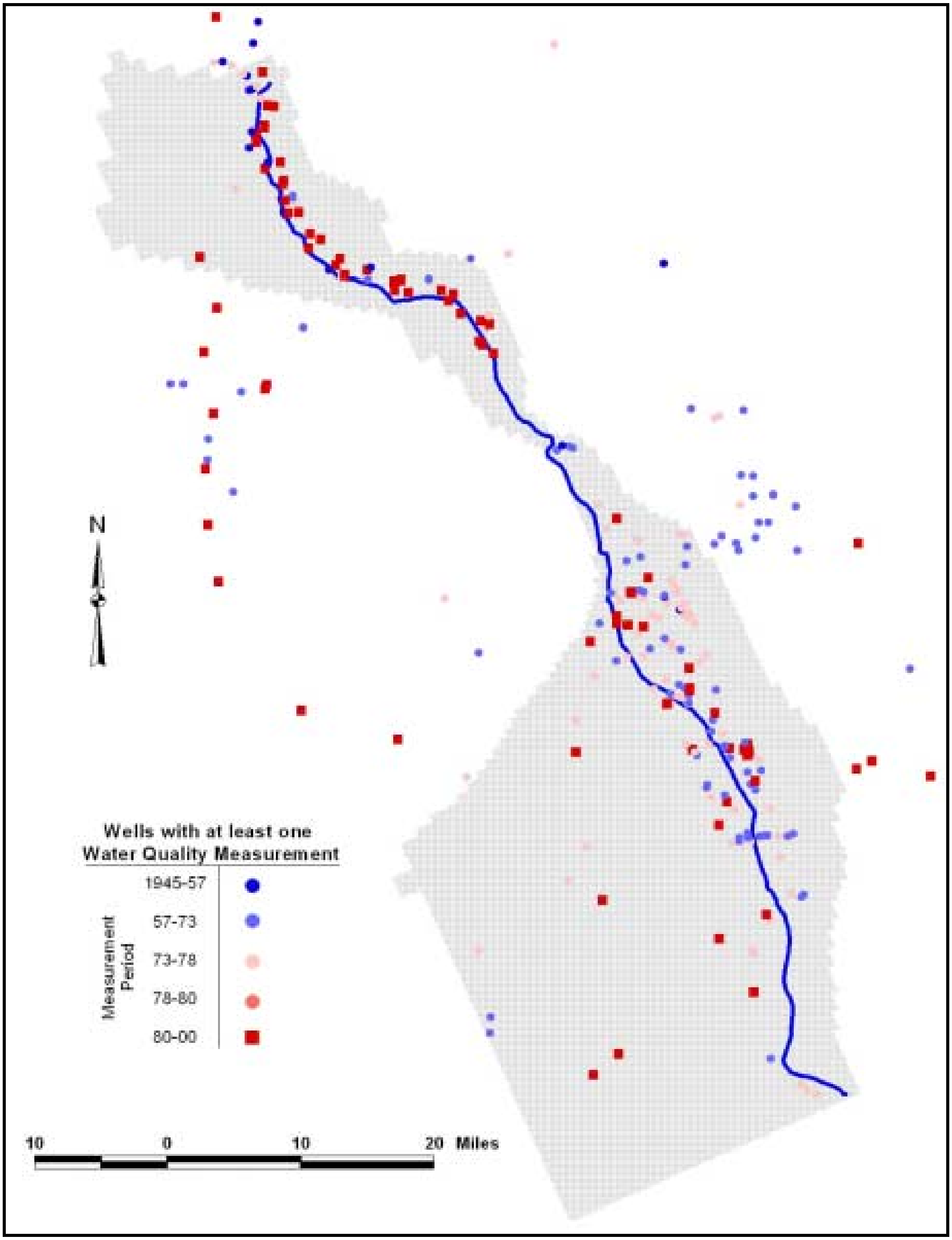

Figure 2-2. Water Quality Measurement Sites

3. Conceptual Model for the Cañutillo Wellfield Modeling Project

3. Conceptual Model for the Cañutillo Wellfield Modeling Project

3.1 Introduction

This section briefly describes the geology, hydrogeology, water budget, and water quality of the Mesilla Basin as examined by researchers over time. A general background of the study area emphasizing parameters related to groundwater flow and solute transport model development is presented. This section generally follows the overall conceptual model presented in Weeden and Maddock (1999) with the addition of water quality information and a focus on the Cañutillo area. While the Weeden and Maddock (1999) study describes the Mesilla and Rincon Valleys of the Rio Grande Basin, this study focuses on the Cañutillo area of the Mesilla Basin. For a more detailed description of the study area, please consult the listed references.

3.2 Area Description

The Mesilla Basin is part of the Lower Rio Grande Basin located in Dona Ana County in New Mexico. A small portion of the basin extends into Texas and a large area extends into Mexico. Hydrologic basins bordering the Mesilla Basin include the Rincon Valley to the north, the Jornada del Muerto Basin to the northeast, the Hueco Bolson to the east and the Mimbres Basin to the west. The basins, except the Mimbres Basin, are believed to be connected to the Mesilla Bolson in varying degrees by a thin alluvial layer. The Mesilla Bolson's connection to the Mimbres Basin is not well understood, but there may be some groundwater movement between basins (Conover, 1954; Wilson, et al., 1981; and Peterson, et al., 1984).

The Mesilla Basin is bordered to the east by the Franklin, Organ, and Dona Ana Mountains; to the west by the Potrillo Mountains and the Aden, Sleeping Lady, and Rough and Ready Hills; and to the north by the Robledo Mountains (King et al., 1971). The area of interest for the current study is the vicinity of Cañutillo, New Mexico, and is generally bounded by Vado, New Mexico to the north; El Paso, Texas to the south; the Basin boundary on the east; and stretches approximately 25 miles from east to west.

3.2.1 Geology/Hydrogeology

The Mesilla Basin is underlain by bedrock composed primarily of Precambrian igneous and metamorphic rock, Paleozoic, Mesozoic, and lower Tertiary sedimentary rock, and Tertiary volcanic rock (Frenzel and Kaehler, 1990). The primary water-bearing units include the upper Santa Fe Group and Rio Grande floodplain alluvium, which are made up of mid-Tertiary to Pleistocene deposits that lie above bedrock.

The Santa Fe Group is nonexistent in some areas near the margins of the Mesilla Basin and extends to as much as 2,500 feet thick in the near west mesa area (Hamilton and Maddock, 1993). It is typically divided into at least three subunits that reflect the varied composition of a depositional environment (Hawley and Lozinski, 1992). These units consist of the Upper Santa Fe unit (USF) with a median hydraulic conductivity of 25 feet per day, the Middle Santa Fe unit (MSF) with a median hydraulic conductivity of 13.5 feet per day, and the Lower Santa Fe unit (LSF) with a median hydraulic conductivity of 12.5 feet per day (Frenzel, 1992). Transmissivities are estimated to range from 2,600 square feet per day (ft^2/day) to 21,000 ft^2/day (Wilson et al., 1981). Weeden and Maddock (1999) estimate storage coefficients ranging from 0.00004 to 0.0006. Groundwater flows generally to the southeast. Based on information from EPWU borings, water quality can vary significantly within a given subunit of the Santa Fe Group.

River alluvium ranges from 50 to 125 feet thick with an average thickness of about 80 feet (Wilson, 1981). Sediments range from fines near the surface to gravels near the base (Frenzel and Kaehler, 1990). Hydraulic conductivity of the river alluvium sediments ranges from 100 to 350 feet per day (Hamilton and Maddock, 1993). Richardson (1972), Frenzel (1990), and Hamilton and Maddock (1993) estimated storage at 0.2. Figures 3-1 through 3-4 present the average hydraulic conductivity and transmissivity from 0 to 200, 200 to 500, 500 to 900, and 900 to 1,300 feet below the ground surface, respectively, as conceptualized by Frenzel and Kaehler (1990) and presented by Weeden and Maddock (1999).

3.3 Water Budget

The majority of surface water enters the Mesilla Basin at its northernmost point. The Rio Grande flows into the basin through the Selden Canyon and exits the Basin at the El Paso Narrows. Additional surface water flow enters the Mesilla Basin through precipitation runoff that generally flows toward the Rio Grande. Flow in the Rio Grande is controlled by releases from Caballo Dam, which plays an integral role in the basin water budget (Weeden and Maddock, 1999). Leasburg Dam and Mesilla Dam divert flows from the Rio Grande for irrigation. Diverted water flows through a complex series of canals and laterals to meet irrigation demands. Water applied to the fields then evapotranspirates and percolates to the water table. In most years, the water table is high enough that a intricate series of drains (shallow, unlined ditches bounding irrigated parcels) will intercept shallow groundwater, flushing salts leached in the irrigation process back into the Rio Grande. Water that seeps into the groundwater and is not intercepted by the drains is the primary source of recharge to the Mesilla Basin aquifer. Some minimal recharge occurs through subsurface flow from other basins. Additional recharge occurs from precipitation primarily through mountain front recharge.

The overall water budget of the Mesilla system varies from year to year depending on a number of factors. In successive years where precipitation is minimal and Rio Grande flow is reduced, less water is available for irrigation diversion. Therefore, less water seeps from the Rio Grande and associated irrigation canals, less water percolates to the aquifer from irrigation application, and less water returns to the Rio Grande in the drains. Because there is still irrigation demand, groundwater is relied upon to make up the decline in surface water diversions. As such, the aquifer experiences reduced inflow and increased withdrawal in dry years. Likewise, in wet years, less water is withdrawn and more water seeps from the Rio Grande and surface water diversion system.

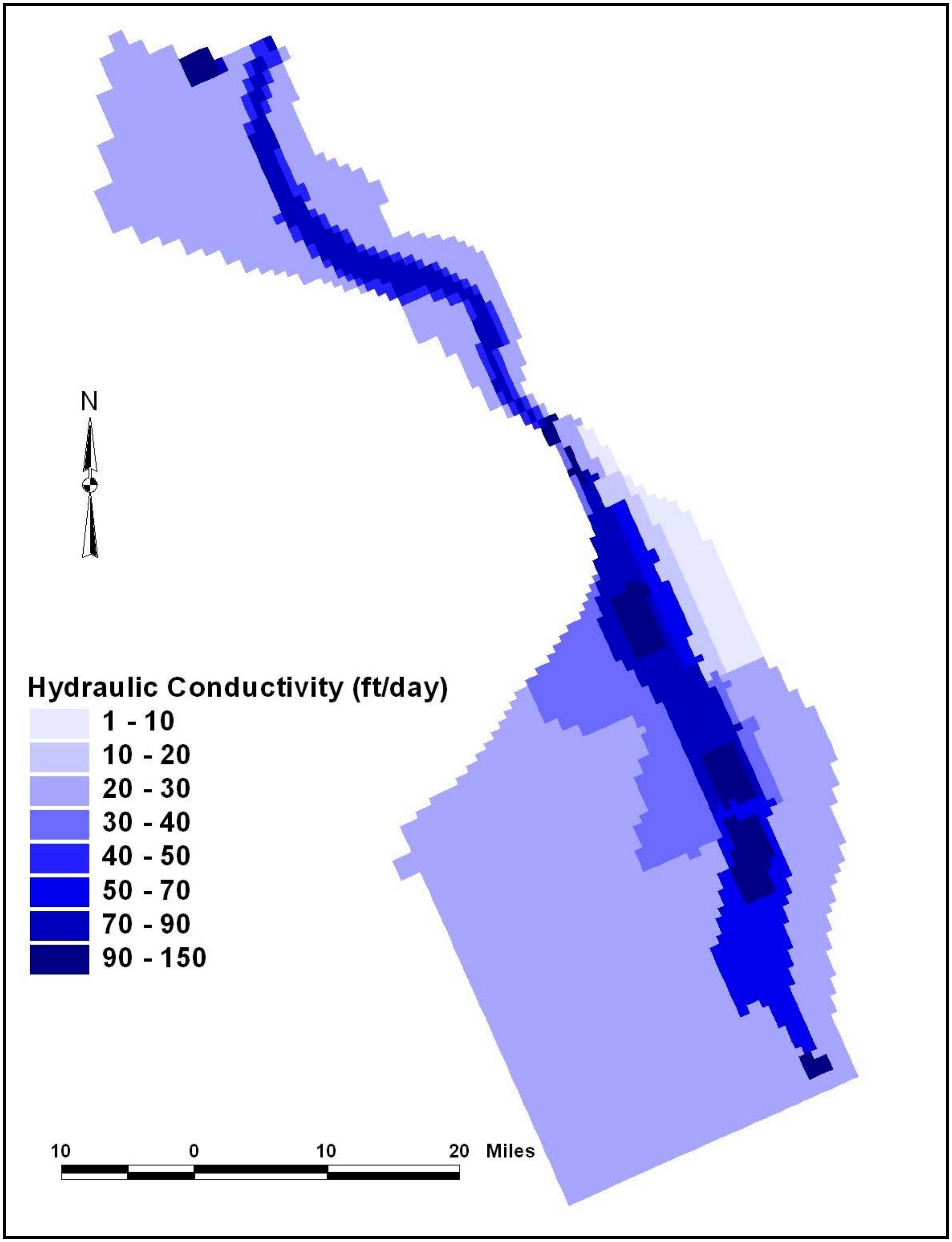

Figure 3-1. Average Hydraulic Conductivity 0 to 200 Feet Belowground Surface

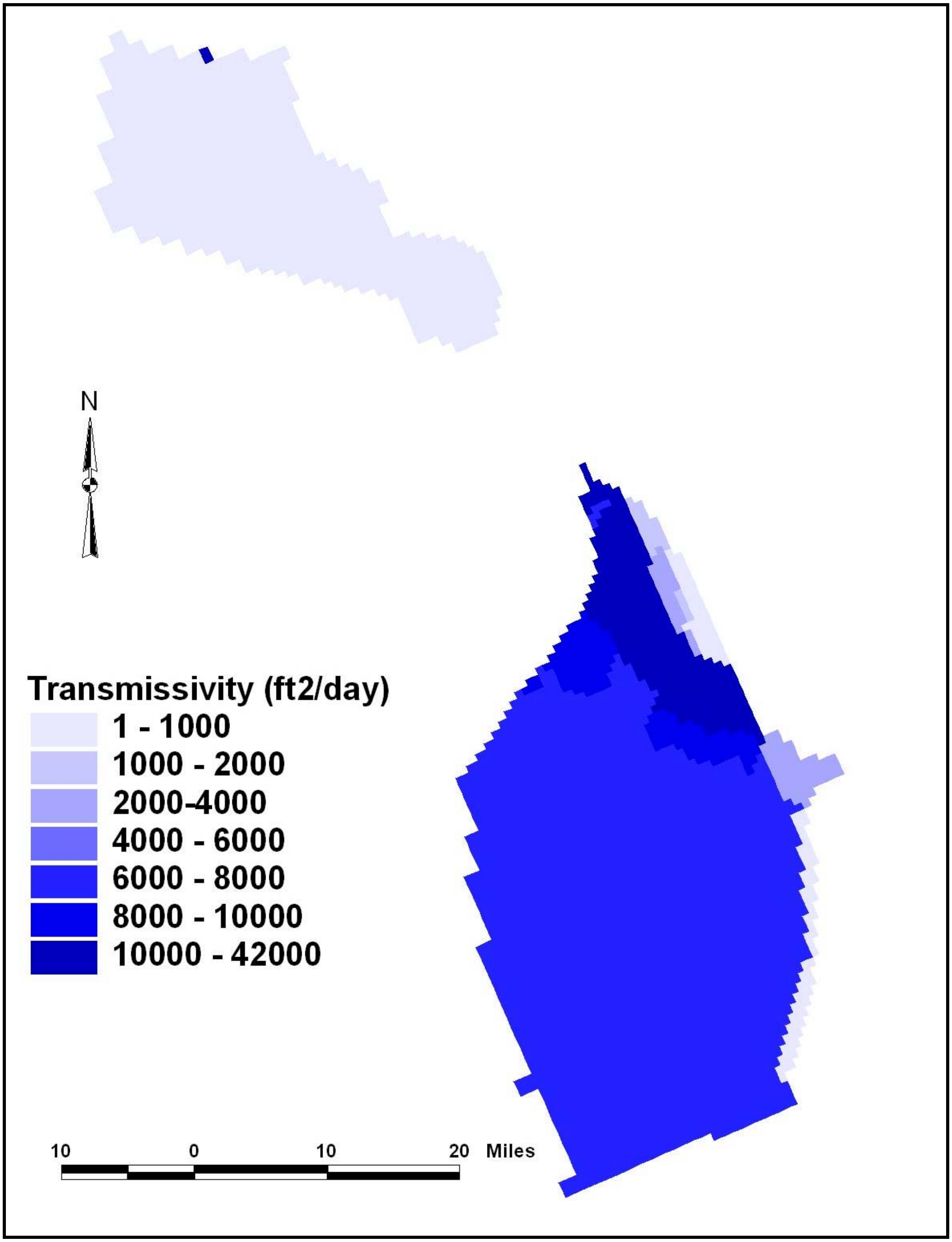

Figure 3-2. Average Transmissivity 200 to 500 Feet Belowground Surface

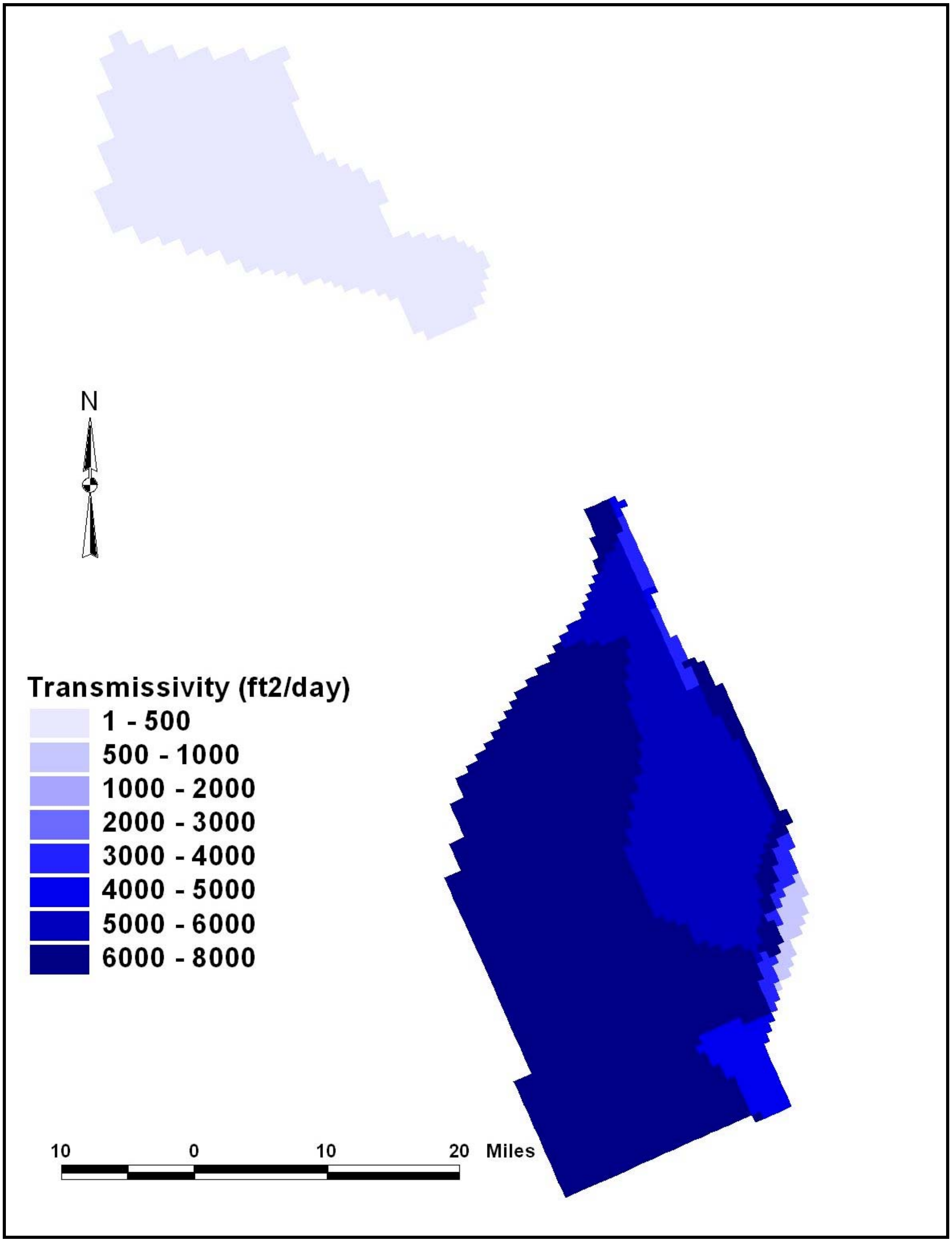

Figure 3-3. Average Transmissivity 500 to 900 Feet Belowground Surface

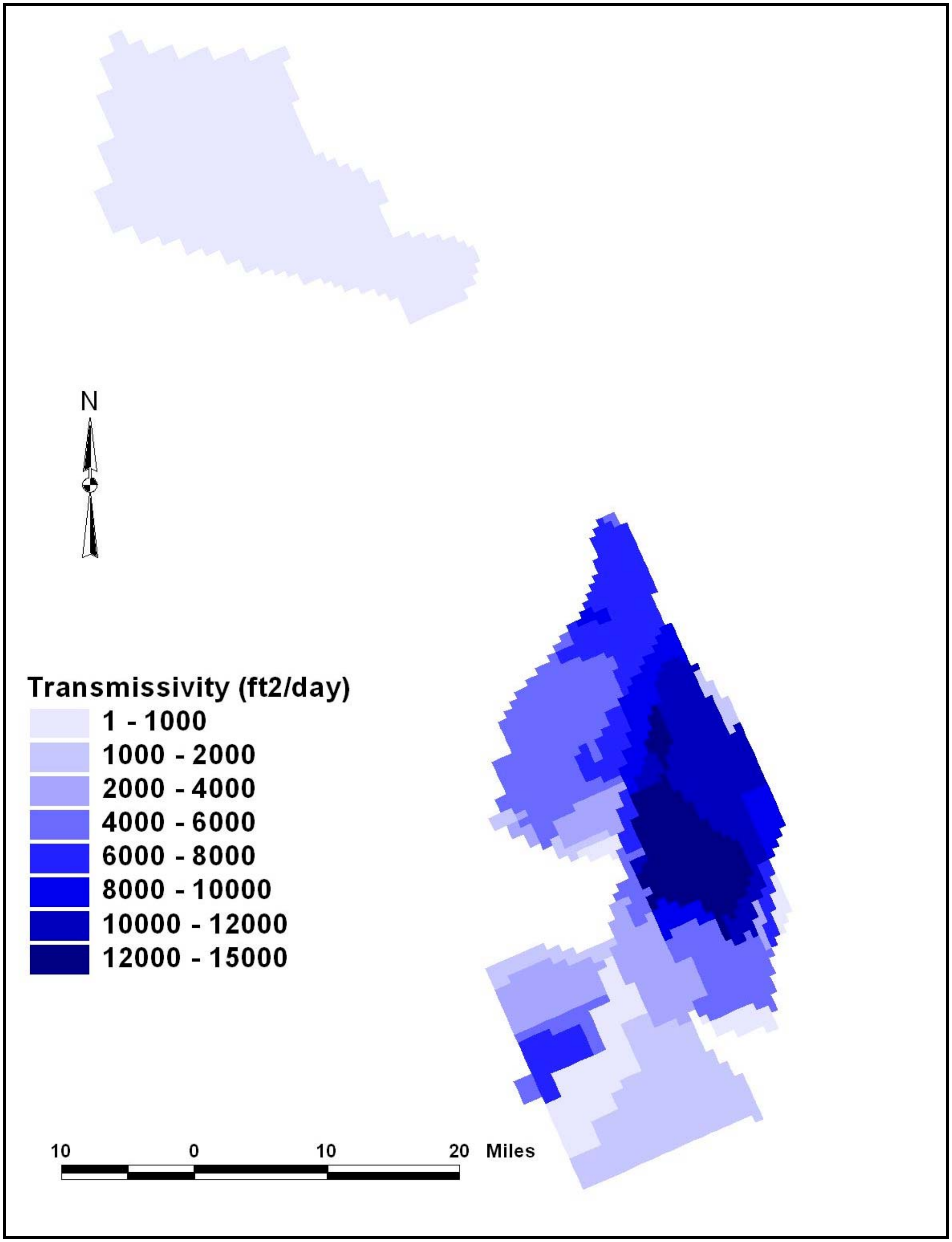

Figure 3-4. Average Transmissivity 900 to 1,300 Feet Belowground Surface

In the Cañutillo area many of the same general processes occur in microcosm of the overall Mesilla Basin. Surface water enters the Cañutillo area through the Rio Grande and through canals carrying flow from upstream diversions at Leasburg Dam. This flow is dependent on releases from Caballo Reservoir. Water is diverted from the Rio Grande at Mesilla and applied to fields for irrigation purposes. Water that is not captured through evapotranspiration percolates through the subsurface to the water table. Open-channel drains capture a portion of this water. The portion not captured and quantities that leak directly from the Rio Grande, canals, and drains recharges the aquifer. Surface water leaves the Cañutillo area at El Paso Narrows. Quantities of water entering and leaving the Cañutillo area vary significantly an annual basis depending on precipitation and irrigation requirements.

Water is also removed from this area by EPWU and other users through wells. Well usage has increased over time as population increases. Agricultural users also use wells to supplement diversions, particularly in drought years. As such, agricultural usage tends to be more variable on an annual basis than municipal and industrial usage. Recharge occurs in the Cañutillo area through mountain front flow off of the Franklin Mountains and slope front flow off of La Mesa. Some underflow occurs from the Hueco Bolson through Anthony gap. In addition, water flows into the Cañutillo area from the north and west from the larger Mesilla Bolson area. Figure 3-5 presents a schematic of the basin water budget.

3.3.1 Inflows

Water flows into the Mesilla Basin through precipitation, seepage from the Rio Grande, seepage from irrigation distribution canals, percolation from applied irrigation, and from subsurface connections to other basins. The following subsections briefly discuss each of these sources of inflow to the Mesilla Bolson aquifer and more specifically the Cañutillo area.

3.3.1.1 Rio Grande Seepage

The Rio Grande is the primary conduit for groundwater recharge in the Mesilla Basin. On average, the Rio Grande is a losing stream (i.e., water flows from the Rio Grande to the aquifer). However, areas north of Las Cruces are gaining (Conover, 1954; Wilson et al., 1981; Nickerson, 1989). Conover (1954) and Nickerson (1994) estimated seepage of the Rio Grande from gauged river flows, diversion amounts, and drain returns. These estimates range from about 0.1 cubic feet per second (ft^3/s) to 1.3 ft^3/s per river mile. Modeling studies by Peterson et al. (1984) generally confirm these results. Overall, the amount of seepage varies from year to year and is dependent on the available flow in the Rio Grande. Weeden and Maddock (1999) examined Rio Grande seepage by comparing Rio Grande depletions between Leasburg and El Paso and by examining seepage study results presented by Nickerson (1997). Figures 3-6 through 3-8 present the Rio Grande depletions over time, seepage per river mile in 1997, and the results of the Nickerson (1994) study, respectively. The Cañutillo area begins approximately at river mile 1280 and extends to El Paso. Average loss rates in this area appear to be consistent with the average loss rates in the Mesilla.

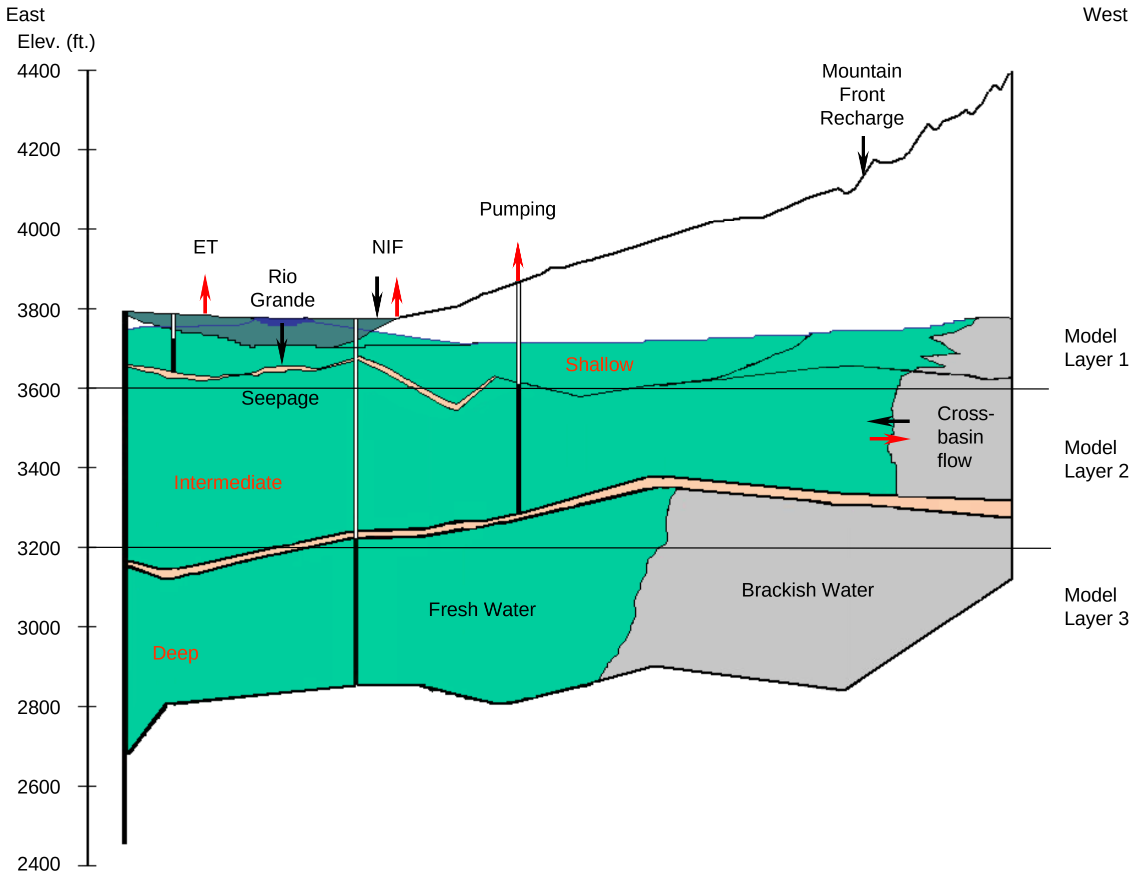

Figure 3-5. Schematic of Aquifer Water Budget in the Cañutillo Area

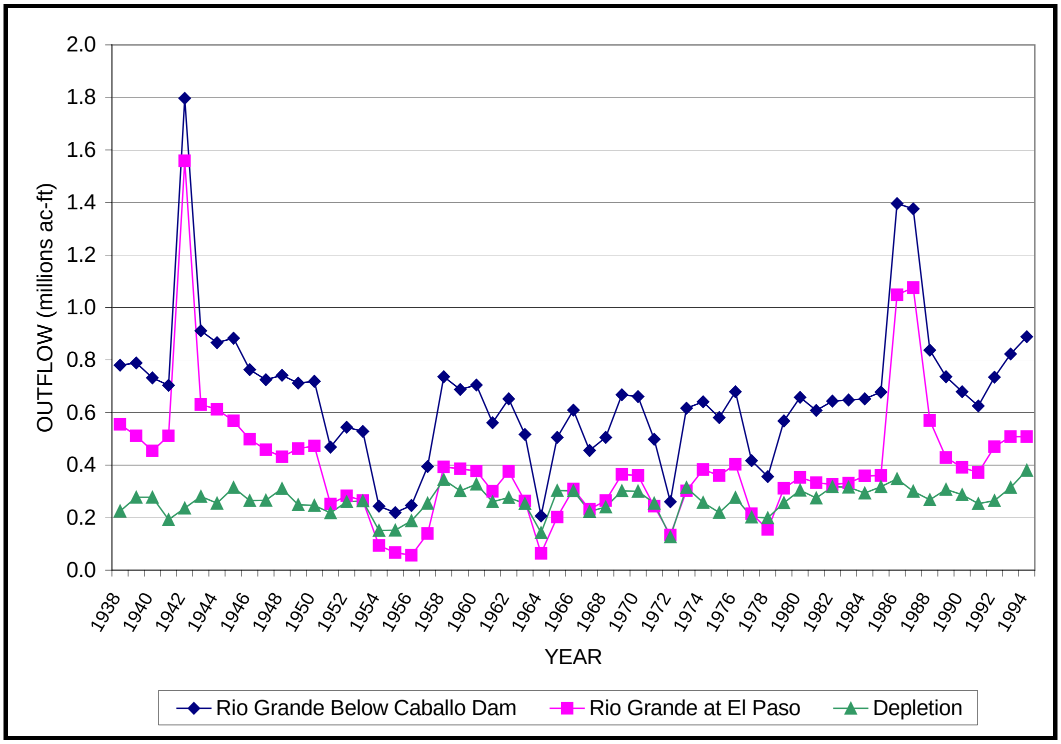

Figure 3-6. Rio Grande Depletions Between Caballo and El Paso

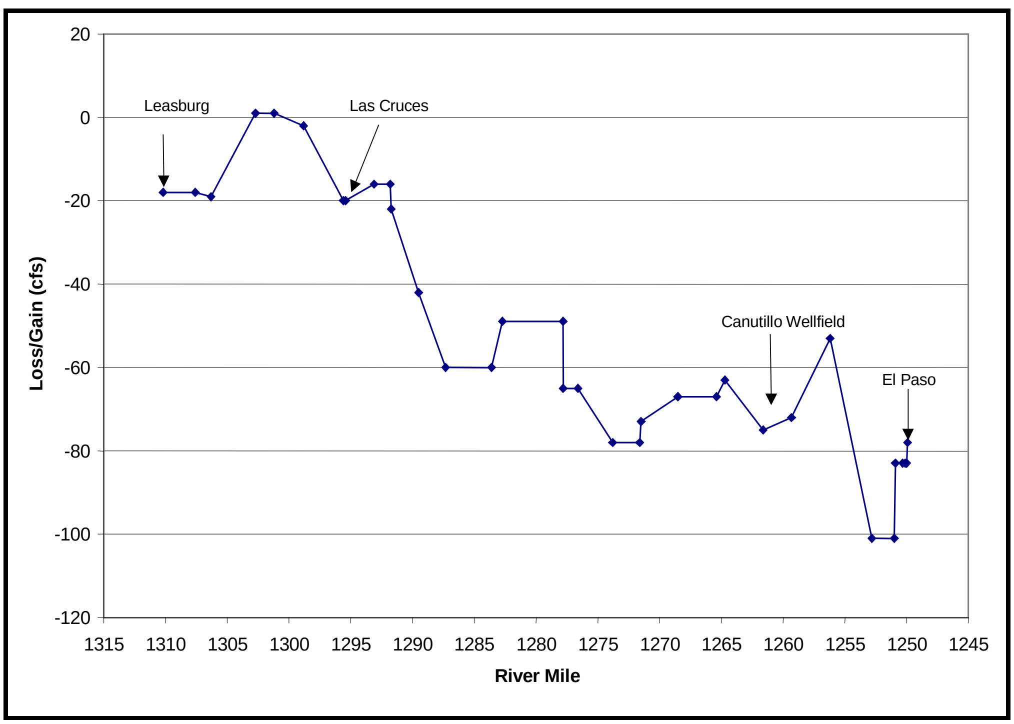

Figure 3-7. 1997 Cumulative Seepage by River Mile from Leasburg to El Paso
(Weeden and Maddock, 1999)

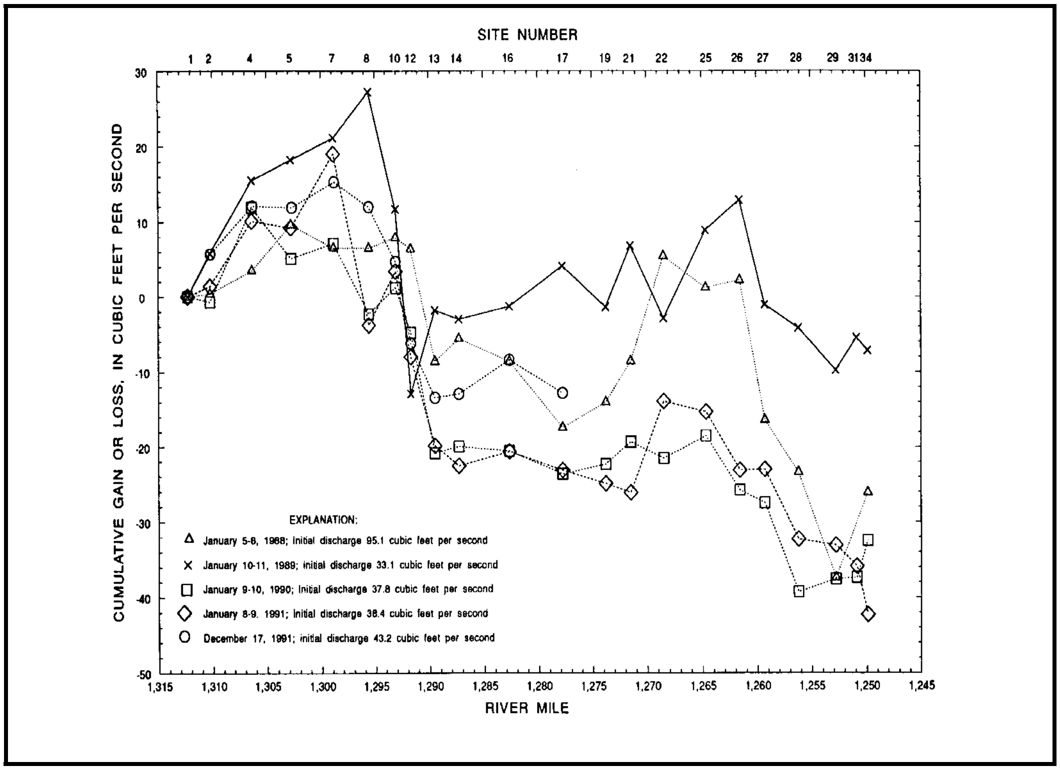

Figure 3-8. Rio Grande Losses by River Mile 1988 through 1991
(Nickerson, 1994)

3.3.1.2 Irrigation Canal, Lateral, and Ditch Seepage

During the irrigation season, low head dams divert water from the Rio Grande into a complex network of canals, laterals, and ditches that distribute it to farmers. The USGS (1997) estimated canal seepage losses to be 10 to 20 percent of initial diversion. Conover (1954) estimated canal losses to be 20 percent of gross diversions. Hamilton and Maddock (1993) and Wilson et al. (1981) estimated canal losses at about 40 percent of diversion through regression analysis of gross diversion. Sammis (1980) estimated canal seepage rates ranging from 0.03 to 0.14 feet per day. Figure 3-9 presents select canal flows over time (Weeden and Maddock, 1999).

Weeden and Maddock (1999) used an estimate of canal seepage in their calculation of applied surface water. Because of the regional nature of the Weeden and Maddock model, they chose to represent only major canals. Because the current modeling effort describes the Cañutillo area in greater detail than the Weedon and Maddock model, additional canals and drains are represented. In addition, Weedon and Maddock's simplified version of the surface water system was replaced with maps from the National Hydrologic Dataset (NHD). In general these surface system are relatively minor and as such measured flow data are not available. However, the addition of these known features provides a better representation of the interaction of the surface and groundwater systems.

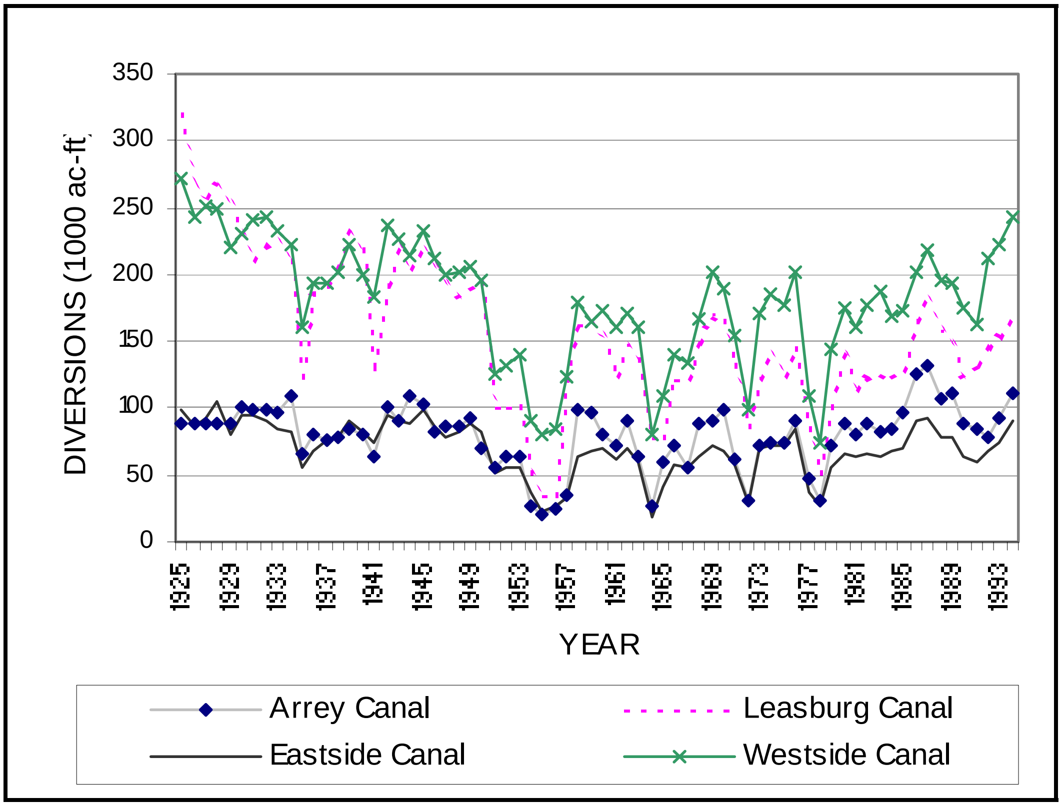

Figure 3-9. Select Canal Flows, 1925 to 1995
(Weeden and Maddock, 1999)

3.3.1.3 Applied Irrigation Water

Conover (1954) estimated that 20 percent of diversions for irrigation are lost to seepage through canal, lateral, and ditch bottoms while another 24 percent return to the Rio Grande. Wilson et al. (1981) noted that delivery became more efficient and therefore only about 15 percent were returned. Applied irrigation water accounts for the remaining 56 percent. Some portion of this water is lost through the evapotranspiration process. The remaining portion percolates to the water table where it recharges deeper aquifers or is intercepted by agricultural drains. Figure 3-10 presents the average annual applied irrigation for the Mesilla Valley as calculated by the method of Weeden and Maddock (1999). Based on acreage about half of this amount is applied in the Cañutillo area.

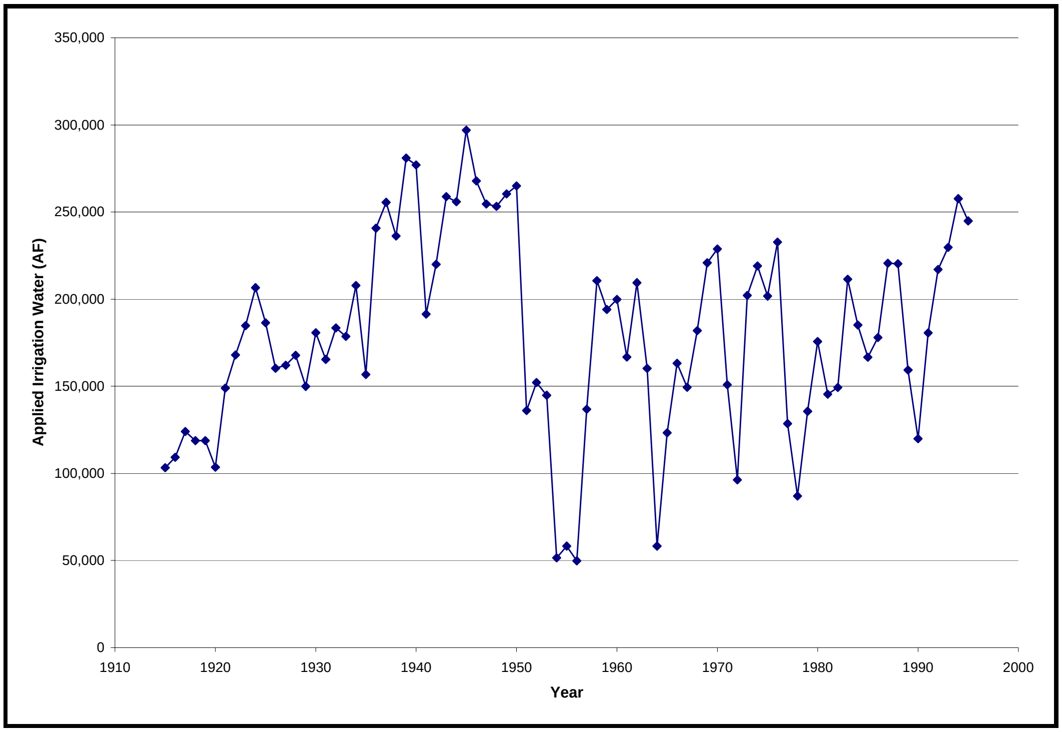

Figure 3-10. Appled Irrigation Water, 1915 to 1995
(Data from Weeden and Maddock, 1999)

3.3.1.4 Precipitation/Mountain Front Recharge

Wilson et al. (1981) reported that recharge by infiltration from precipitation on the valley floor is negligible. However, because mountain fronts typically intersect aquifer material in such a way as to pinch the material out toward the surface, mountain fronts typically act as good conduits for precipitation recharge to aquifer systems. Mountain front recharge is dependent on the area of drainage, the slope of the basin, and the amount of precipitation. It is difficult to quantify the amount of this type of recharge over the basin and estimates of this type of recharge will have significant uncertainty. However, estimates of this recharge are relatively small when compared to other sources. Peterson et al. (1984) estimated mountain front recharge to be approximately 40 ft^3/s. Frenzel and Kaehler (1990) estimate the steady-state recharge of the Mesilla Basin to be approximately 18 ft^3/s. Frenzel (1992) estimated mountain front recharge at 15 ft^3/s.

Weeden and Maddock (1999) represent a small amount of mountain front recharge at the base of the Potrillo Mountains. Based on personal communications with Sperka (2000), this recharge may not occur. Sperka indicated that well sample data from this area does not indicate the presence of a fresh water source. The Cañutillo area includes slope and mountain front recharge at the same rate as the Weedon and Maddock model. Because the western most boundary of the Mesilla Bolson is not represented in the Cañutillo model, recharge in this area is not included.

3.3.1.5 Subsurface Flow

As stated above there is some connection between the Mesilla Basin and surrounding basins. Wilson et al. (1981) estimates that very little water enters the Mesilla Basin from Selden Canyon. According to King et al. (1971), no water from the Jornada del Muerto Basin enters the Mesilla Basin.

3.3.2 Outflows

A very small amount of water is estimated to flow out of the basin at its boundaries. Overall, basin surface water losses dramatically overshadow estimates of groundwater losses due to basin underflow. Drain flow represents significant aquifer loss, but drain flow generally originates as applied irrigation water, therefore resulting in little effective loss. In dry years, pumping for irrigation reduces the groundwater table. As the water table drops, the drains intercept less water.

3.3.2.1 Drain Flows

Wilson et al. (1981) reported 1974 drain flow that averaged about 153 ft^3/s. CH2M HILL (2000a) calculated the 10-year average drain flows 1986 through 1995 for select drains that typically make up more than 80 percent of total flow at 197 ft^3/s. Weeden and Maddock (1999) reported drain flows on an annual basis from 1925 through 1996 that averaged 186 ft^3/s. Figure 3-11 shows the combined drain flows for Selden, Picacho, East, Del Rio, La Mesa, and Montoya drains. The Cañutillo area includes the East, Del Rio, La Mesa and

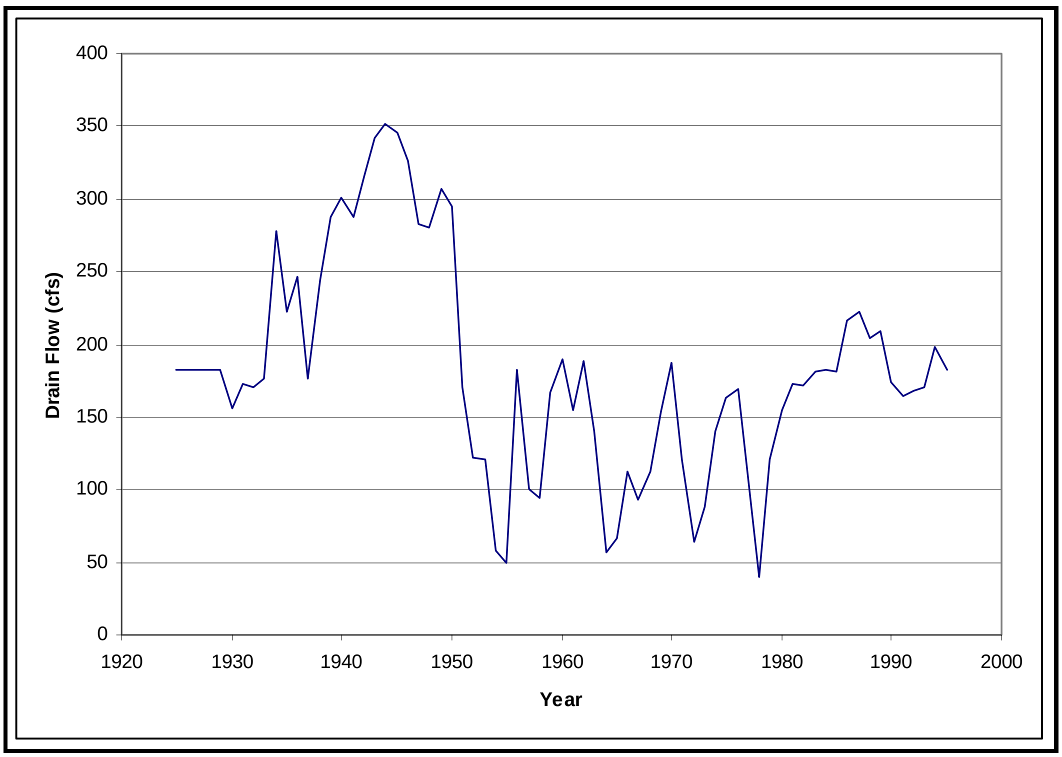

Figure 3-11. Primary Combined Drain Flow, 1915 to 1995
(Data from Weeden and Maddock, 1999)

Montoya Drains. Because these drains make up most of the drain return flow in the Mesilla, the average drain flow in the Cañutillo area is roughly the same as the Mesilla Bolson for the 1925 to 1995 period.

3.3.2.2 Pumping

Wilson et al. (1981) reported 1975 total groundwater pumping for the Mesilla and Rincon Valleys as approximately 180 ft^3/s. Approximately 70 percent of this withdrawal were for irrigated agriculture. Frenzel and Kaehler (1990) used U.S. Census data to estimate overall nonagricultural pumping at 122 gallons per capita per day (gpcd) over time. With population data, this value results in a total nonirrigation pumping withdrawal of about 60 ft^3/s for 1995 (Weeden and Maddock, 1999). However, Weeden and Maddock (1999) also reported that possibly twice this amount of nonirrigation withdrawal might occur. Figure 3-12 presents Frenzel's (1992) estimate of nonirrigation withdrawal. About half of the 60 ft^3/s occurs in the Cañutillo area.

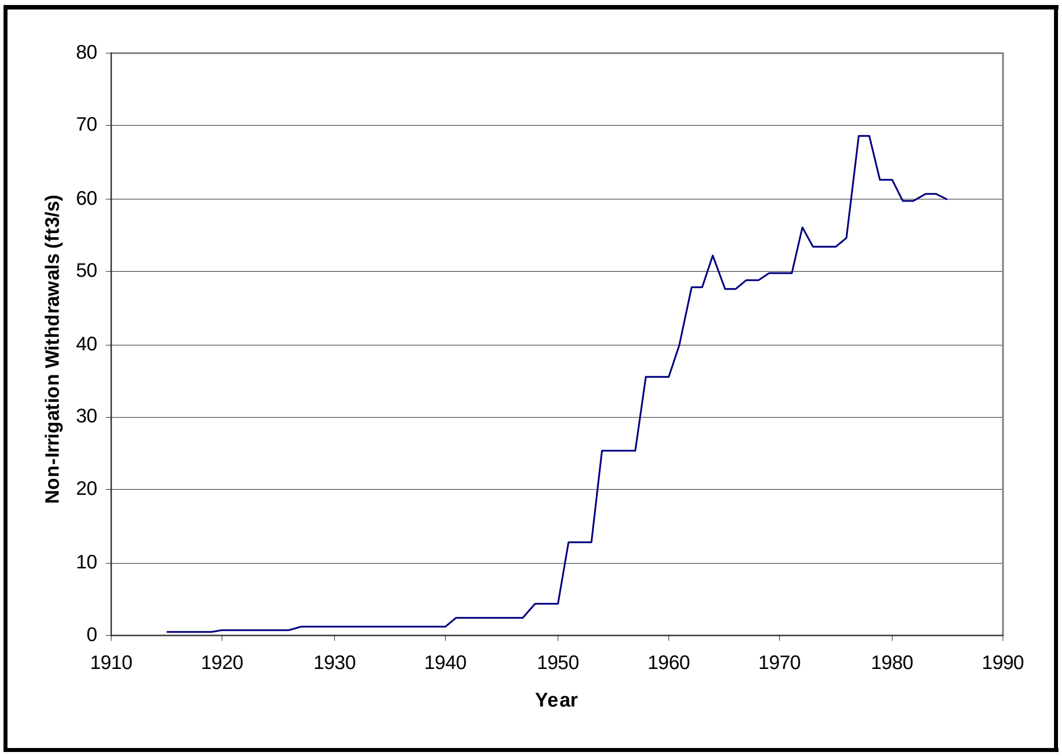

Figure 3-12. Nonirrigation Withdrawal
(Data from Frenzel, 1992)

3.3.2.3 Subsurface Flow

Hamilton and Maddock (1993) estimated that a small amount of water flows from the Mesilla Bolson to the Hueco Bolson at Fillmore Pass, and that water may exit along the southwestern border into the Mimbres Basin. Weeden and Maddock represented some exchange between the Mesilla and Hueco Bolson. A similar quantity of leakage is simulated in the Cañutillo area.

3.3.2.4 Evapotranspiration

The bulk of Mesilla Basin evapotranspiration takes place near the Rio Grande in irrigated areas where the water table is relatively close to the ground surface. Evapotranspiration consumes a significant amount of applied irrigation water. Peterson et al. (1984) estimates evapotranspiration for agriculture at 1.85 to 2.2 acre-feet (ac-ft) per acre based on crops typically grown in the Mesilla Valley. Peterson estimated the total irrigated acreage at 70,000 acres. Peterson et al. (1984) also reported that Richardson (1972) estimated an additional 22, 500 acre-feet per year (ac-ft/yr) of evapotranspiration due to phreatophytes along the Rio Grande. Figure 3-13 shows net annual irrigation evapotranspiration for the Mesilla Valley as calculated by Frenzel (1992). Of these 70,000 acres, approximately half lie within the Cañutillo area. Because a bulk evapotranspiration rate was used for the model area, it was assumed that evapotranspiration in the Cañutillo area is half that of the Mesilla basin.

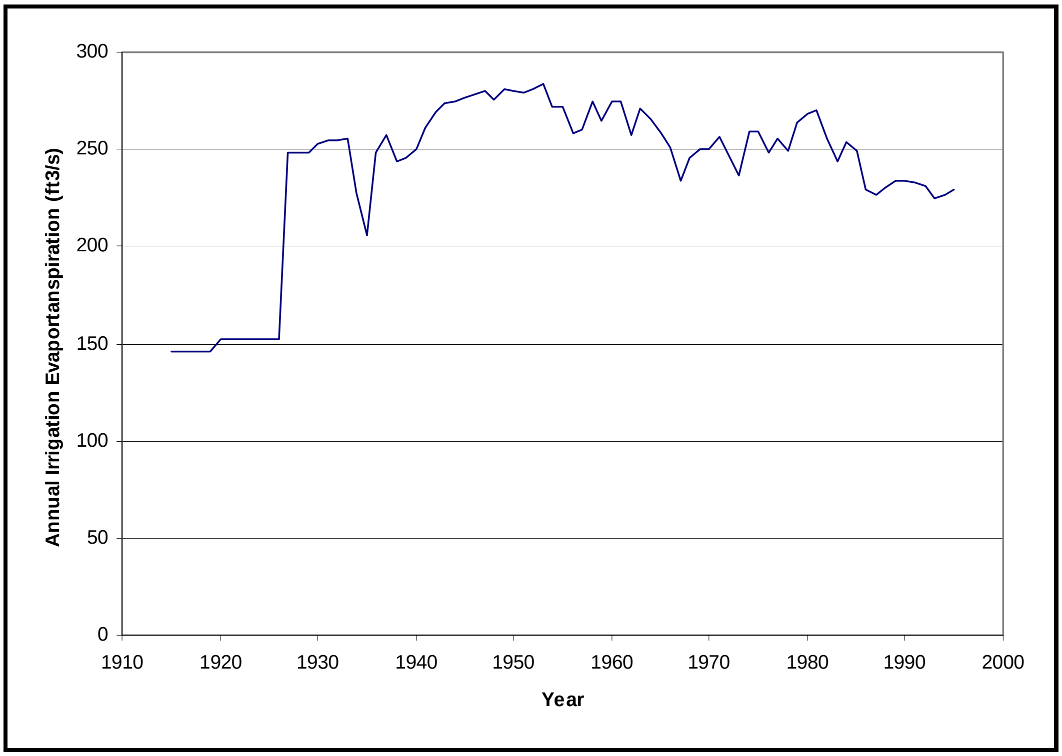

Figure 3-13. Net Annual Evapotranspiration of Agricultural Irrigation
(Data from Weeden and Maddock, 1999)

3.4 Water Quality

Water quality varies significantly within the Mesilla Bolson. The quality of excess irrigation water and the quality of river and canal seepage water affects groundwater quality. River and canal seepage are freshwater inflows into the shallow alluvium, while excess irrigation water typically is of lower quality. As such, the shallow alluvium usually has lower TDS concentrations near the Rio Grande. TDS concentrations typically increase proportionally moving away from the river. Rio Grande quality typically deteriorates moving downstream due to drain returns. Groundwater in the shallow alluvium is often higher in TDS than deeper groundwater. TDS concentrations generally decrease with depth until a zone of water containing TDS less than 500 milligrams per liter (mg/L) is reached. Below this zone the TDS concentration increases (Wilson and White, 1984). The thickness of fresh water varies significantly over the Mesilla Basin. The zone of slightly saline water in the shallow alluvium increases in thickness moving away from the Rio Grande. The thickness of the freshwater zone ranges from 400 feet under the northwest mesa area to 2,400 feet near Mesilla Dam. Freshwater thickness generally decreases moving from north to south and moving away from the Rio Grande (Wilson et al., 1981). Water quality degradation in some EPWU wells has been noted over time. The mechanism for this degradation appears to be capture of lower quality water from upper layers where salts are concentrated through the irrigation process.

In general, water quality data have primarily been collected in areas of anthropogenic activity. Therefore, very little data are available on the eastern and western areas of the model. Significant amounts of data have been collected in the Cañutillo area. Water quality data are regularly collected by both EPWU and the USGS. However, in part due to the model-layering scheme and in part due to spatial and temporal data gaps, some level of generalization and synthesis of data are required to represent the Cañutillo area in three dimensions. As such, data collected over several years from various locations was used to produce "average" water quality profiles for "historical" and "present" conditions. Wilson et al. (1981) compiled all available water quality data, conducted an extensive electroresistivity survey, and plotted water quality cross-sections for the Mesilla Bolson that cover portions of the Cañutillo area. These cross-sections were used in this study to fill in some data gaps with respect to initial model water quality.

3.4.1 Surface Water Quality

3.4.1.1 Rio Grande

Water quality in the Rio Grande is somewhat variable from year to year and deteriorates considerably from Caballo Dam to El Paso. Data in Wilson and White (1983) for the period from 1943 to 1980 show a variation in Rio Grande TDS concentration at El Paso ranging from 862 mg/L to 1,905 mg/L. The lowest concentration occurs with the greatest river flow. Likewise, the greatest concentration occurs with the smallest river flow. Concentrations of TDS tend to increase in low flow years because there is less water in the Rio Grande to dilute irrigation returns from drain flows. TDS concentrations in groundwater also tend to increase in low flow years because less fresh water is available to flush salts. Nickerson (1995) presented Rio Grande analyses conducted during seepage investigations that indicate deteriorating water quality from north to south in the basin. Table 3-1 presents average TDS, chloride, sodium, sulfate, and Sodium Absorption Ratio (SAR) values for various gages. Figure 3-14 presents the flow and TDS concentrations in the Rio Grande over time at Mesilla and El Paso. This figure shows that TDS concentration increases downstream and that TDS concentration is lower in high flow years and higher in low flow years.

TABLE 3-1
Rio Grande Average Concentrations of Selected Constituents and Water Quality Parameters

Location	Time Period	TDS (mg/L)	Chloride (mg/L)	Sodium (mg/L)	Sulfate (mg/L)	SAR [a]
USGS Gage at San Marcial 08358400	Primary Irrigation Season	420	33	60	144	2.0
	Secondary Irrigation Season	409	38	60	117	1.9
	Annual Average	416	34	60	136	1.9
USGS Gage Below Elephant Butte Dam 08361000	Primary Irrigation Season	335	24	45	98	1.4
	Secondary Irrigation Season	309	23	42	93	1.2
	Annual Average	329	24	45	97	1.4
USGS Gage at El Paso 08364000	Primary Irrigation Season	716	117	145	244	3.3
	Secondary Irrigation Season	1,349	263	319	490	6.8
	Annual Average	933	165	202	325	4.5
USGS Gage at Fort Quitman 08370500	Primary Irrigation Season	3,559	1,261	873	903	12
	Secondary Irrigation Season	2,982	1,028	749	795	11
	Annual Average	3,357	1,180	830	866	12

[a] Sodium Adsorption Ratio calculated based on TDS values.

Source: USGS, 1996.

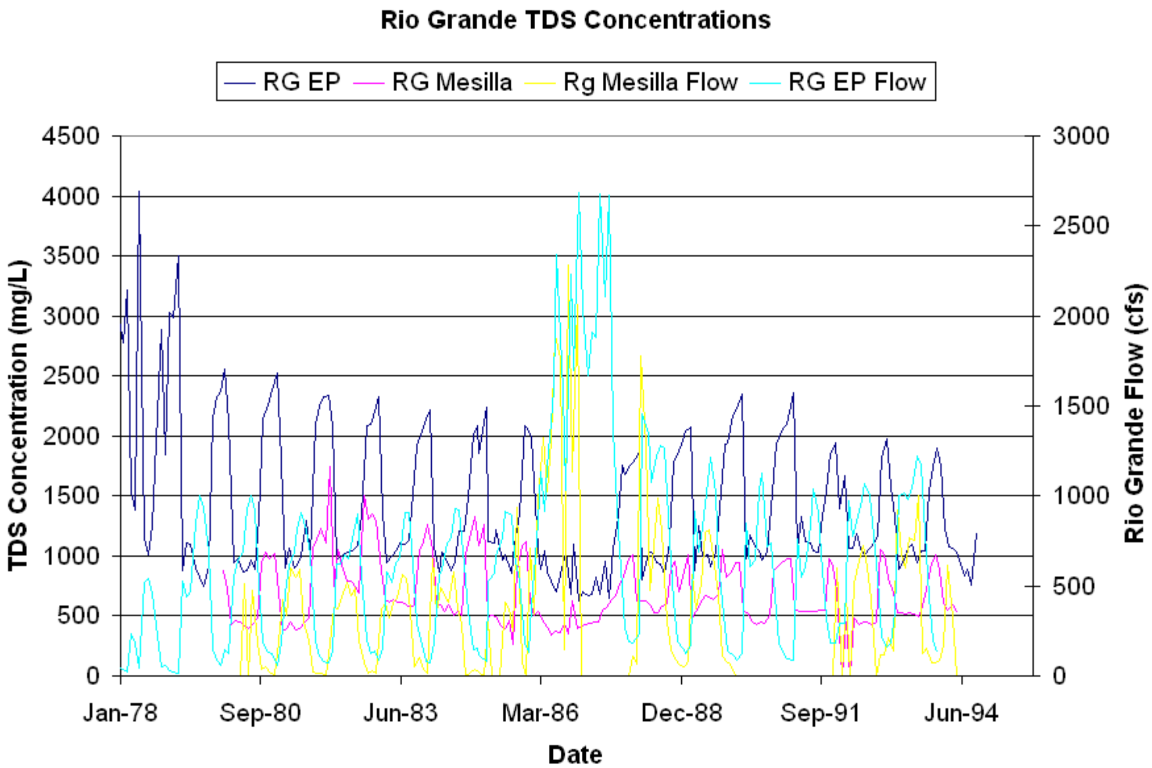

Figure 3-14. Flow and TDS Concentration With Distance Along the Rio Grande Over Time

3.4.1.2 Canals, Laterals, and Ditches

Canal flows are supplied by water diverted from the Rio Grande; therefore, canal water quality reflects that of the Rio Grande at the diversion. Water quality in the canals will likely tend to decrease moving downstream due to lower quality agricultural runoff.

3.4.1.3 Drains

Drains intercept excess irrigation water seepage and keep the water table below the root zone on agricultural lands. The primary purpose of drains is to remove salts from the subsurface so that detrimental buildups do not occur. As such, TDS concentrations in drains are generally higher than those in canals or in the Rio Grande. Drain returns to the Rio Grande drive the increase in TDS from north to south in the basin. Table 3-2 presents average TDS concentrations in select drains.

TABLE 3-2
Drain Average TDS Concentration

Drain	Primary Irrigation Season (mg/L)	Secondary Irrigation Season (mg/L)	Annual Average (mg/L)
Del Rio	1060	1150	1105
La Mesa	1220	2900	2060
East	1580	1450	1515
Montoya	1340	1780	1560

Source. CH2M HILL, 2000a

3.4.2 Groundwater Quality

Groundwater quality generally deteriorates and the thickness of the freshwater zone tends to decrease moving away from the river. There are relatively large amounts of TDS and other concentration data at discrete depth intervals in the Cañutillo area. However, there are little groundwater quality data in the western portion of the Mesilla Basin.

Wilson et al. (1981) presents most early data in cross-sections. Wilson compiled all available water quality data, conducted an extensive electroresistivity survey, and plotted water quality cross-sections for the Mesilla Bolson that cover portions of the Cañutillo area. These cross-sections were used in this study to fill in some data gaps with respect to initial model water quality. These data provide the best known historical starting point for constructing TDS profiles. Water quality degradation has been noted in some EPWU wells. It appears that this degradation is the result of lower quality water from the upper zones migrating into pumping wells. However, this process is not ubiquitous and therefore cannot be inferred with certainty.

Data compiled for this study from the WRRI, the USGS, and EPWU provide information on recent conditions. From each of these data sets, plots were constructed that represent the TDS concentration in three-dimensional space. Figure 3-15 presents wells with at least one water quality measurement. This compiled data will be used with data interpretations from Wilson et al. (1981) to produce a transport model starting point. However, in part due to the model layering scheme and in part due to spatial and temporal data gaps, some level of generalization and synthesis of data is required to represent water quality in the Cañutillo area in three dimensions. As such, data collected over several years from various locations was used to produce "average" water quality profiles for "historical" and "present" conditions. In general, in areas where significant time series data are available, care was taken to represent historical or present conditions accurately. In particular, in wells where marked changes in groundwater quality occur over the time period of interest, data were used for the starting year and ending year (1970 and 1995) rather than averaging the water quality changes. The generalizations in water quality representation will increase uncertainty associated with simulation results. Individual wells will serve as targets in solute transport modeling.

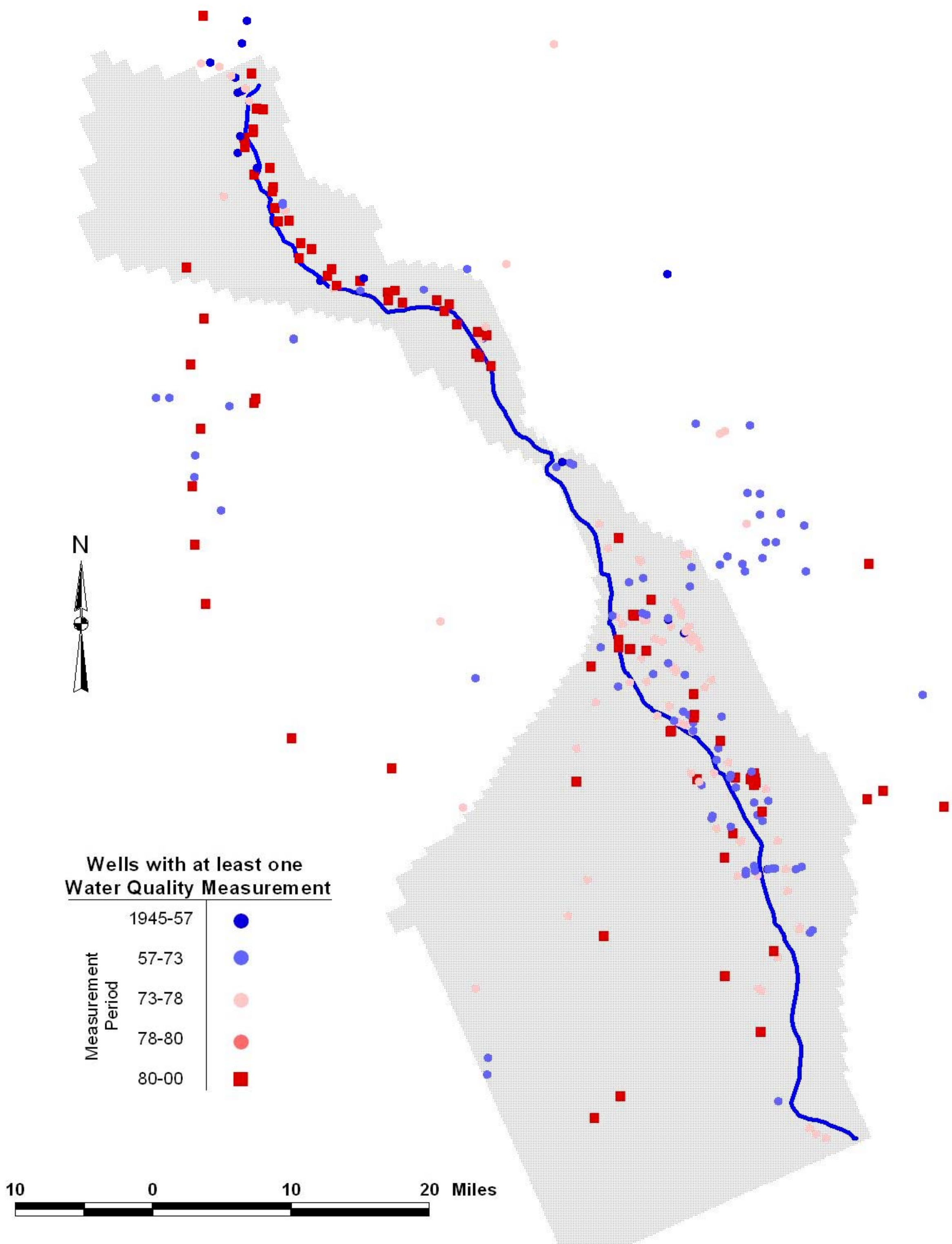

Figure 3-15. Locations of Wells With Water Quality Data

4. Flow Model Development

4. Flow Model Development

4.1 Introduction

This section briefly describes the process and results of development of a localized flow model for the Cañutillo wellfield. This model was developed directly from Weeden and Maddock (1999), and as such relies heavily on the data and assumptions used to create the regional model. This model was developed to provide additional refinement in the Cañutillo wellfield area. This additional refinement is required to produce a viable solute transport model. The combined flow and transport models will be used to aid in long-term planning and decision making with respect to EPWU's groundwater resources on the West Side. The following subsections are generally organized in order that they were completed beginning with the installation of Weeden and Maddock (1999) and ending with a description of the Cañutillo model.

4.2 Maddock Model Installation

The Weeden and Maddock model (1999) of the Rincon and Mesilla basins was installed and tested to ensure all files transferred properly and that MODFLOW simulation results are the same as those reported. The Weeden and Maddock model files were downloaded from the University of Arizona (UA) File Transfer Protocol (FTP) site through anonymous FTP. Simulations were completed with the provided compiled version of MODFLOW and with the updated MODFLOW-96 program. In both cases volumetric budgets, contours of head, and output file contents were compared with those provided on the UA FTP site. There were no discernable differences in the output as calculated by Weeden and Maddock and that calculated on local machines with either version of MODFLOW. To facilitate batch file processing and incorporate updates to MODFLOW, the MODFLOW-96 version was used exclusively during development of the Cañutillo model.

4.3 Regional Analysis of Maddock Model Assumptions and Limitations

As with any groundwater model there are data gaps and limitations that require extrapolation and assumptions. This subsection briefly examines some of the more important parameters and discusses some of the assumptions and limitations for these parameters.

4.3.1 Horizontal Hydraulic Conductivity

Values of horizontal hydraulic conductivity in the Maddock model correspond well with values obtained over time through aquifer testing and with specific capacity measurements used as a surrogate for hydraulic conductivity. While the model does not necessarily capture individual conductivity measurements, the model values appear to represent the regional conductivity well. However, for the area covered, there are relatively few overall measurements and very few measurements that target specific hydrogeologic units. Therefore, there are many areas where specific hydraulic conductivity measurements do not exist.

4.3.2 Streamflow

The Rio Grande and its complex network of canals and drains are extremely important in the simulation of long-term aquifer conditions. Flows in and out of this system largely determine water levels in the upper aquifer. In addition, because this system is so complicated and arguably self-compensating (increased river/canal losses are generally associated with increased drain flows, etc.), it is difficult to know precisely where gains and losses occur. Short-term studies by Nickerson (1989) have attempted to better quantify gains and losses.

Hamilton and Maddock (1993) and Weeden and Maddock (1999) attempted to address this complicated network through use of a modified version of the Prudic streamflow package for MODFLOW. This package calculates streamflow based on known inflows, known diversions (including diversions from individual segments for application to crops), and aquifer interaction.

4.3.2.1 Streambed Elevations

Maddock estimated streambed elevations by linearly interpolating between points selected from USGS 7.5-minute topographic maps. These values were then altered by subtracting elevation for drains and increasing elevation for canals until simulated flows matched gaged flows. While this method produces the correct flows, it is difficult to determine if the streambeds are in fact at the correct elevation and therefore interact with the aquifer correctly. It is recognized that streambed elevations are not constant and that elevations have changed somewhat over time with agradation and degradation as well as dredging.

4.3.2.2 Vertical Hydraulic Conductivity

Vertical hydraulic conductivity of streambeds is difficult to measure and can vary significantly over small distances (Calver, 2001). Estimates of loss rates between gages coupled with estimates of evapotranspiration are used to provide large-scale estimates of streambed vertical hydraulic conductivity. However, such work completed to date has been carried out over relatively short time periods, generally in the nonirrigation season.

Conductivities at any given point can vary seasonally depending on whether that reach is gaining or losing. Losing streams tend to deposit sediments in the riverbed pore space resulting in a reduction in conductivity over time. With the addition of more detailed streambed elevation data, additional flow measurements for accurate volumetric balances, and/or shallow piezometers that measure local gradients at drains and canals, numerical simulation could more accurately estimate vertical hydraulic conductivity and thus more reliably represent aquifer stream interaction.

4.3.3 Evapotranspiration

Weeden and Maddock used the MODFLOW evapotranspiration package (ET) to estimate only ET from nonirrigated lands. ET from irrigated lands was incorporated into a calculation of "Net Irrigation Flux" (NIF) that was applied in the MODFLOW recharge package. For both ET on nonirrigated lands and NIF, the rates were applied over the Mesilla valley where irrigation typically occurs with factors applied to reflect the portion of irrigated or nonirrigated land. Based on vegetative cover and anthropogenic activity, little ET would be expected outside of the Mesilla Valley.

Weeden and Maddock (1999) used seasonal evapotranspiration rates on non-irrigated land of 4.7 feet and 0.57 feet for the primary and secondary irrigation seasons, respectively. The total rate adds to 5.27 feet per year, which is close to the 5.5 feet per year used in previous versions of the model. Weeden and Maddock stated that "...secondary irrigation season rate is 12% of the primary irrigation season rate, and is based on pan evaporation data from Wilson et. al. (1981)". Potential evapotranspiration data was also presented in Wilson et al. (1981). This data indicates that the secondary season rate was about 8 percent of the primary season rate and that the overall annual rate should be about 4.2 feet. All of these data were based on average data presented in a report by Lesperance (1977). Pan evaporation data and potential evapotranspiration data are available or can be calculated from historic data on a seasonal or an annual basis.

Weedon and Maddock (1999) used an average evapotranspiration rate of approximately 2.4 feet per year on irrigated land based on Frenzel (1992). Frenzel calculated evapotranspiration rate based on annual reported crop mix in the Mesilla Valley. The Weedon and Maddock evapotranspiration rate was used in the calculation of NIF as described in the following section.

4.3.4 Agricultural Pumping

It is assumed by Weeden and Maddock (1999) that the full evapotranspiration demand of irrigated areas as calculated by the Blaney and Hanson method (1965) is met each year. Agricultural pumping is the portion of ET demand that is not met through surface water sources. Agricultural pumping corresponds to a negative NIF, whereas a positive NIF represents recharge to the aquifer. NIF is calculated seasonally by estimating the ET demand and then subtracting precipitation and the amount of surface water delivered to valley farms for irrigation. These rates are applied over the entire Mesilla valley after being proportioned to reflect the amount of irrigated land.

There are two primary concerns with this particular technique as follows:

1. The researchers included precipitation for the entire valley rather than only precipitation on irrigated lands. Because the amount of this precipitation that offsets agricultural ET is low, it is unlikely that it significantly affects the overall water balance. However, the inclusion of this rainfall implies that NIF will be overstated in wet years and under-represented during drought.

2. In years of severe drought, crop demand in excess of available surface water will not always be met through increased groundwater withdrawals. Some farmers will likely not irrigate and potentially sell their surface water to other farmers. Alternatively,

reported annual crop yields could be used with diversion records to estimate the quantity of water required to produce the recorded yield. From this analysis, the volume of groundwater withdrawals required can be estimated. More study is likely required to determine a more appropriate estimation method.

As part of the NIF calculation measurements of annual diversions and of canal return flows are used with estimates of conveyance losses to determine the amount of water actually delivered to irrigators. In the Weeden and Maddock (1999) update, the calculated values of canal return flows for 1985 through 1995 did not correspond with measured values. These calculated values were altered to reflect measured data in the modified version of the Weeden and Maddock model. Weedon and Maddock implemented NIF as specified flux values in the MODFLOW recharge package. When more water was applied to irrigated areas than theoretically required, the MODFLOW recharge package injects this excess water into the model. In drought years where less water is available for irrigation, the recharge package withdraws water from the aquifer.

4.3.5 Recharge

Mountain-front and slope-front recharge were estimated by Frenzel and Kaehler (1990), Hamilton and Maddock (1993), and Weeden and Maddock (1999) based on annual precipitation, drainage area, and basin slope. Weeden and Maddock state

> "The flows calculated by this method are probably highly inaccurate. Frenzel and Kaehler (1990) estimate an error of +100% to –50% using this method. However, no better estimation method could be found. In comparison to other fluxes in the system the volume of mountain front recharge is very small and therefore, the error not considered significant."

Based on water quality data, it was determined that mountain-front recharge is not occurring along the southwestern most portion of the model. This recharge was removed from the modified version of the Weeden and Maddock model. Weedon and Maddock implemented mountain and slope front recharge as specified flux values in the MODFLOW well package (injection).

4.3.6 Municipal and Industrial Pumping

Annual municipal and industrial pumping rates were compiled by Frenzel and Kaehler (1990), Frenzel (1992), and Hamilton and Maddock (1993). Where data are available, actual measured withdrawals were used. Historic data, small users, and domestic users were largely estimated from population data. Agricultural withdrawals were not specifically represented as "pumping" in the model. As stated above, a NIF was calculated and represented as recharge (negative for pumping). Data from 1990 were repeated from 1991 to 1995 in the Weeden and Maddock update. These data were corrected to measured data for this time period for the City of El Paso in the modified version of the Weeden and Maddock model. Possible limitations include:

1. Weeden and Maddock did not attempt to update the pumping rates of users from 1991 to 1995. All pumping rates from 1990 were repeated in the 1991 to 1995 period.

2. *De minimus* users may make up a significant volume of withdrawals. It is possible that there are a relatively large number of unknown and unregulated users of water in the Mesilla Bolson.

4.3.7 Layering

Layer 1 is 200 feet thick below the 1976 water table elevation as defined by Wilson et al. (1981). Layer 2 is 400 feet thick. Layer 3 is 600 feet thick. Layer 4 varies in thickness. This layering does not correspond to the generally recognized "shallow", "intermediate", and "deep" hydrostratigraphic layers of the Santa Fe Group (Hawley and Lozinsky, 1992). As such, layer properties were derived by using a weighted average of the properties of each hydrostratigraphic unit. While this technique is generally appropriate for the level of detail of the regional model, some uncertainties are generated. For example, when determining aquifer heads in the vicinity of the Cañutillo wellfield in layer 3, what hydrostratigraphic unit does the result represent? The result likely represents an average of the aquifer heads in the hydrostratigraphic units represented. For areas where there is a significant difference in aquifer head, this layering will likely result in simulated values that are different than measured values. Figure 4-1 presents an example from Frenzel (1992) of model layering.

The model-layering scheme used by Weedon and Maddock presents significant obstacles in the simulation of contaminant transport. There are often large differences in concentrations within individual hydrostratigraphic units. In this layering system, these differences must be averaged along with concentrations from distinct hydrostratigraphic units to produce the layer concentration. Averaging will result in incorrect simulated estimates of concentrations at individual wells. Likewise, vertical barriers to migration of elevated concentrations will not be accurately represented in the numerical model. To accurately simulate groundwater flow and contaminant transport at the local scale, model layering should at a minimum represent the actual hydrostratigraphic units and ideally represent zones of large differences in concentration within individual hydrostratigraphic units.

4.4 Changes to Maddock Model

The Weeden and Maddock (1999) model was modified to be used as a base from which a localized groundwater flow and contaminant transport model could be developed. Modifications were proposed to correct known issues with the Weeden and Maddock model. Most changes to the Maddock model were generally described above and are listed as follows:

- The eastern boundary was extended toward the Franklin Mountains. Data from wells in this area indicate that the aquifer extends further to the east. The model was extended by approximately 0.5 miles in this direction.
- Recharge on the southwestern boundary was removed. Based on water quality data obtained from EPWU, it did not appear that significant freshwater recharge was occurring on the southwestern boundary.

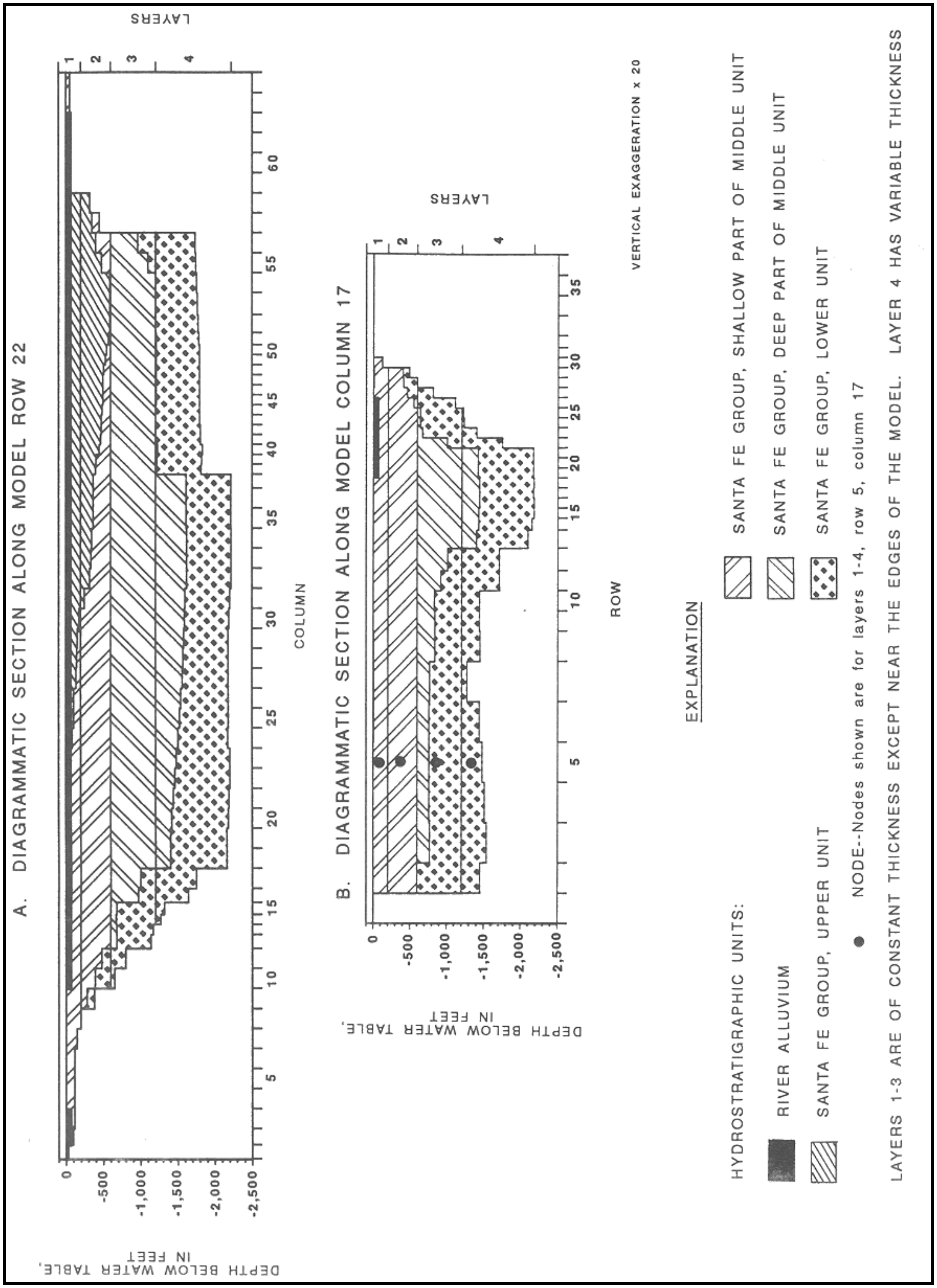

Figure 4-1. Example of Model Layering

- Pumping data was updated with EPWU records. The Weeden and Maddock (1999) update repeated EPWU pumping from 1990 over the 1991 to 1995 period. Actual EPWU pumping was input for this period. Likewise, modeled EPWU pumping from approximately 1950 to 1990 did not exactly match EPWU records. Model files were updated to more accurately reflect EPWU records.
- Canal return flows were modified to reflect measured values. Canal return flows have been measured from 1985 to present. Hamilton and Maddock and Weeden and Maddock's estimates were replaced with measured values. This update in turn resulted in the recalculation of the quantity of water delivered to farms, NIF, and agricultural diversions.

The combination of these changes resulted in relatively minor overall change in the model results — primarily a lowering in aquifer head (~2 feet) along the southwestern border where recharge was removed. Assessment of calibration including measured versus simulated flows in the streamflow system (drains, Rio Grande) and aquifer heads, were unchanged or slightly improved. Figures 4-2 and 4-3 show the modified Weeden and Maddock model. In Figure 4-2 additional model cells are shown in red. In Figure 4-3 removed recharge points are shown in red.

4.5 Cañutillo Model

The Cañutillo model was developed from a modified version of the Weeden and Maddock (1999) model to better represent local conditions in the Cañutillo wellfield and to facilitate the eventual development of a contaminant transport model. In addition to the changes noted above, the following changes were incorporated into the Cañutillo model:

- The model area was decreased from the Rincon and Mesilla valleys. The southern and eastern boundaries remained the same, the northern boundary was moved to near Mesquite, and the western boundary moved to approximately 7.4 miles to the west of the Cañutillo wellfield.
- The grid was made uniform at a spacing of approximately 200 meters.
- Additional canals, drains, and laterals were added. Because the grid spacing is much smaller than the original model, additional canals, drains, and laterals can be represented.

This model was developed using the Telescoping Mesh Refinement (TMR) procedure as provided by Groundwater Vistas, a pre- and post-processor for visualizing groundwater model data. The TMR process allows the modeler to select an area of an existing model to create a new smaller, more refined model from the existing models results. Head values at the chosen boundaries are computed in the existing model for each time step. These values then become constant head cells for each stress period in the new model.

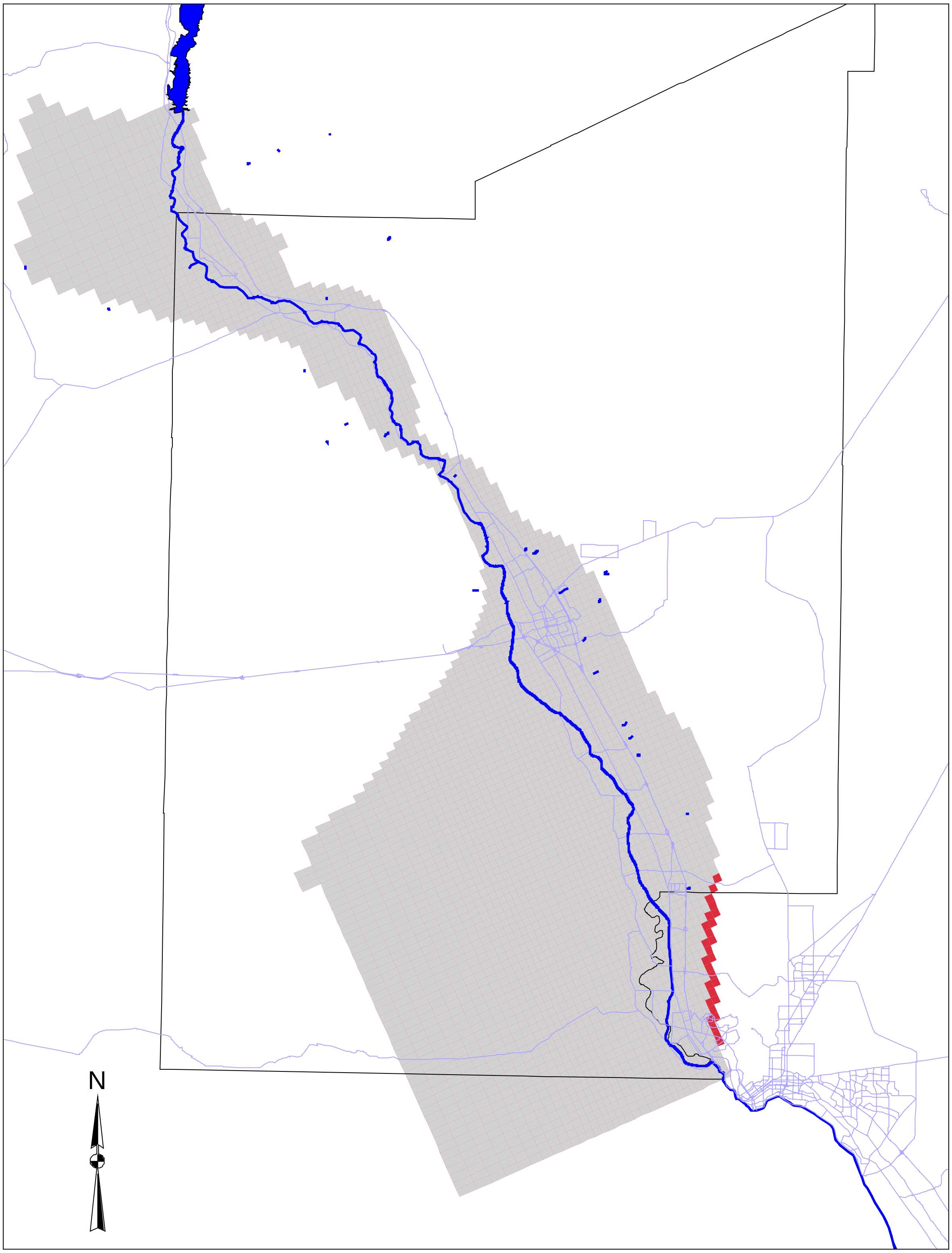

Figure 4-2. The Modified Maddock Model, Eastern Boundary

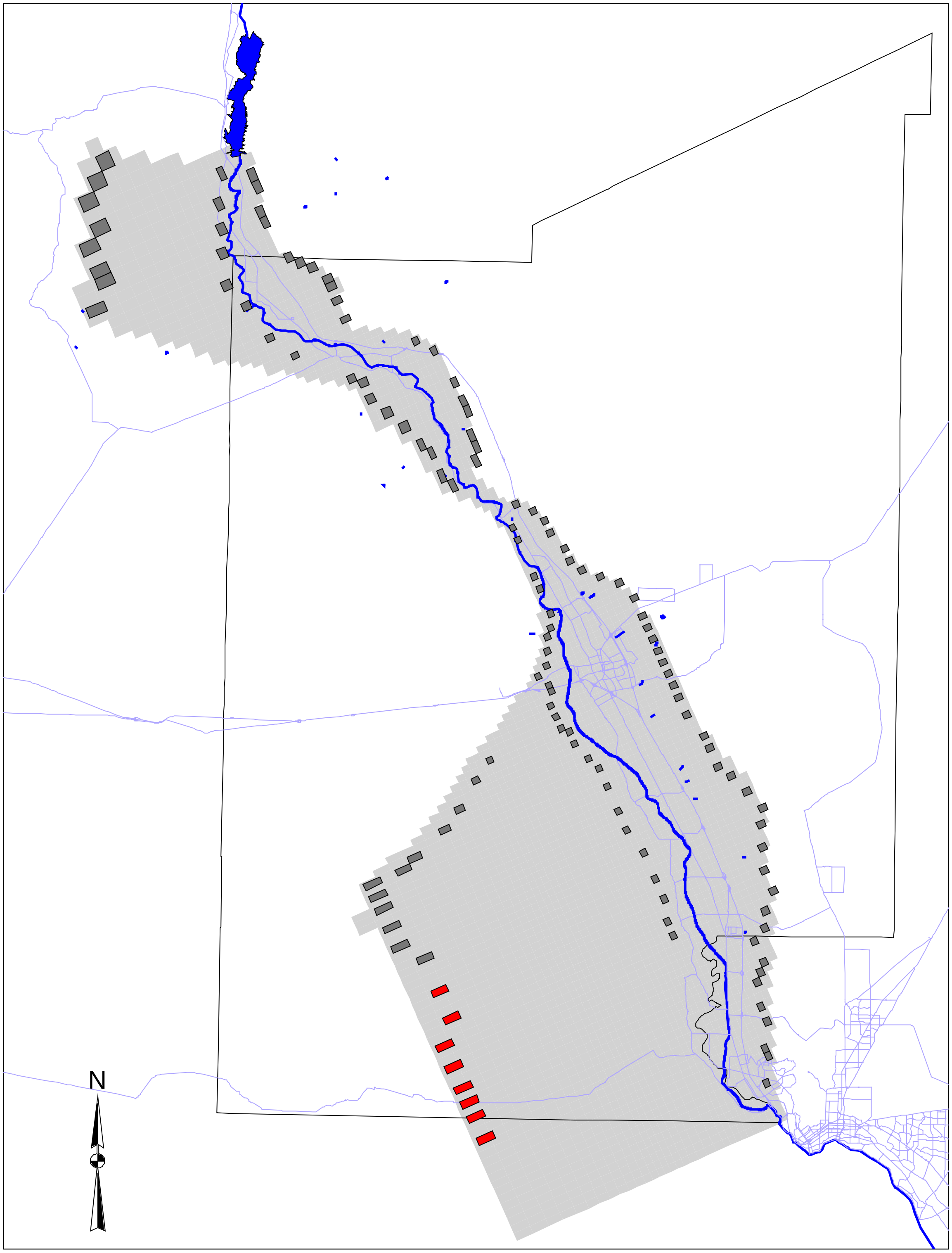

Figure 4-3. The Modified Maddock Model, Recharge

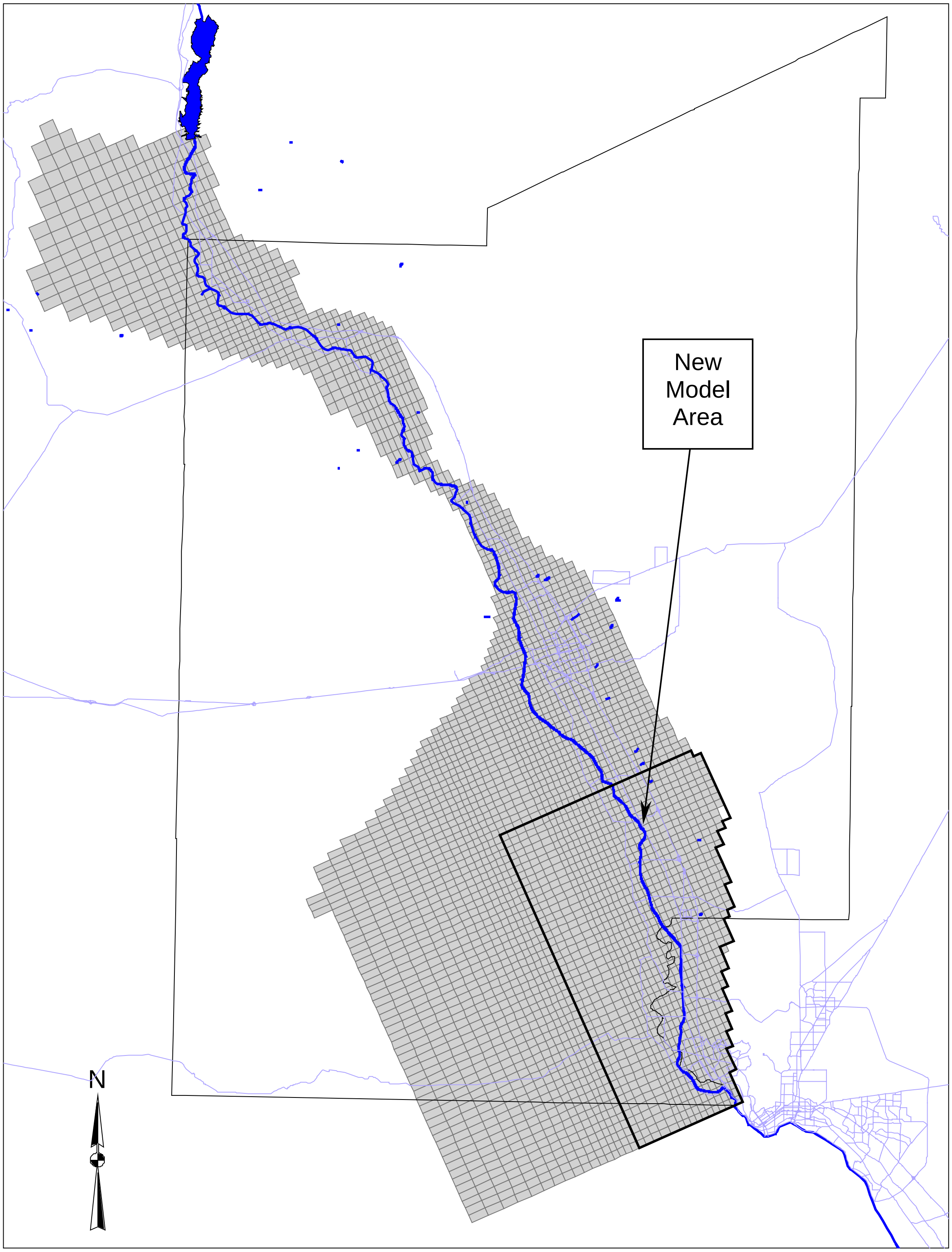

Figure 4-4. Cañutillo Model Shown as a Subset of the Modified Weeden and Maddock Model

Hydrostratigraphic data is transferred directly to the new grid (hydraulic conductivity, layer bottoms, storage, etc.). Wells are moved to the new model cell closest to the center of the original well cell. Constant head and no flow boundaries remain the same. Figure 4-4 shows the Cañutillo model as a subset of the Weeden and Maddock model. The area of the Cañutillo model is outlined with a black line.

4.5.1 Boundary Conditions

Boundary conditions for the Cañutillo model are the same as the modified Weeden and Maddock model on the east (no flow at the escarpment of the Franklin mountains) and south (no flow at a potential groundwater divide in Mexico). As stated above, the northern and western boundaries are made up of constant head cells derived from a modified Weeden and Maddock model simulation. As stresses in the modified Weeden and Maddock model change, the aquifer heads in each layer change. For each stress period, a new aquifer head value is calculated for each cell. The heads in the boundary cells of the Cañutillo model are computed for each stress period from the corresponding Weeden and Maddock model simulation. The heads in the new boundary cells are assumed to be constant over any given stress period. Figure 4-5 shows the constant head boundaries of the Cañutillo model.

4.5.2 Spatial and Temporal Descretization

As previously stated, the Cañutillo model was constructed with a uniform grid with a spacing of approximately 200 meters. In the area of the tightest grid spacing of the Weeden and Maddock model (the Cañutillo wellfield area), the Cañutillo cells are approximately 1/16th the area of the Weeden and Maddock model cells (800mx800m vs. 200mx200m). Figure 4-6 shows the Cañutillo model grid.

Because the Cañutillo model was developed as a subset of the Weedon and Maddock model, a similar temporal descritization was required in order to match Weedon and Maddock model heads at the Cañutillo model boundaries. Descritization is the process of dividing a continuous function (time, distance, etc.) into smaller pieces that can be managed numerically by a model. Typically, the smaller the divisions, the more accurate the results and the longer the processing time required.

4.5.3 River, Canal, and Drain Development

Precise representation of the Rio Grande, irrigation canals and laterals, and drains in the Weeden and Maddock model was not possible due to the relatively coarse grid size. In some cases, multiple features were represented in individual cells. The Cañutillo model was gridded to represent stream features with a more detailed coverage and additional canals, drains, and laterals were included. Most of the added features are relatively minor and the addition of these features did not significantly change model calibration or results. Added features include:

- Mesquite Drain
- Central Drain
- An unnamed drain
- San Miguel Lateral

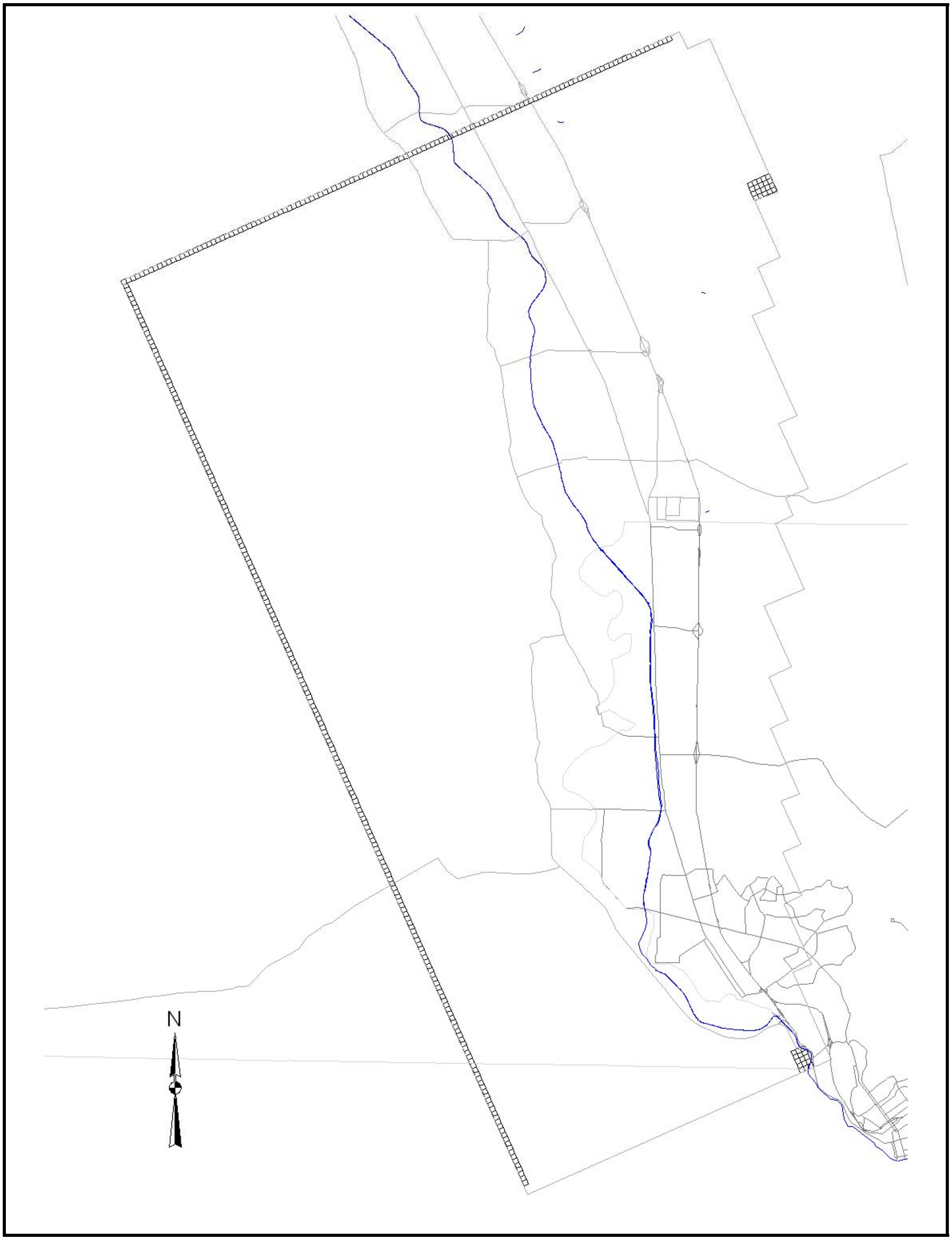

Figure 4-5. Constant Head Cells in the Cañutillo Model

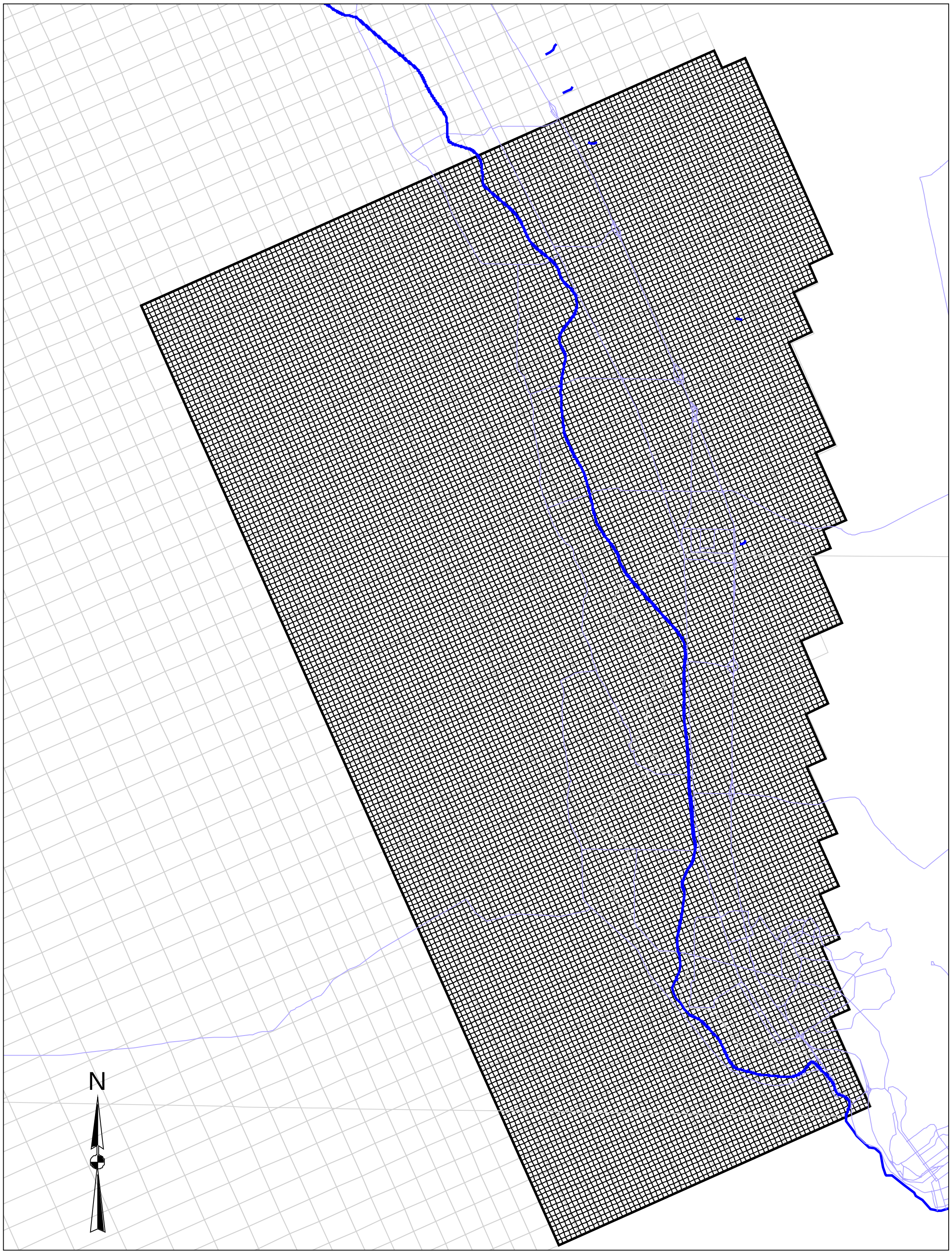

Figure 4-6. The Cañutillo Model Grid with the Weeden and Maddock Grid for Reference

- Anthony Lateral
- Cañutillo Lateral
- Vinton Drain
- Montoya Lateral
- Baker Lateral
- Little La Union Lateral
- Crawford Lateral

Figure 4-7 shows the added stream features. New drains are yellow. New canals and laterals are green.

4.5.4 Wells

Well locations and pumping rates were altered slightly from the original Weeden and Maddock model. Locations of simulated withdrawals (i.e., cell center) in the Weeden and Maddock model did not necessarily match the actual locations of EPWU production wells. The EPWU production wells were moved to their correct locations on the reference grid. Likewise, production rates in the Weeden and Maddock model did not exactly match the EPWU production records. Pumping rates were updated to reflect EPWU production records.

Mountain front recharge was represented in the Maddock model with specified flux cells (well package) spaced at regular intervals. In the TMR process, these fluxes were moved to the new model cell closest to the center of the old cell. Because there is no evidence to suggest the actual location of mountain front recharge, these modified locations were not moved back to the model boundary.

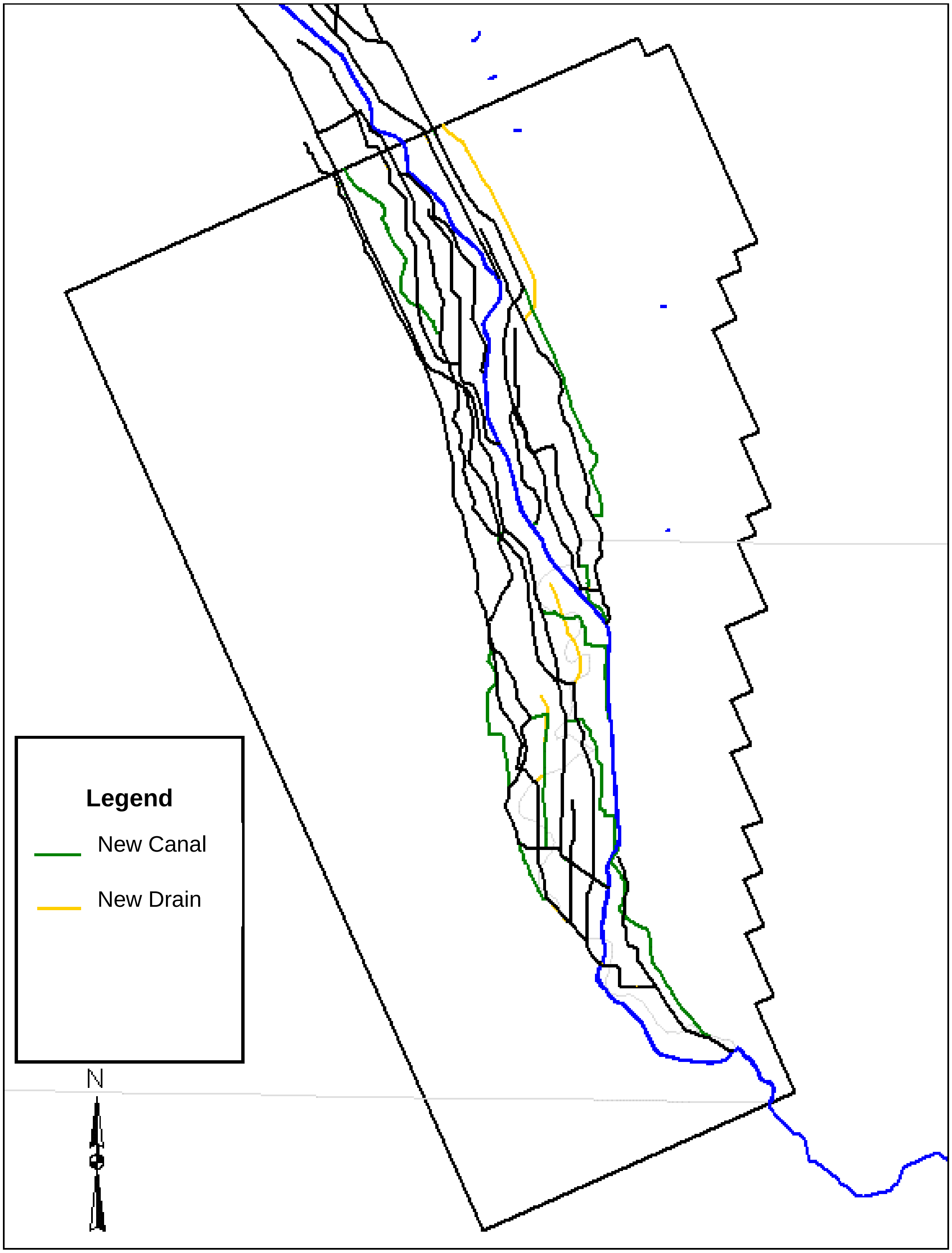

Figure 4-7. The Cañutillo Model with Additional Drain, Canal, and Lateral Features

5. Flow Model Calibration

5. Flow Model Calibration

5.1 Introduction

During development of a groundwater flow model, parameters such as hydraulic conductivity are input to the model based on available test data, knowledge of the aquifer hydrogeology, and extrapolation between known values. Because there are relatively few test values for a given parameter, large areas of a model grid are typically assigned values based on extrapolation with the best available information. With the knowledge that parameters are largely extrapolated, the process of model calibration adjusts these parameters within reasonable limits established through field testing. These adjustments are made to produce model results that more closely match values, such as aquifer heads that have been observed over time. Because many different combinations of parameters can result in the same overall model solution, a model solution is not unique. The process of model calibration attempts to find a model solution that matches observed data well and is realistic based on known data. Often the process of model development results in new insight to hydrogeologic parameters.

For the Cañutillo model, it was determined that observational data of aquifer heads, flow in the Rio Grande, canal return flows, drain flows, and Rio Grande seepage should be used to assess model results. If the model can reproduce these observed values within a reasonable tolerance, the model will be calibrated. During the process of calibration, it was noted that the canal return flow data are limited compared to other available data and that these data appeared to be incomplete. Unfortunately, without knowing how much water is returned to the Rio Grande through the canal system, it is difficult to determine how much water should be seeping to and from the Rio Grande. The net seepage may be correct, but the magnitude of inflow and outflow from the surface water system to the aquifer may not represent actual conditions. Further, inflow and outflow of the surface water system are quite sensitive to and largely driven by differences in elevation in aquifer head and that of the surface water system.

Some of the uncertainty associated with unknown parameter values can be mitigated through sensitivity analysis. During the process of sensitivity analysis, parameter values are changed and the effects on model results are noted. If minor changes in a model parameter result in large changes in model results, the model is "sensitive" to that parameter. In this way it can be determined what type of data to collect to improve the model results. If the model is sensitive to hydraulic conductivity, then aquifer testing data can be collected to reduce the number of possible conductivity values and therefore constrain the model to a smaller number of possible solutions. Likewise, if the model is insensitive to hydraulic conductivity, additional data collection may not result in any appreciable improvement in model accuracy.

The following subsections describe the calibration process and results.

5.2 Baseline Simulation

A model simulation was completed using the parameters derived from the Weeden and Maddock (1999) model in the TMR process. The results of this simulation were then used as a baseline to gage model improvement during calibration. Likewise, the baseline simulation was compared to the original results of the Weeden and Maddock model to ensure that parameters were properly assigned. Calibration targets in this model are the following items:

- Rio Grande flow at El Paso
- Rio Grande losses in the Mesilla Valley
- Drain flows
- Aquifer heads

The following two subsections briefly describe the results of the baseline run.

5.2.1 River and Drain Simulation

Observed Rio Grande flow data are available over the model period for the USGS gage at El Paso. Releases from Caballo, irrigation diversions at Mesilla, and drain flows are also known. For the overall water balance of the surface water system to be accurately simulated, the model must reproduce Rio Grande flows at El Paso while correctly simulating drain flows. As stated previously, canal return flows are not well known. Therefore, surface water system seepage, canal return flows, and surface water system losses to evapotranspiration are lumped together to produce a net gain or loss of surface water that results in the final flow at El Paso. The surface water system is also somewhat self compensating. For example, Hamilton and Maddock (1993) indicate that increases in seepage from canals will generally result in increased drain flows, which result in little overall change in Rio Grande flows. Figures 5-1 and 5-2 present the simulated and observed flows at El Paso for the primary and secondary irrigation season, respectively.

While the model cannot be constrained to specifically determine Rio Grande seepage, Nickerson has conducted a number of empirical studies (1995, 1998) of Rio Grande seepage in the secondary irrigation season that can be compared to simulated Rio Grande seepage. Weeden and Maddock (1999) stated "…studies by Nickerson determine seepage over one or two day study runs, while the model simulation calculates the average seepage over a particular season…". Therefore, Nickerson's seepage and simulated seepage should only be compared generally. Figure 5-3 presents simulated secondary season Rio Grande seepage for the 1994/1995 secondary irrigation season and observed seepage in January 1997 (observed from Weeden and Maddock, 1999). The large offset in predictions by Weedon and Maddock and the Cañutillo model is likely due to changes in the representation of the surface water system including:

- More detailed representation of surface water components with smaller cell size.
- Inclusion of more surface water components.
- Changes in bottom elevations and vertical hydraulic conductivities as a result of changed cell sizes.

Figure 5-4 shows the variation in observed seepage as presented by Nickerson (1998).

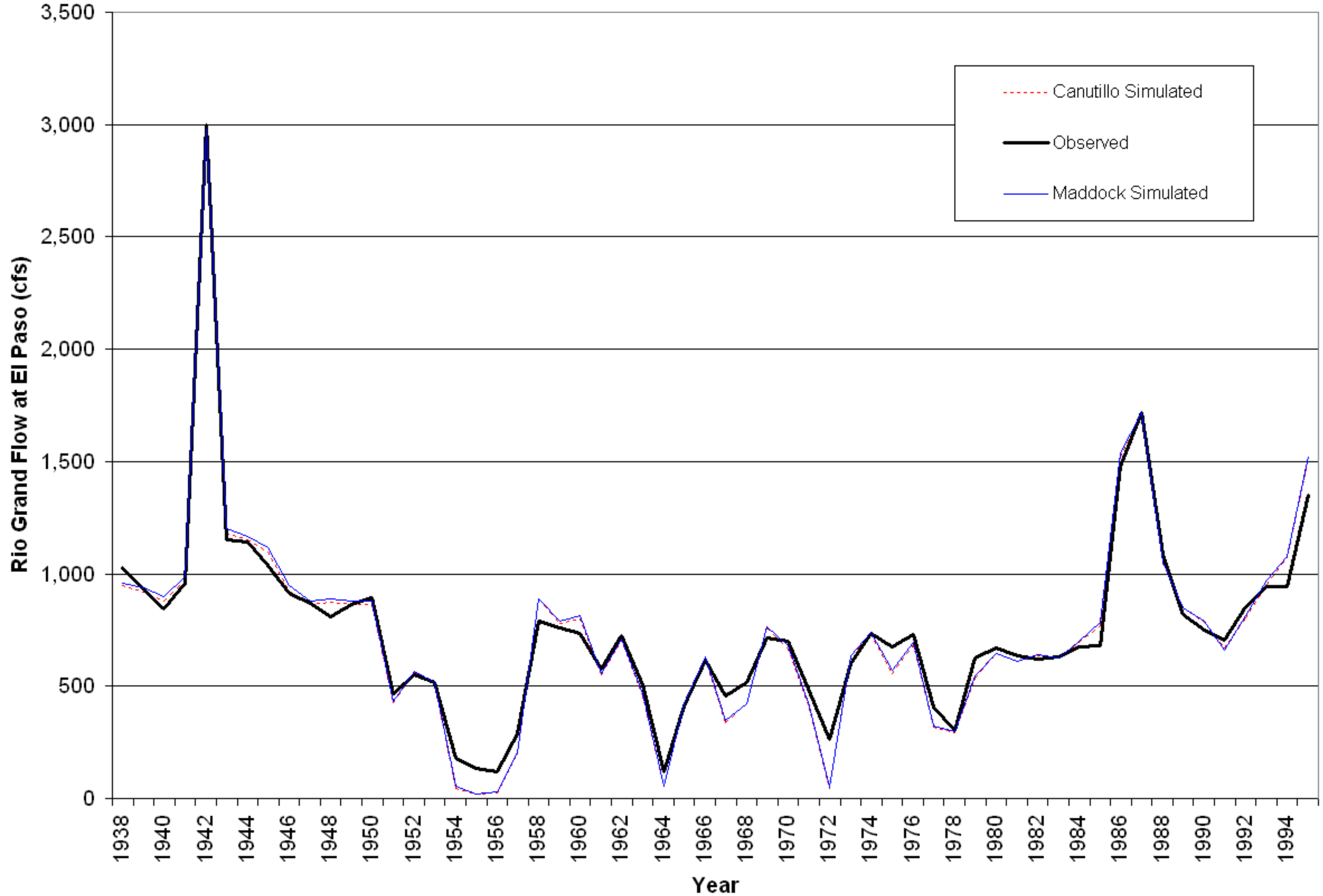

Figure 5-1. Simulated and Observed Flow at El Paso, Primary Irrigation Season

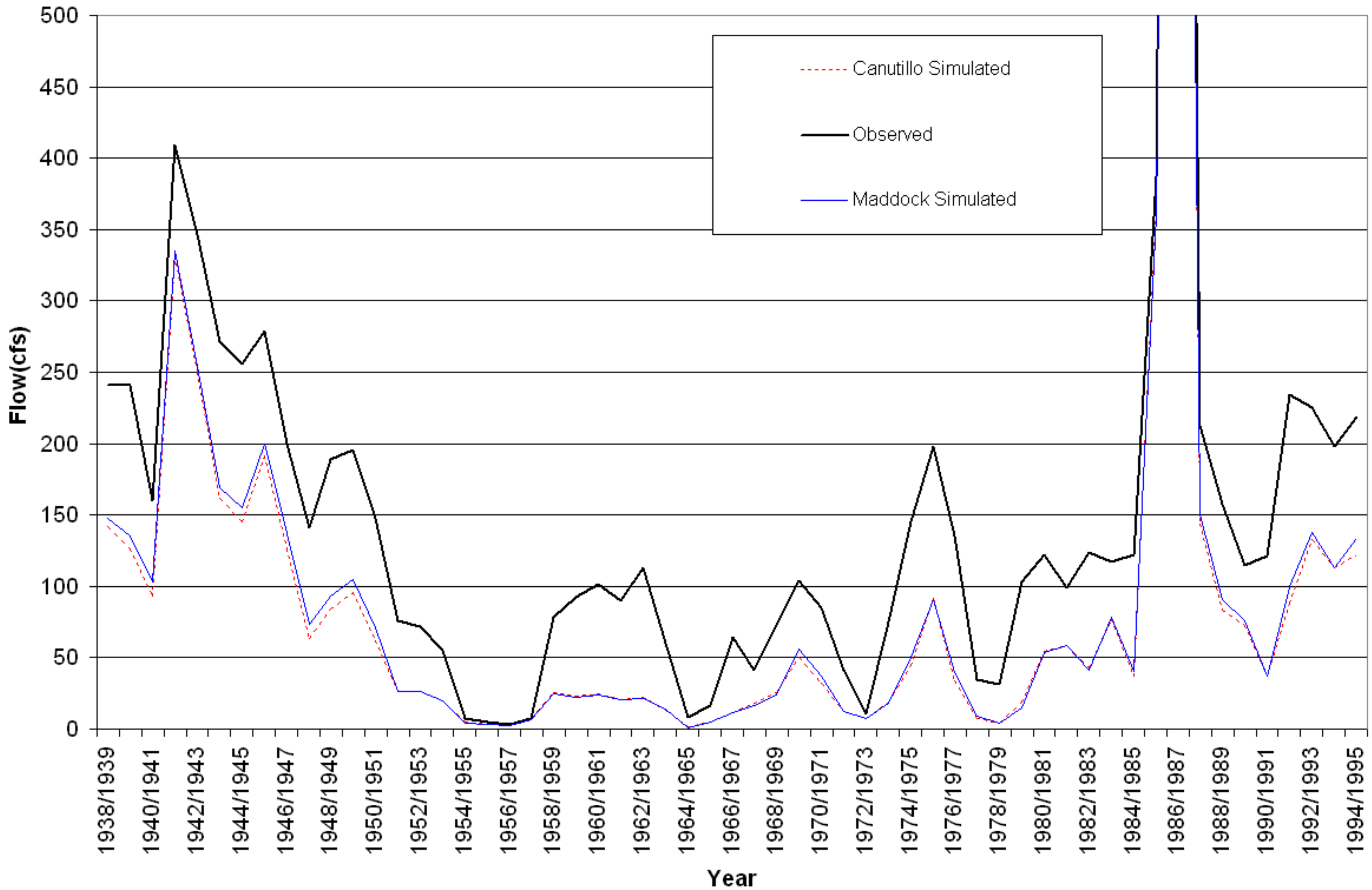

Figure 5-2. Simulated and Observed Flow at El Paso, Secondary Irrigation Season

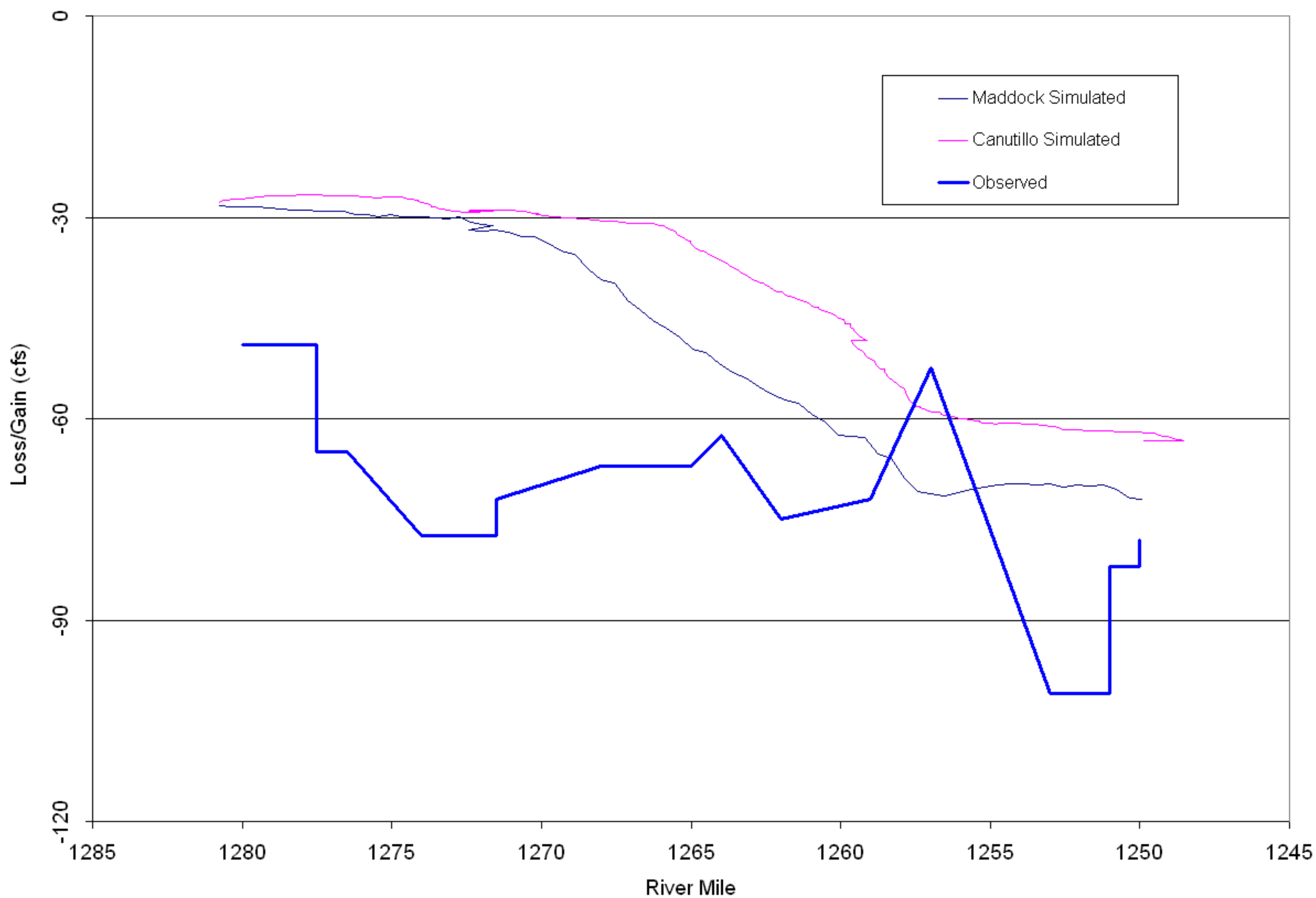

Figure 5-3. Rio Grande Seepage in the Lower Mesilla Valley 1994/1995 Secondary Irrigation Season

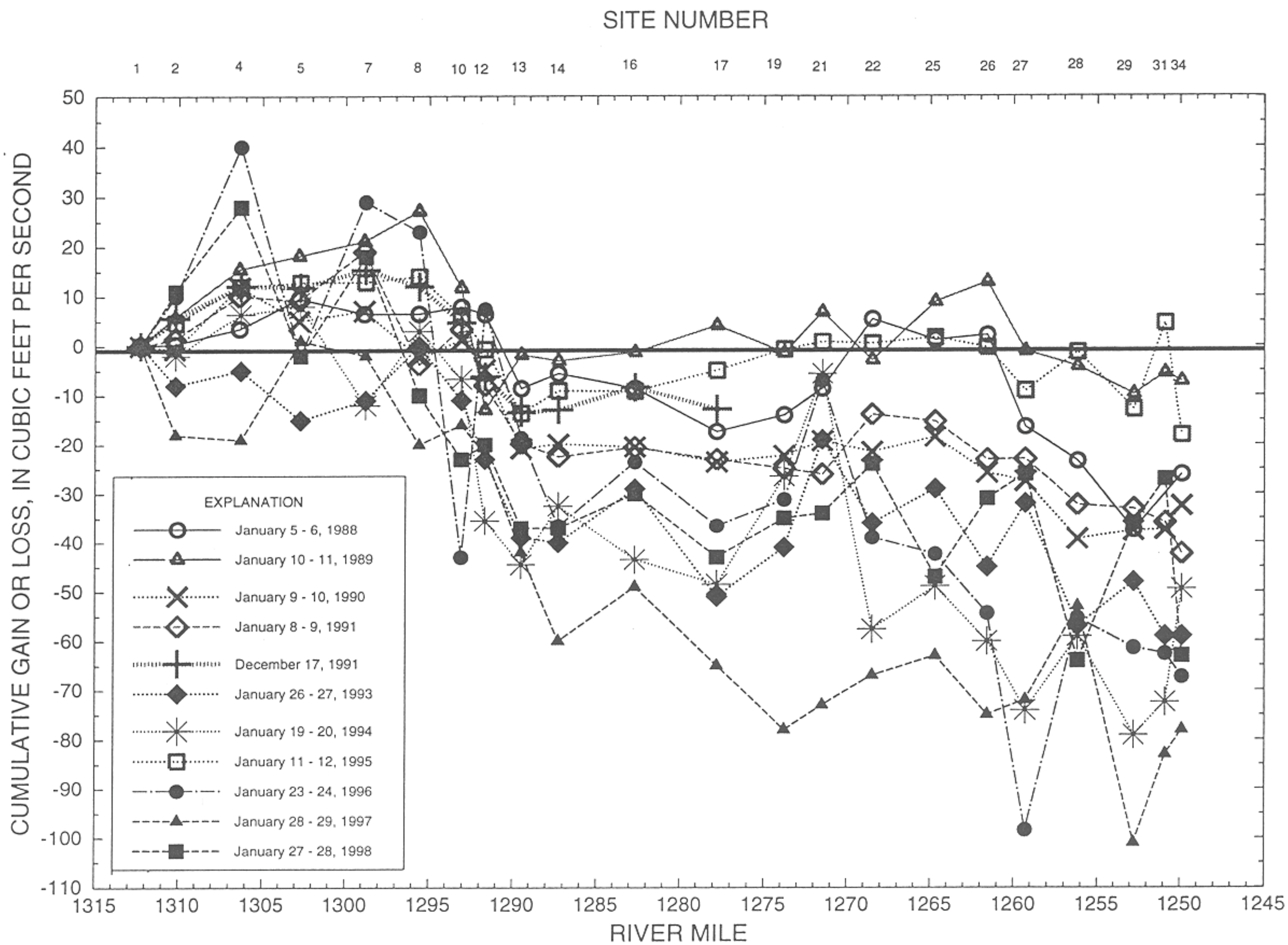

Figure 5-4. Variation in USGS-Observed Rio Grande Seepage Over Time

Drain return flows have been measured over the modeled period. Where measurements are missing, Hamilton and Maddock extrapolated values, used correlations to Rio Grande flow, or used values from published sources as appropriate. Figures 5-5 through 5-12 present the simulated and observed drain flows for Del Rio Drain, Montoya Drain, East Drain, and La Mesa Drain for the secondary and primary irrigation seasons, respectively. To determine the overall fitness of the surface water simulation, the root mean squared (RMS) error was calculated for Rio Grande flows at El Paso and for each drain presented above as well as for the combination of all of these. RMS error is calculated as shown in Equation 5-1. RMS error is the standard deviation or the average of the squared differences in measured and simulated heads.

$$\sqrt{\sum_{n}^{i=1}\frac{(X_{oi}-X_{si})^2}{n}}$$

Equation 5-1, Root Mean Squared Error

In this way the goodness of fit of individual solutions can be balanced with the overall surface water system fitness. Table 5-1 presents the RMS error for the surface water system compared to the RMS error in the Weeden and Maddock model. Other measures of fitness including the average residual and the absolute average residual are also included. The combination of fitness measures can often provide insight to a problem that individual measures do not. For instance, the negative average values indicated that the solutions tend to be more negative than positive. However, this effect could be because of a single outlier. Taking the absolute value of residuals prior to averaging results in a measure of the range in residuals. A residual is the difference between a measured and a simulated value. The RMS error seems to provide the best overall comparable measurement of solution fitness. Values are included for the entire simulation period (1915-1995) and for a subset of this period beginning in 1938 [labeled "(38)"]. The 1938 period was analyzed because the observed data appear to be more complete from this point forward.

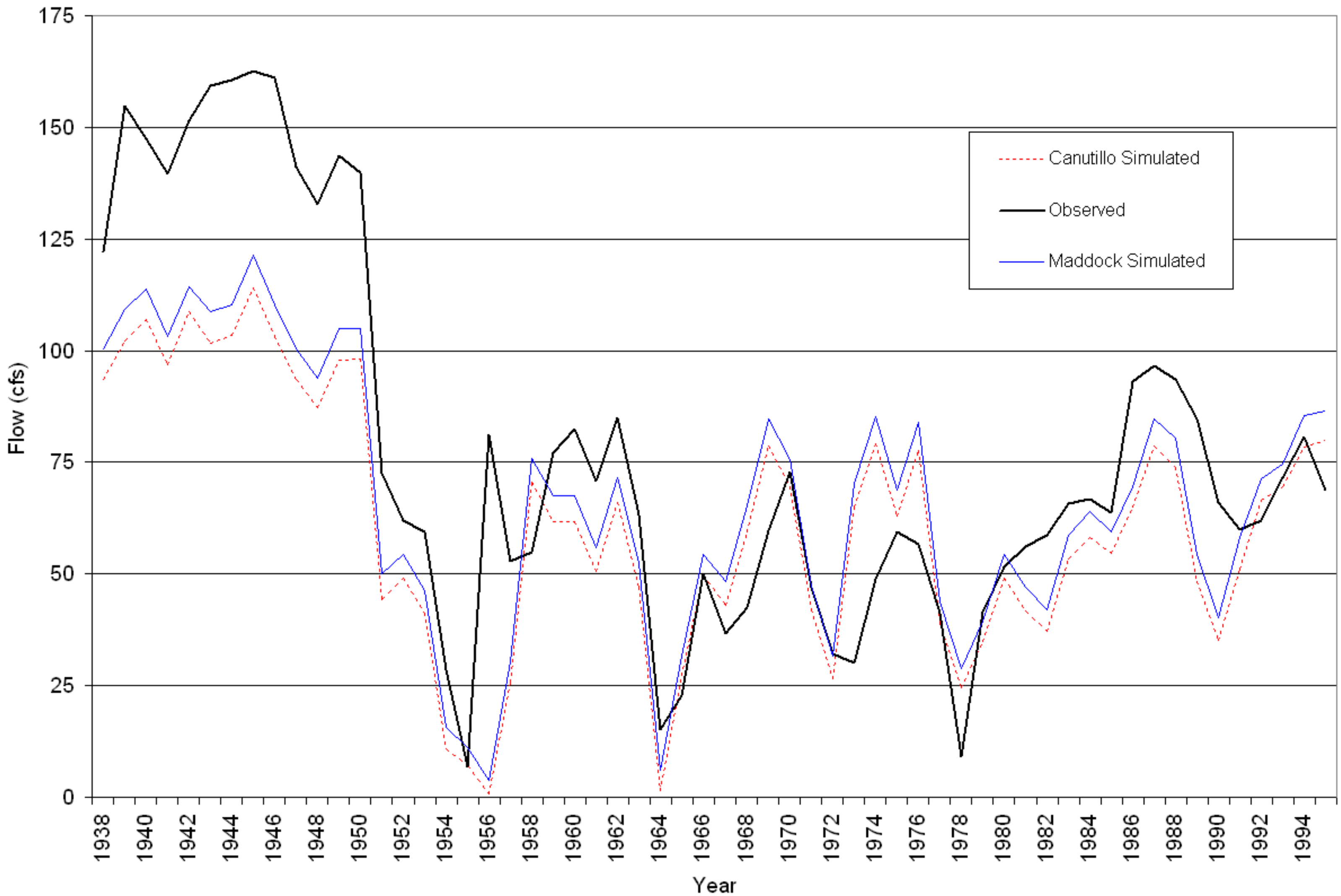

Figure 5-5. Simulated and Observed Del Rio Drain Flow in the Primary Irrigation Season

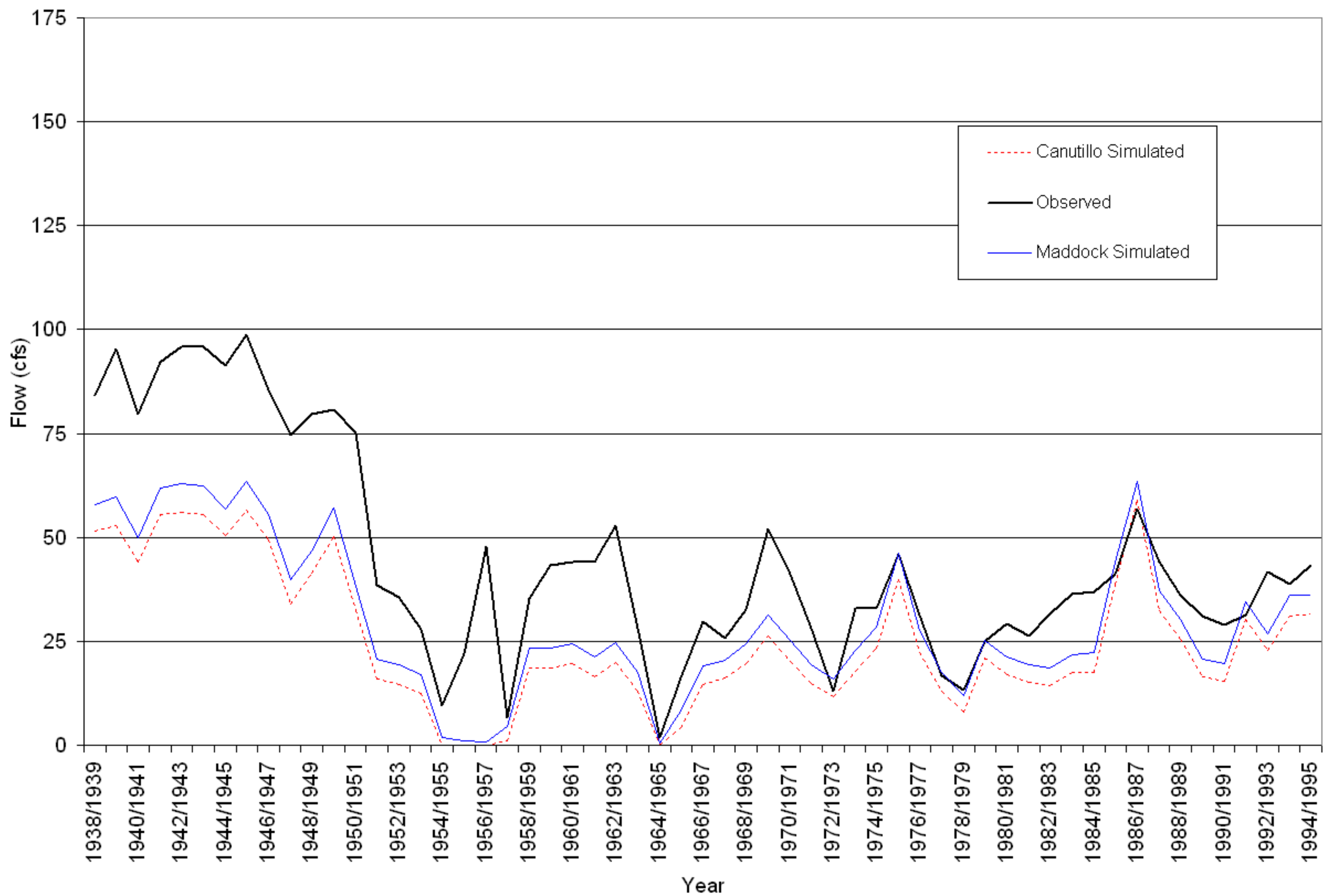

Figure 5-6. Simulated and Observed Del Rio Drain Flow in the Secondary Irrigation Season

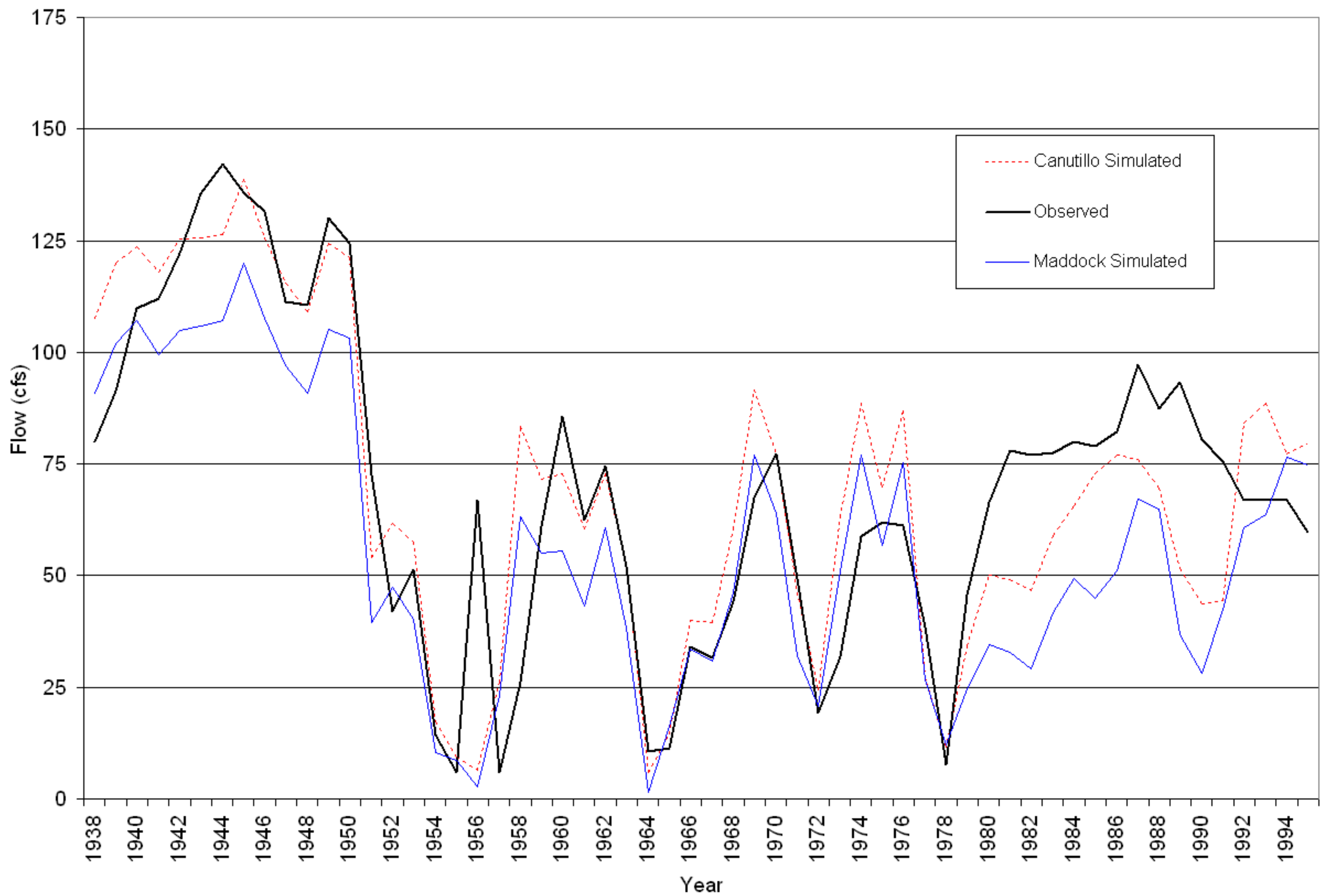

Figure 5-7. Simulated and Observed Montoya Drain Flow in the Primary Irrigation Season

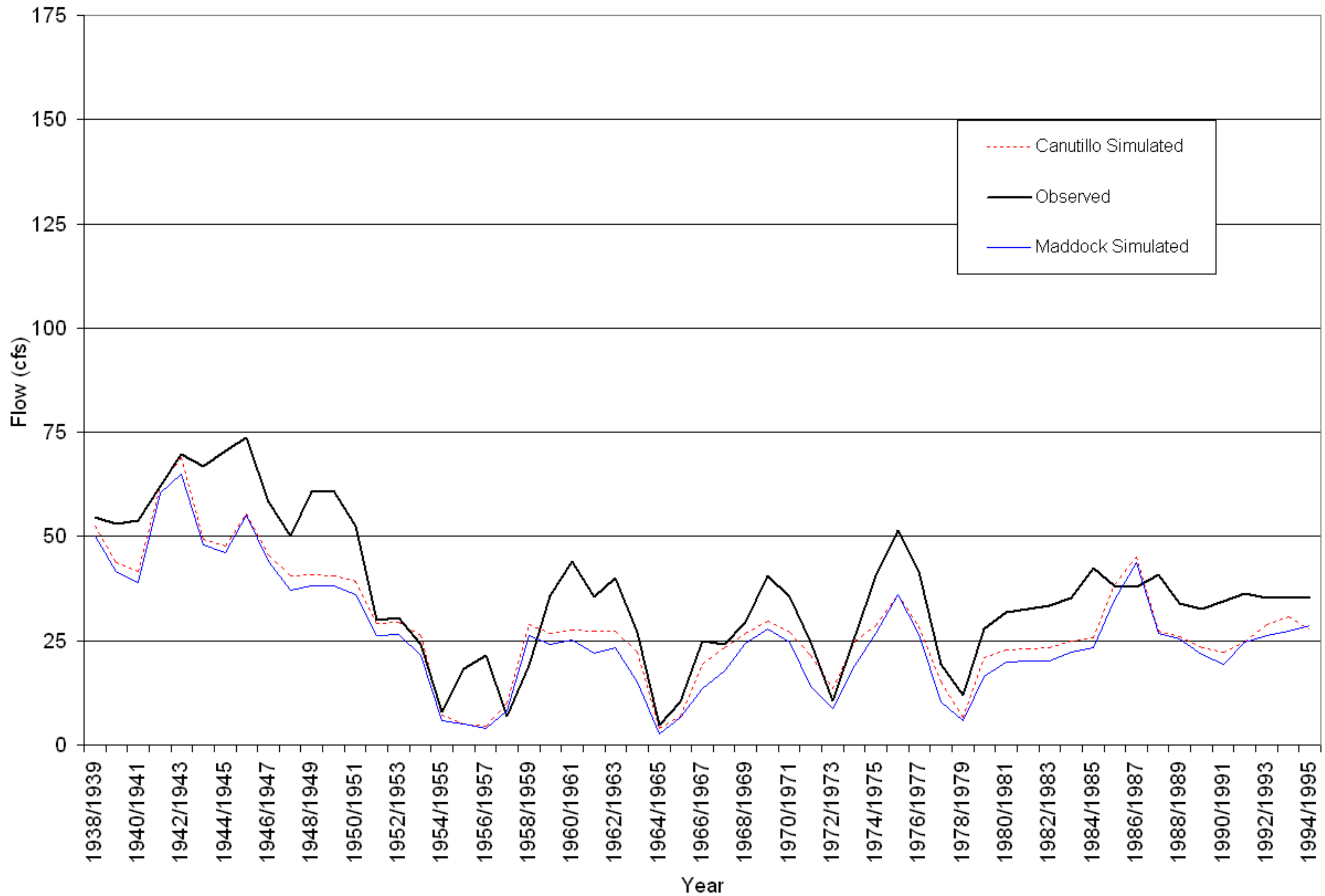

Figure 5-8. Simulated and Observed Montoya Drain Flow in the Secondary Irrigation Season

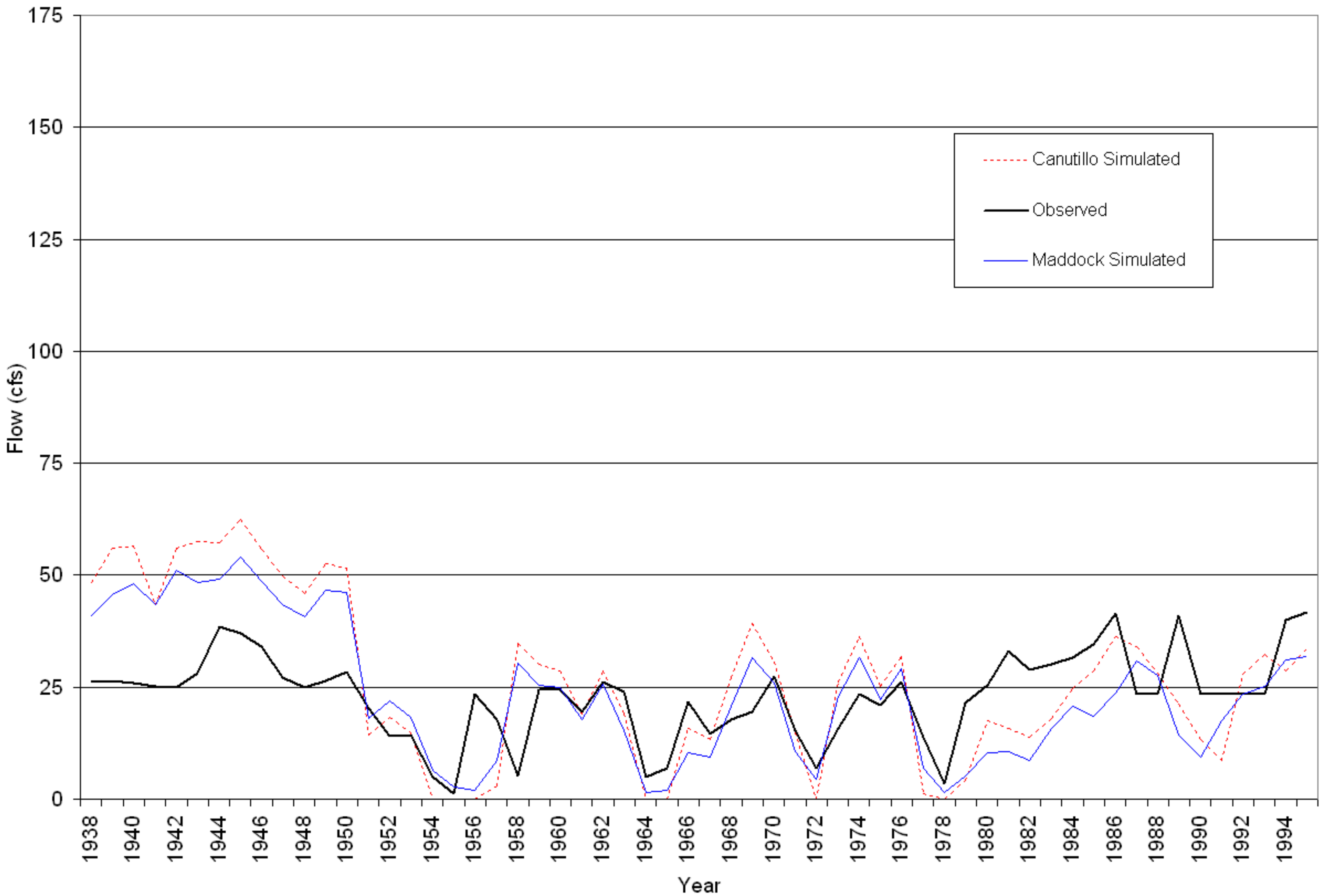

Figure 5-9. Simulated and Observed East Drain Flow in the Primary Irrigation Season

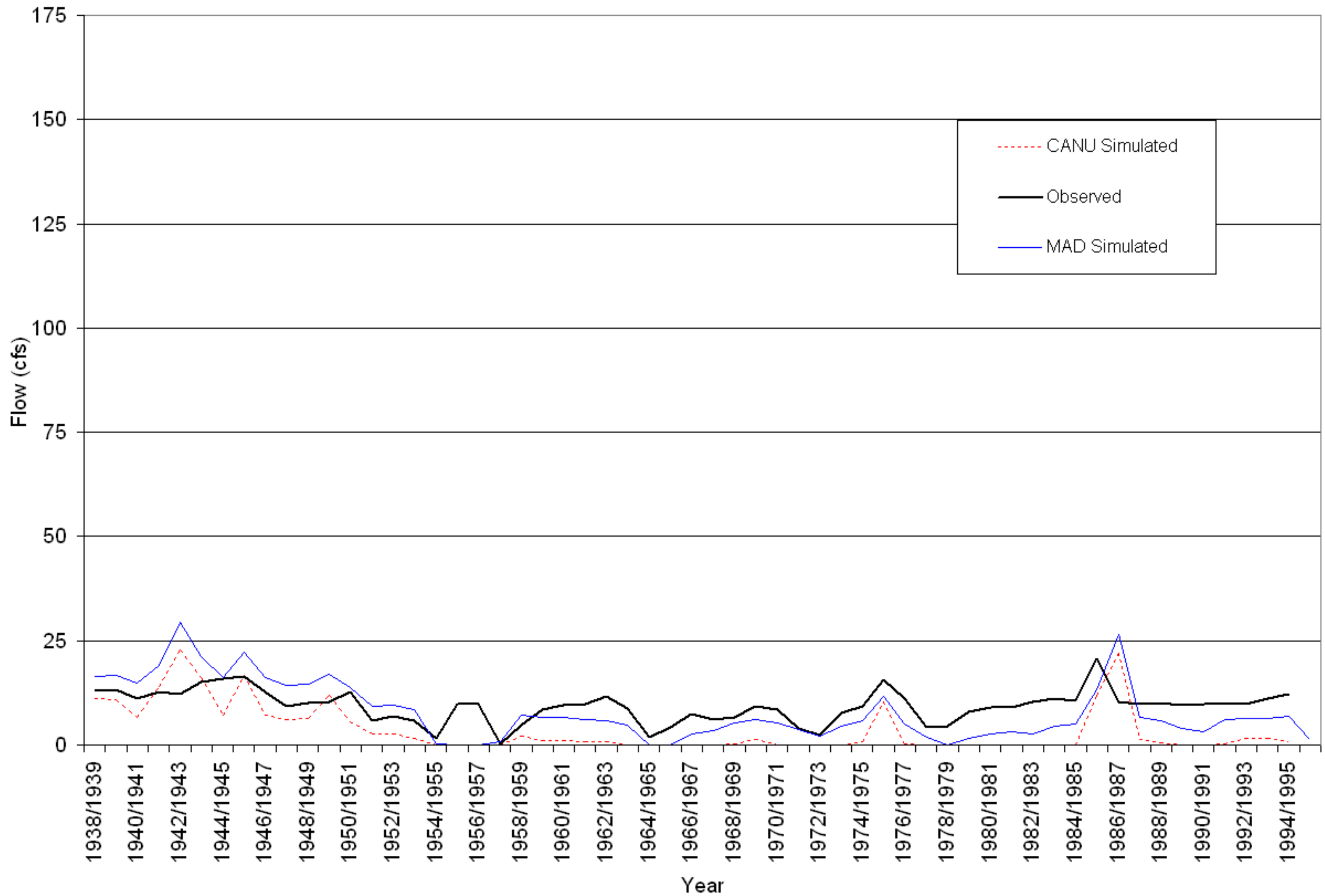

Figure 5-10. Simulated and Observed East Drain Flow in the Secondary Irrigation Season

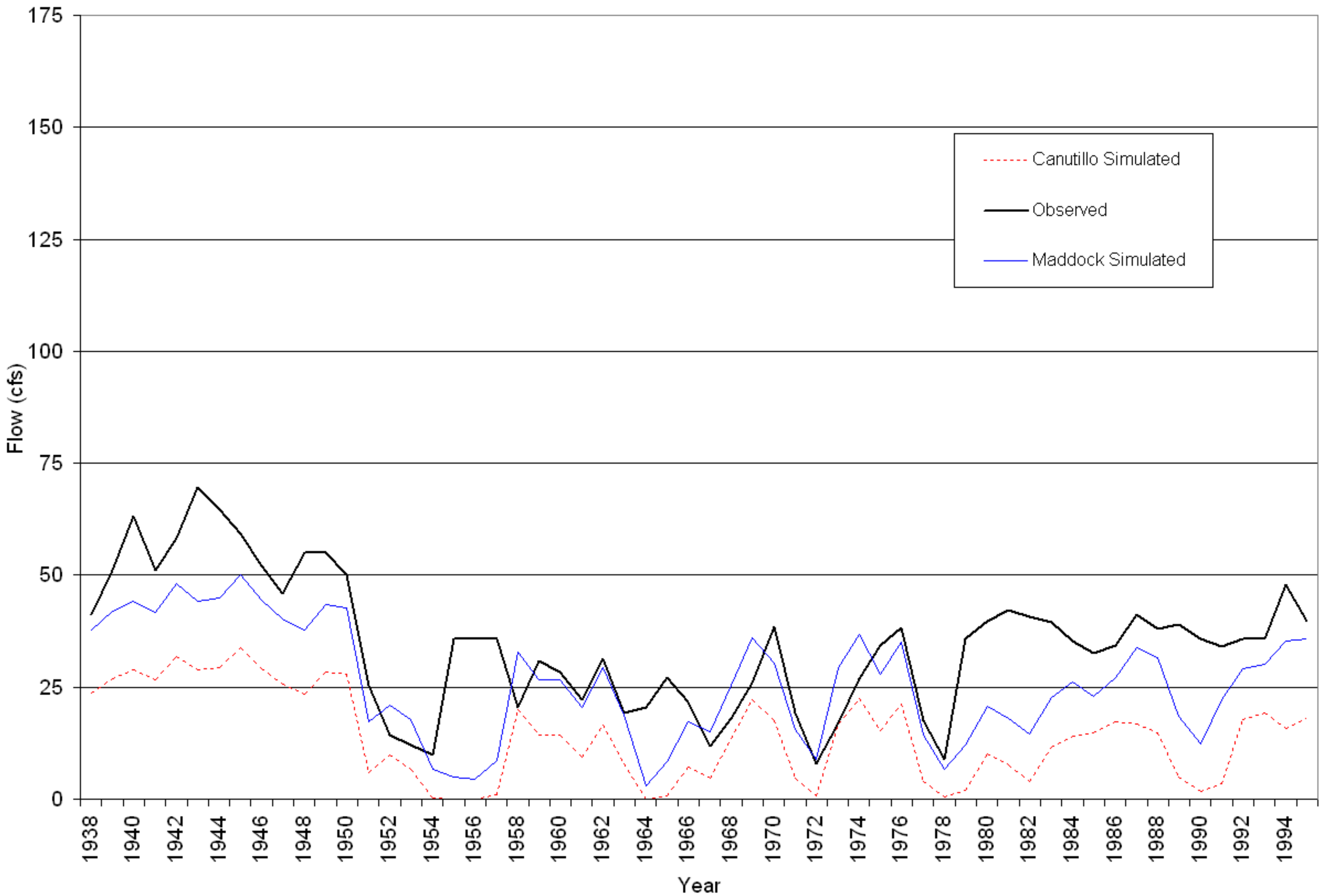

Figure 5-11. Simulated and Observed La Mesa Drain Flow in the Primary Irrigation Season

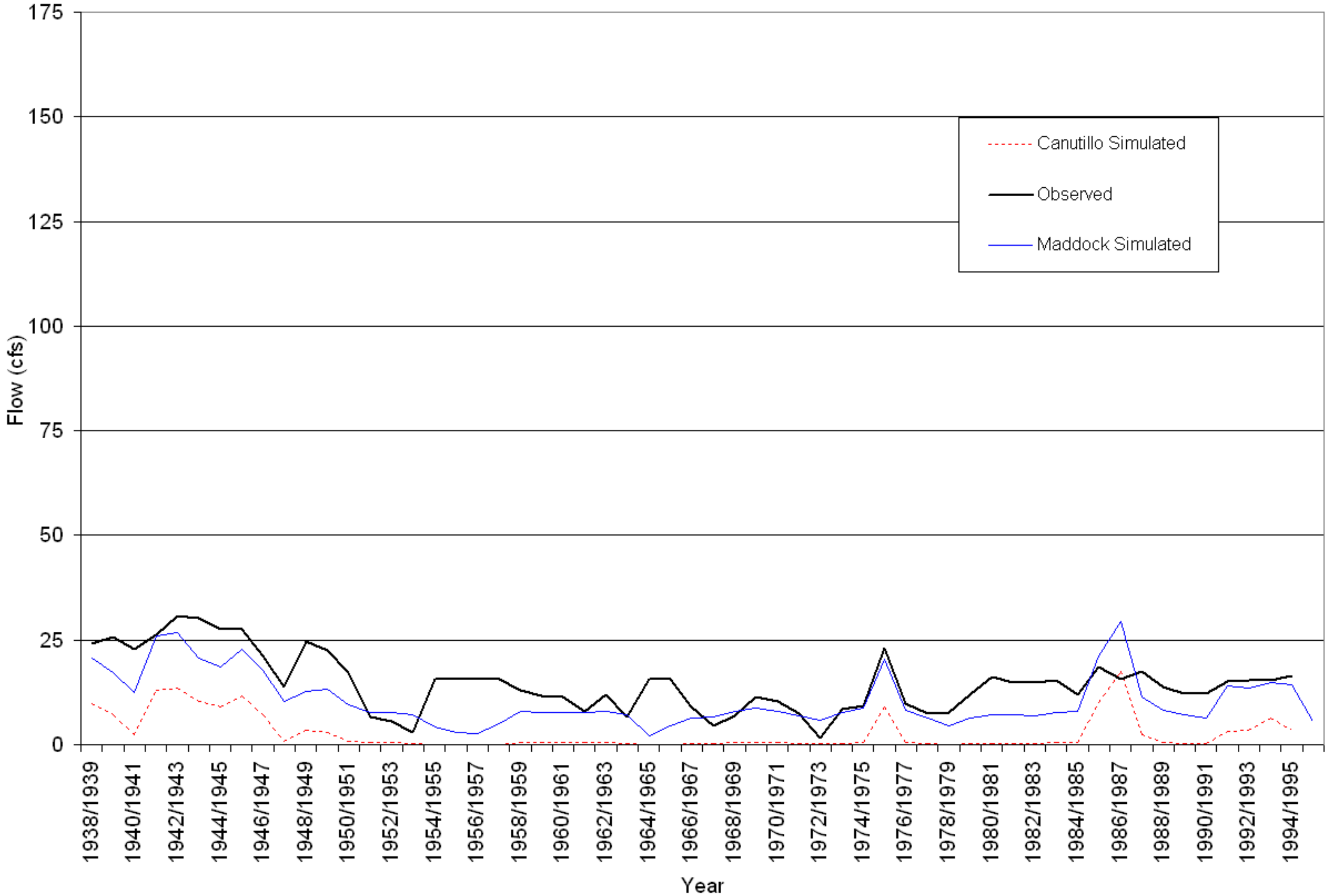

Figure 5-12. Simulated and Observed La Mesa Drain Flow in the Secondary Irrigation Season

TABLE 5-1
Difference in Simulated and Observed Flows for the Cañutillo (CANU) and Maddock (MAD) Models

	Rio Grande		Del Rio		La Mesa		East		Montoya	
	CANU	MAD	CANU	MAD	CANU	MAD	CANU	MAD	CANU	MAD
Average	-49	-44	-9	-3	-14	-4	5	3	7	-3
Average (38)	-39	-34	-18	-13	-16	-6	0	0	-4	-12
Primary (38)	-14	-6	-16	-11	-21	-9	5	1	0	-13
Secondary (38)	-66	-64	-19	-14	-12	-4	-6	-1	-7	-10
Absolute Avg.	87	86	25	23	15	9	12	9	19	18
Abs Avg (38)	59	58	21	18	16	8	9	7	12	15
Absolute Pri (38)	51	52	23	20	21	11	12	10	15	20
Absolute Sec (38)	66	64	19	15	12	5	6	5	9	11
Tot RMS	158	156	32	31	18	12	16	11	27	24
RMS (38)	73	71	26	23	19	11	12	10	16	19
Primary RMS (38)	68	69	29	26	23	14	15	13	20	24
Sec RMS (38)	76	73	23	19	13	6	7	6	10	12

	MAD	CANU
Total RMS	72	73
Total RMS (38)	35	36

5.2.2 Model Heads

Transient aquifer head targets from Frenzel, Hamilton and Maddock, and Weeden and Maddock were used to gage how well the model simulates aquifer head. RMS error was also calculated for 104 targets to determine the goodness of simulated aquifer head fit. Table 5-2 presents the RMS error for the Cañutillo model and the Weedon and Maddock model. Targets are distributed over time and space. Targets and residuals used from Weeden and Maddock only include those that intersect the area of interest. Calibration to these targets will allow for comparison to the Weeden and Maddock model. Additional time series water level data are available in the Cañutillo wellfield area. Additional temporal calibration points would allow for the evaluation of water level trends. However, with the current model layering calibration to additional points will not likely result in additional model accuracy. Future model revisions that explore the Cañutillo area in more detail should include additional spatial and temporal calibration points.

TABLE 5-2
Difference in Simulated and Observed Heads for the
Cañutillo (CANU) and Maddock (MAD) Models

	CANU	MAD
Abs. Res. Mean	1.7	2.4
Head Range	20.6	76.8
Max. Residual	8.6	65.7
Min. Residual	-12.1	-11.2
Res. Std. Dev.	2.7	7.0
Residual Mean	-0.3	0.5
Std/Head Range	0.1	0.1
Sum of Squares	779.7	5082.8
RMS	2.7	7.0
Count	104	104

5.3 Calibration

The process of model calibration involves changing model parameters such as hydraulic conductivity, surface water system elevations, and surface water system vertical conductances to improve the overall goodness of fit. Changes to hydraulic conductivity are considered in subsection 5.4 in the discussion of the inverse model. Numerous simulations were made altering elevations and/or vertical conductances of individual components of the surface water system and combinations of components to attempt to improve calibration. Generally, individual components were targeted for changes based on attempting to produce primary and secondary irrigation seasons results whose average error is zero. As stated previously, the surface water system is somewhat self-compensating. So, changes that increase flows of Del Rio Drain for instance may reduce flows in other drains or canals. The following subsections present the results of the calibration process.

5.3.1 Rio Grande Flow at El Paso

As can be seen in Table 5-1, error in Rio Grande flow at El Paso dominates the overall error of the surface water system. When error is normalized with average flow, the error in Rio Grande flow at El Paso is relatively small compared to other streamflow components. However, to minimize overall streamflow system error, the error in Rio Grande flow must clearly be reduced. Likewise, the Rio Grande is the most important component of the surface water system. Figures 5-13 and 5-14 present observed and simulated Rio Grande flow at El Paso for the calibrated Cañutillo model in the primary and secondary irrigation seasons, respectively.

5.3.2 Rio Grande Seepage

As stated previously, the scale and timing of the observed Rio Grande seepage values do not allow them to be directly compared to the simulated values. However, Figure 5-15 indicates that the general trend of simulated Rio Grande seepage matches the observed trend. Likewise, the rate and magnitude of simulated seepage appear to match observed seepage reasonably well.

5.3.3 Drain Return Flows

Numerous simulations were made changing individual parameters and examining results. Parameters changed included drain elevations and drain vertical hydraulic conductivities. Once it was determined that improvements could be made, additional simulations were made combining the most successful individual parameter changes. It was found that changing the elevation of various drains and reducing the horizontal hydraulic conductivity of the Rio Grande simultaneously resulted in the best overall surface water system fitness. In general simulated drain return flows match the observed drain return flows well. Simulated primary irrigation season flows tend to match observed flows better than secondary irrigation season flows. Figures 5-16 through 5-23 present the simulated and observed flows for Del Rio Drain, Montoya Drain, East Drain, and La Mesa Drain for the primary and secondary irrigation seasons, respectively. Table 5-3 tabulates the final surface water system error.

5.3.4 Model Heads

Final simulated heads for layers 1 through 4 are presented in Figures 5-24 through 5-27, respectively. Table 5-4 presents the final error in simulated versus observed heads. The cumulative probability of head residuals is presented in Figure 5-28. This plot shows that there is close to a 50 percent probability of a zero residual. Likewise, residuals between –1 and 1 meter make up most of the distribution. Figure 5-29 presents calculated verses observed heads by layer and observation point in time. These values generally form a straight line with relatively few outliers. The residual verses the observed values are shown in Figure 5-30. These values are generally well scattered with similar numbers of negative residuals to positive residuals and no obvious spatial bias (clusters of similar residuals around a given observation point). Changes to the surface water system resulted in little or no change to overall model heads. Likewise, as is discussed in subsection 5.4, minor changes to hydraulic conductivity also resulted in little change to overall model heads.

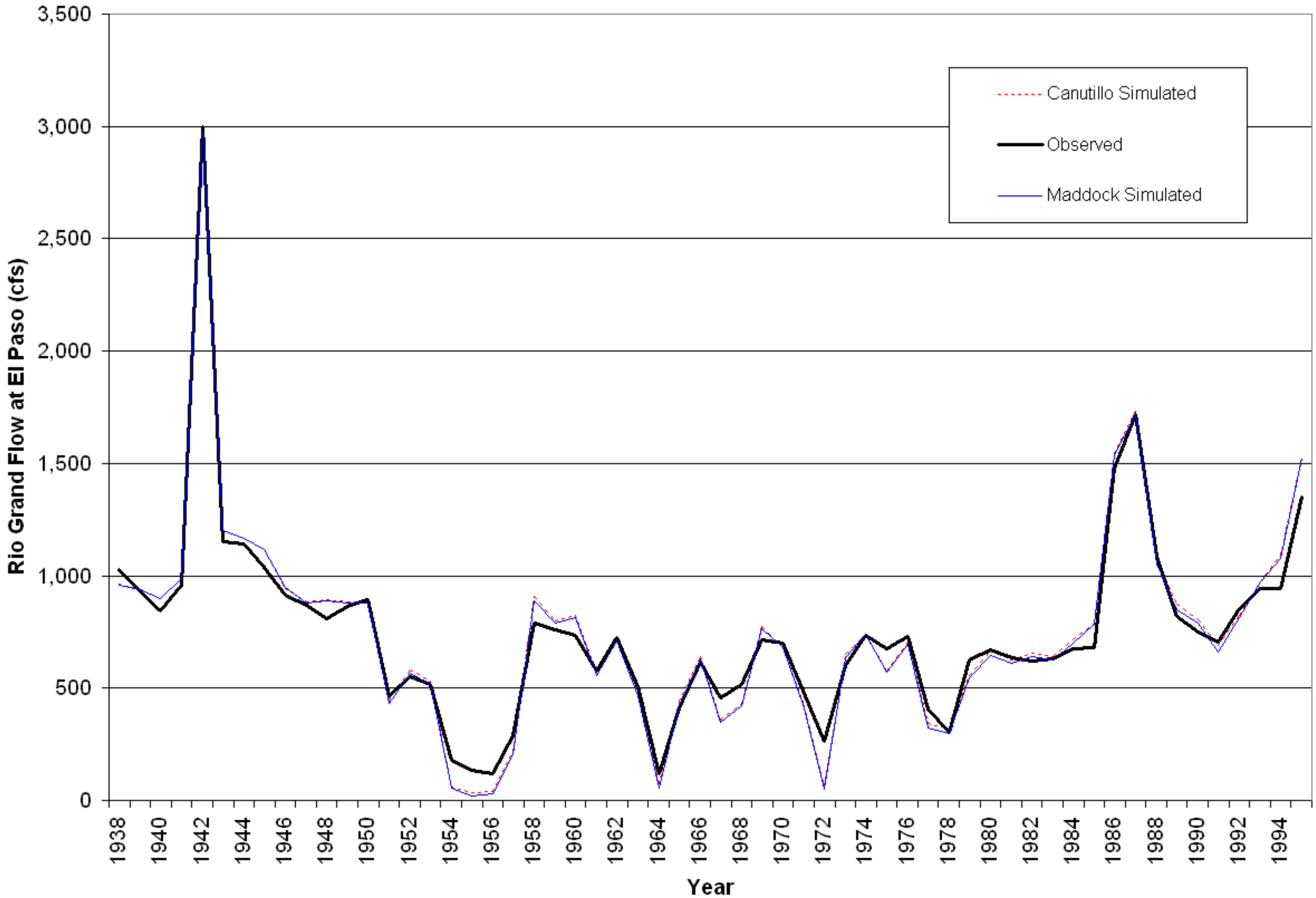

Figure 5-13. Simulated and Observed Primary Irrigation Season Rio Grande Flow at El Paso

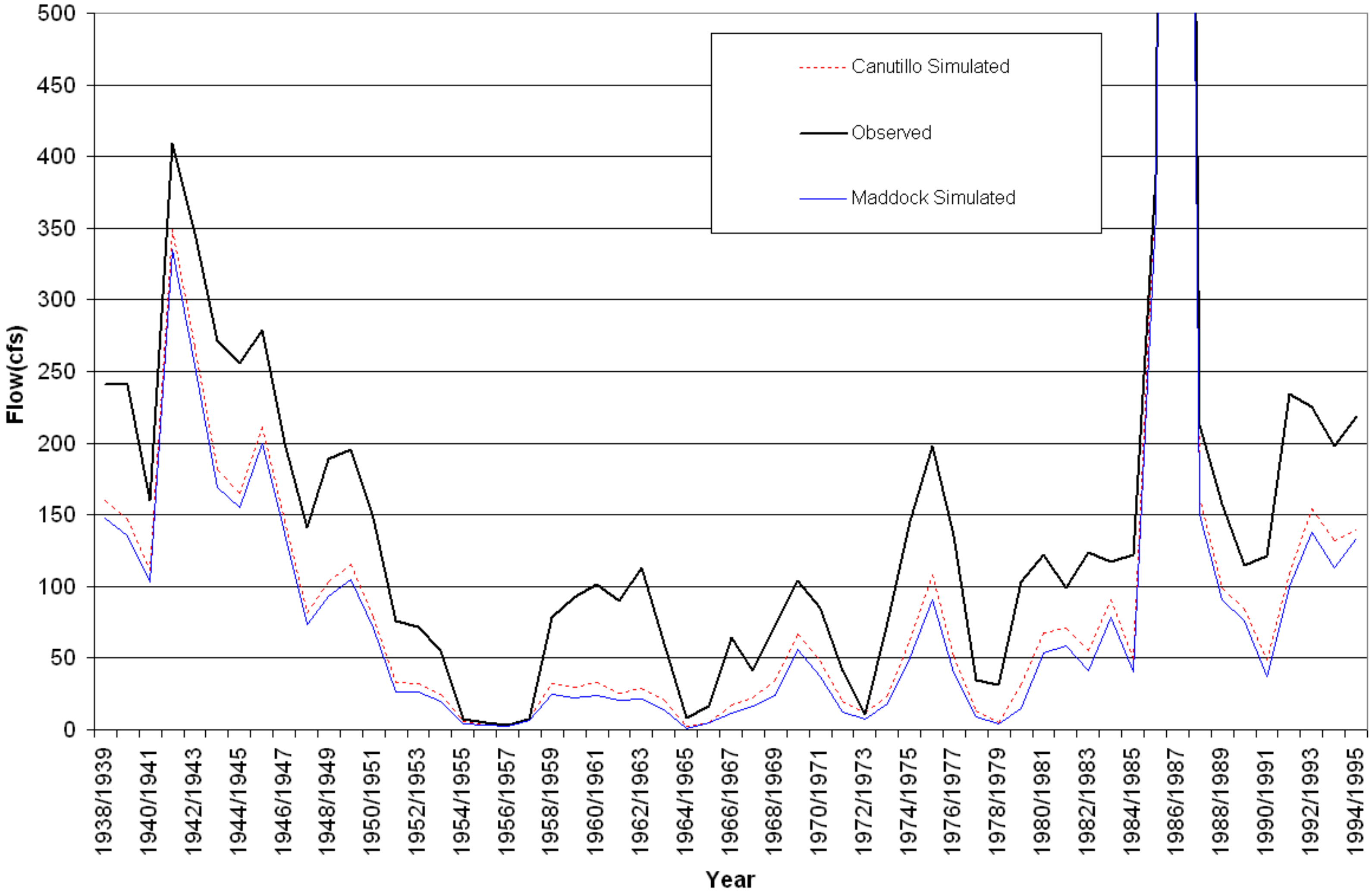

Figure 5-14. Simulated and Observed Secondary Irrigation Season Rio Grande Flow at El Paso

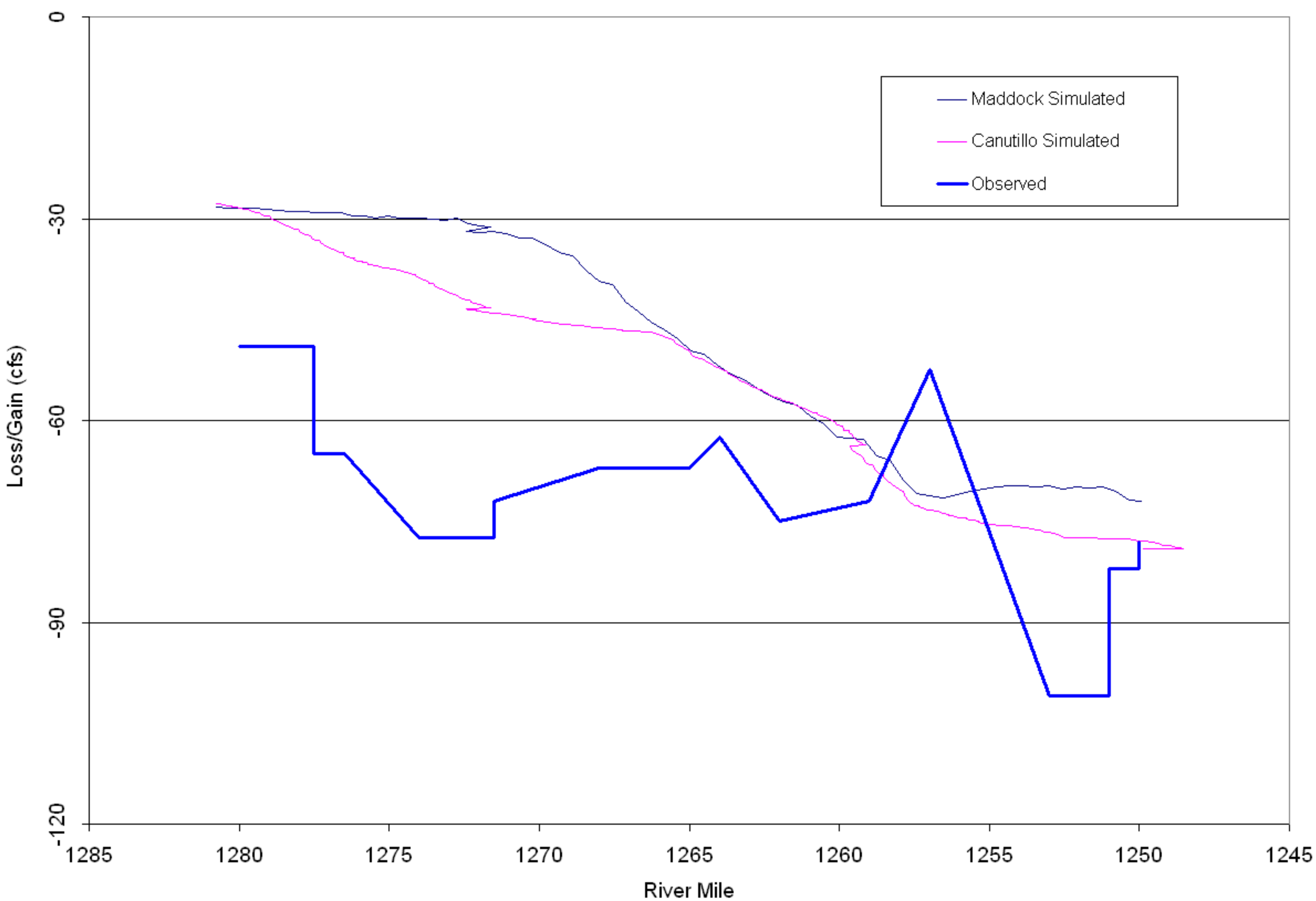

Figure 5-15. Rio Grande Seepage in the Lower Mesilla Valley 1994/1995 Secondary Irrigation Season

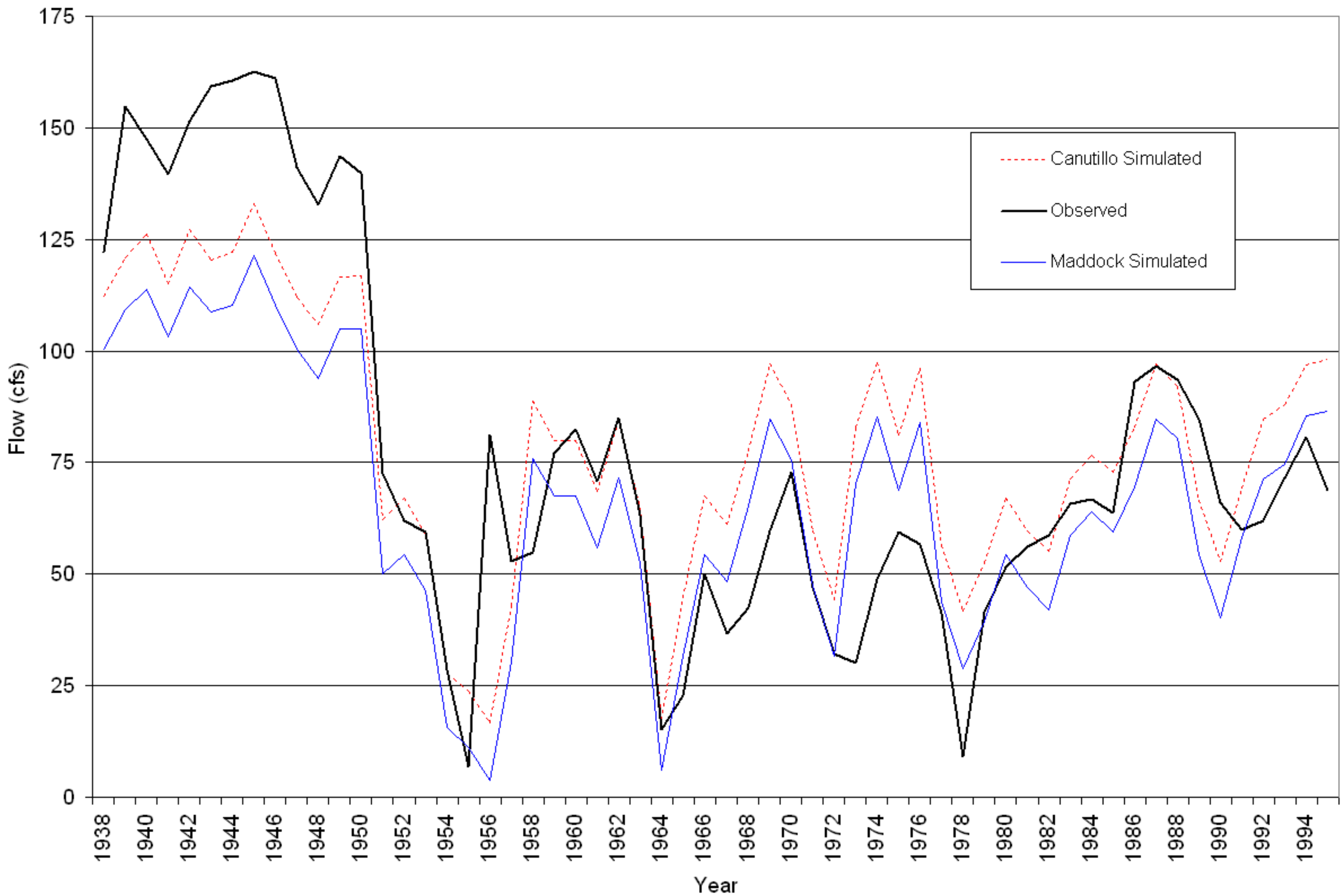

Figure 5-16. Simulated and Observed Del Rio Drain Flow in the Primary Irrigation Season

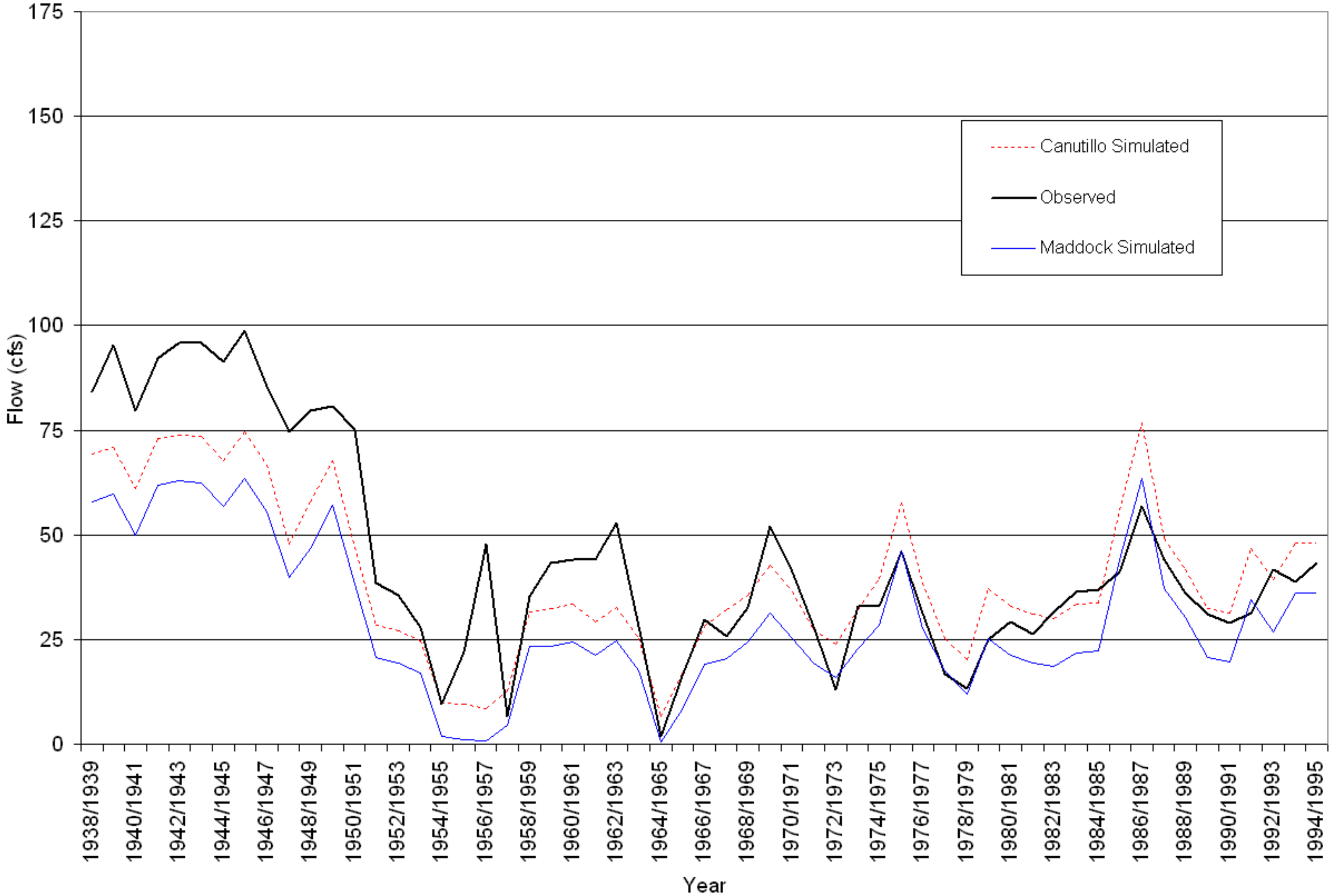

Figure 5-17. Simulated and Observed Del Rio Drain Flow in the Secondary Irrigation Season

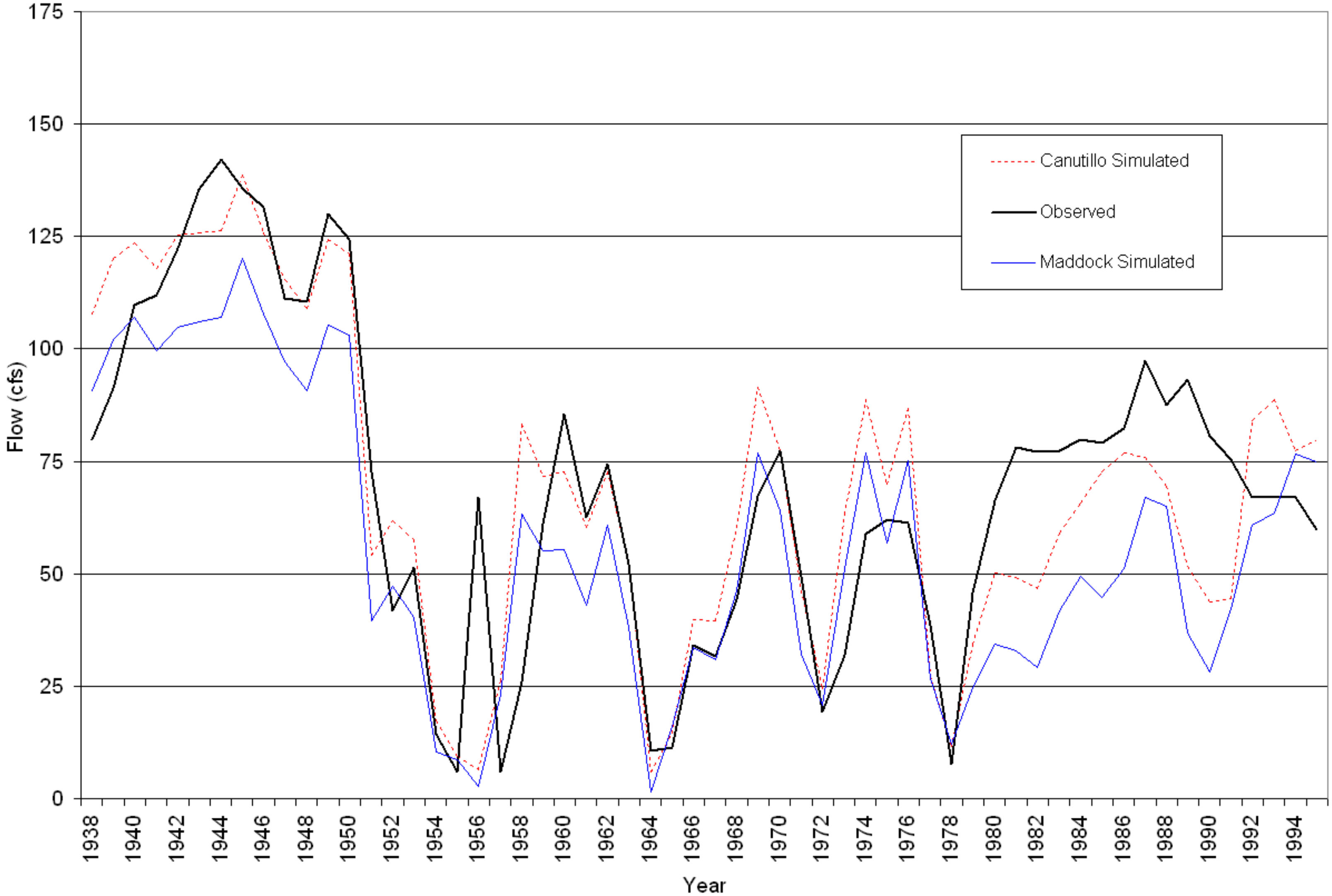

Figure 5-18. Simulated and Observed Montoya Drain Flow in the Primary Irrigation Season

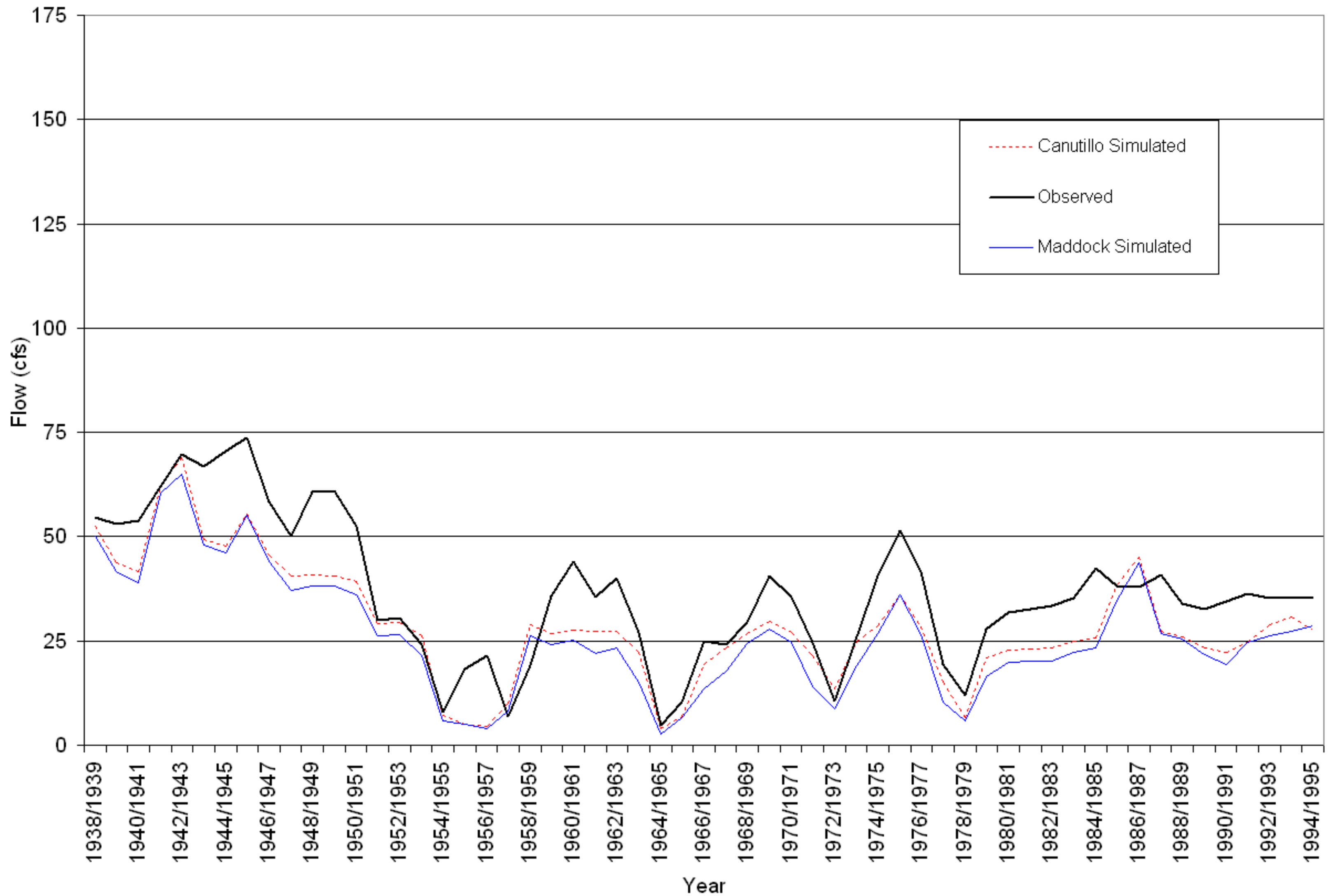

Figure 5-19. Simulated and Observed Montoya Drain Flow in the Secondary Irrigation Season

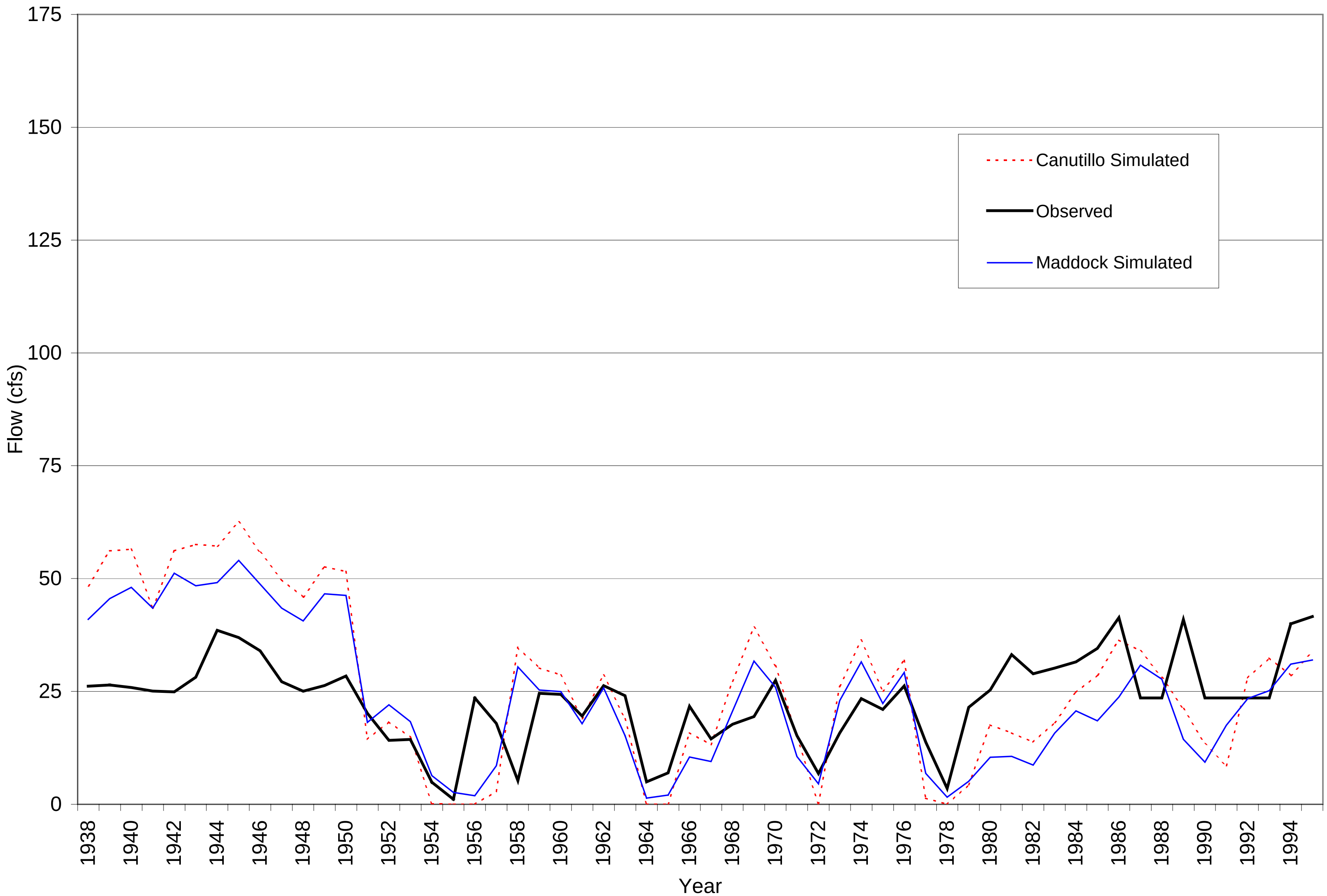

Figure 5-20. Simulated and Observed East Drain Flow in the Primary Irrigation Season

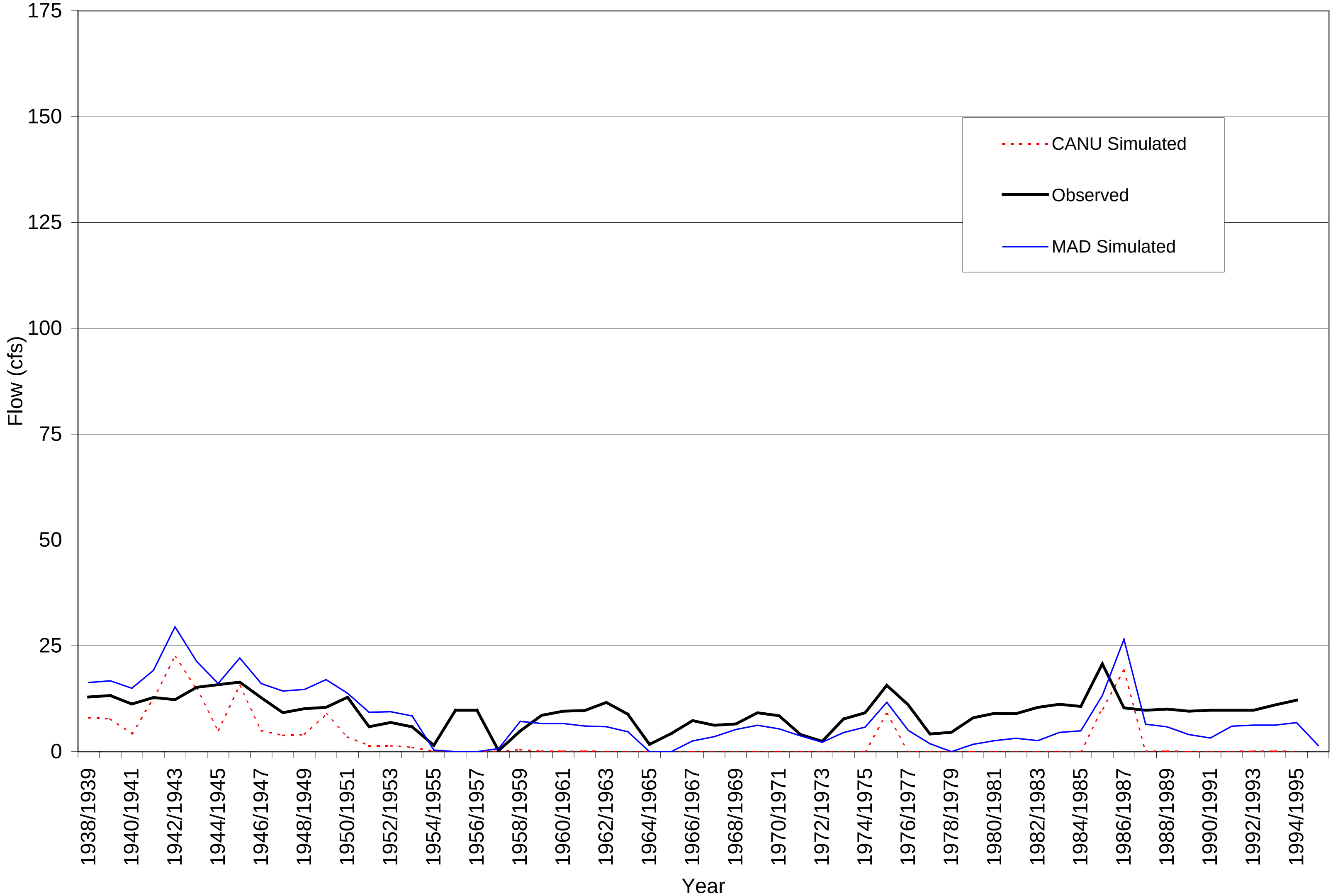

Figure 5-21. Simulated and Observed East Drain Flow in the Secondary Irrigation Season

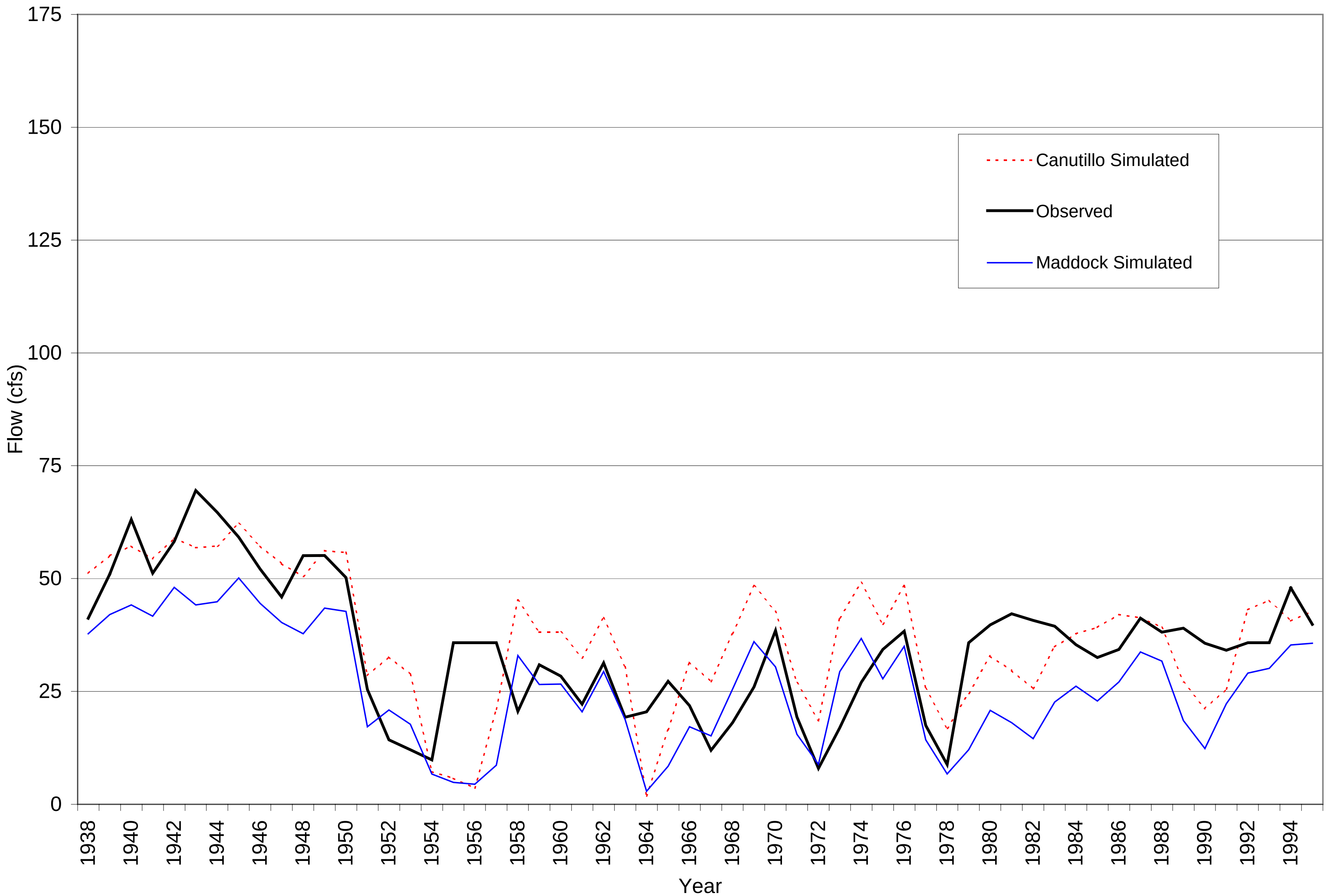

Figure 5-22. Simulated and Observed La Mesa Drain Flow in the Primary Irrigation Season

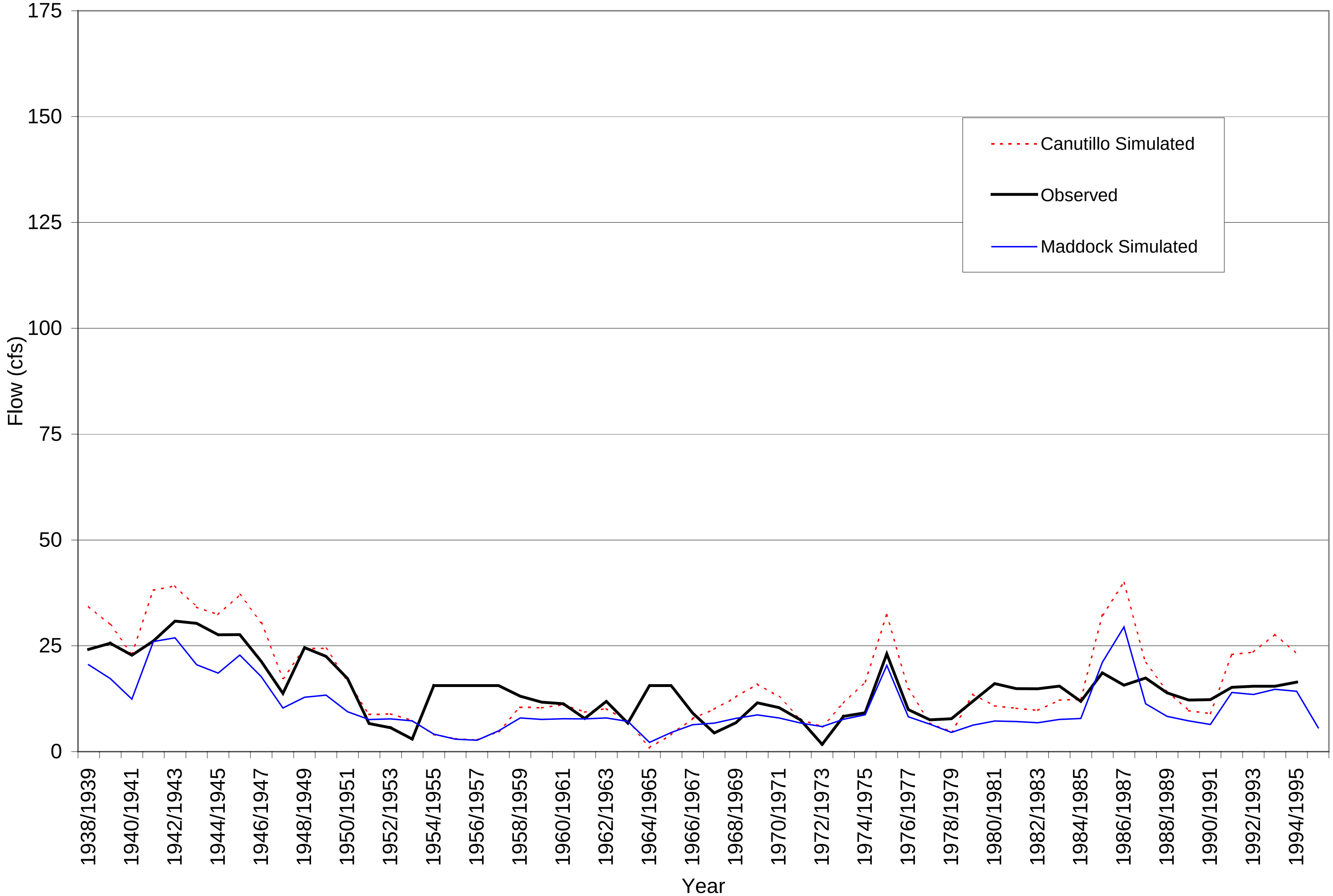

Figure 5-23. Simulated and Observed La Mesa Drain Flow in the Secondary Irrigation

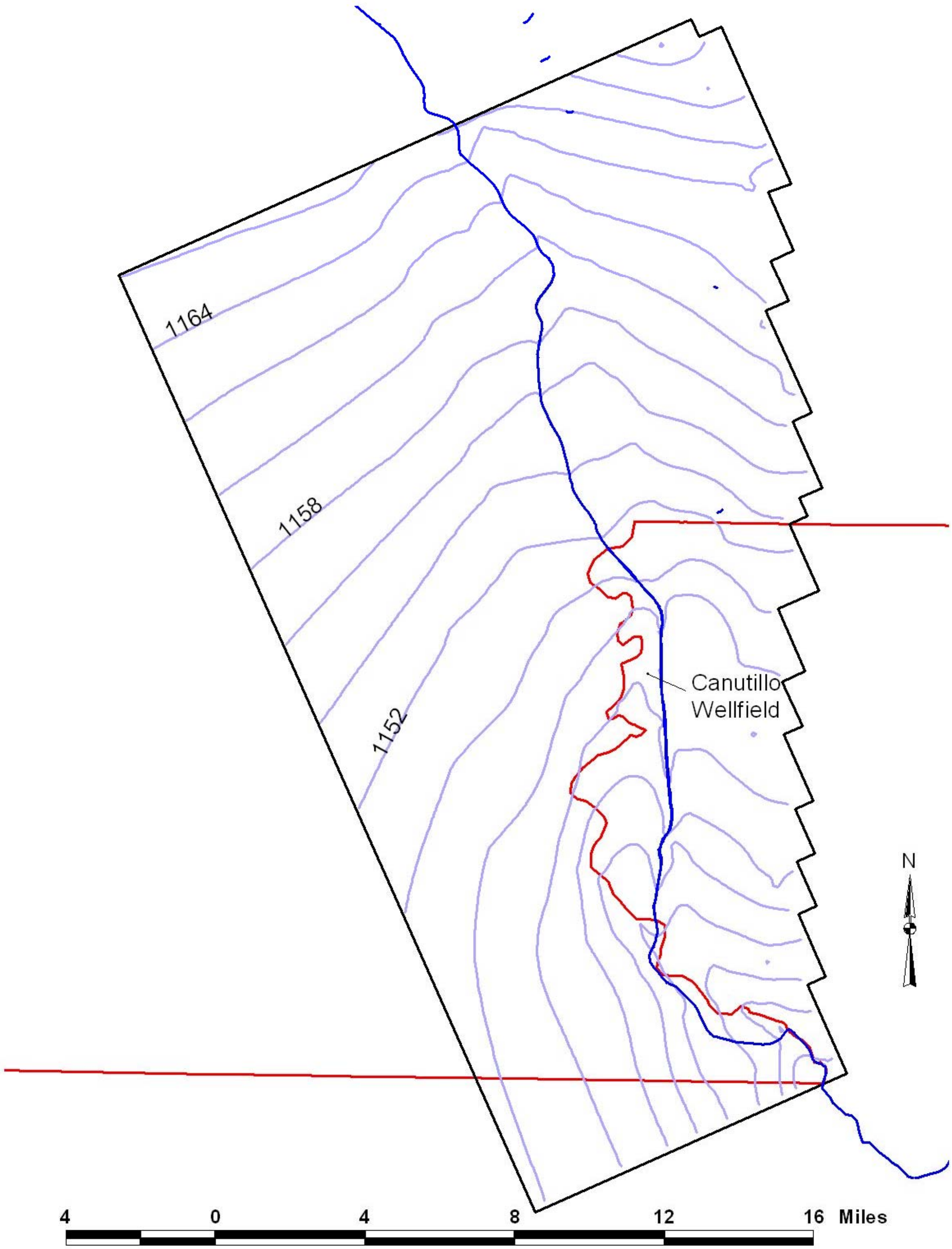

Figure 5-24. Layer 1 Head, 1994/1995 Secondary Irrigation Season

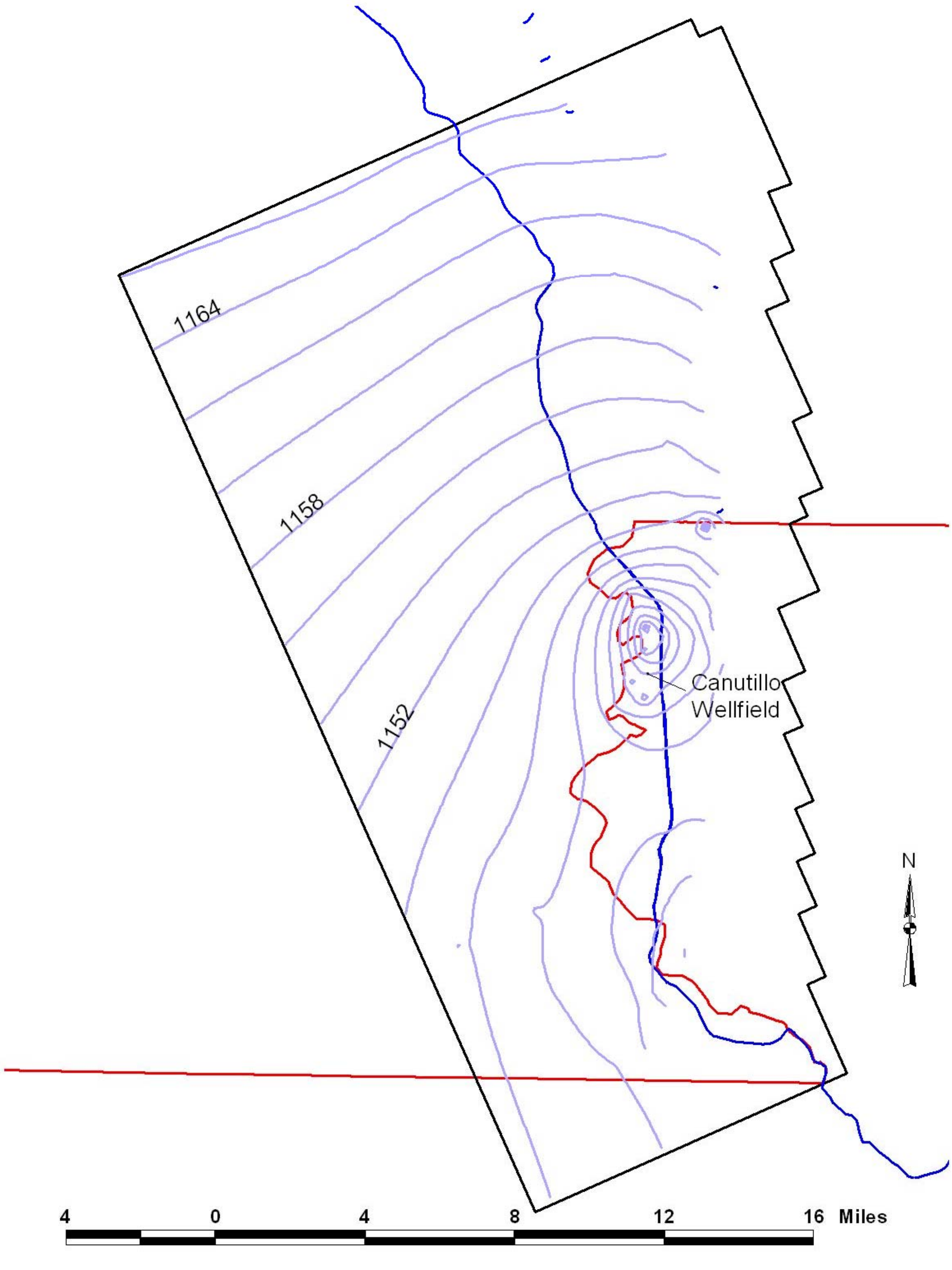

Figure 5-25. Layer 2 Head, 1994/1995 Secondary Irrigation Season

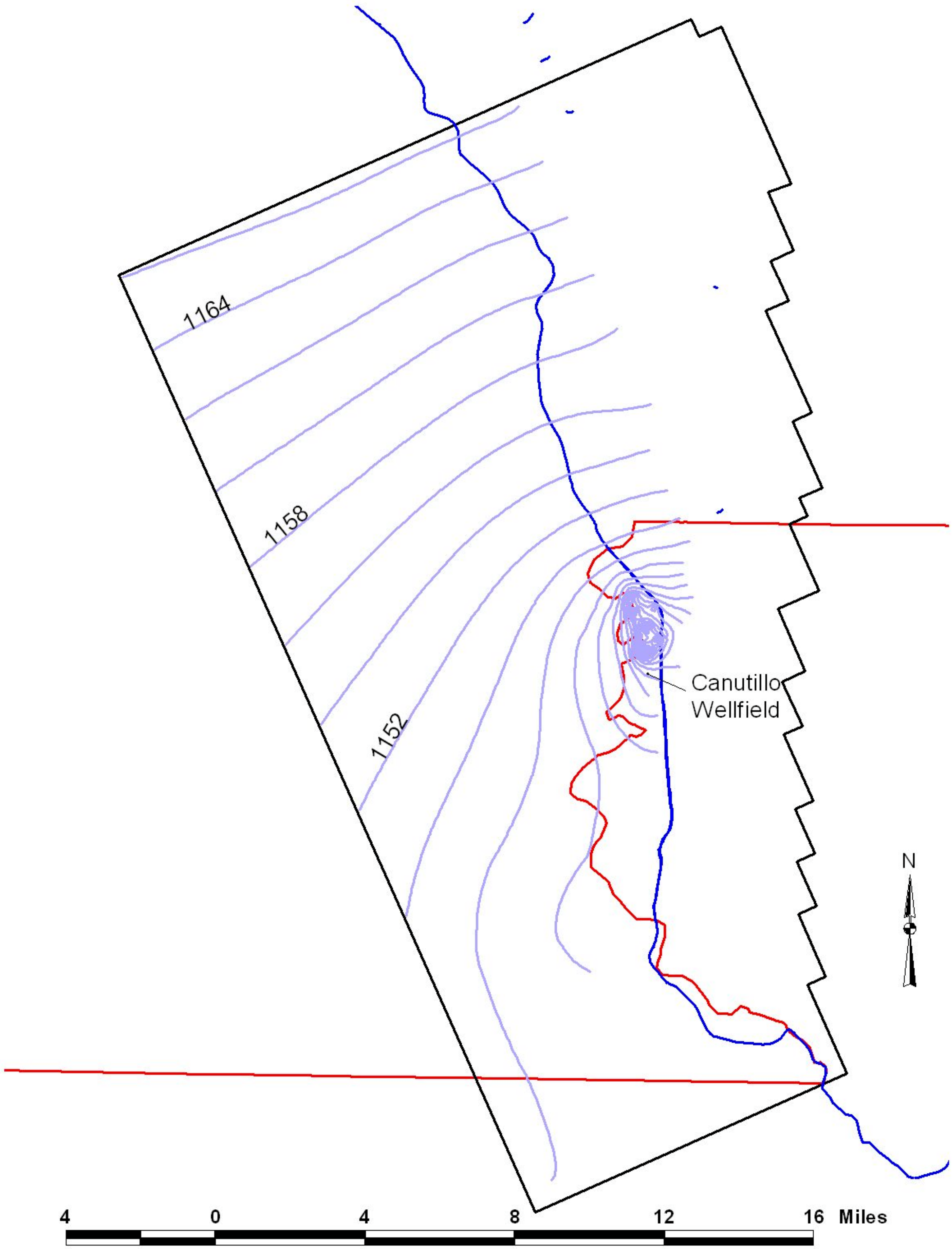

Figure 5-26. Layer 3 Head, 1994/1995 Secondary Irrigation Season

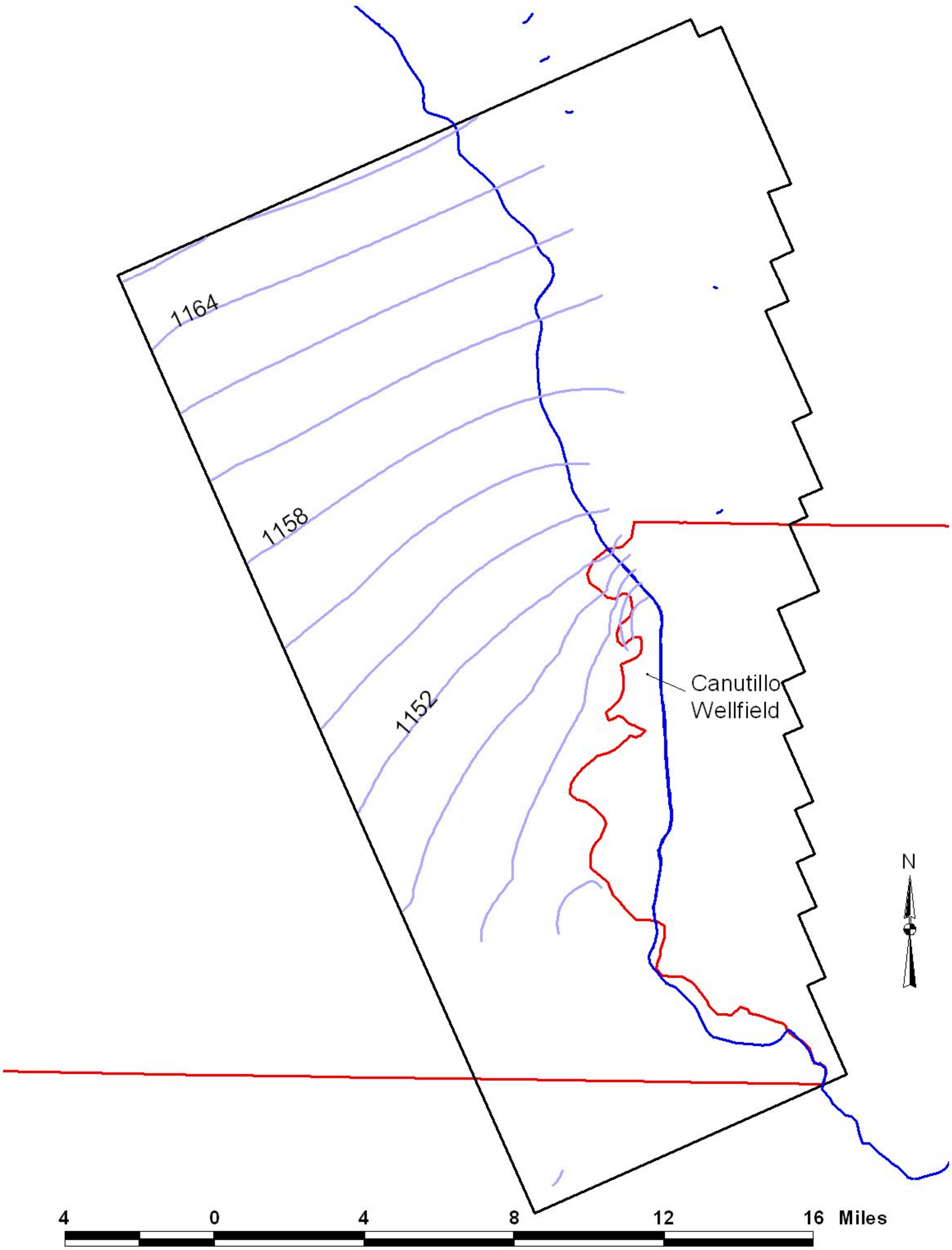

Figure 5-27. Layer 4 Head, 1994/1995 Secondary Irrigation Season

TABLE 5-3
Final Difference in Simulated and Observed Flows for the Cañutillo (CANU) and Maddock (MAD) Models

	Rio Grande		Del Rio		La Mesa		East		Montoya	
	CANU	MAD	CANU	MAD	CANU	MAD	CANU	MAD	CANU	MAD
Average	-33	-44	8	-3	5	-4	4	3	7	-3
Average (38)	-24	-34	-1	-13	2	-6	-1	0	-4	-12
Primary (38)	4	-6	2	-11	2	-9	4	1	0	-13
Secondary (38)	-54	-64	-4	-14	2	-4	-6	-1	-7	-10
Absolute Avg	80	86	22	23	10	9	12	9	19	18
Abs Avg (38)	53	58	15	18	8	8	10	7	12	15
Absolute Pri (38)	51	52	19	20	10	11	12	10	15	20
Absolute Sec (38)	54	64	11	15	6	5	7	5	9	11
Tot RMS	153	156	32	31	14	12	16	11	27	24
RMS (38)	65	71	20	23	10	11	12	10	16	19
Primary RMS (38)	67	69	24	26	12	14	15	13	20	24
Sec RMS (38)	64	73	14	19	7	6	8	6	10	12

	MAD	CANU
Total RMS	72	71
Total RMS (38)	35	32

TABLE 5-4
Measures of Model Fitness by Year for the Final Cañutillo Model and The Maddock Model

	Cañutillo Final	Cañutillo Original	MAD
Abs. Res. Mean	2.0	1.7	2.4
Head Range	27.0	20.6	76.8
Max. Residual	20.1	8.6	65.7
Min. Residual	-6.9	-12.1	-11.2
Res. Std. Dev.	3.6	2.7	7.0
Residual Mean	0.6	-0.3	0.5
Std/Head Range	0.1	0.1	0.1
Sum of Squares	1369.8	779.7	5082.8
RMS	3.6	2.7	7.0
Count	104	104	104

Cañutillo					Maddock				
1947					1947				
	Total	L1	L2	L3		Total	L1	L2	L3
Abs. Res. Mean	1.4	1.4	NA	NA	Abs. Res. Mean	1.7	1.7	NA	NA
Head Range	8.4	8.4	NA	NA	Head Range	9.3	9.3	NA	NA
Max. Residual	3.4	3.4	NA	NA	Max. Residual	4.0	4.0	NA	NA
Min. Residual	-5.1	-5.1	NA	NA	Min. Residual	-5.3	-5.3	NA	NA
Res. Std. Dev.	2.0	2.0	NA	NA	Res. Std. Dev.	2.3	2.3	NA	NA
Residual Mean	0.5	0.5	NA	NA	Residual Mean	0.4	0.4	NA	NA
Std/Head Range	0.2	0.2	NA	NA	Std/Head Range	0.2	0.2	NA	NA
Sum of Squares	72.8	72.8	NA	NA	Sum of Squares	89.9	89.9	NA	NA
RMS	2.0	2.0	NA	NA	RMS	2.2	2.2	NA	NA
Count	18	18	NA	NA	Count	18	18	NA	NA

1974					1974				
	Total	L1	L2	L3		Total	L1	L2	L3
Abs. Res. Mean	2.0	1.3	2.2	6.0	Abs. Res. Mean	2.7	1.1	2.7	13.3
Head Range	24.8	10.8	8.8	24.1	Head Range	72.8	10.3	10.4	72.8
Max. Residual	20.1	6.1	6.5	20.1	Max. Residual	65.7	5.7	9.0	65.7
Min. Residual	-4.7	-4.7	-2.4	-4.0	Min. Residual	-7.1	-4.6	-1.4	-7.1
Res. Std. Dev.	3.6	2.0	2.8	9.1	Res. Std. Dev.	9.1	1.8	3.1	27.9
Residual Mean	0.6	-0.1	1.5	3.7	Residual Mean	1.2	-0.2	2.1	9.1
Std/Head Range	0.1	0.2	0.3	0.4	Std/Head Range	0.1	0.2	0.3	0.4
Sum of Squares	742.3	153.7	94.0	494.6	Sum of Squares	4637.4	125.8	132.9	4378.8
RMS	3.6	2.0	3.1	9.1	RMS	9.1	1.8	3.6	27.0
Count	56	40	10	6	Count	56	40	10	6

TABLE 5-4
Measures of Model Fitness by Year for the Final Cañutillo Model and The Maddock Model

	1984			
	Total	**L1**	**L2**	**L3**
Abs. Res. Mean	1.2	1.1	1.6	NA
Head Range	5.8	3.8	4.4	NA
Max. Residual	2.0	2.0	0.7	NA
Min. Residual	-3.8	-1.8	-3.8	NA
Res. Std. Dev.	1.6	1.3	2.5	NA
Residual Mean	-0.1	0.2	-0.9	NA
Std/Head Range	0.3	0.3	0.6	NA
Sum of Squares	30.4	15.7	14.7	NA
RMS	1.5	1.3	2.2	NA
Count	13	10	3	NA

	1984			
	Total	**L1**	**L2**	**L3**
Abs. Res. Mean	1.6	1.5	1.8	NA
Head Range	10.5	7.6	5.2	NA
Max. Residual	6.2	6.2	1.0	NA
Min. Residual	-4.3	-1.4	-4.3	NA
Res. Std. Dev.	2.4	2.2	2.8	NA
Residual Mean	0.5	0.9	-1.0	NA
Std/Head Range	0.2	0.3	0.5	NA
Sum of Squares	71.7	52.4	19.3	NA
RMS	2.3	2.3	2.5	NA
Count	13	10	3	NA

	1994			
	Total	**L1**	**L2**	**L3**
Abs. Res. Mean	3.7	2.1	2.4	7.3
Head Range	21.7	8.6	6.2	19.5
Max. Residual	14.8	1.7	5.4	14.8
Min. Residual	-6.9	-6.9	-0.8	-4.8
Res. Std. Dev.	5.6	3.2	3.2	7.9
Residual Mean	1.1	-1.5	1.9	5.4
Std/Head Range	0.3	0.4	0.5	0.4
Sum of Squares	524.4	100.8	31.0	392.6
RMS	5.6	3.3	3.2	8.9
Count	17	9	3	5

	1994			
	Total	**L1**	**L2**	**L3**
Abs. Res. Mean	2.6	2.0	1.2	4.6
Head Range	16.7	8.4	3.5	16.7
Max. Residual	5.5	1.7	0.6	5.5
Min. Residual	-11.2	-6.8	-2.9	-11.2
Res. Std. Dev.	3.9	3.0	1.9	6.3
Residual Mean	-1.6	-1.5	-0.7	-2.1
Std/Head Range	0.2	0.4	0.5	0.4
Sum of Squares	283.8	91.5	8.9	183.4
RMS	4.1	3.2	1.7	6.1
Count	17	9	3	5

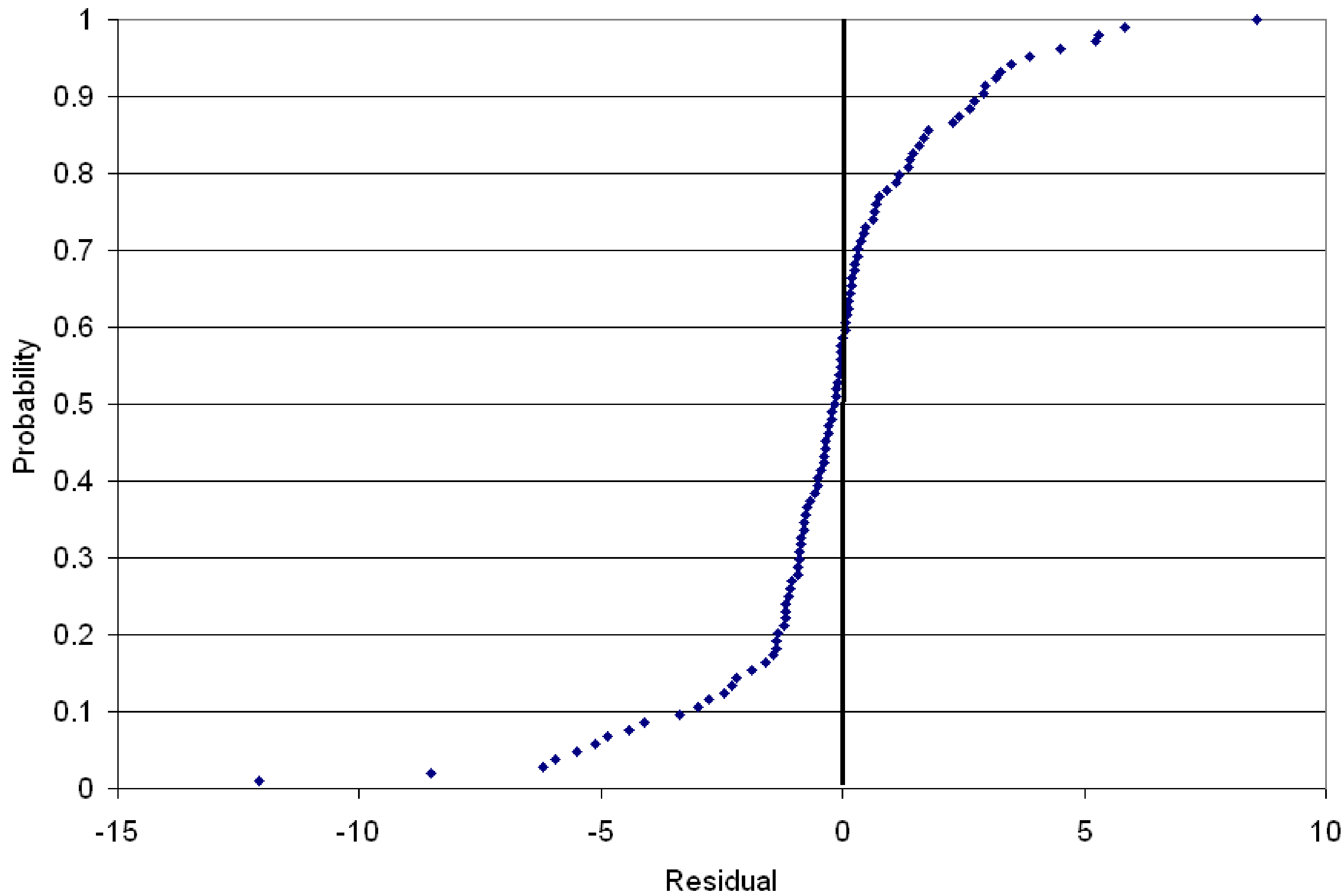

Figure 5-28. Cumulative Probability Distribution of Head Residuals

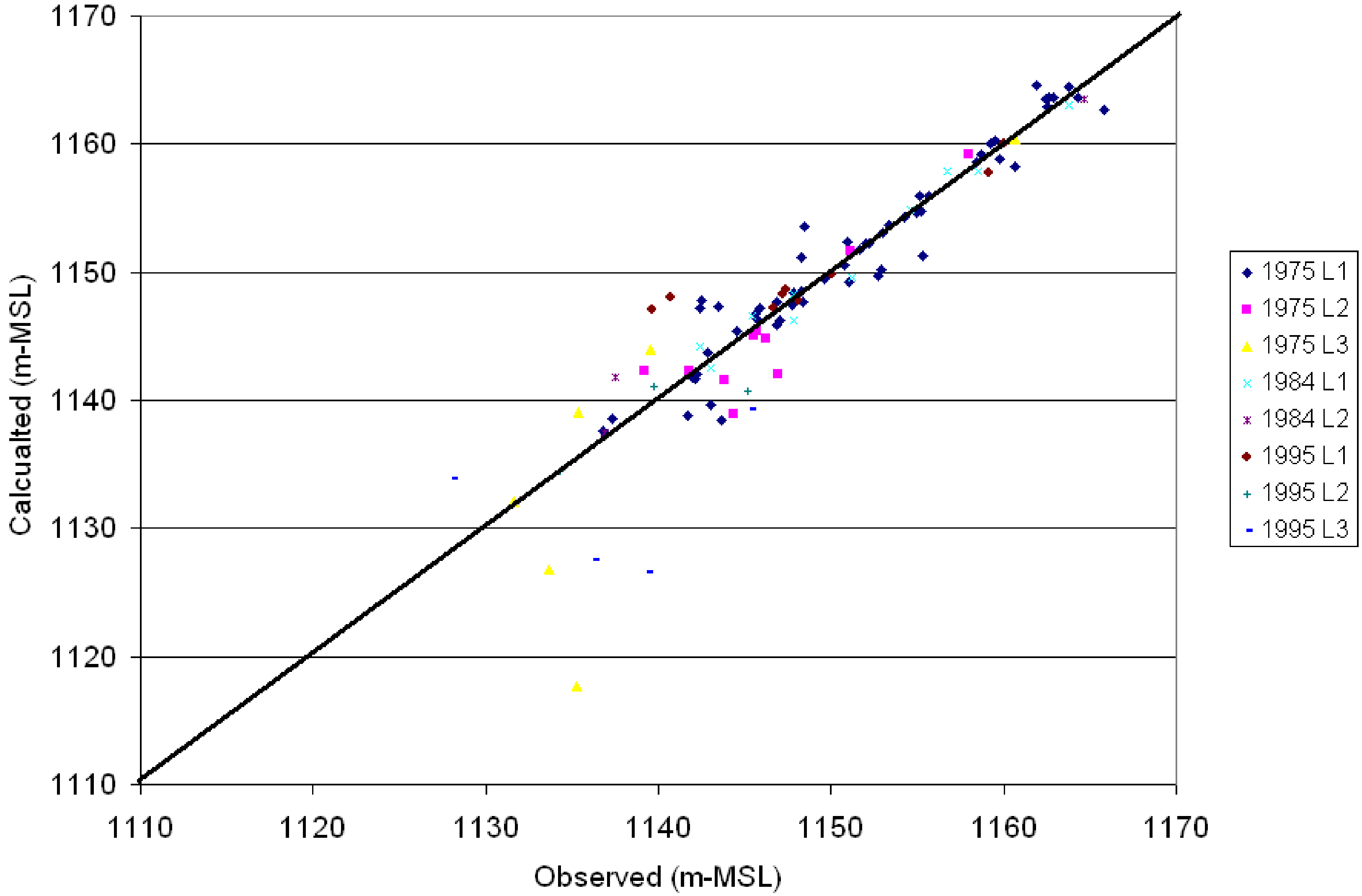

Figure 5-29. Simulated Versus Observed Heads

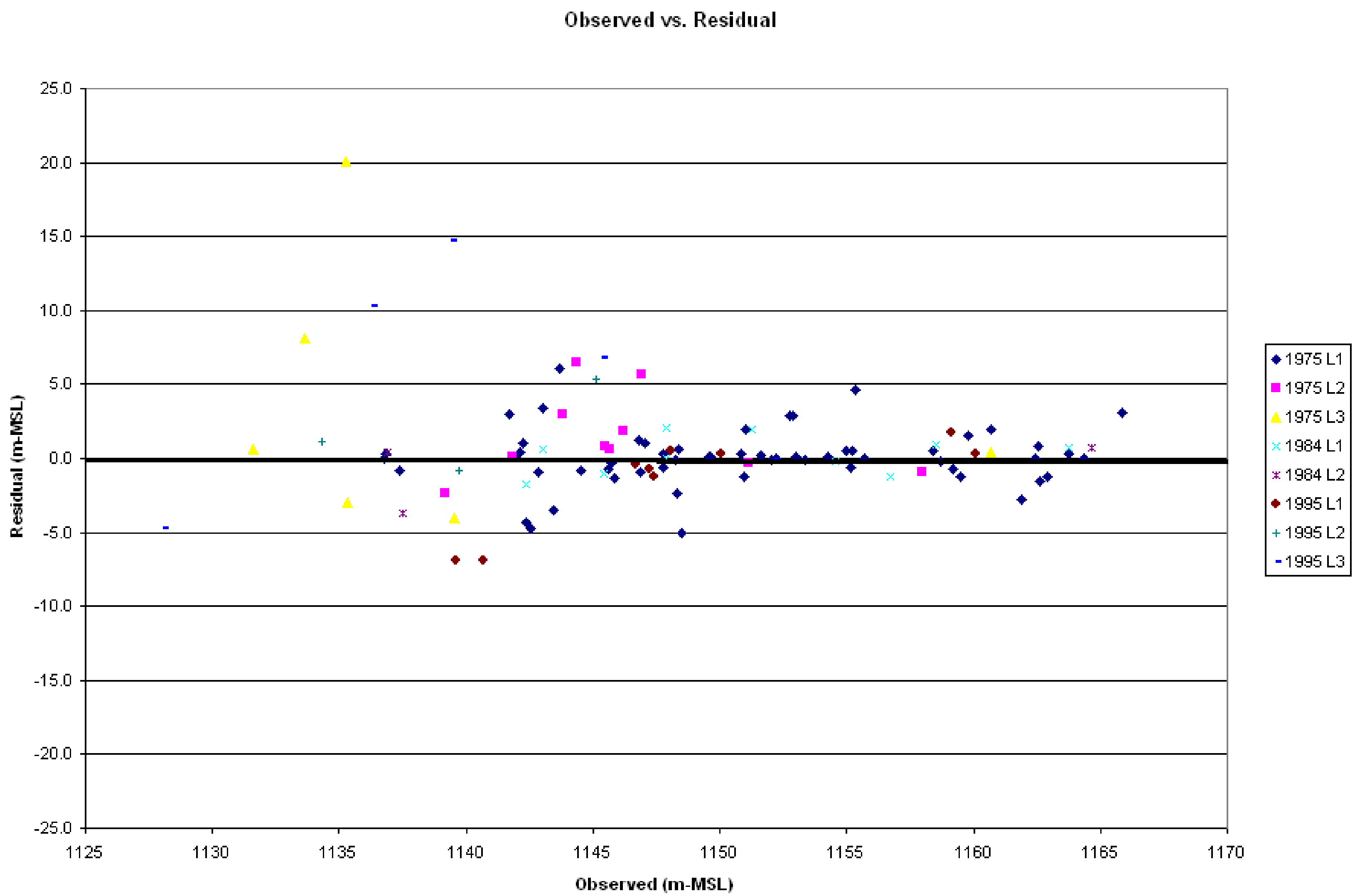

Figure 5-30. Residuals Versus Observed Heads

5.4 Inverse Model

An inverse model simulation was completed to attempt to determine if further refinement in hydraulic conductivity would result in additional improvement to the model. A universal parameter estimation code, UCODE, developed by the USGS was used for this simulation. UCODE uses nonlinear regression to match simulated values to observed values. Multiple simulations are completed and compared through an automated process.

Because the model generally matches aquifer heads well, it was assumed that for the current model hydraulic conductivities are near a local optimum. Therefore, a simulation was undertaken that only allowed minor changes to hydraulic conductivities. In this way, the inverse model could be used to fine-tune the current solution to obtain an optimal solution or a solution closer to a local optimum. The changes in conductivity resulted in so little change in the error that the changes were not statistically significant. As such, hydraulic conductivities were not changed in the final model.

5.5 Sensitivity Analysis

A sensitivity analysis was conducted to determine which parameters are important to the Cañutillo model. This analysis was conducted on the following parameters:

- Hydraulic conductivity
- Streambed elevation
- Streambed vertical conductance
- Storage
- Mountain front and slope recharge

Each parameter was changed by ±10 percent of the final calibrated value and changes in the RMS error in aquifer head and RMS error in the streamflow system were noted. Figures 5-31and 5-32 show the RMS error in the streamflow system and the RMS error in head for the analysis completed, respectively. These results show that the model is most sensitive to changes in mountain- and slope-front recharge with respect to head and most sensitive to storage with respect to streamflow. It should be noted that reducing Rio Grande bottom elevations by 10 percent resulted in a lack of convergence.

In Figure 5-31, it can be seen that some of the changes resulted in some small improvement in the model's representation of aquifer heads. However, the same changes resulted in more significant degradation of the model's representation of streamflow. Figure 5-32 demonstrates that the model is near a local optimum as none of the changes resulted in improvement in the overall goodness of fit.

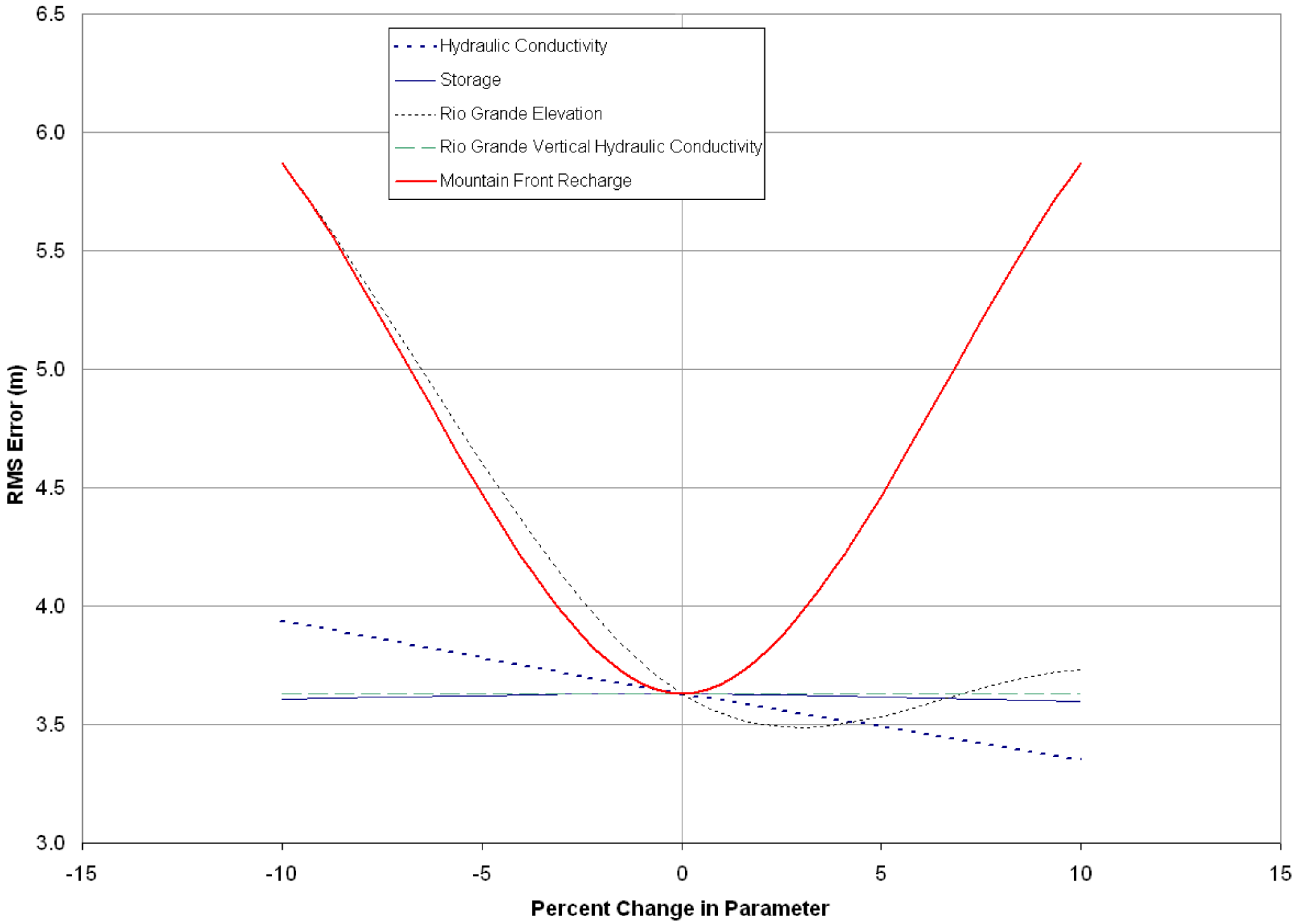

Figure 5-31. Sensitivity of RMS Error in Head to Change in Select Parameters

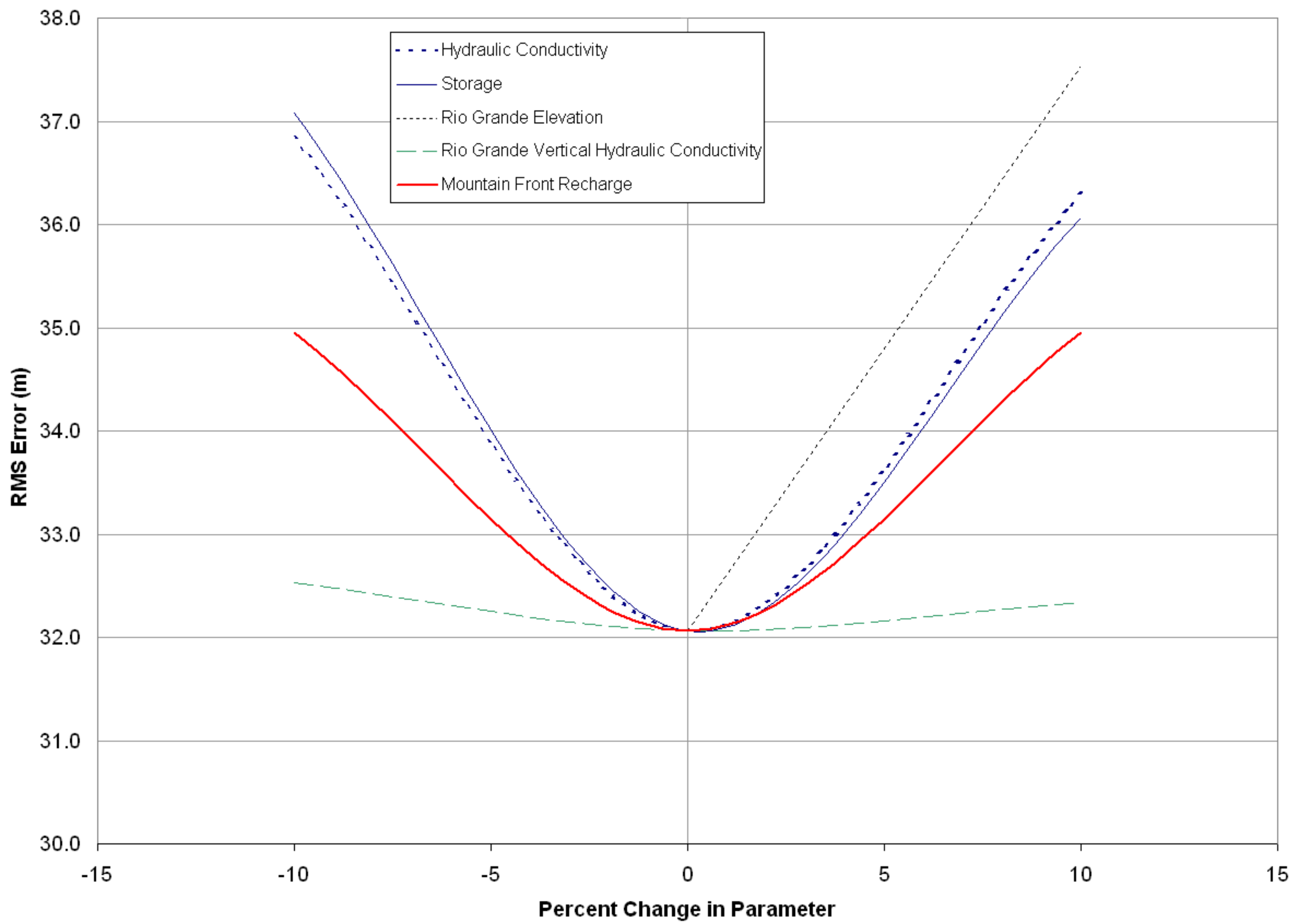

Figure 5-32. Sensitivity of RMS Error in Streamflow to Change in Select Parameters

6. Transport Model Development

6. Transport Model Development

6.1 Introduction

The Cañutillo wellfield flow and transport model was developed to provide more reliable estimates of changes in water quality over time than can be produced analytically. The transport model covers the same area as the Cañutillo flow model and uses the solved head distribution from the flow model as an input. The flow model solution is used along with estimates of initial concentration and potential concentration inflows over time to simulate changes in constituent concentration over time. Changes in concentration occur as constituents move by advection. Advection is the process of transport of particles along flow lines. The following sub-sections briefly describe the components of a transport model and the specific development of the Cañutillo wellfield transport model.

6.2 Numerical Implementation

Solute transport is described numerically with the advection-dispersion equation. This equation is extremely complicated with hyperbolic and parabolic components that cannot be readily solved by a single technique. The solution to this equation is nonlinear and discontinuous. Solutions to this equation have typically been by Eulerian methods, Lagrangian methods, or mixtures of these two techniques. The solute transport model chosen for this task, MT3DMS, provides a number of different solution techniques—the appropriateness of each depending on the aquifer system and model setup.

The following discussion of numerical implementation is based on Zheng and Wang (1998). The partial differential equations governing fate and transport of an individual species (k) in a three-dimensional transient groundwater flow system is written as shown in Equation 6.1.

$$\frac{\partial(\theta C^k)}{\partial t} = \frac{\partial}{\partial x_i}\left(\theta D_{ij}\frac{\partial C^k}{\partial x_i}\right) - \frac{\partial}{\partial x_i}\left(\theta v_i C^k\right) + q_s C_s^k + \sum R_n$$

Equation 6.1

where

C^k	is the dissolved concentration of species k, ML^{-3}
θ	is the porosity of the subsurface medium, dimensionless
t	is time, T
x_I	is the distance along the respective Cartesian coordinate axis, L
D_{ij}	is the hydrodynamic dispersion coefficient tensor, L^2T^{-1}
v_i	is the seepage or linear pore water velocity, LT^{-1} (related to the specific discharge or Darcy flux through the relationship, $v_i=q_i/\theta$)
q_s	is the volumetric flow rate per unit volume of aquifer representing fluid sources and sinks, T^{-1}

C_s^k is the concentration of the source or sink flux for species k, ML^{-3}

$\sum R_n$ is the chemical reaction term, $ML^{-3}T^{-1}$.

The left-hand side of this equation represents the rate of change in solute mass. This rate of change is then made up of the components of the right-hand side described in the following subsections.

6.2.1 Advection/Dispersion

The first term on the right-hand side is the rate of mass change due to dispersion in the x direction. Dispersion is a measure of the spread of a constituent due to the inability to follow a straight line path when traveling through the subsurface. The second term is the change in mass due to advection. Typically, solute transport problems are dominated by the advection term. Based on the local hydrogeology, it is expected that flow in the Cañutillo wellfield area will be advection dominated. Changes in macroscopic hydraulic conductivity over the model scale that result in physical dispersion are relatively small. Therefore, most change in solute mass over the model area will be due to advection.

A previous solute transport modeling effort of the Cañutillo area completed by Turnbull (1985) used relatively small dispersivities. Turnbull determined that model results were insensitive to changes in dispersivity because of the "advectively controlled flow system in the Cañutillo Well Field." Turnbull also cites studies by Pinder (1973) and Konikow and Bredhoft (1974) where similar dispersivities were used effectively on similar aquifer systems. Hill (1979) indicates that dispersion can be neglected when the width of the transition zone is small compared to the area of interest or when the contaminant is widely distributed over the area of interest. Dispersivities become most important in sharp-front type problems where a spreading of concentrations will result in the loss of model representation of high concentration spikes.

For advectively dominated problems, solution of the transport equations can result in numerical dispersion and/or artificial oscillation. Each of these problems results in incorrect model results. These problems can be mitigated with MT3DMS by choosing the method of characteristics (MOC) or third-order total-variation-diminishing (TVD) solutions or by using a fine model grid.

6.2.2 Source/Sink

The third term represents the change in solute mass due to source or sinks. Sources and sinks include aerially distributed types such as recharge and evapotranspiration and point types, such as injection or extraction wells, constant head boundaries, streamflow boundaries, and constant flux boundaries. There are a number of sources and sinks in the Cañutillo wellfield model. Sources require that a solute mass concentration be specified for each constituent. Sinks generally remove solute mass based on the model calculated concentration at the sink location. One exception is the evapotranspiration term. It is assumed that solute mass remains in the aquifer in evapotranspiration losses. In this way, solute mass is concentrated in these locations.

6.2.3 Reactions

The fourth term represents the change in mass due to reactive species. This term includes chemical reactions with other constituents, retardation, and/or radioactive decay and biodegradation. The species modeled in the Cañutillo flow and transport model include chloride, sodium, and TDS. Chloride is widely modeled as a conservative (nonreactive species). Sodium will be removed from solution through ion exchange with calcium and magnesium in clayey materials. However, because clayey materials are generally not continuous on the scale of the model, are relatively small compared to the model volume, and are not explicitly represented in the model, sodium was assumed to be conservative. This assumption may result in a mis-representation of sodium in the deeper layers in the Cañutillo area where a known locally continuous layer of clay is present. However, the model layering scheme does not explicitly account for this relatively thin layer and therefore, the assignment of a reaction location would be suspect. Assuming that sodium is a non-reactive species produces the most conservative model results. TDS is an amalgamated parameter that includes a number of different constituents. The primary components that make up TDS are sodium, chloride, bicarbonate, and sulfate. At a relatively constant pH bicarbonate will be stable. Under the typical aerobic conditions in the aquifer, sulfate will not be broken down. Because the primary components of TDS can be assumed to be conservative, TDS is assumed to be conservative. As with sodium, assuming that TDS is non-reactive produces the most conservative model results.

For both TDS and sodium linear correlations to chloride concentration were examined. These correlations indicated that it is reasonable to assume that these species are relatively conservative in the Cañutillo area. Because the Cañutillo flow and transport model examines only species assumed to be conservative, the fourth term of Equation 6.1 is zero.

For a complete description of the theory underlying MT3DMS and available solution techniques, please refer to Zheng and Wang (1998).

6.3 Model Development

The Cañutillo wellfield flow and transport model was developed to provide more reliable estimates of changes in water quality over time than can be produced analytically. The transport model covers the same area as the Cañutillo flow model and uses the solved head distribution from the flow model as an input. The flow model solution is used along with estimates of initial concentration and potential concentration inflows over time to simulate changes in constituent concentration over time. Changes in concentration occur as constituents move by advection along flow lines. The rate at which constituents move is dependent on the aquifer porosity and the degree to which the concentration is diluted through dispersion. The following subsections provide information on the development of initial input parameters for the transport model.

6.3.1 Boundary Conditions

As in the Cañutillo flow model, boundary conditions are established that represent the aquifer interaction with outside water systems. For each boundary condition in the flow model, a boundary condition with respect to constituent concentration is established. At each boundary, water flowing out of the model (except through evapotranspiration) leaves with a model calculated mass of constituent and water flowing into the model has some predetermined concentration. The following subsections describe how concentrations were assigned over time at each of the flow model boundary types. All concentration boundaries in this model can be described as or specified concentration for each stress period.

6.3.1.1 Constant Head Boundaries

Constant head cells are used to represent the aquifer boundaries on the west and north. These heads change slightly with each stress period in response to stress in the model. These heads were assigned as part of the production of the Cañutillo model through the TMR process. The concentration at each of these cells was estimated by overlaying the assumed initial concentrations with the model grid. It was assumed that concentrations would remain constant in these cells over time. Because these boundaries are relatively distant from pumping centers, it was assumed that only small amounts of water are drawn from these areas. In addition, because these boundaries are distant, any errors in initial concentration should not propagate to the pumping center within the proposed simulation period.

6.3.1.2 Constant Flux Boundaries

Constant flux boundaries are used to represent interaction between the Mesilla and Hueco Bolson as well as mountain- and slope-front recharge. Where water is flowing from the Hueco Bolson to the Mesilla Bolson, time series sample data from wells were analyzed. The average value of this inflow was used to represent concentrations in these cells. Mountain- and slope-front recharges were initially assigned based on typical recharge concentrations as presented in Chebotarev, I.I. (1955). However, after initial simulations were complete, these concentrations resulted in "bull’s-eye" patterns of higher quality water at the recharge locations. Because there is no evidence of such patterns occurring naturally, the recharge locations were assumed to have concentrations similar to present water quality in these locations. In addition, mountain- and slope-front recharge is represented as a series of injection wells at regular intervals along the mountain front and the mesa, respectively. In actuality, recharge is likely spread over a larger area resulting in relatively small volumes of water blending with groundwater thus producing little net change in local groundwater quality. Any future detailed study of recharge should include a water quality component.

Evapotranspiration is the lumped process by which water is evaporated from the groundwater surface where depth to water is relatively shallow and the uptake of water by plants resulting in transpiration to the atmosphere. As a result of either process, dissolved solids are left behind and accumulate in the groundwater. Because the model represents evapotranspiration from agricultural lands as a "net irrigation flux", it is likely that the effects of salt buildup due to evapotranspiration are under-represented.

Aquifer withdrawals as the result of pumping remove constituent mass based on the model-calculated concentration for a given cell. Agricultural wells and *de minimis* (domestic and small use) wells are not explicitly represented in the model. Agricultural wells are represented as an aerially distributed negative recharge. The recharge flux is a calculated “net irrigation flux” that includes seasonal diversion, evapotranspiration, and precipitation.

6.3.1.3 Variable Type Boundaries

The interaction of the surface water system is described as a variable type boundary condition, such that changes in aquifer head affect the amount of water that flows to or from the aquifer system. For the transport model, the hydrologic record from 1975 to 1995 was used. Where available, measured values of TDS, Cl, and Na concentrations in individual stream components were used. Where measured values were not available correlations were determined between flow and TDS concentration and/or TDS and Cl or Na concentrations. Average values for Cl and Na for drains reported by Boyle and Parsons (1999) were used where insufficient data for individual drains were available. Flow and TDS values were generally available for the Rio Grande stations and the drains. Table 6-1 presents the range of concentrations used in the surface water system.

TABLE 6-1
Concentrations Used in Surface Water System (mg/L)

	TDS	Na	Cl
Rio Grande	390-1950	70-460	40-380
Drains	670-2580	300-440	220-380
Canals	390-1650	70-430	40-300

Rio Grande concentrations were assumed to vary linearly between observation points. It is possible that Rio Grande concentrations are relatively constant until drain return flows are intercepted. However, there is not sufficient data to characterize the change in concentration at this scale.

Drain and canal concentrations were assumed to be constant over the drain or canal length. Drain concentrations are likely to decrease moving upstream. However, because drain elevations are closest to the water table near where they discharge to the river, they are most likely to leak to the subsurface near where they discharge to the river. Because drain samples were taken near the discharge point, these concentrations were assumed to be representative of drain leakage and conservative. Canal concentrations will generally increase moving downstream due to the addition of tail water runoff. However, because the increase will likely be relatively small and there is not sufficient data to characterize the increase, canal concentrations were assumed to be constant and reflect Rio Grande concentrations at the point of diversion.

6.3.2 Temporal Descritization

In the Cañutillo wellfield flow model, the simulation is divided into stress periods representing the primary and secondary irrigation season. Each of these stress periods is divided into four equally spaced time steps. Because of stability and accuracy requirements, these steps are generally too large for transport simulation. Therefore, each time step is typically further divided into transport steps. MT3DMS includes an automated procedure for determining the appropriate transport step length. The MT3DMS automated procedure was used for most of the Cañutillo flow and transport model simulations and resulted in further divisions of individual flow model time steps. Smaller divisions were input manually to examine changes to solution accuracy. It was determined that the smaller divisions did not result in significant changes to model accuracy and required considerably more processor time for computations.

6.3.3 Spatial Descritization

The Cañutillo transport model uses the same spatial descritization as the Cañutillo flow model. The Cañutillo flow model grid was chosen to be relatively fine and regular to avoid potential numerical dispersion errors in the transport model. Large grid cells and highly deformed grids can result in numerical dispersion errors in a solute transport model.

6.3.4. Hydraulic Parameters

Hydraulic parameters that control the change in concentration in the aquifer include porosity and dispersivity. The following paragraphs briefly discuss these hydraulic parameters.

6.3.4.1 Effective Porosity

Porosity is a measure of the open space in the subsurface that could contain water or other substances. In solute transport modeling, the effective porosity is used as a measure of the pore space available for flow. In most systems some portion of the true porosity is made up of dead end or unconnected pores. Because water or other substances cannot flow through these pores, they do not contribute directly to the flow field. Therefore, some smaller portion of the overall pore space is available for flow. In the advective-dispersive equation, the effective porosity acts as an acceleration parameter. The smaller the porosity, the more quickly constituents must move through the subsurface to reproduce the observed flow field.

Table 6-2 presents typical values of porosity for a range of aquifer media along with typical effective porosities from Domenico and Schwartz (1990). Turnbull (8955) used an effective porosity of 0.3 for the Mesilla Bolson. Turnbull (1985) also cited like values used in similar aquifers by Pinder (1973) and Konikow and Bredhoft (1974). Effective porosities in the range of 0.18 to 0.3 have been proposed for the Hueco Bolson transport model (Heywood 2001). As a starting point, effective porosities of 0.2 and 0.3 are proposed for this modeling effort for layers 1 and 2 through 4, respectively. These values are likely to change in the calibration process.

TABLE 6-2
Typical Porosities and Effective Porosities
(Domenico and Schwartz, 1990)

Material	Porosity (%)
Sedimentary	
Gravel, coarse	24 - 36
Gravel, fine	25 - 38
Sand, coarse	31 - 46
Sand, fine	26 - 53
Silt	34 - 61
Clay	34 - 60
Sedimentary Rocks	
Sandstone	5 - 30
Siltstone	21 - 41
Limestone, dolomite	0 - 20
Karst limestone	5 - 50
Shale	0 - 10
Crystalline Rocks	
Fractured crystalline rocks	0 - 10
Dense crystalline rocks	0 - 5
Basalt	3 - 35
Weathered granite	34 - 57
Weathered gabbro	42 - 45

TABLE 6-2, CONTINUED
Range in Values of Total Porosity and Effective Porosity

Material	Total Porosity (%)	Effective Porosity (%)
Anhydrite [a]	0.5 - 5	0.05 - 0.5
Chalk [a]	5 - 20	0.05 - 0.5
Limestone, dolomite [a]	5 - 15	0.1 - 5
Sandstone [a]	5 - 15	0.5 - 10
Shale [a]	1 - 10	0.5 - 5
Salt [a]	0.5	0.1
Granite [b]	0.1	0.0005
Fracture crystalline rock [b]	--	0.00005 - 0.01

[a] Data from Croff and others (1985).
[b] Data from Norton and Knapp (1977).

6.3.4.2 Dispersivity

Dispersivity is the sum of several components that result in a measure of the spread of constituents. While the groundwater flow equations result in flow along head gradients, in actuality, groundwater flows through a relatively tortuous path generally along the head gradient. As a result of the flow path, concentration in groundwater are often spread along a front whose width is described by dispersivity. Unfortunately, because dispersivity is a lumped parameter, it cannot be directly measured in the field. In addition, numerous researchers have shown that dispersivity changes with the scale of the problem considered both temporally and spatially.

To represent the concept of dispersivity, a number of assumptions are made. These assumptions are generally not satisfied for real-world solute transport problems. As such, the resulting representation of dispersivity is a lumped parameter that allows for additional spreading of sharp-front concentrations than would be represented by pure advection. Dispersivity values cannot be measured directly and are generally determined through simulation. In addition, dispersivity varies according to the scale of the problem. For example, in the case of the Mesilla Bolson, local areas of the aquifer can be somewhat homogeneous with changes occurring gradually at distance. Problems on this scale would generally have little dispersion. However, increasing the scale to larger areas, there is more likelihood for wholesale changes in hydraulic conductivity either through changes in depositional material or through intrusions of something such as volcanics. At this scale, dispersivity could play a greater role in concentration changes, particularly for sharp concentration fronts. In addition, the magnitude of the simulated dispersivity is somewhat dependent on the hydrogeologic representation of the aquifer. Greatly simplified representations of hydraulic conductivity generally require larger values of dispersivity to replicate the spread of constituents in the more complex natural environment.

As stated in subsection 6.1.1, it is expected that this problem is advection dominated and that dispersion can be ignored. A previous solute transport modeling effort of the Cañutillo area completed by Turnbull (1985) used relatively small dispersivities. Turnbull determined that model results were insensitive to changes in dispersivity because of the "advectively controlled flow system in the Cañutillo Well Field." Turnbull also cites studies by Pinder (1973) and Konikow and Bredhoft (1974) where similar dispersivities were used effectively on similar aquifer systems. Hill (1979) indicates that dispersion can be neglected when the width of the transition zone is small compared to the area of interest or when the contaminant is widely distributed over the area of interest. The constituents of interest in the Cañutillo wellfield area are distributed over the area of interest and generally have small transitions zones from elevated concentrations to lower concentrations when compared to the model area. Therefore, the effects of dispersivity are assumed to be small and can be ignored. Dispersivity will be examined in the calibration process as a sensitivity parameter.

6.3.5 Initial Concentrations

Initial concentrations were generated from EPWU data, Texas Water Commission (TWC, now Texas Natural Resources Conservation Commission) data, WRRI data, and data collected by Wilson et al. (1981). EPWU, TWDB, and WRRI data consist of actual sample values over time for various constituents. Data were compiled for the model layers based on average sample elevations. Generally, samples that were taken in a layer interval were used in the generation of initial concentrations for that layer. However, in a few cases, samples that were taken near the intersection of two layers and whose results were more consistent with the data in the layer above or below were assigned to the other layer. In this way, results that were not consistent with a given layer but were technically within the layer did not inappropriately skew the initial concentrations in that layer.

It should be noted that the model layering follows Weeden and Maddock (1999). Weeden and Maddock (1999) generally represented each layer as a uniform thickness. Model layering does not correspond to hydrostratigraphic units or to known concentration changes within hydrostratigraphic units. Because of this layering system, individual data known to be in distinct hydrostratigraphic units were often averaged to estimate the individual cell concentration. Likewise, borings often show that concentrations can vary by an order of magnitude within a single hydrostratigraphic unit. This practice results in error in starting concentration as well as final concentration throughout much of the model area. Therefore, initial and final concentrations should be examined as general or average values and not specific to a given well.

Initial concentrations were generated using individual point measurements gridded with universal Kriging using Surfer™. Surfer™ uses Kriging to generate data between data points. Kriging is a statistical interpolation method that chooses the best linear unbiased estimate. Unlike other interpolation techniques, Kriging considers the spatial structure of the data and preserves observed values in the final structure (Anderson and Woessner, 1990). The gridded concentration data were then examined and compared to the concentration cross-sections generated by Wilson et al. (1981). Wilson's cross-sections incorporated data from 1939 through 1976, with most values from 1978. Wilson used both direct and indirect methods to generate the cross-sections. Wilson examined samples taken at individual wells and electric resistivity measurements at various points. The results of Wilson's methods were incorporated into the other concentration data by adding select well data from Wilson's cross-sections to the other point data. The results were then again processed with Surfer™ and imported into the model as starting conditions. Figures 6-1 through 6-3 present plan and select example profile views of the Wilson cross-sections used in this analysis. Figures 6-3 through 6-7 present the initial TDS concentrations in model layers 1 through 4, respectively. Figures 6-8 through 6-11 present the initial Na concentrations in model layers 1 through 4, respectively. Figures 6-12 through 6-15 present the initial Cl concentrations in model layers 1 through 4, respectively.

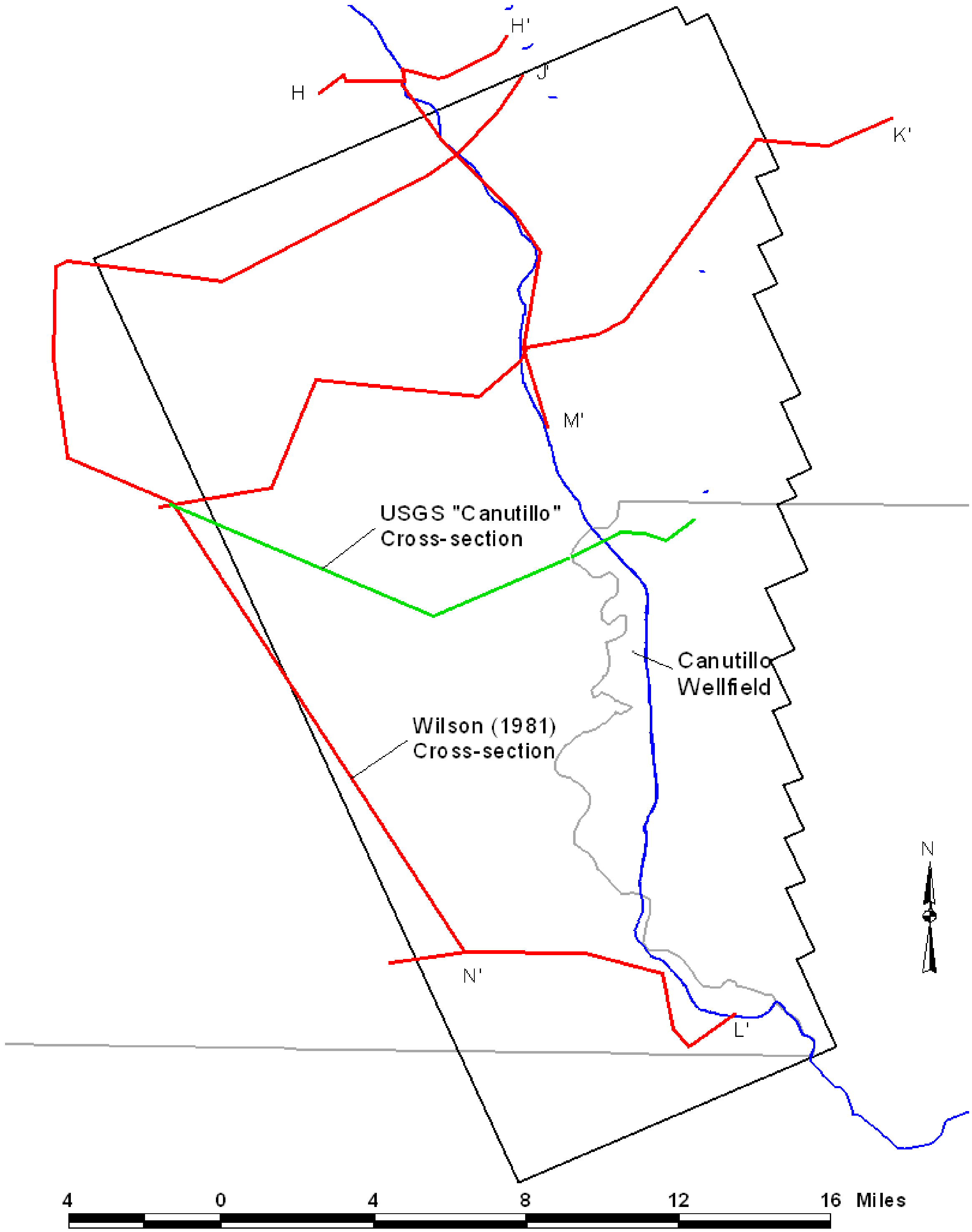

Figure 6-1. Plan View of Cross Sections Used with Individual Well Data to Generate Initial Concentrations

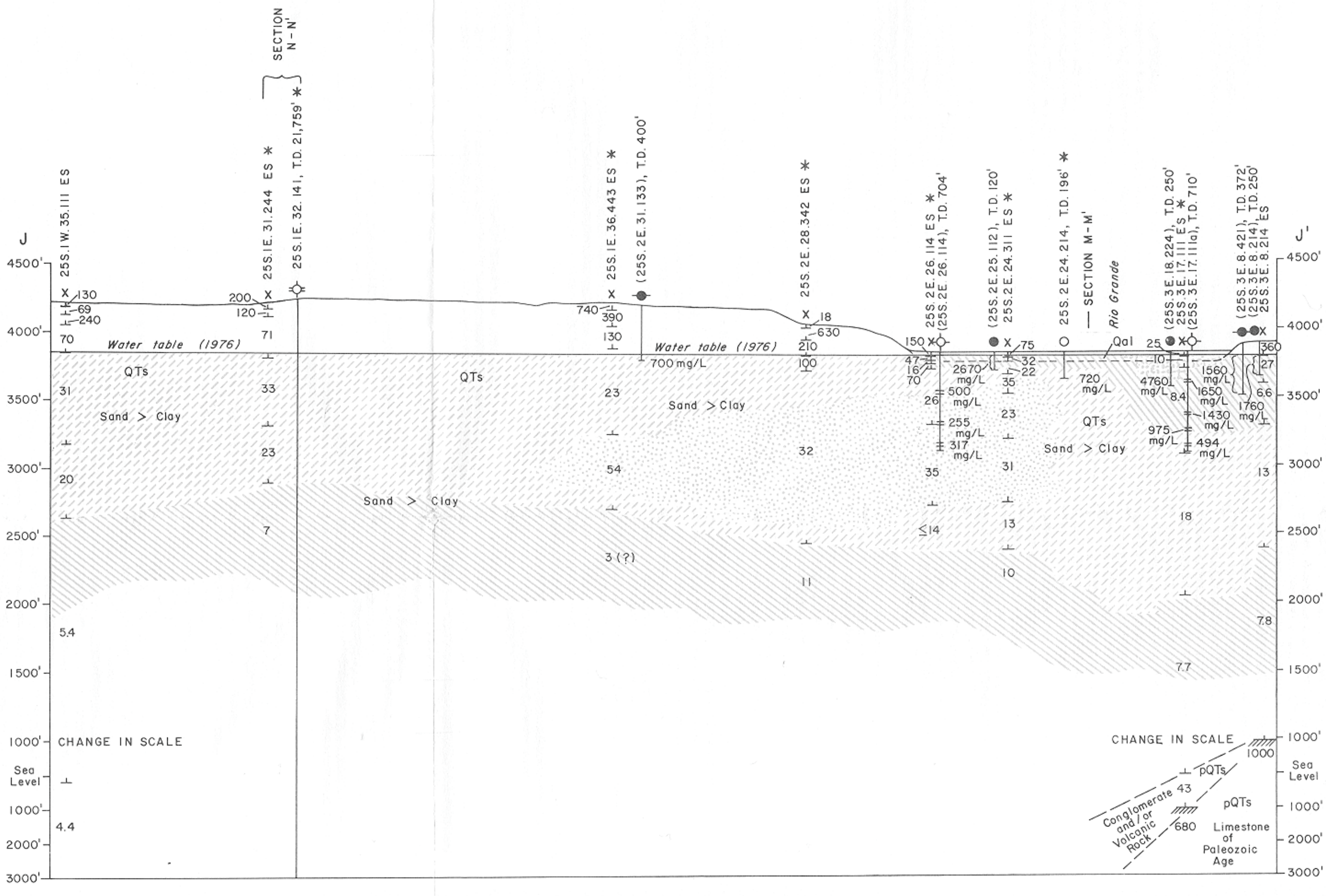

Figure 6-2. Wilson Cross-Section J-J'

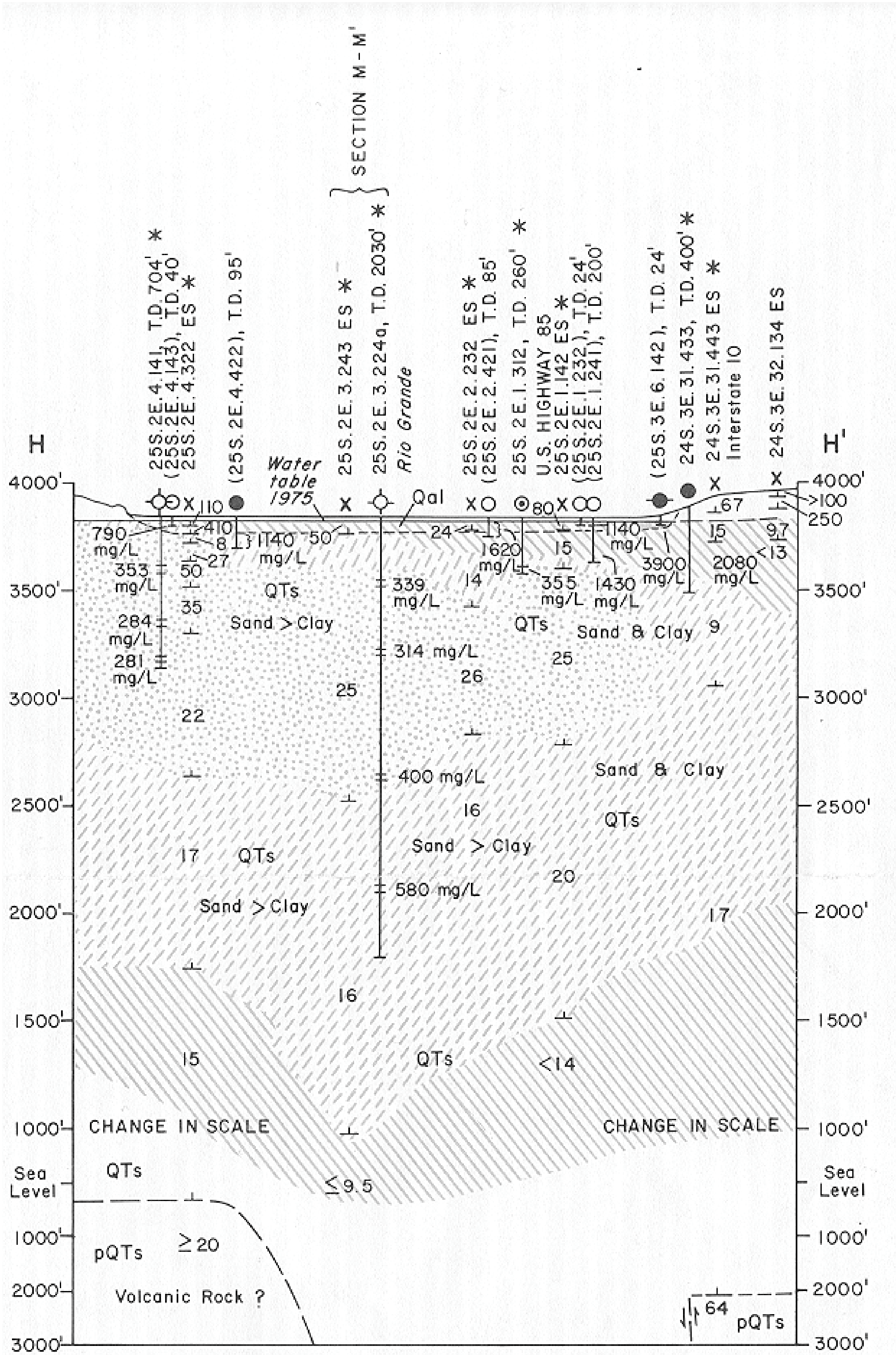

Figure 6-3. Wilson Cross-Section H-H'

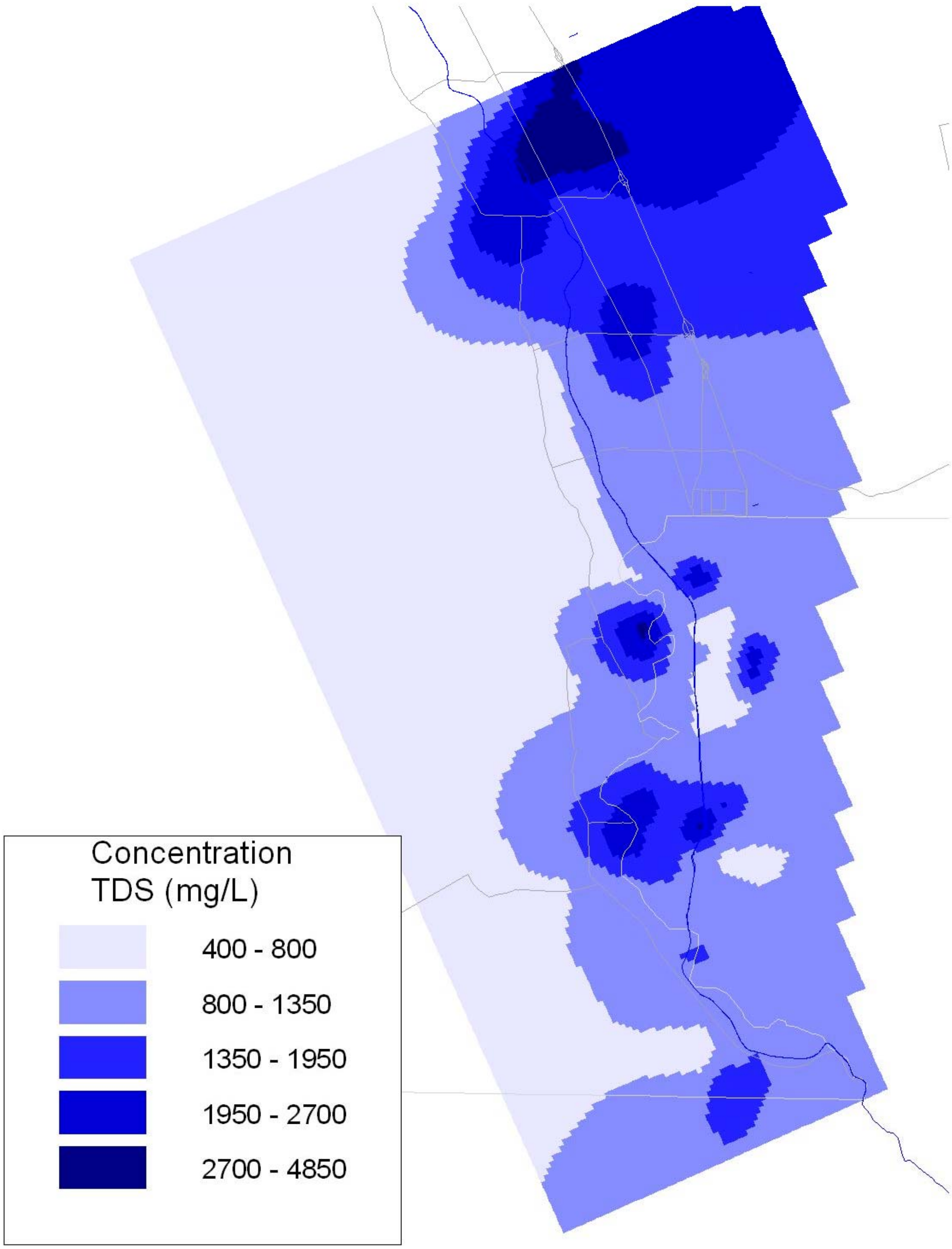

Figure 6-4. Initial TDS Concentration Layer 1

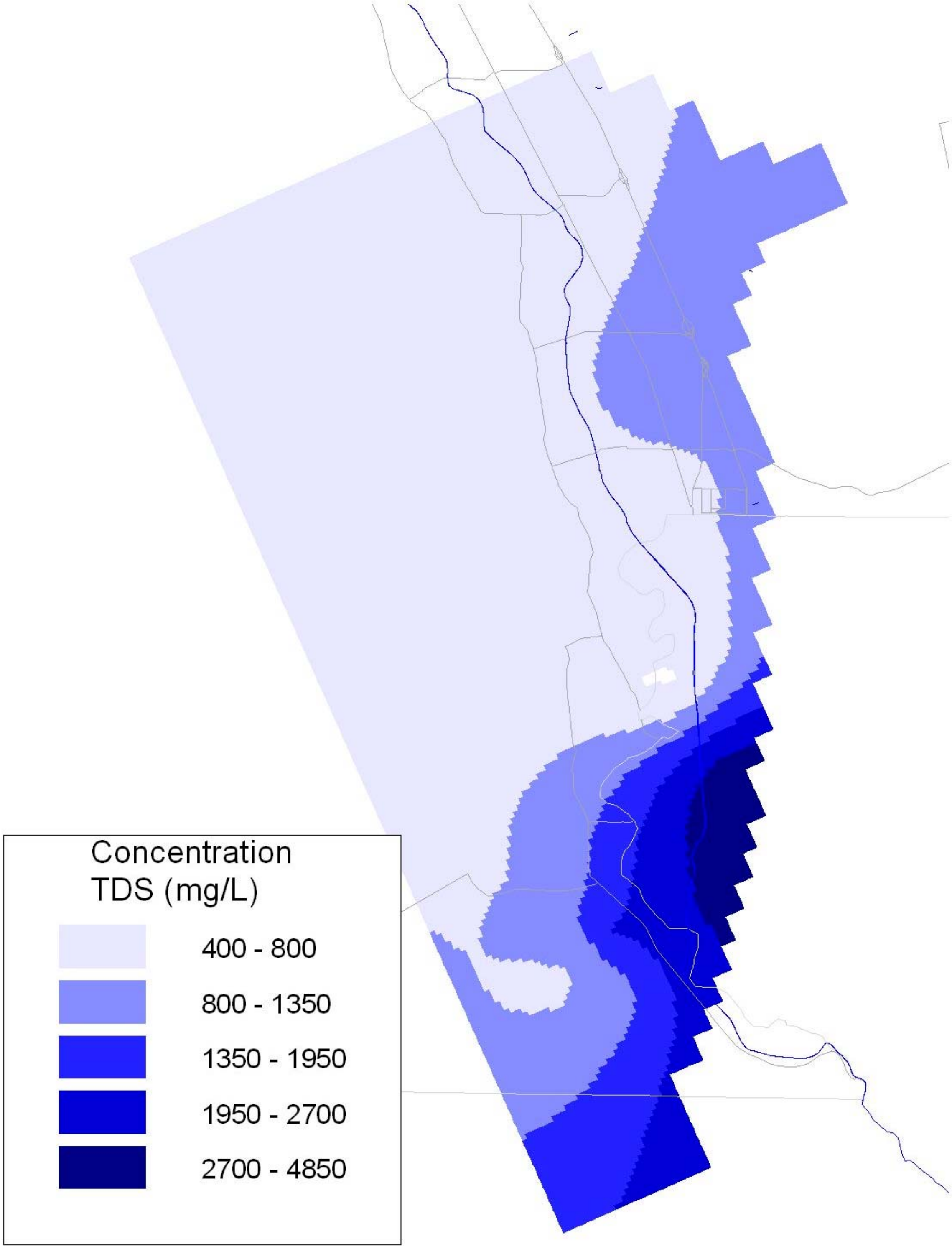

Figure 6-5. Initial TDS Concentration Layer 2

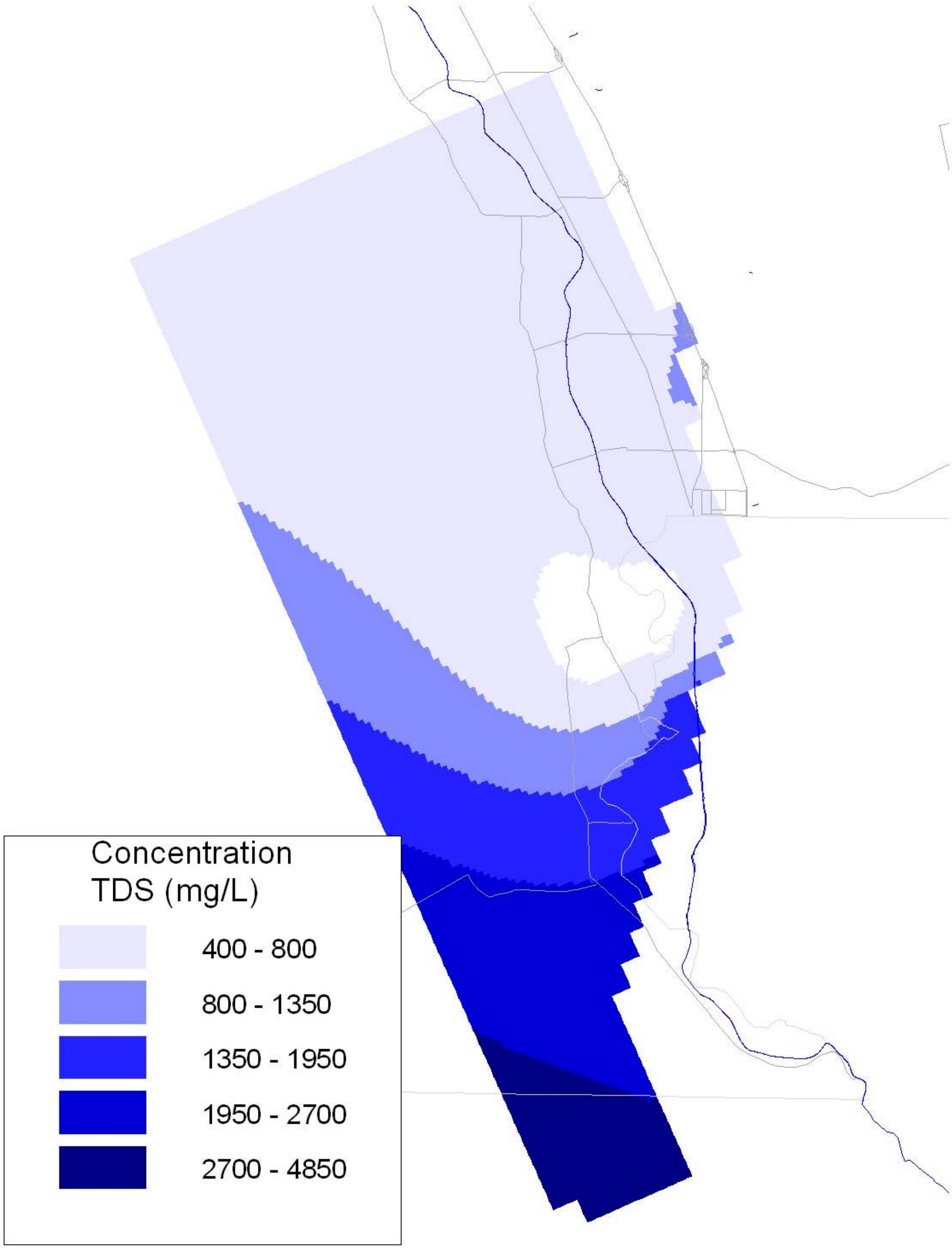

Figure 6-6. Initial TDS Concentration Layer 3

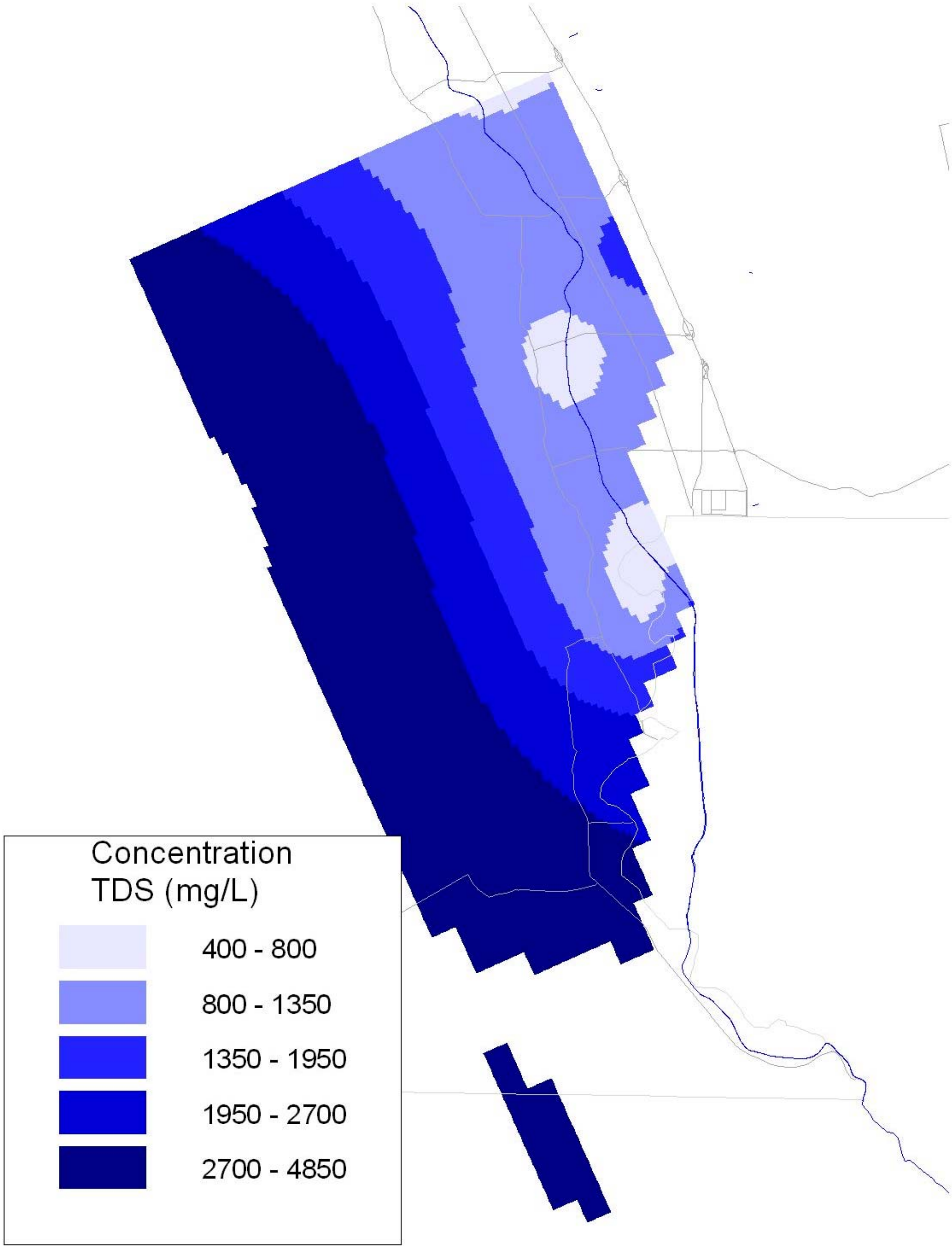

Figure 6-7. Initial TDS Concentration Layer 4

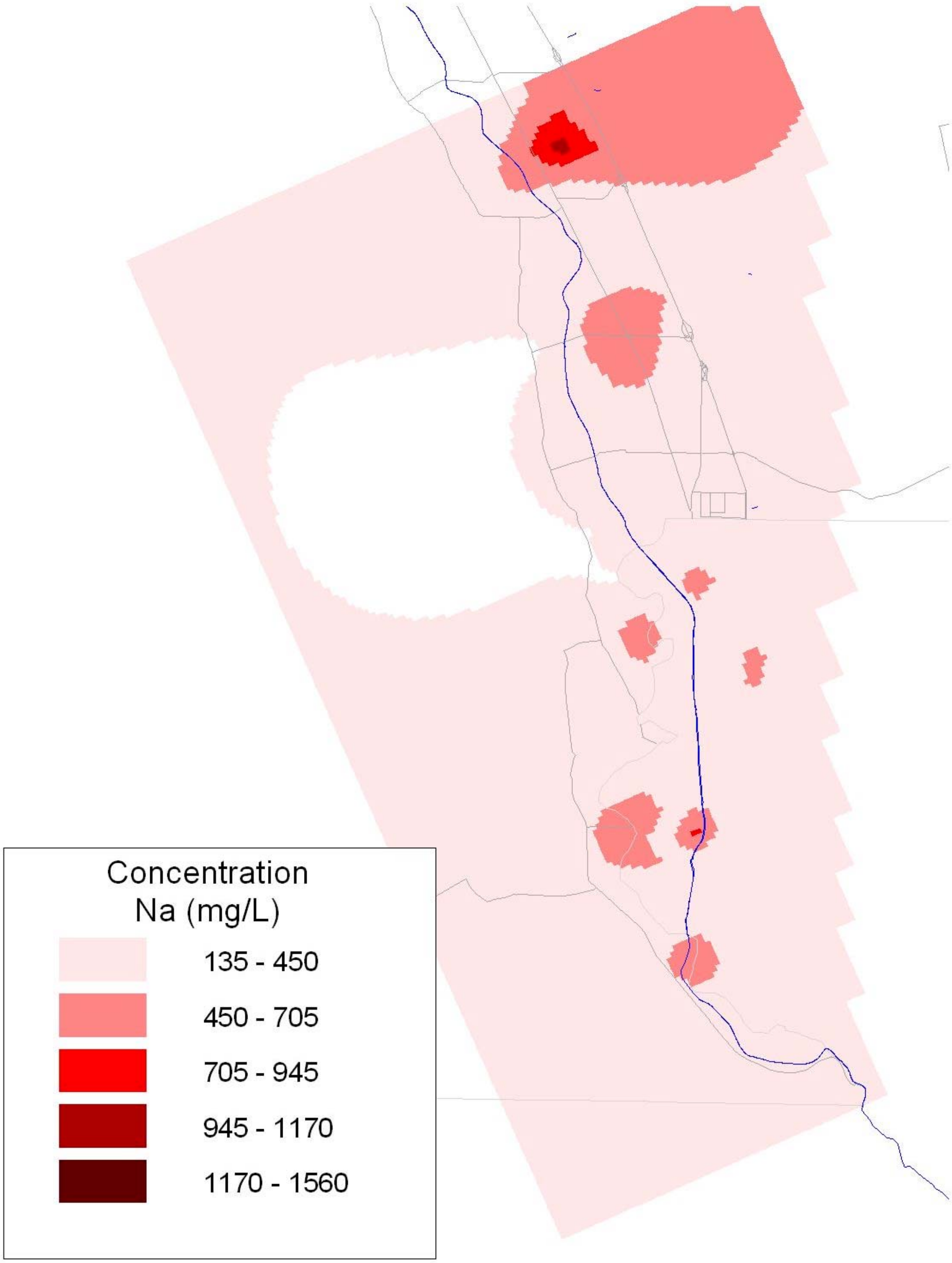

Figure 6-8. Initial Na Concentration Layer 1

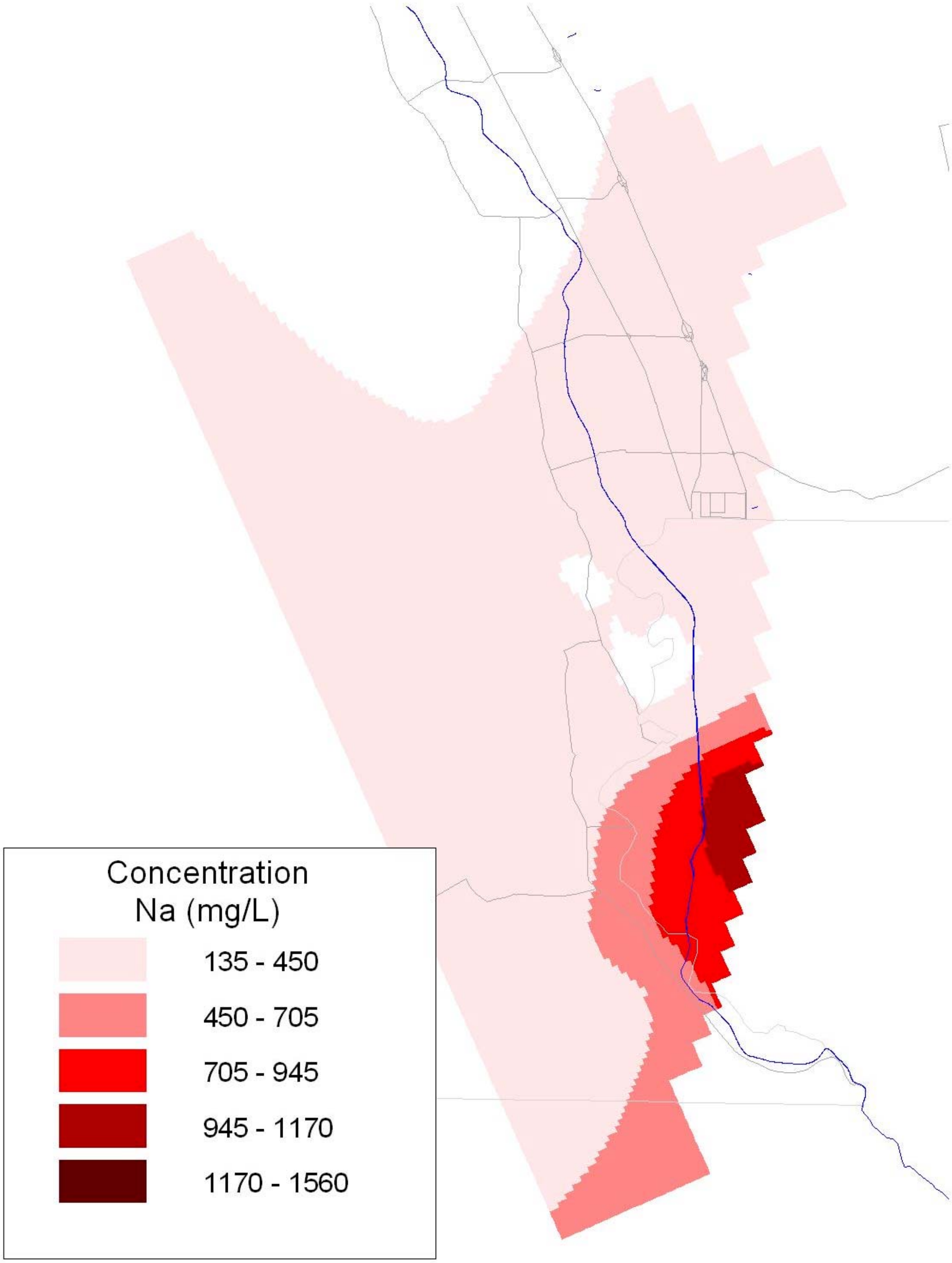

Figure 6-9. Initial Na Concentration Layer 2

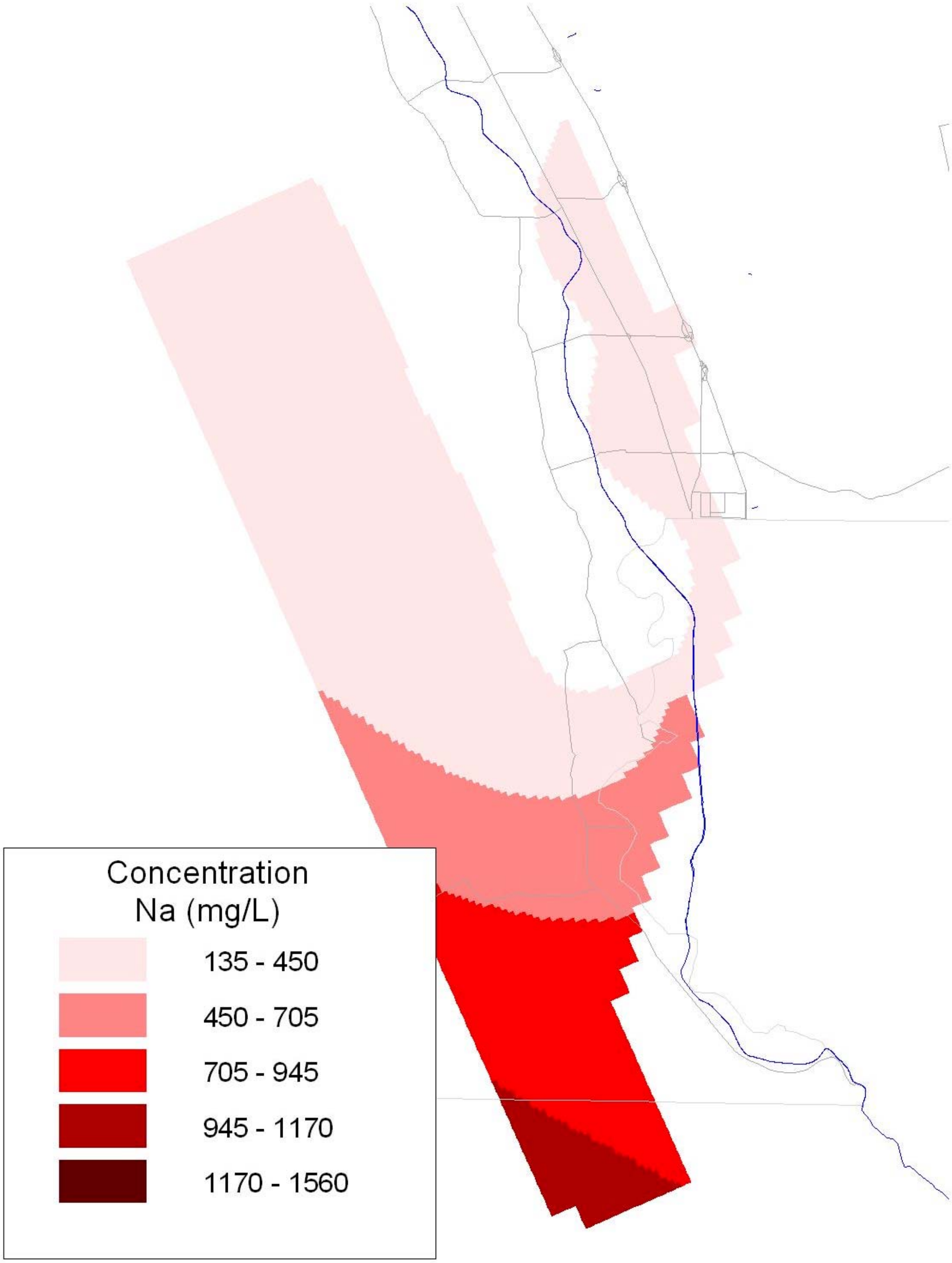

Figure 6-10. Initial Na Concentration Layer 3

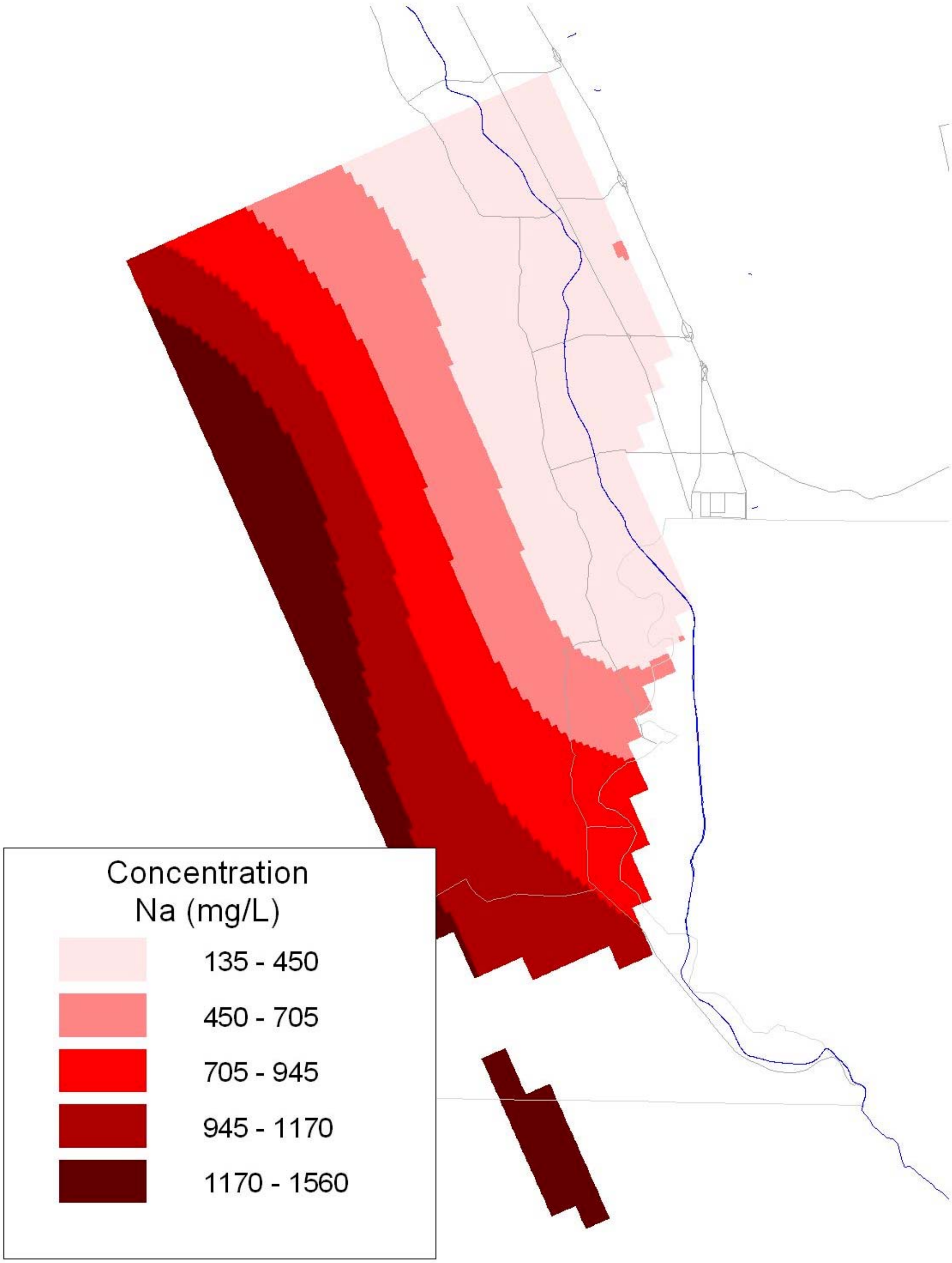

Figure 6-11. Initial Na Concentration Layer 4

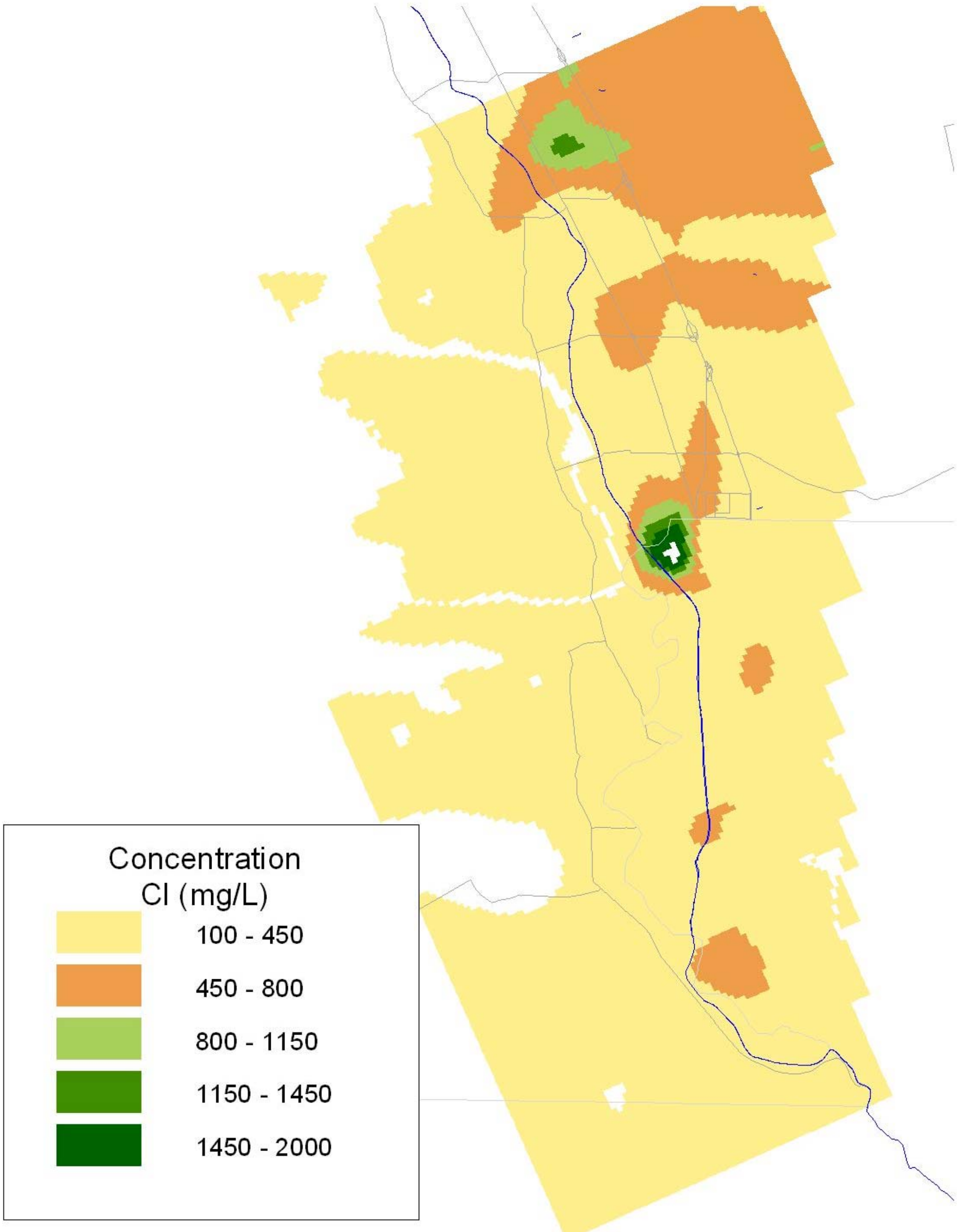

Figure 6-12. Initial Cl Concentration Layer 1

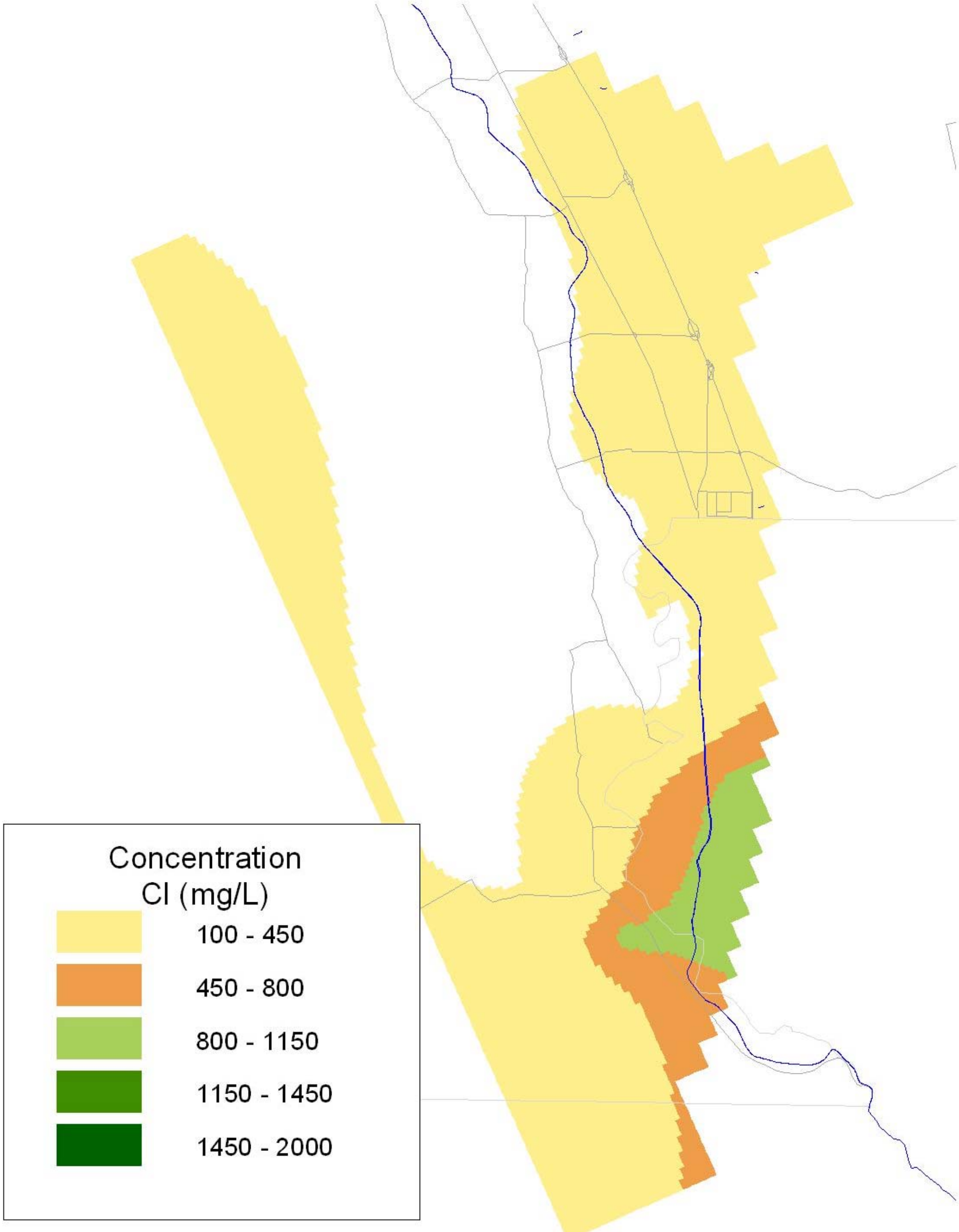

Figure 6-13. Initial Cl Concentration Layer 2

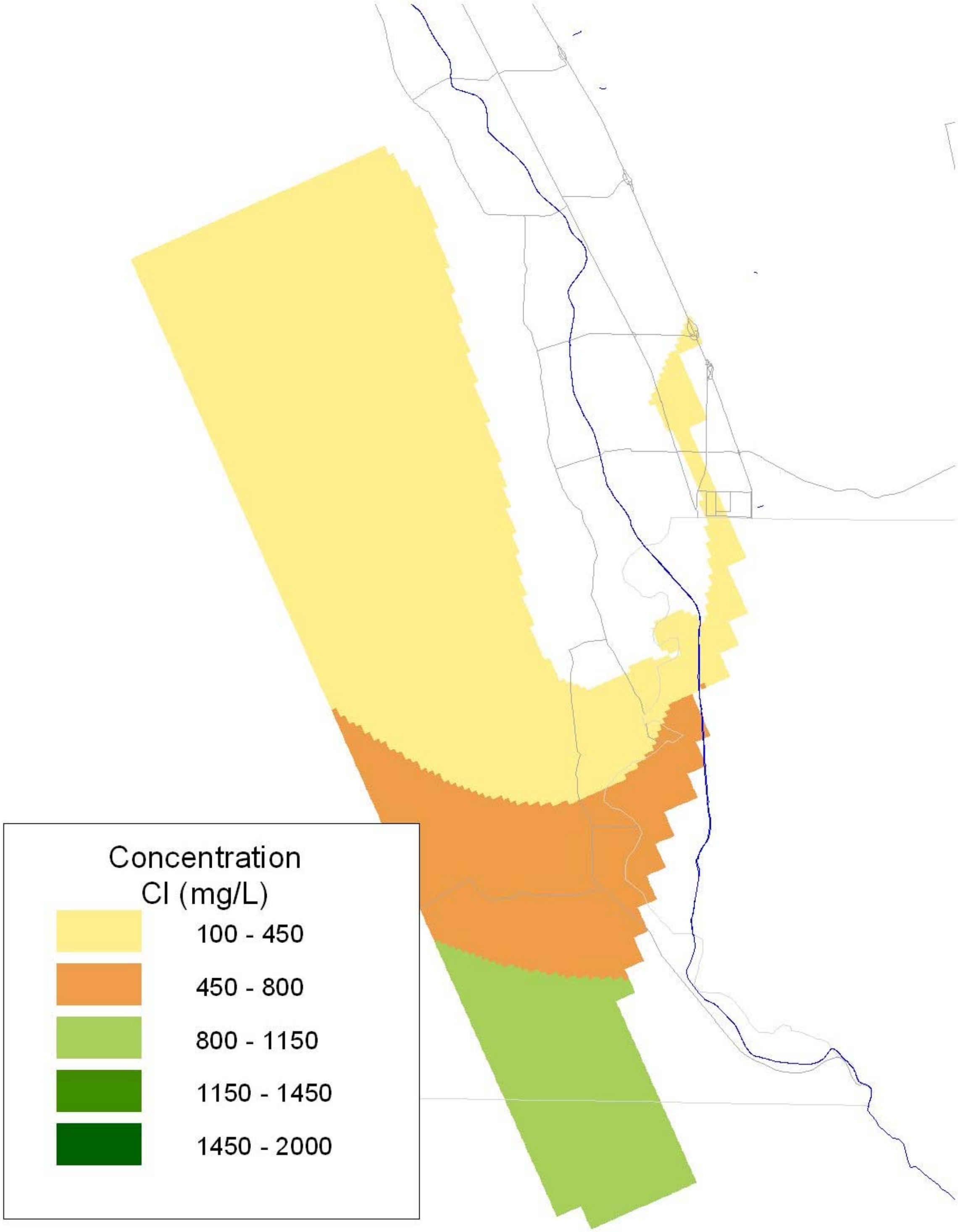

Figure 6-14. Initial Cl Concentration Layer 3

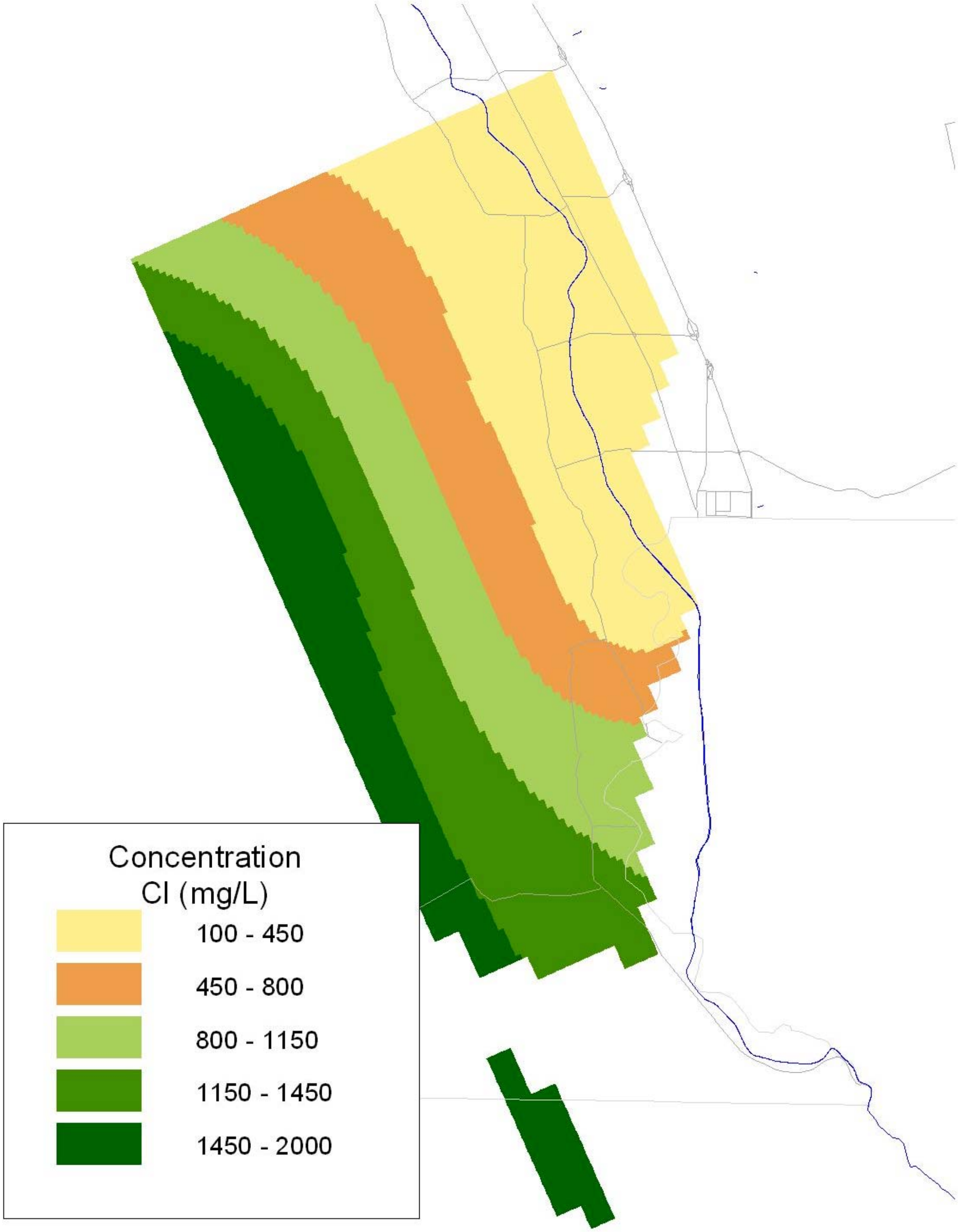

Figure 6-15. Initial Cl Concentration Layer 4

7. Transport Model Calibration

7. Transport Model Calibration

7.1 Introduction

To produce better estimates of future waster quality in the Cañutillo wellfield area than can be achieved through analytical calculations, a transport model has been developed and calibrated. Calibration of a groundwater transport model requires that concentrations in individual wells are matched over time through changing select parameters, boundary conditions, and initial concentrations. Model parameters specifically associated with the transport model such as porosity and dispersivity are altered and simulations are completed until the best model fit of simulated and observed concentrations is achieved.

In part due to the model layering scheme used by Weedon and Maddock and in part due to spatial and temporal data gaps, some level of generalization and synthesis of data are required to represent water quality in the Cañutillo area in three dimensions. As such, data collected over several years from various locations was used to produce "average" water quality profiles for "historical" and "present" conditions. In general, in areas where significant time series data are available, care was taken to represent historical or present conditions accurately. In particular, in wells where marked changes in groundwater quality occur over the time period of interest, data were used for the starting year and ending year (1970 and 1995) rather than averaging the water quality changes. The generalizations in water quality representation will increase uncertainty associated with simulation results. The following subsections describe the calibration process and results.

7.2 Target Concentrations

A relatively large database of sample results from production wells, monitoring wells, and test borings was compiled to produce not only initial concentrations but also transport model target concentrations. Most of the data points consist of individual measurements with no information on reliability. In addition, the vast majority of the data points are in the shallowest layer near centers of anthropogenic activity.

To calibrate the solute transport model, it is desirable to have calibration points that are well distributed over the model area, both horizontally and vertically. Because of the lack of consistent data over the calibration period, the Cañutillo Solute Transport model was calibrated to a single point in time. The effective calibration point in time that was selected is the end of the secondary irrigation season 1994/1995. However, sample data used for target concentrations were chosen that included dates both earlier and later than this date. In general, in the vicinity of the Cañutillo wellfield, sample data were available that were collected near this point in time. However, in some areas of the model, only a single sample has been taken over the entire calibration period. To gain broad horizontal and vertical coverage, these points were sometimes used for calibration even if they were measured significantly prior to the end of the 1994/1995 secondary irrigation season. Fortunately, these points were generally in areas of the model somewhat distant from pumping centers and where it is anticipated that little or no change in water quality has occurred over the period of interest. Calibrating to a single point in time does not allow for the analysis changes in water quality over time which could be important in examining mechanisms for degradation in EPWU wells. However, the current model-layering calibration to additional points will not likely result in additional model accuracy. Future model revisions that explore the Cañutillo area in more detail should include additional spatial and temporal calibration points.

In the Cañutillo wellfield area numerous samples from production and monitoring wells are available for use in the calibration. As discussed previously, at some locations a single layer may contain portions of several hydrostratigraphic units. In addition, the water quality within any given zone can vary by an order of magnitude. Initial concentrations were arrived upon by averaging sample concentrations in a given layer both horizontally and vertically. Model results and calibration results will reflect this averaging. As such, care was taken in choosing calibration points that represent average conditions at a given location. Figures 7-1 through 7-3 present the wells used as concentration calibration targets. Table 7-1 provides a listing of the wells used as concentration calibration targets and their TDS, Na, and Cl values used in calibration.

In the calibration process parameters are changed in an attempt to minimize the residuals between the simulated results and the observed values. An initial best estimate of likely parameter values is simulated to produce the baseline values. Results from each additional simulation are then compared to the baseline simulation to gage model improvement.

7.3 Baseline Simulation

A baseline simulation using the most likely model parameters was completed. This simulation was completed to have a basis for comparing subsequent calibration simulations. An initial effective porosity value of 0.3 was input to the model based on the work of Turnbull (1985), and the work of Pinder (1973) and Konikow and Bredhoft (1974) cited by Turnbull. Because drains are designed to intercept excess irrigation water, it was assumed that solute concentrations in drains would be similar to recharge concentrations. Recharge TDS concentrations of 1,412 mg/L were input to the model based on the calculated average concentration of drains return flow over the calibration period. Initial concentrations, concentrations in constant head cells, and surface water system concentrations were input as discussed in Chapter 6. Table 7-2 presents the composite results of this simulation. The RMS values will be compared to other simulations in later sections. As discussed in Chapter 6, the effect of dispersivity will be analyzed as part of the model sensitivity analysis.

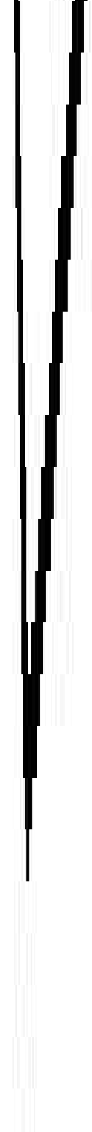

Figure 7-1. Layer 1 Wells Used for Concentration Target

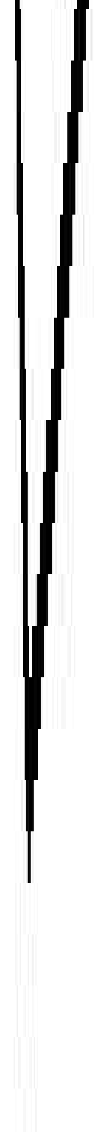

Figure 7-2. Layer 2 Wells Used for Concentration Target

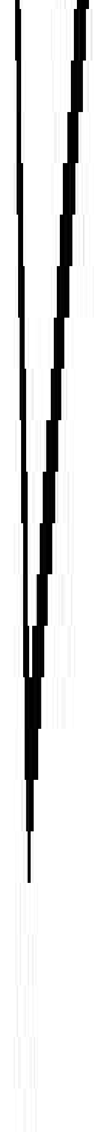

Figure 7-3. Layer 3 Wells Used for Concentration Target

TABLE 7-1
Target Wells and Concentration Data

Well Number	Well Name	Easting (m)	Northing (m)	Sample Elevation (ft)	Calculated TDS (mg/L)	Na (mg/L)	Cl (mg/L)	Layer
JL-49-04-182	AT 2	346753.6	3539211.1	3545	787	212	72	1
JL.49.04.417	CR-1	347895.2	3533819.6	3632	801	223	130	1
JL-49-04-508	El Paso County	351335.5	3534739.0	3650	1084	168	278	1
JL.49.04.415	EPWU 101	348339.5	3533296.5	3707	742	134	103	1
JL.49.04.412	EPWU 102	348274.0	3533892.5	3683	766	144	105	1
JL.49.04.406	EPWU 103	348207.7	3534568.7	3687	780	138	108	1
JL.49.04.409	EPWU 109	347179.4	3534189.6	3695	1286	217	150	1
JL.49.04.408	EPWU 111	346900.3	3533778.5	3663	681	114	76	1
JL.49.04.407	EPWU 112	346573.6	3533748.7	3661	742	144	100	1
JL.49.04.424	EPWU 116	348195.8	3535615.7	3644	780	178	120	1
JL.49.04.426	EPWU 117	347624.4	3535623.9	3644	1383	310	339	1
JL.49.04.428	EPWU 118	348352.4	3532778.9	3651	834	255	170	1
JL.49.04.495	EPWU 207	348444.3	3536744.6	3504	745	211	95	1
JL.49.04.116	EPWU 308	347188.7	3537567.3	3557	858	207	190	1
27S.02E.13.331	MT-3	339359.4	3536490.8	3620	427	160	80	1
JL-49-04-179	Sam Blount	348623.4	3537828.0	3596	1144	301	299	1
28S.03E.29.442	Santa Teresa #17	343863.7	3523577.0	3598	851	225	220	1
JL-49-04-754	Singh Test	347935.0	3528598.1	3706	1205	294	160	1
JL-49-04-488	Valley Acres Mobile	346537.8	3533577.8	3521	452	123	62	1
JL-49-04-202	Westway 2	351185.3	3537051.2	3579	1050	180	260	1
JL-49-04-507	Westway 3	350784.8	3536595.0	3515	1026	179	274	1
JL-49-04-180	Wet & Wild	350337.3	3540112.8	3683	858	200	300	1
25S.03E.06.2324A		342500.3	3559574.3	3825	2037	785	518	1
25S.03E.06.2324		342449.0	3559606.0	3845	2077	646	710	1
25S.03E.06.2433		342524.5	3559420.0	3826	1993	813	562	1
28S.02E.23.324	Santa Teresa #14	338016.0	3525439.0	3727	634	240	43	1
JL-49-04-149	Anthony 3	348250.0	3540975.0	3297	541	140	100	2
JL-49-04-174	Anthony 4	347902.0	3540518.0	3302	606	150	140	2
JL-49-04-184	Anthony 5	347941.0	3541349.0	3444	552	166	105	2
JL-49-04-183	AT 2	346754.0	3539211.0	3545	664	180	84	2
JL-49-03-335	AT 3	345669.0	3538642.0	3290	462	123	57	2
JL-49-04-172	BS 3	350298.0	3537434.0	3280	1112	274	325	2
JL.49.04.115	CR-4	347607.0	3536856.0	3400	530	135	86	2

TABLE 7-1
Target Wells and Concentration Data

Well Number	Well Name	Easting (m)	Northing (m)	Sample Elevation (ft)	Calculated TDS (mg/L)	Na (mg/L)	Cl (mg/L)	Layer
JL-49-04-753	Cullers Test	346899.0	3531355.0	3182	1807	583	496	2
JL.49.04.495	EPWU 207	348444.0	3536745.0	3504	609	179	140	2
JL.49.04.107	EPWU 301	347645.0	3536841.0	3353	457	125	80	2
JL.49.04.410	EPWU 302	347606.0	3533935.0	3400	723	194	150	2
JL.49.04.423	EPWU 304	348227.0	3536508.0	3500	631	166	140	2
JL.49.04.404	EPWU 305	347050.0	3534562.0	3484	494	123	90	2
JL.49.04.427	EPWU 306	347644.0	3535883.0	3428	613	152	150	2
JL.49.04.425	EPWU 307	348173.0	3535616.0	3461	501	131	110	2
JL.49.04.110	EPWU 309	347020.0	3538311.0	3421	725	181	138	2
JL-49-04-171	La Tuna 8	348806.0	3539519.0	3510	631	186	125	2
27S.02E.13.331	MT-3	339359.0	3536491.0	3282	425	195	46	2
28S.03E.30.412	Santa Teresa #30	341792.0	3524077.0	3519	1032	320	360	2
28S.03E.29.333	Santa Teresa #31	342640.0	3523335.0	3546	966	310	160	2
28S.02E.04.213	Santa Teresa #6	340096.0	3526254.0	3501	683	250	85	2
JL-49-04-488	Valley Acres Mobi	346538.0	3533578.0	3521	562	150	83	2
JL-49-04-173	Vinton 16 Joint	349735.0	3538428.0	3277	889	204	220	2
JL-49-04-181	Vinton Village Es	349423.0	3536831.0	3362	854	270	51	2
JL-49-04-202	Westway 2	351185.0	3537051.0	3495	1072	240	350	2
JL-49-04-507	Westway 3	350785.0	3536595.0	3515	1026	179	274	2
JL-49-03-926	Wieland Testhole	344598.0	3530373.0	3255	1727	507	379	2
JL-49-04-174	Anthony 4	347902.0	3540518.0	3082	379	100	50	3
JL-49-04-184	Anthony 5	347941.0	3541349.0	2904	497	120	73	3
JL-49-04-183	AT 1	347331.0	3540927.0	2619	464	136	65	3
JL-49-04-182	AT 2	346754.0	3539211.0	2905	314	85	45	3
JL-49-03-335	AT 3	345669.0	3538642.0	3015	367	96	50	3
JL.49.04.419	CR-2	347728.0	3536386.0	2950	304	86	37	3
JL.49.04.416	CR-3	347751.0	3534898.0	3093	1000	200	280	3
JL.49.04.111	CR-6	347630.0	3537757.0	2973	285	86	44	3
JL.49.04.402	EPWU 201	347628.0	3535907.0	2950	383	120	85	3
JL.49.04.106	EPWU 202	347644.0	3536870.0	2955	281	81	40	3
JL.49.04.104	EPWU 203	347222.0	3537591.0	2874	275	83	45	3
JL.49.04.105	EPWU 204	348017.0	3537818.0	3029	315	88	50	3
JL.49.04.401	EPWU 205	348235.0	3536386.0	3096	429	133	130	3

TABLE 7-1
Target Wells and Concentration Data

Well Number	Well Name	Easting (m)	Northing (m)	Sample Elevation (ft)	Calculated TDS (mg/L)	Na (mg/L)	Cl (mg/L)	Layer
JL.49.04.113	EPWU 206	347054.0	3538247.0	2864	307	97	68	3
JL.49.04.495	EPWU 207	348444.0	3536745.0	3014	379	115	54	3
JL-49-04-171	La Tuna 8	348806.0	3539519.0	3070	545	163	102	3
JL-49-03-926	Wieland Testhole	344598.0	3530373.0	2905	3303	943	608	3
27S.02E.13.331	mt-3	339359.0	3536491.0	2508	301	110	40	3

Notes:

1. Easting and Northing based on UTM Zone 13, NAD 1927 meters.
2. Where multiple measurements were available over the period from 1990 to 1995, values were averaged. If a 1995 value was available it was used.
3. There is not enough information to pose targets in layer 4.

TABLE 7-2
Results of Baseline Simulation for TDS Concentration

Statistic	Value
Residual Mean	-30.4
Res. Std. Dev.	100.4
Sum of Squares	791,818
Abs. Res. Mean	83.7
Min. Residual	-233.6
Max. Residual	149.2
Residual Range	382.8
Sdv/Range	0.3
RMS	104.9

7.4 Calibration Simulations

Once the baseline simulation was complete, a series of simulations was completed with effective porosity values both higher and lower than the initial value. Smaller effective porosity values will result in concentrations moving more quickly along head gradient lines than in the base case. While larger effective porosities will result in solutes moving less quickly and therefore covering a smaller distance than in the base case.

The MODFLOW recharge package in the Cañutillo model is used to represent NIF. Recharge concentrations represent the concentration of water seeping from irrigation areas to the aquifer. Because recharge concentrations are represented with average values, recharge concentrations were also varied in the simulations. As with effective porosity, individual simulations were completed for each change in recharge holding all other parameters the same as the baseline simulation. Residuals for each individual simulation were then compared model wide and on a layer-by-layer basis to the baseline simulation. In this way, the results that best reproduce the target concentrations were found. It should be noted that based on the current representation of agricultural irrigation, recharge to the aquifer may be under-represented. Therefore, estimated recharge concentrations may be artificially elevated (if the recharge flow is low then higher concentrations are required in the model to produce the same results.

Because RMS error in concentration continued to decrease with increasing effective porosity, simulations were completed with porosities that are outside of values that would be considered reasonable for this aquifer system (i.e., 0.4). Table 7-3 presents a comparison of RMS error values for TDS for various scenarios. It is apparent from this table that in general increasing the effective porosity results in a better fit of simulated to observed values. However, porosities of 0.4 and 0.5 are clearly outside of reasonable values for this type of aquifer as presented in Table 6-1. Changing recharge (excess applied agricultural water) concentration in ±10 percent intervals has little effect on the overall model fitness. The best overall model fit of simulated to observed values was achieved with porosities of 0.25 for layer 1 and 0.3 for layers 2 through 4 and with the initial TDS recharge concentration of 1,412 mg/L.

TABLE 7-3
Comparison of TDS Results for Various Calibration Parameters

Scenario	Total	Layer 1	Layer 2	Layer 3
P=0.1	155	147	132	200
P=0.2	118	129	94	137
P=0.25, 0.3 (Final)	104	126	77	108
P=0.3 (Baseline)	105	127	78	108
P=0.4	100	129	72	93
P=0.5	99	130	72	84
R=1,130	105.7	130.0	76.0	107.5
R=1,270	104.8	128.0	76.5	107.7
R=1,412 (Baseline/Final)	104.0	126.0	76.7	107.8
R=1,553	104.5	126.6	77.0	108.0
R=1,695	105.1	127.4	77.0	108.0

Notes:
1. Effective porosity values greater than or equal to 0.4 would be considered unrealistic for this aquifer.
2. P (effective porosity).
3. R (recharge TDS concentration).

Table 7-4 presents simulated versus observed concentrations for the chosen calibration scenario on a well by well basis for TDS, Na, and Cl. This table also includes summary statistics for each constituent. Simulated Cl appears to have the best fit.

TABLE 7-4
Final Cañutillo Model Simulated 1995 Results

Well Number	Well Name	Simulated TDS (mg/L)	Simulated Na (mg/L)	Simulated Cl (mg/L)	TDS Residual	Na Residual	Cl Residual	Layer
JL-49-04-182	AT 2	1026	270	218	-239	-58	-146	1
JL.49.04.417	CR-1	735	175	122	66	48	8	1
JL-49-04-508	El Paso County	1274	294	318	-190	-126	-40	1
JL.49.04.415	EPWU 101	708	146	106	34	-12	-3	1
JL.49.04.412	EPWU 102	626	140	89	140	4	16	1
JL.49.04.406	EPWU 103	630	141	90	151	-3	18	1
JL.49.04.409	EPWU 109	1181	266	214	105	-49	-65	1
JL.49.04.408	EPWU 111	731	165	116	-51	-51	-39	1
JL.49.04.407	EPWU 112	629	141	94	113	3	6	1
JL.49.04.424	EPWU 116	659	148	99	121	30	22	1
JL.49.04.426	EPWU 117	1243	297	291	140	13	48	1
JL.49.04.428	EPWU 118	721	151	111	113	104	59	1
JL.49.04.495	EPWU 207	705	152	108	40	59	-13	1
JL.49.04.116	EPWU 308	852	207	148	5	0	42	1
27S.02E.13.331	MT-3	422	159	99	5	1	-19	1
JL-49-04-179	Sam Blount	1061	281	225	83	20	74	1
28S.03E.29.442	Santa Teresa #17	931	228	204	-80	-3	16	1
JL-49-04-754	Singh Test	1324	324	243	-119	-30	-83	1
JL-49-04-488	Valley Acres Mobile	603	134	88	-151	-11	-26	1
JL-49-04-202	Westway 2	999	174	233	51	6	27	1
JL-49-04-507	Westway 3	1255	268	330	-228	-89	-56	1
JL-49-04-180	Wet & Wild	869	199	287	-11	1	13	1
25S.03E.06.2324A		2233	522	618	-196	263	-100	1
25S.03E.06.2324		2237	522	620	-160	123	90	1
25S.03E.06.2433		2163	505	587	-170	308	-25	1
28S.02E.23.324	Santa Teresa #14	694	193	50	-60	47	-7	1
JL-49-04-149	Anthony 3	619	174	112	-78	-34	-12	2
JL-49-04-174	Anthony 4	601	162	116	5	-12	24	2

TABLE 7-4
Final Cañutillo Model Simulated 1995 Results

Well Number	Well Name	Simulated TDS (mg/L)	Simulated Na (mg/L)	Simulated Cl (mg/L)	TDS Residual	Na Residual	Cl Residual	Layer
JL-49-04-184	Anthony 5	554	163	110	-2	3	-5	2
JL-49-04-183	AT 2	612	162	110	52	18	-26	2
JL-49-03-335	AT 3	517	135	56	-56	-13	1	2
JL-49-04-172	BS 3	1005	209	254	107	65	71	2
JL.49.04.115	CR-4	666	173	102	-136	-38	-16	2
JL-49-04-753	Cullers Test	1837	571	379	-30	12	117	2
JL.49.04.495	EPWU 207	647	173	129	-39	5	11	2
JL.49.04.107	EPWU 301	660	173	103	-203	-48	-23	2
JL.49.04.410	EPWU 302	728	214	177	-5	-20	-27	2
JL.49.04.423	EPWU 304	605	160	119	26	6	21	2
JL.49.04.404	EPWU 305	503	134	100	-9	-11	-10	2
JL.49.04.427	EPWU 306	603	153	105	10	-1	45	2
JL.49.04.425	EPWU 307	526	138	109	-25	-7	1	2
JL.49.04.110	EPWU 309	636	165	108	89	16	30	2
JL-49-04-171	La Tuna 8	631	170	130	0	16	-5	2
27S.02E.13.331	MT-3	425	194	50	-1	1	-4	2
28S.03E.30.412	Santa Teresa #30	1025	295	234	7	25	126	2
28S.03E.29.333	Santa Teresa #31	928	275	254	38	35	-94	2
28S.02E.04.213	Santa Teresa #6	860	243	81	-177	7	4	2
JL-49-04-488	Valley Acres Mobi	648	190	127	-86	-40	-44	2
JL-49-04-173	Vinton 16 Joint	845	215	220	44	-11	0	2
JL-49-04-181	Vinton Village Es	742	187	179	112	83	-128	2
JL-49-04-202	Westway 2	1157	211	288	-85	29	62	2
JL-49-04-507	Westway 3	1040	223	273	-14	-44	1	2
JL-49-03-926	Wieland Testhole	1688	498	249	39	9	130	2
JL-49-04-174	Anthony 4	496	121	50	-117	-21	0	3
JL-49-04-184	Anthony 5	558	145	98	-61	-25	-25	3
JL-49-04-183	AT 1	502	127	51	-38	9	14	3
JL-49-04-182	AT 2	369	98	51	-55	-13	-6	3
JL-49-03-335	AT 3	346	93	50	21	3	0	3
JL.49.04.419	CR-2	454	129	82	-150	-43	-45	3
JL.49.04.416	CR-3	851	221	272	149	-21	8	3
JL.49.04.111	CR-6	416	124	75	-131	-38	-31	3

TABLE 7-4
Final Cañutillo Model Simulated 1995 Results

Well Number	Well Name	Simulated TDS (mg/L)	Simulated Na (mg/L)	Simulated Cl (mg/L)	TDS Residual	Na Residual	Cl Residual	Layer
JL.49.04.402	EPWU 201	484	131	92	-101	-11	-7	3
JL.49.04.106	EPWU 202	450	133	99	-169	-52	-59	3
JL.49.04.104	EPWU 203	405	119	71	-130	-36	-26	3
JL.49.04.105	EPWU 204	458	138	80	-143	-50	-30	3
JL.49.04.401	EPWU 205	520	145	105	-91	-12	25	3
JL.49.04.113	EPWU 206	384	108	63	-77	-11	5	3
JL.49.04.495	EPWU 207	531	152	102	-152	-37	-48	3
JL-49-04-171	La Tuna 8	505	136	54	40	27	48	3
JL-49-03-926	Wieland Testhole	3204	917	599	99	26	9	3
27S.02E.13.331	mt-3	310	114	51	-9	-4	-11	3

Summary Statistics

	TDS	Na	Cl
Maximum Negative Residual	-239	-126	-146
Maximum Positive Residual	151	308	130
Average	-28	5	-1
Abs Average	84	35	35
RMS	104.4	61.5	49.7

Figures 7-4 through 7-12 present the residuals by layer for TDS, Na, and Cl, respectively. These figures demonstrate the absence of spatial bias in the results. A model with spatial bias tends to have a separation of positive and negative residuals rather than the random pattern demonstrated in these figures. Because of a lack of deep monitoring wells, residuals were not calculated for layer 4.

Figure 7-13 provides the probability distribution of TDS residuals. The probability of a zero residual is approximately 50 percent. Ideally, the residual values should make a sharp “s” curve with most of the values falling along an almost vertical section near 0 rather than the gradual sloping curve shown. However, as stated previously, the model layering scheme and the lack of concentration data requires averaging of concentration data. As such it is difficult to minimize residuals at individual observation points. Figure 7-14 presents simulated versus observed values of TDS concentration by layer. Most values fall relatively near the 1:1 sloped diagonal line indicating a good overall fit. Figure 7-15 shows TDS residuals versus observed TDS concentration. This plot shows that errors appear to be distributed randomly.

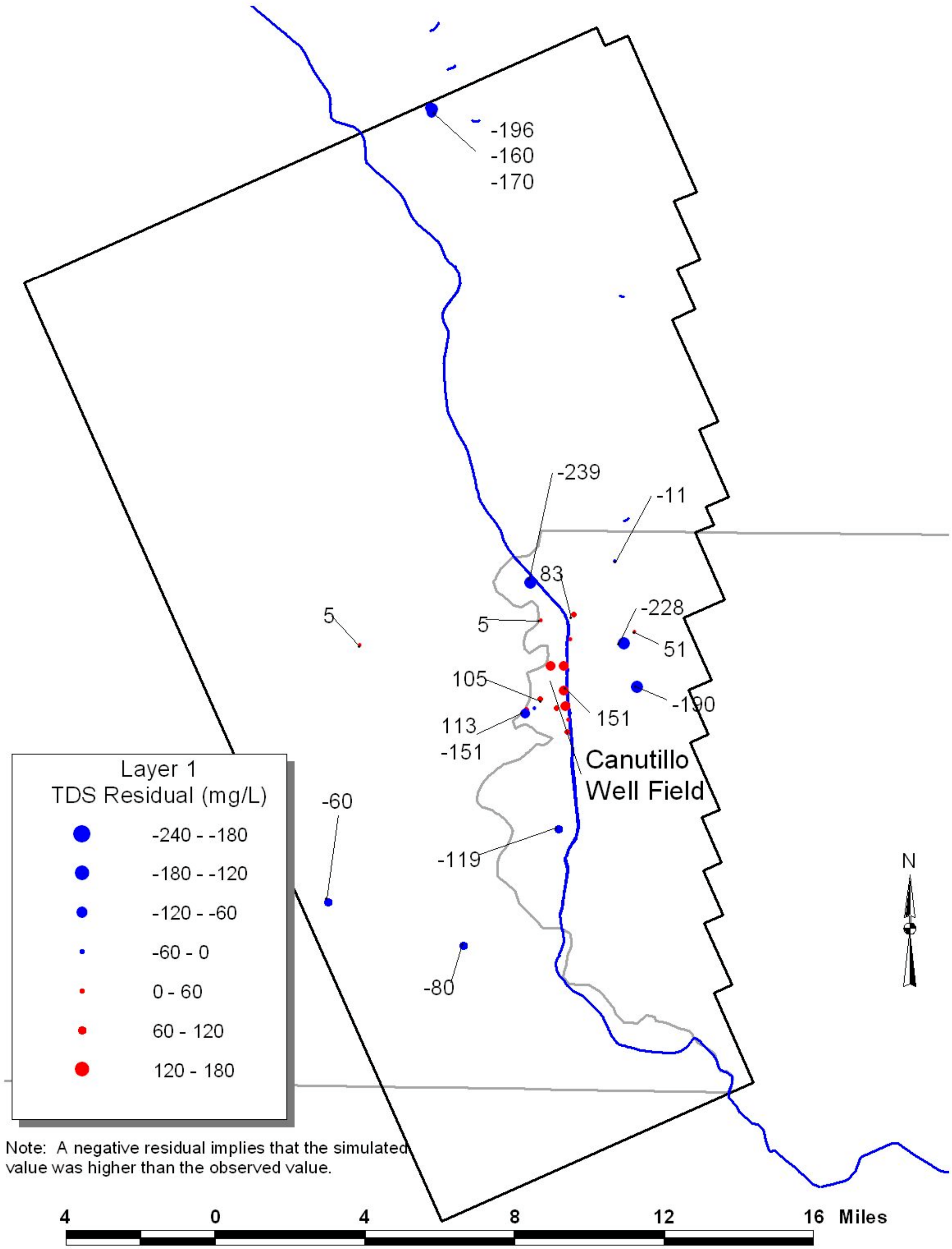

Figure 7-4. Layer 1 TDS Residual

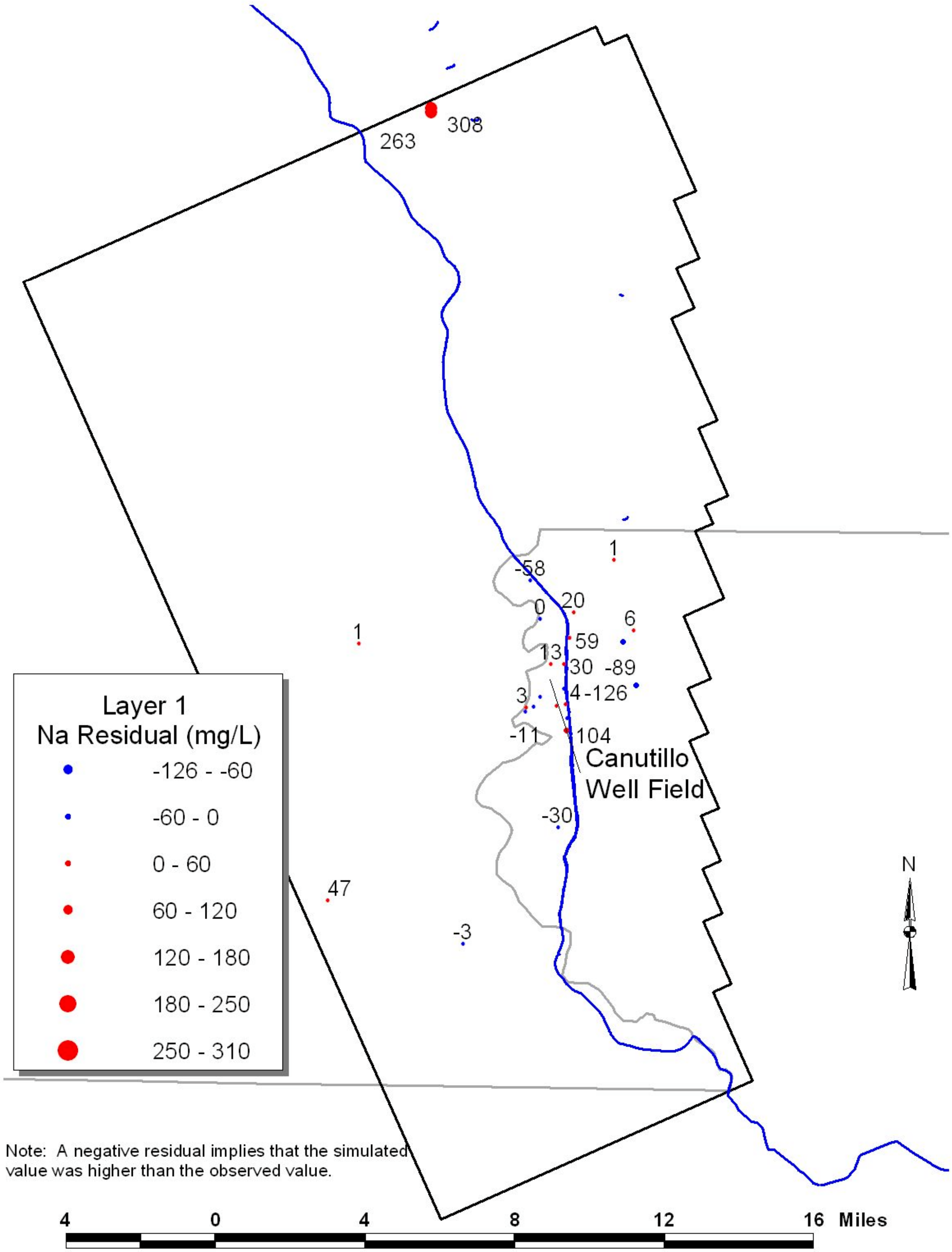

Figure 7-5. Layer 1 Na Residual

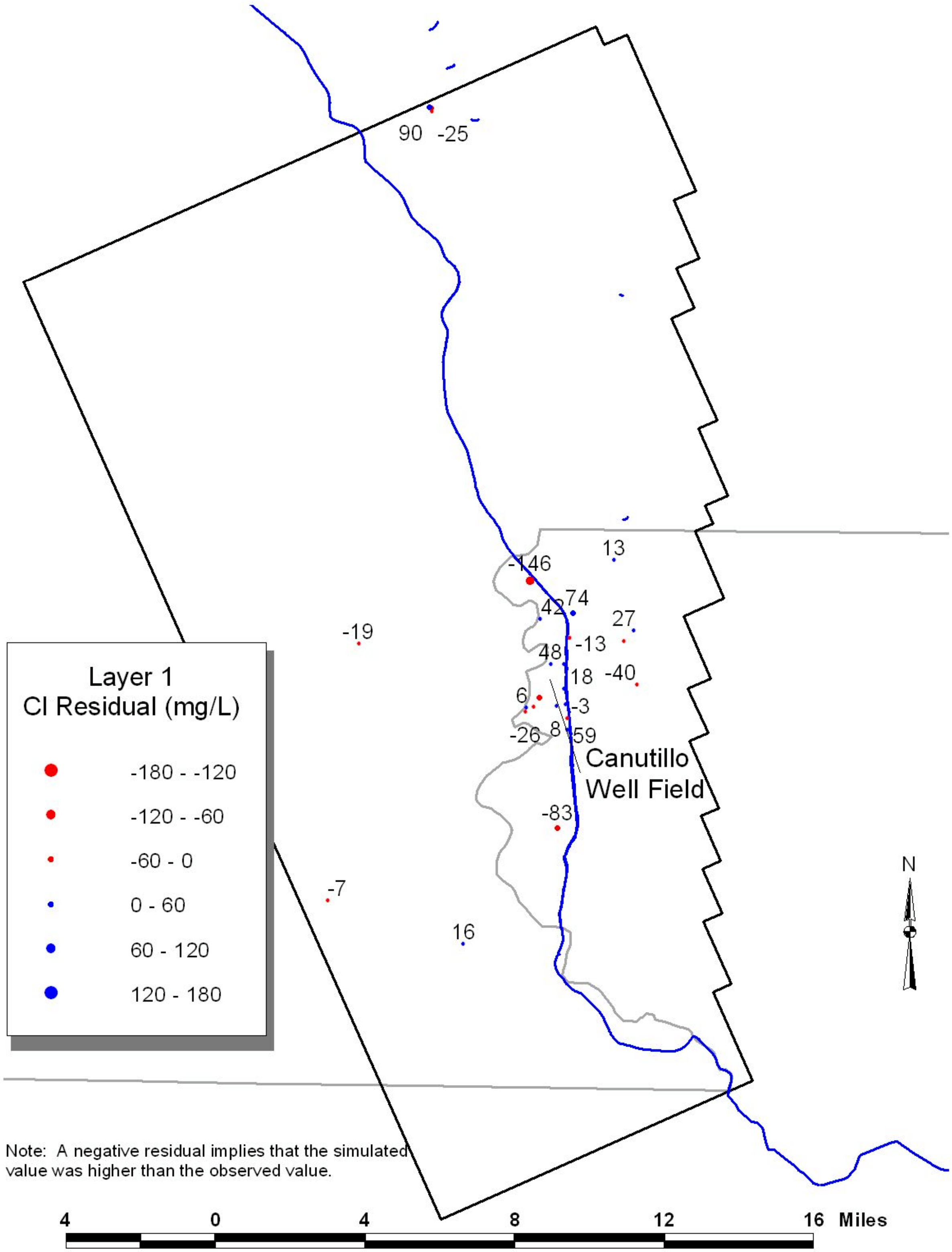

Figure 7-6. Layer 1 Cl Residual

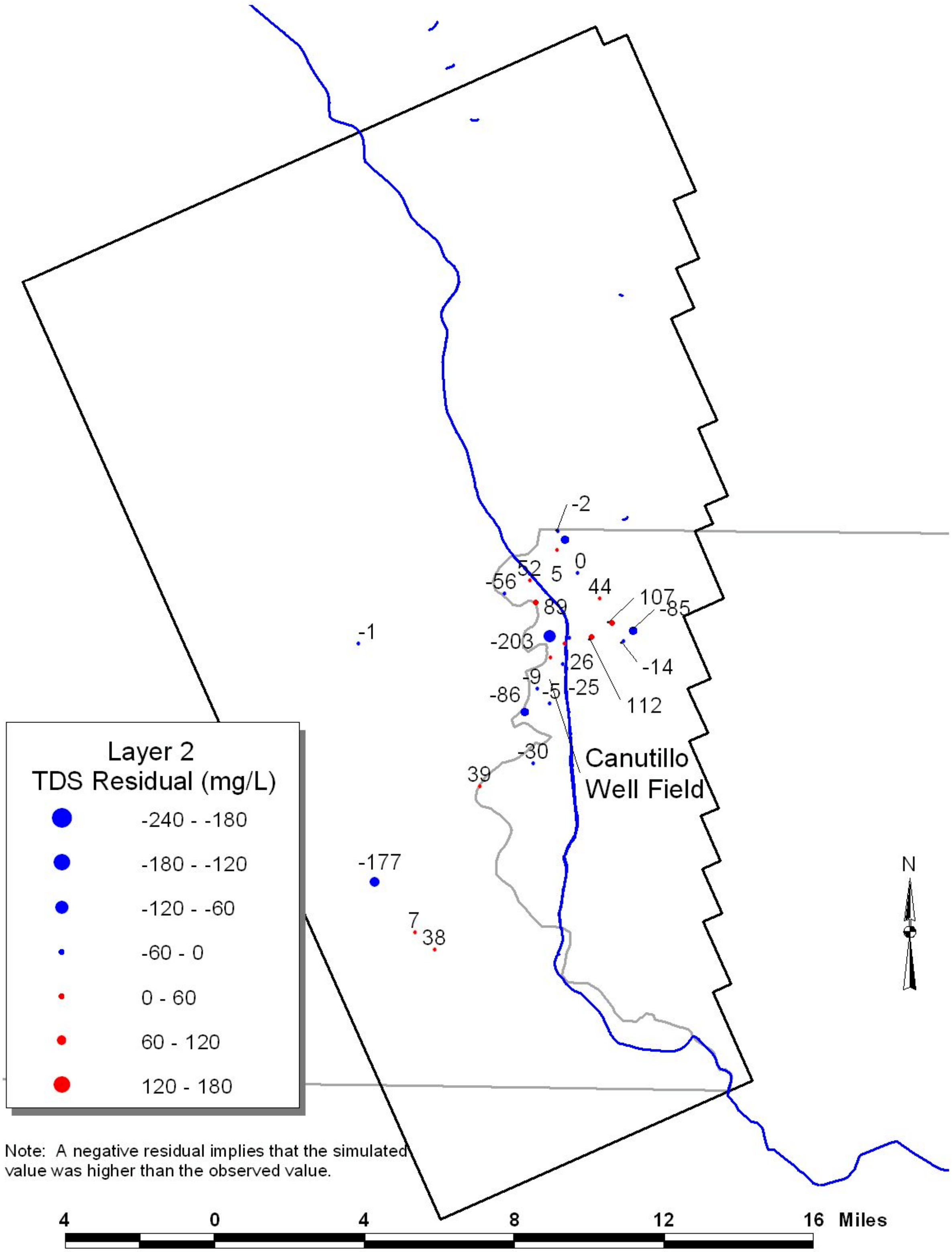

Figure 7-7. Layer 2 TDS Residual

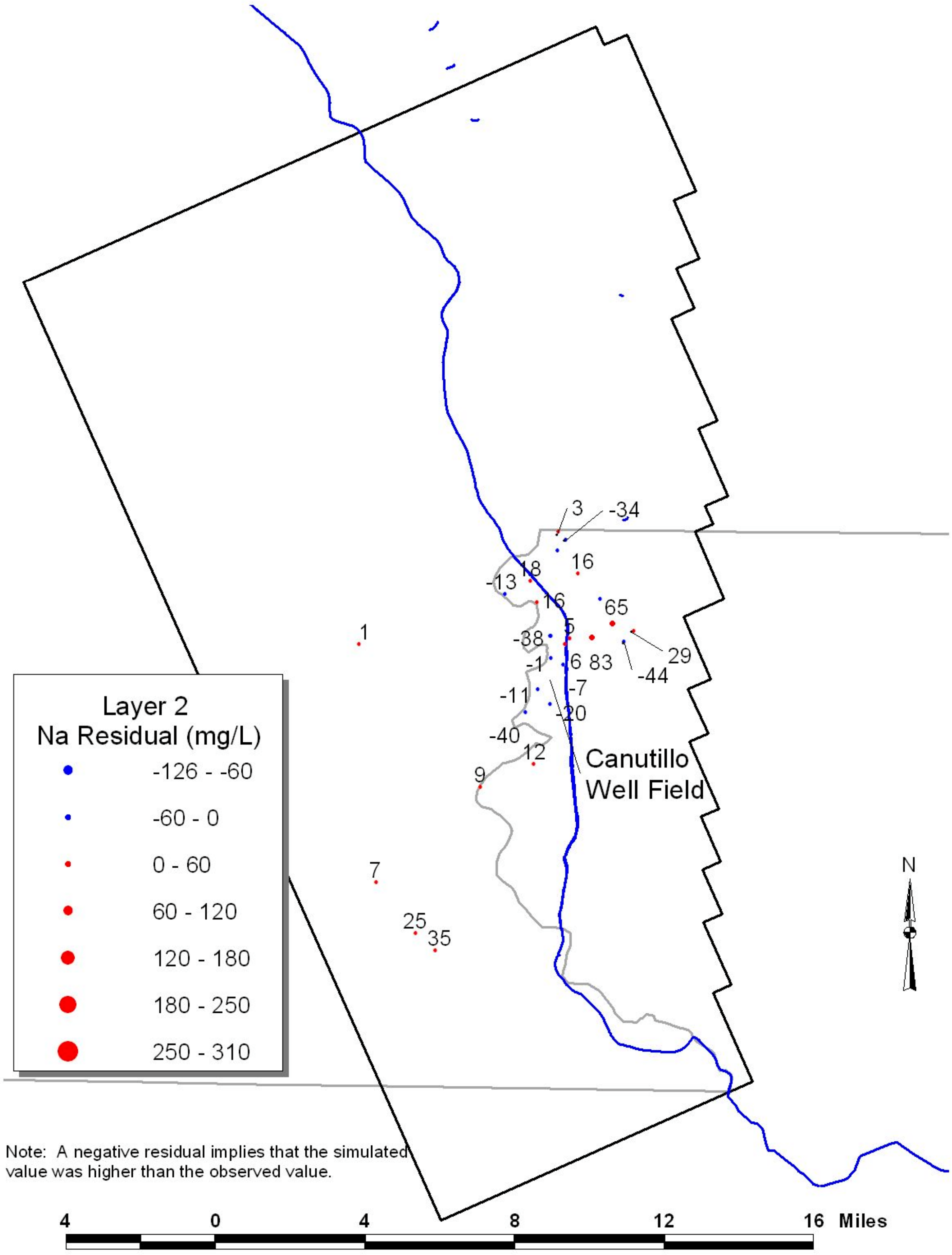

Figure 7-8. Layer 2 Na Residual

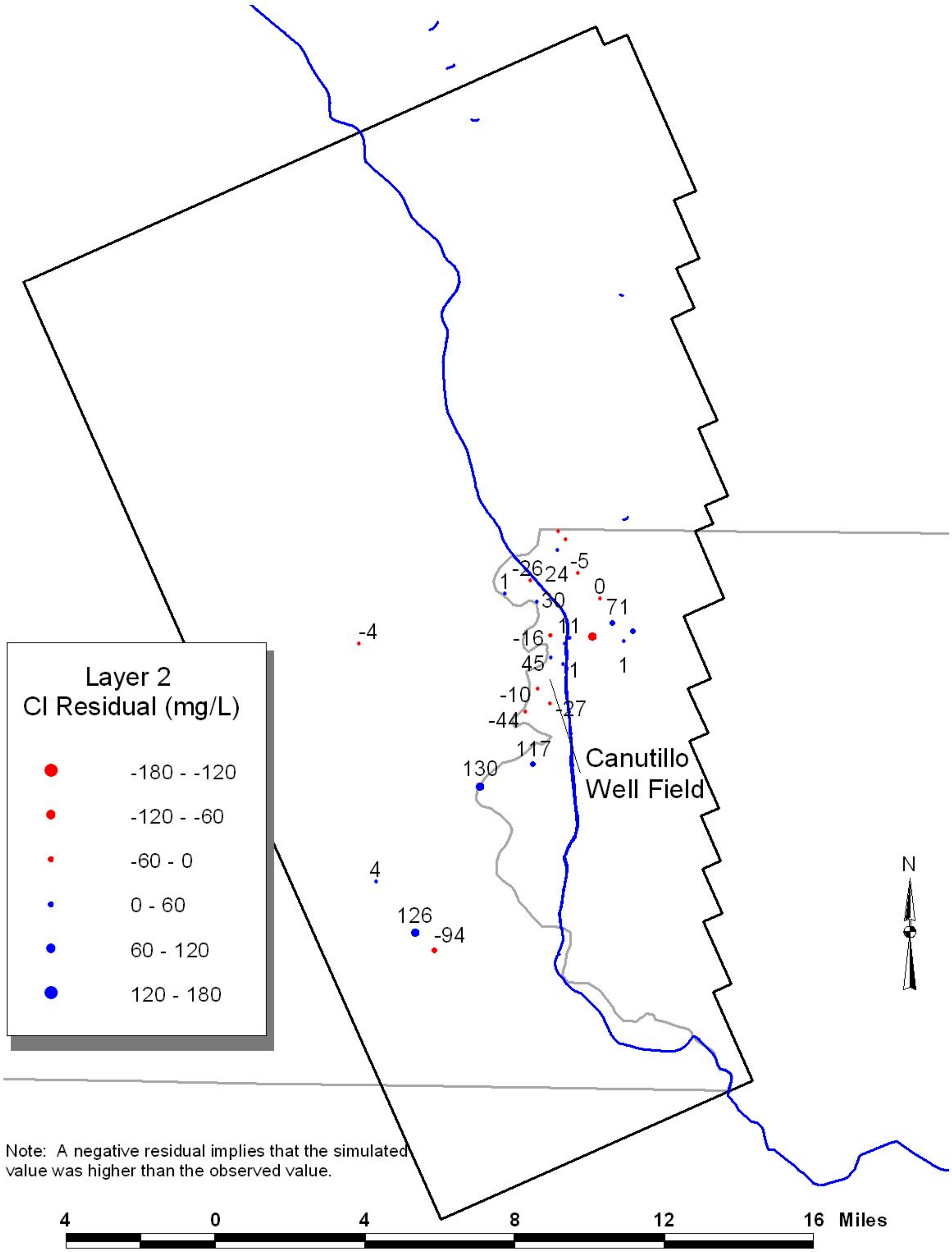

Figure 7-9. Layer 2 Cl Residual

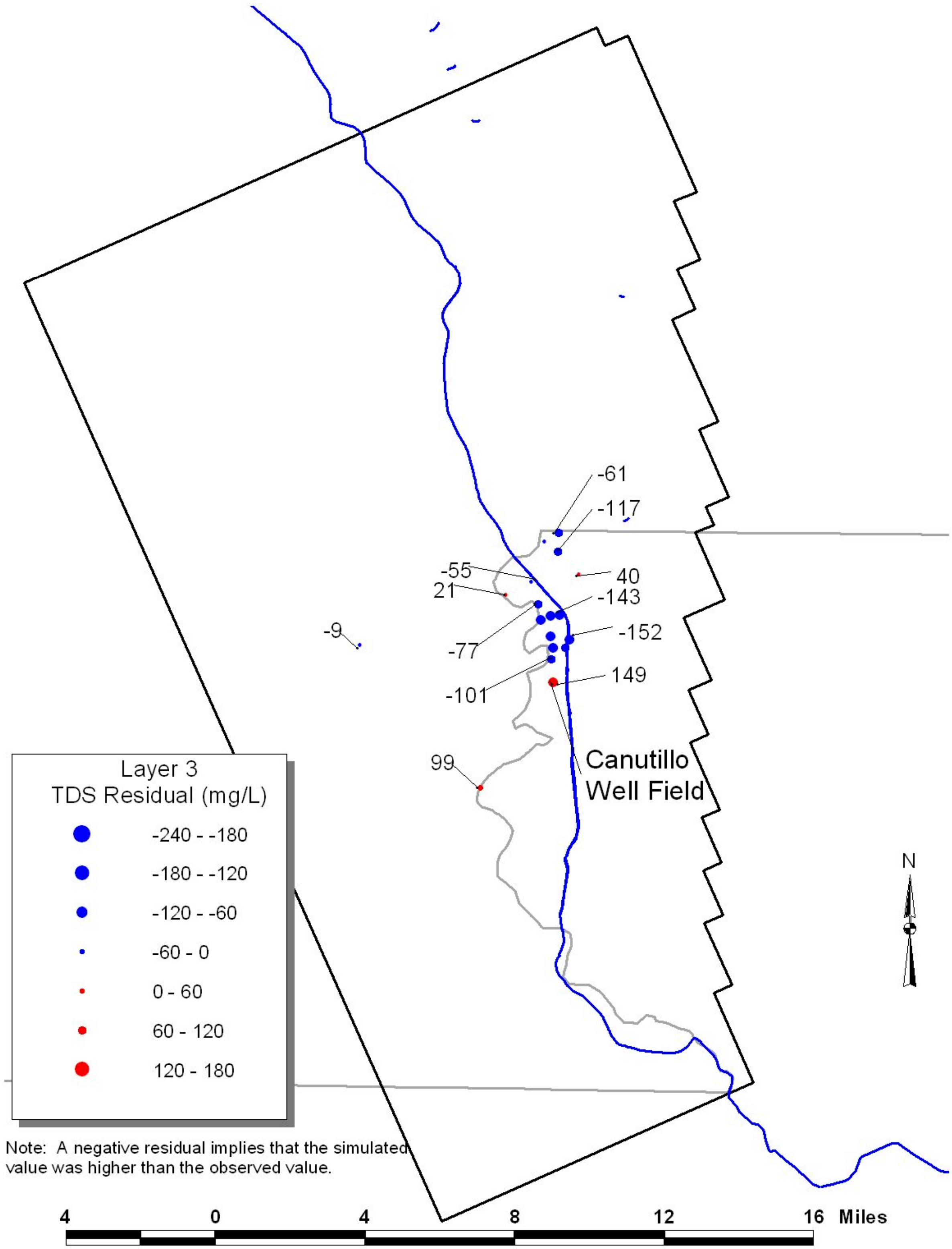

Figure 7-10. Layer 3 TDS Residual

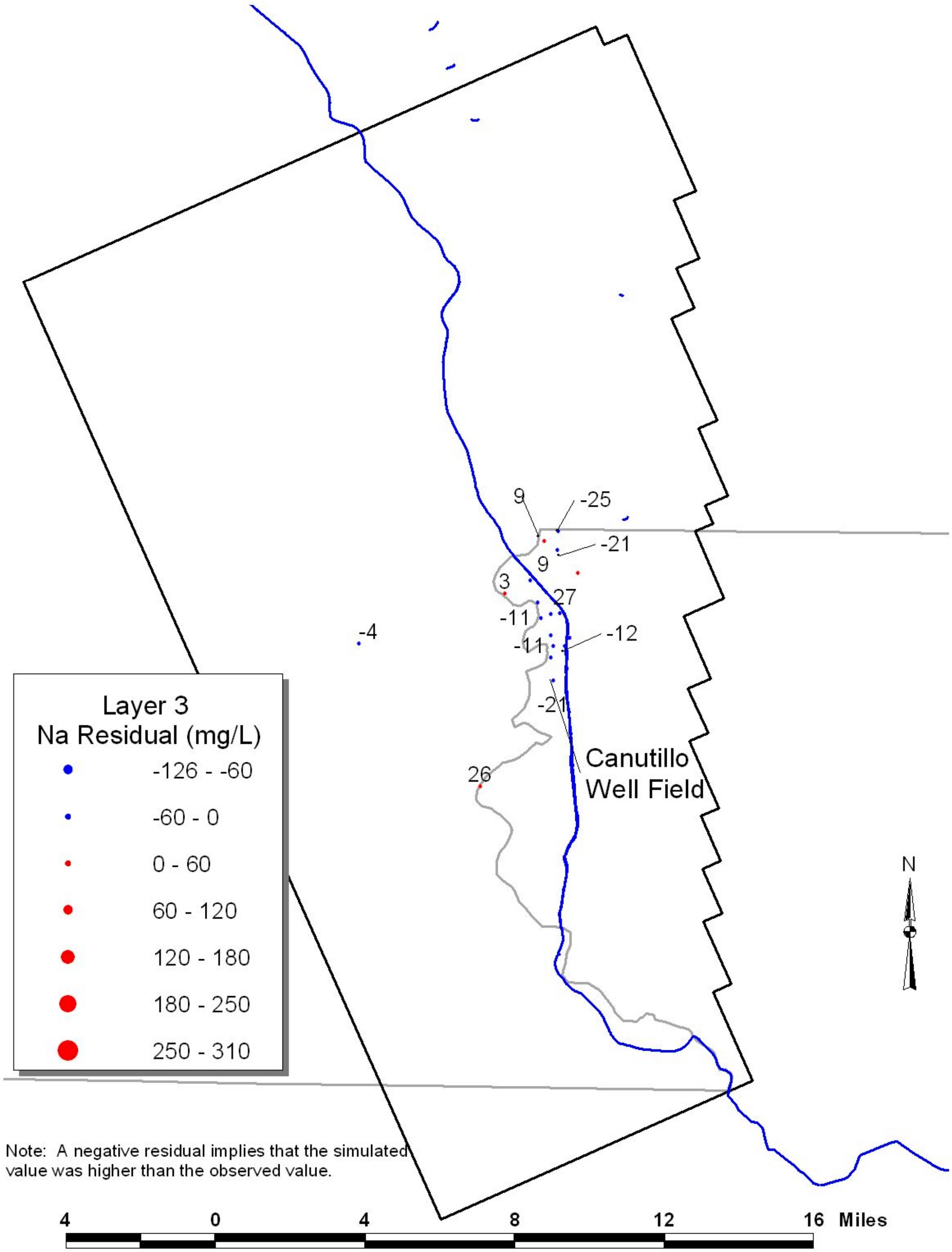

Figure 7-11. Layer 3 Na Residual

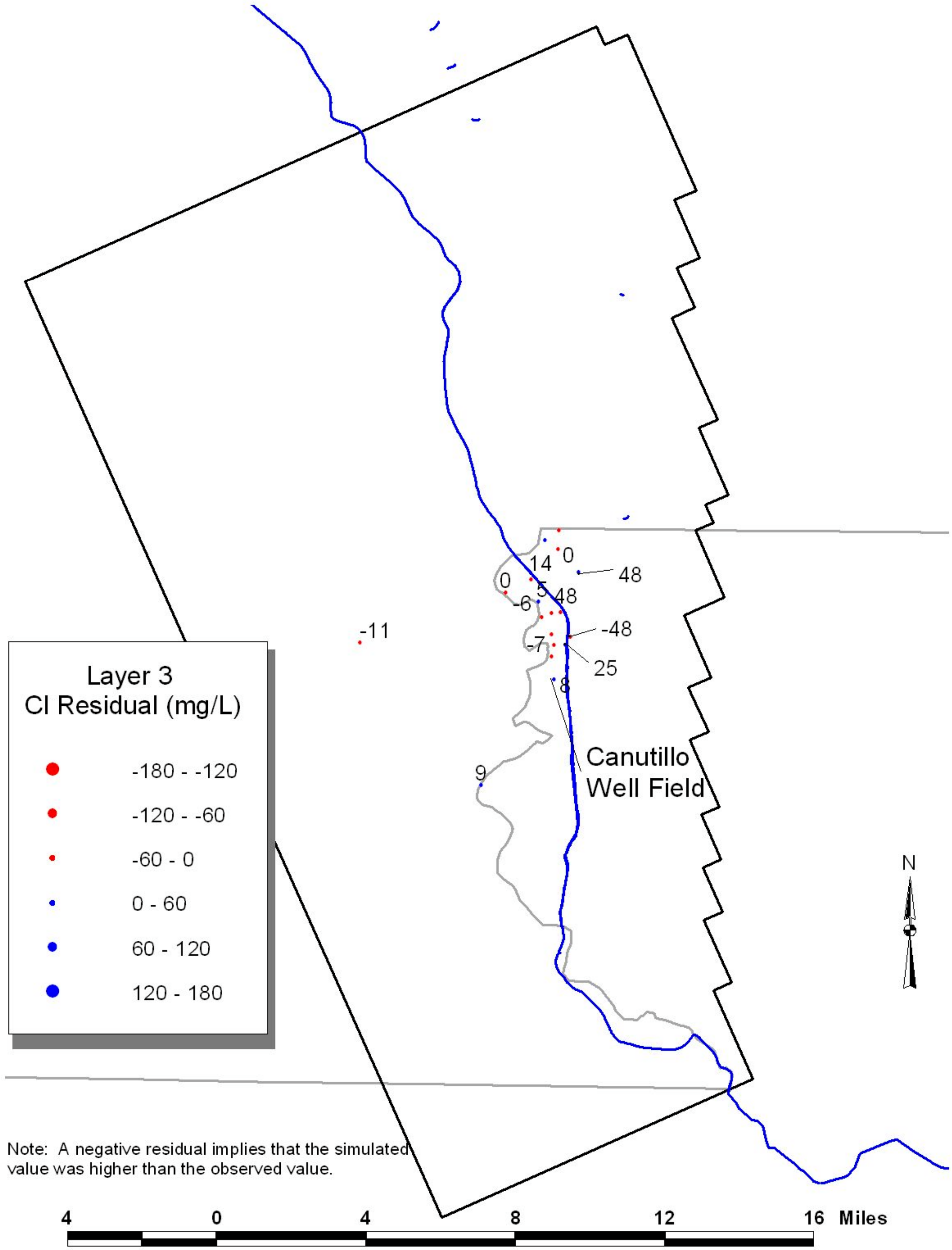

Figure 7-12. Layer 3 Cl Residual

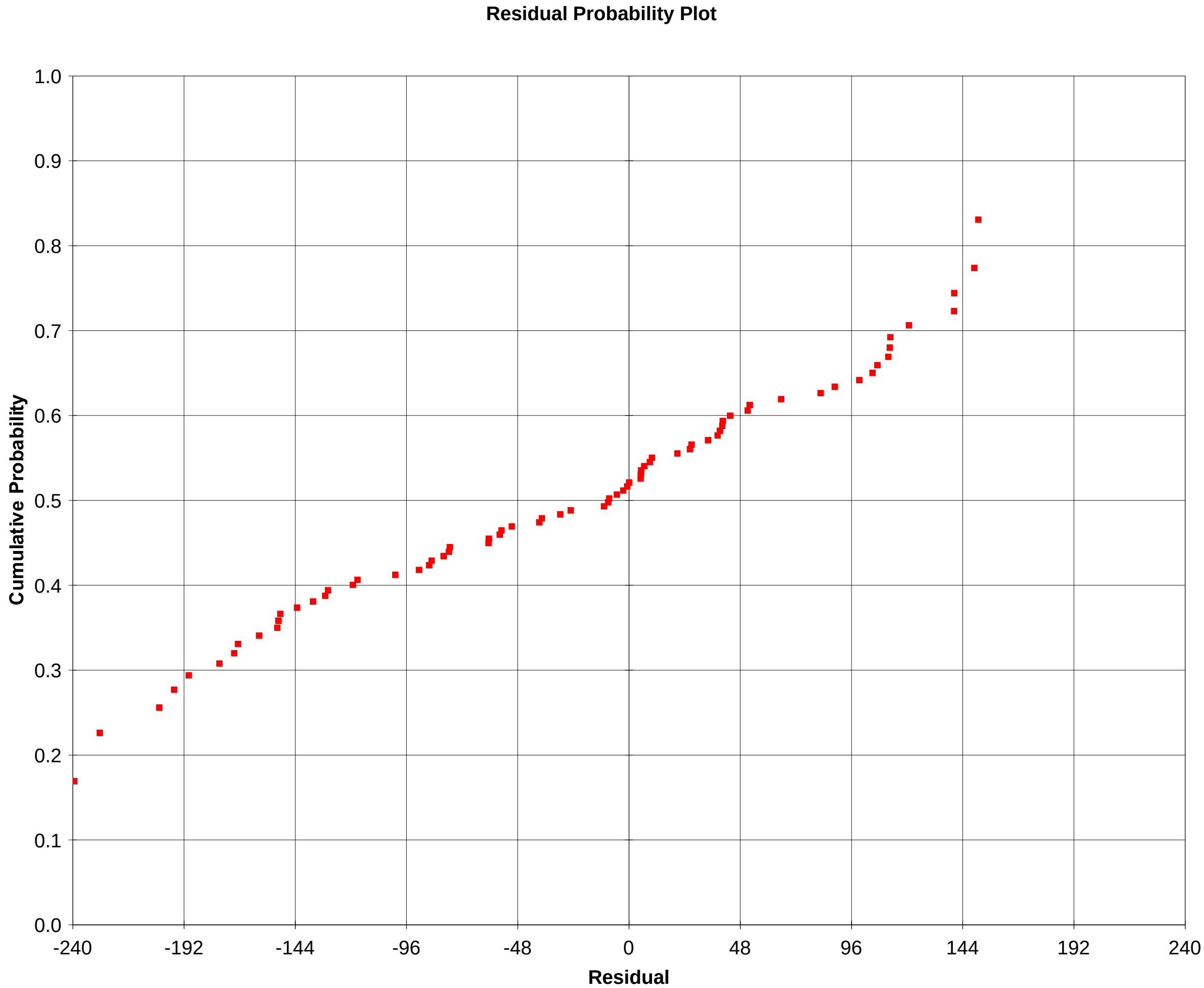

Figure 7-13. Residual Probability

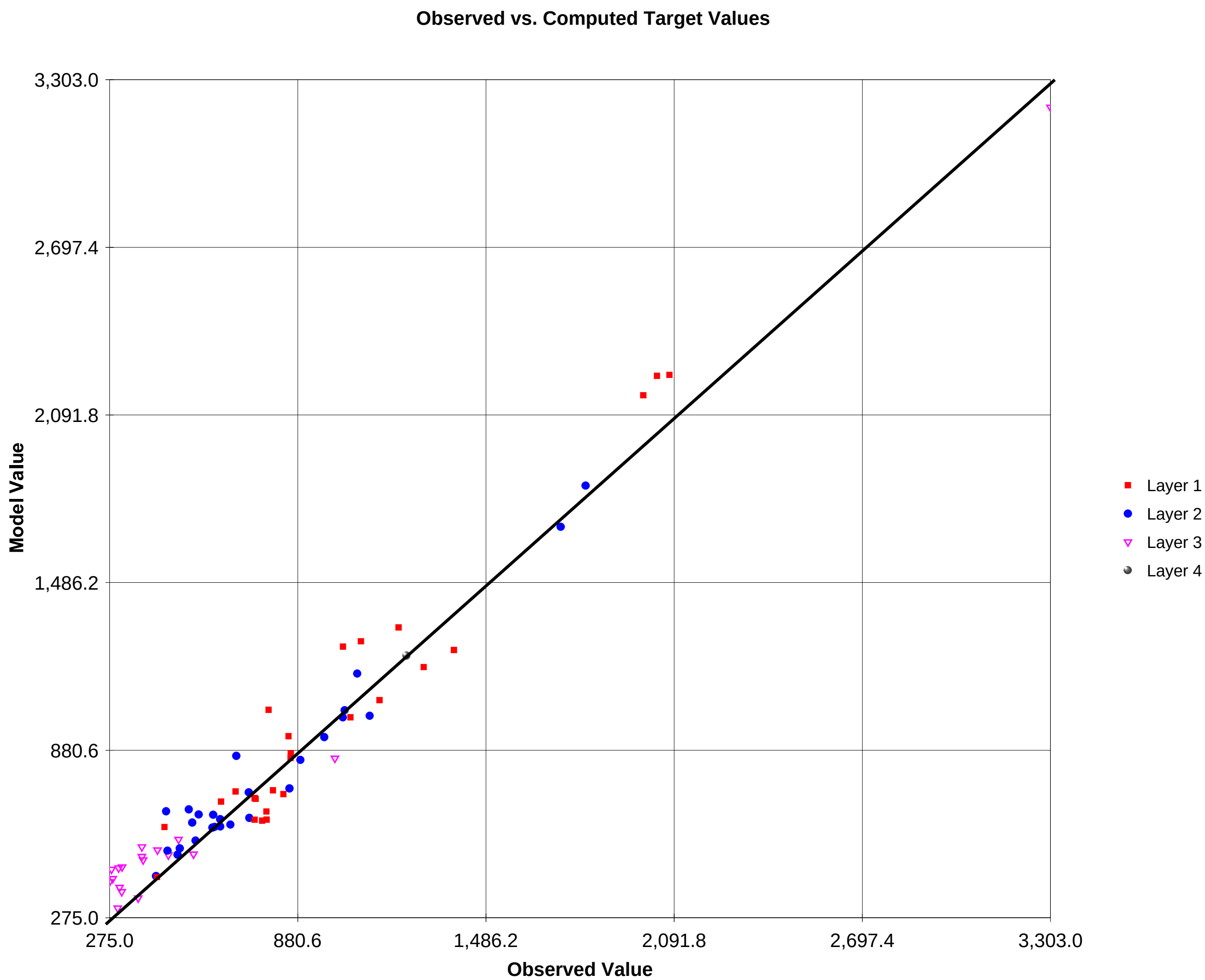

Figure 7-14. Simulated Versus Observed TDS Concentration (mg/L)

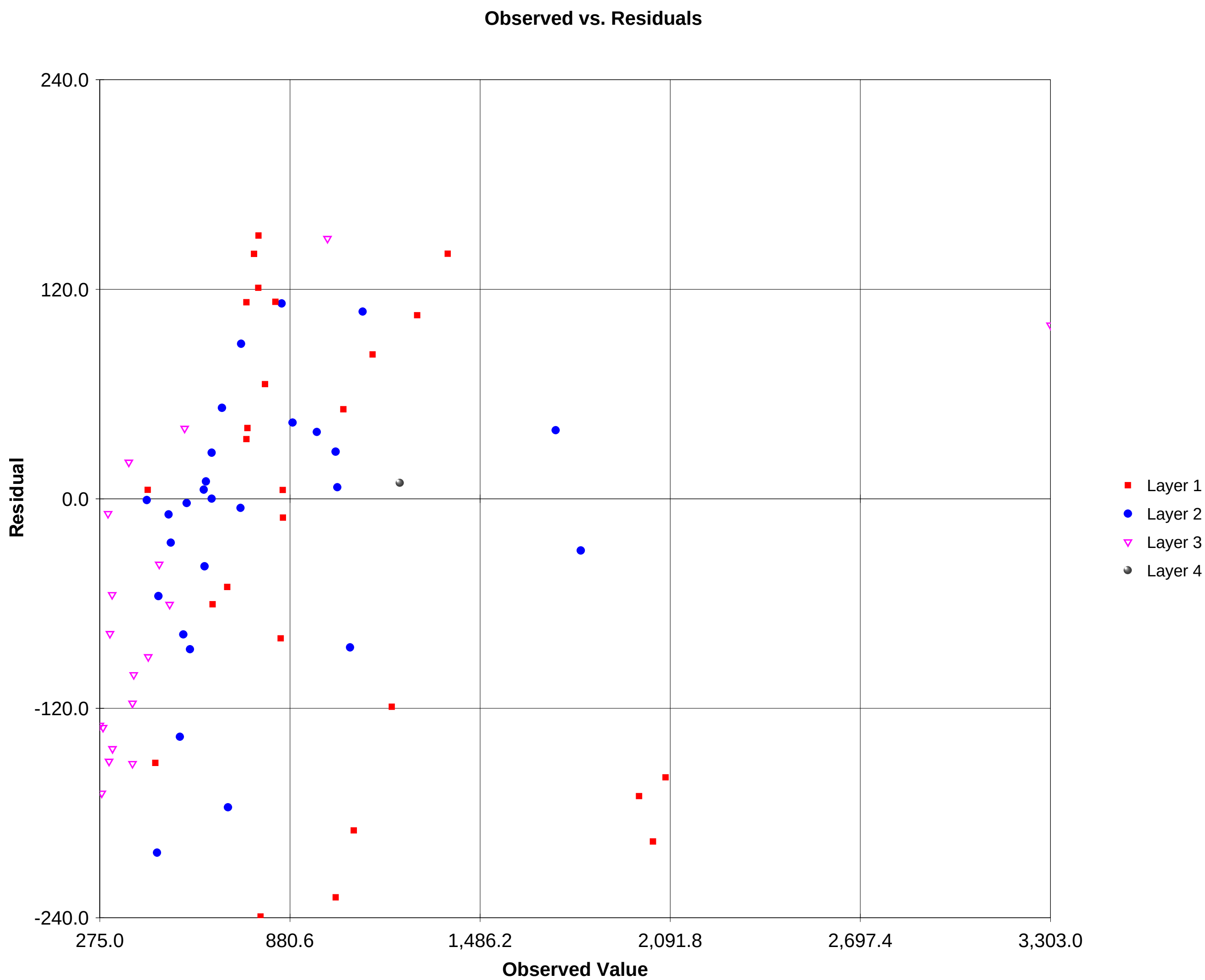

Figure 7-15. Residual Versus Observed TDS Concentration (mg/L)

Figures 7-16 through 7-27 present the calibrated 1995 TDS, Na, and Cl concentrations by model layer, respectively.

Figure 7-28 through 7-59 present hydrographs of individual EPWU wells over time with observed and simulated TDS concentration. As stated previously, the model-layering scheme from Weedon and Maddock requires that concentrations are averaged across discrete hydrostratigraphic units introducing additional uncertainty into the model results. These figures demonstrate this uncertainty. For example, Figure 7-28, Simulated Versus Observed EPWU 101, shows that the model simulated TDS at this point adequately. Whereas, the model under represented TDS concentrations in wells 102 and 103 (Figures 7-29 and 7-30) and over-represented concentrations in well 201 (Figure 7-44). In general the number of wells where concentrations are predicted correctly or are over-predicted is greater than the number of wells where concentrations are under-predicted. Therefore, the model results can be viewed as being conservative. Likewise, concentrations in a significant number of wells in the EPWU 100 series were under-predicted. Many of these wells are no longer used by EPWU for production. It should be noted that several EPWU wells are screened across multiple model layers. These wells are represented with two simulated plots representing the concentration in each model layer.

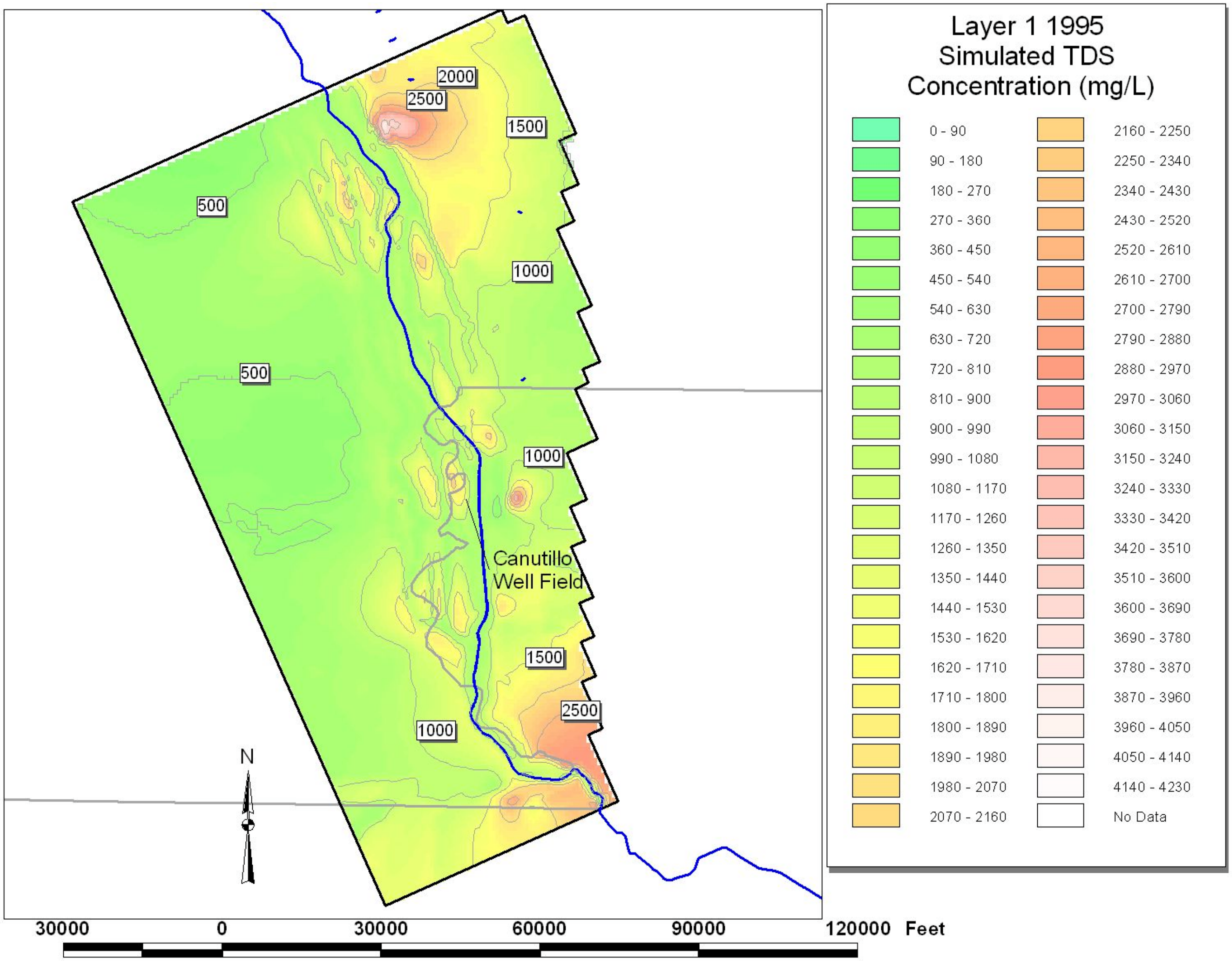

Figure 7-16. Layer 1 Simulated 1995 TDS Concentration

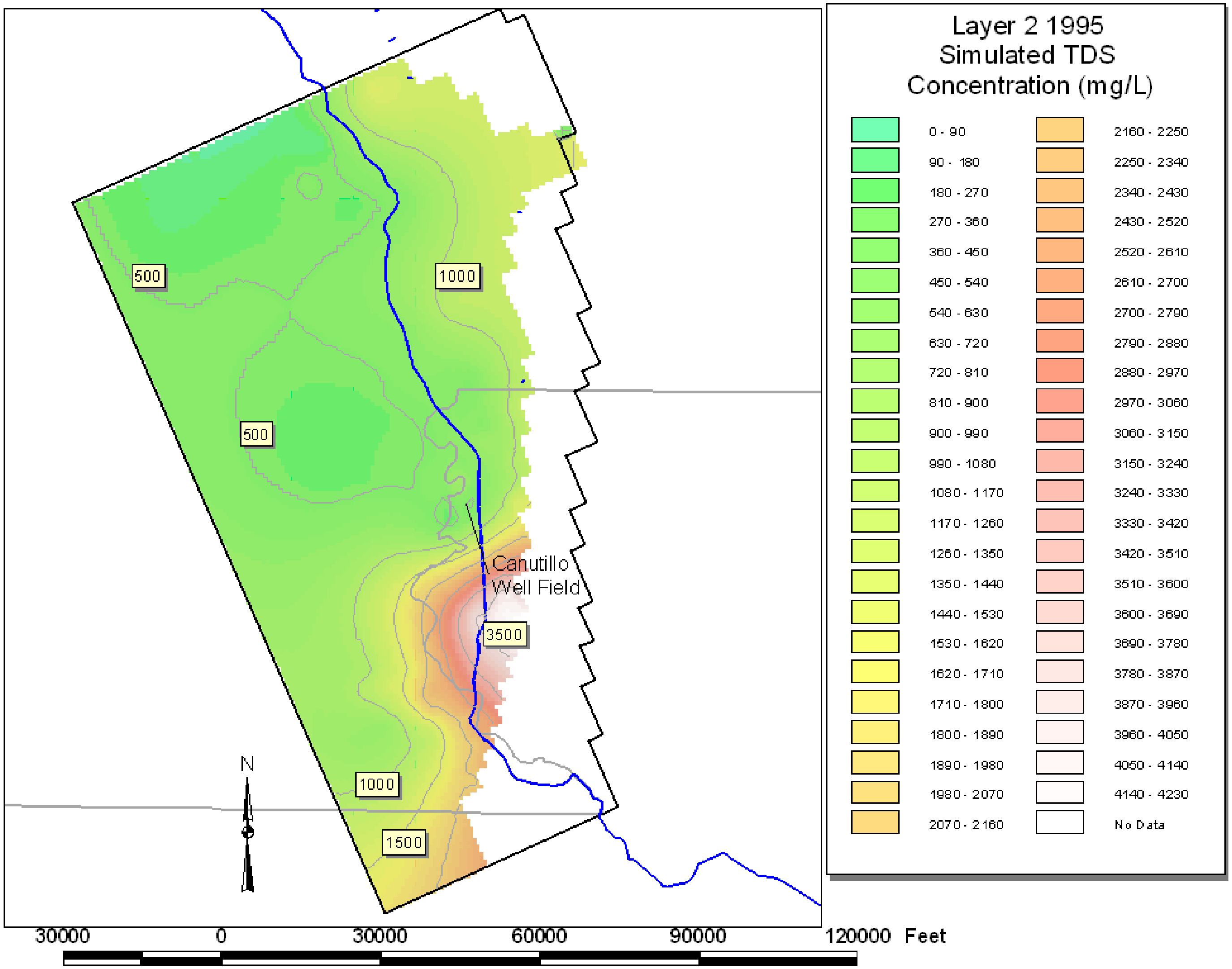

Figure 7-17. Layer 2 Simulated 1995 TDS Concentration

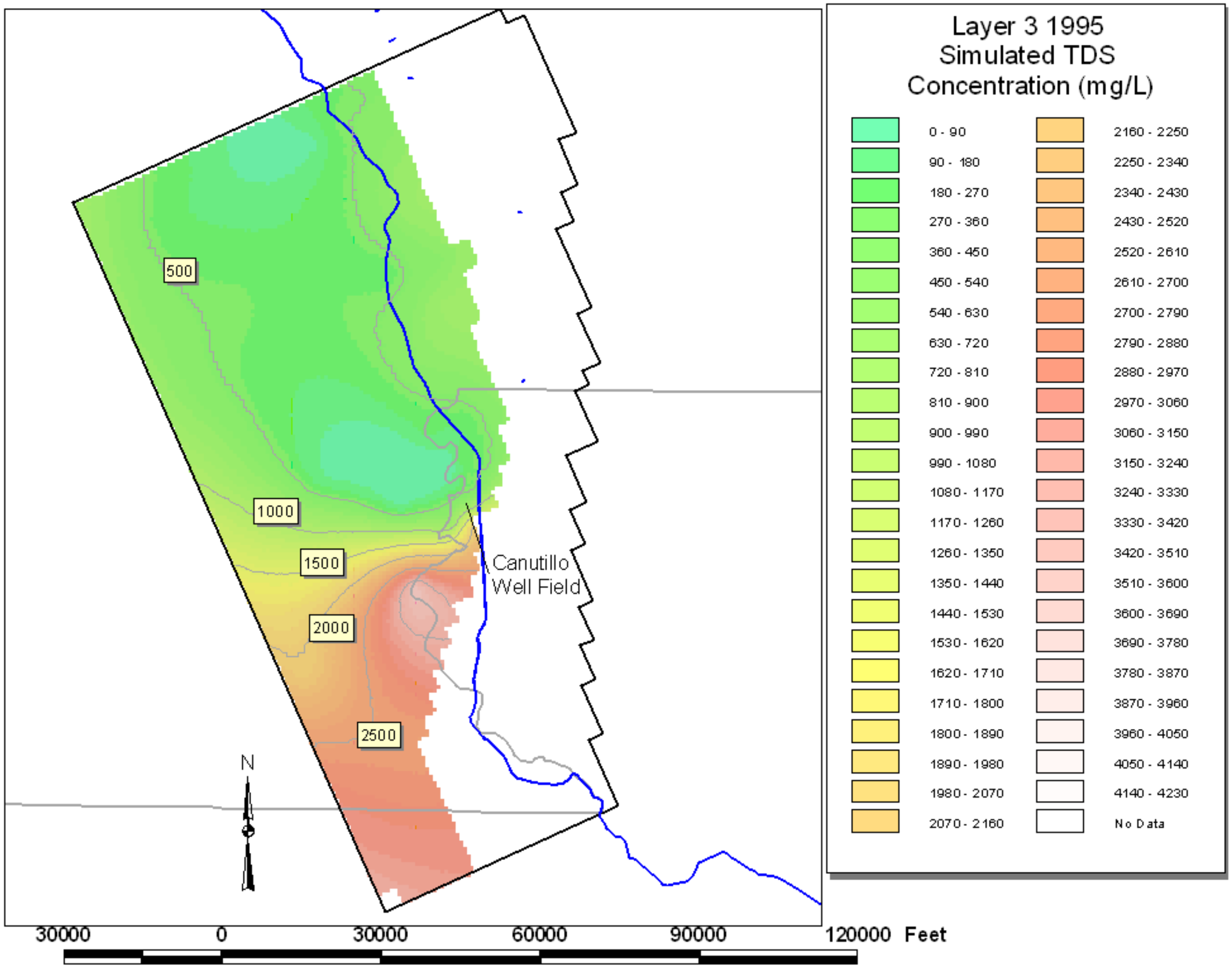

Figure 7-18. Layer 3 Simulated 1995 TDS Concentration

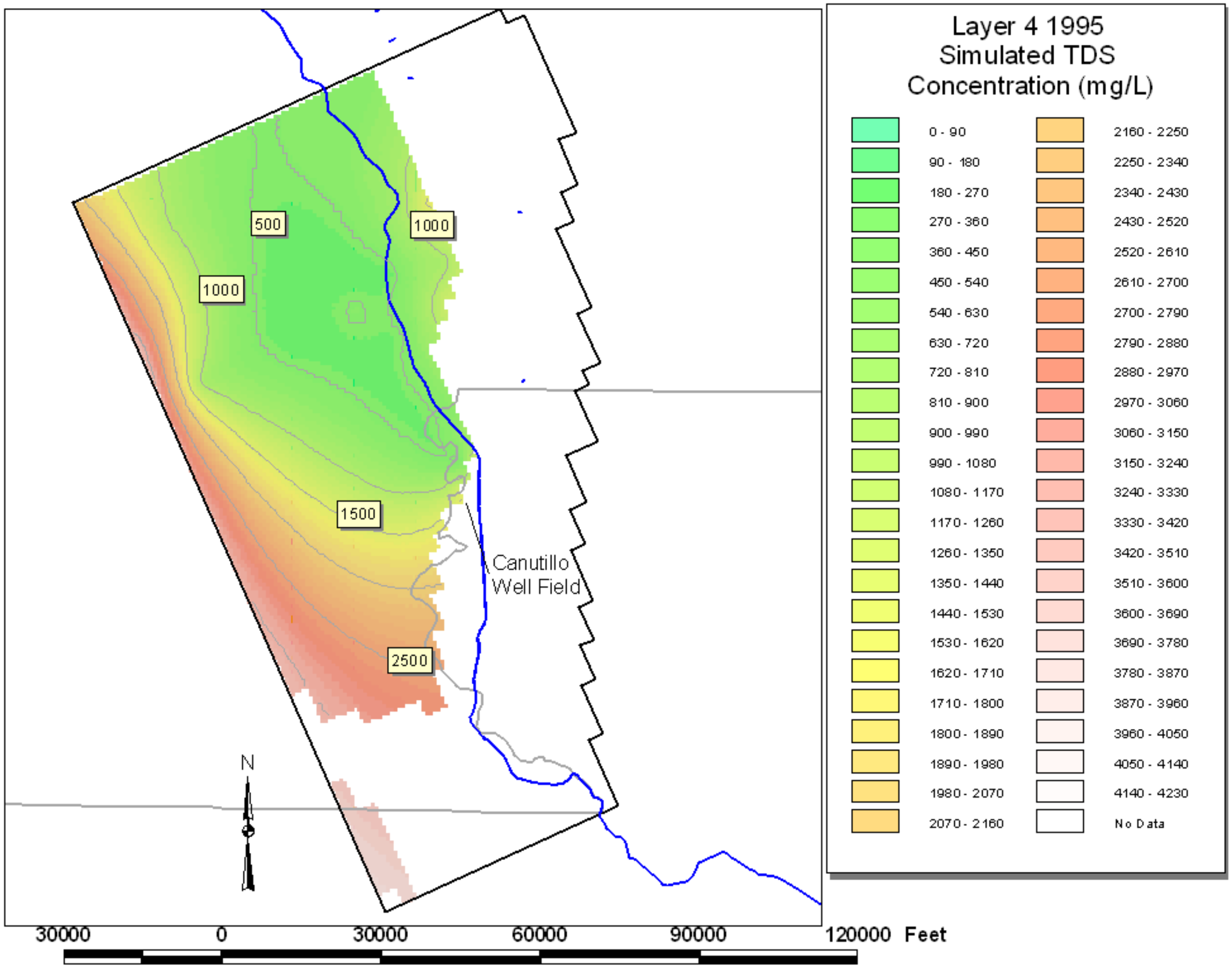

Figure 7-19. Layer 4 Simulated 1995 TDS Concentration

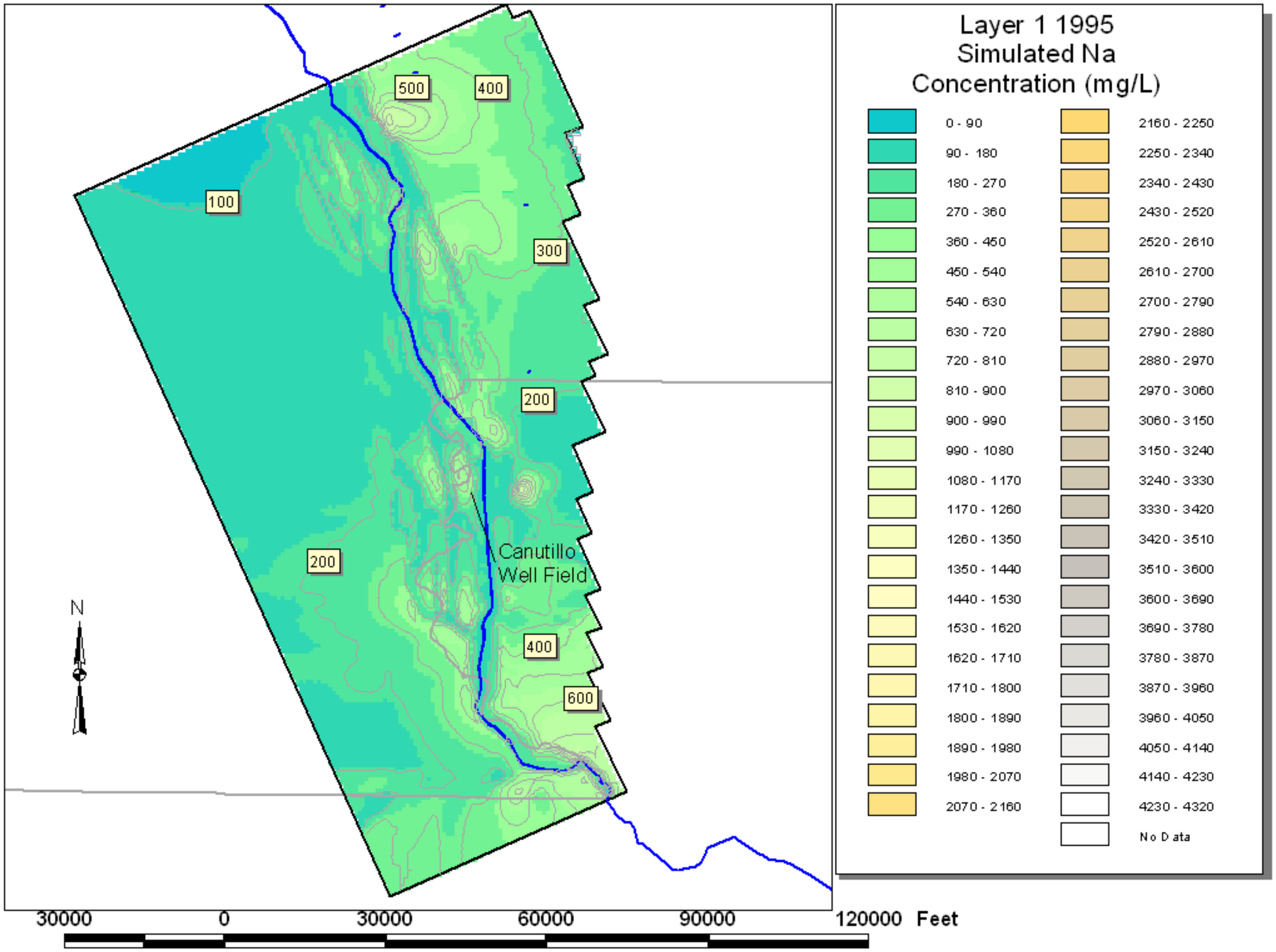

Figure 7-20. Layer 1 Simulated 1995 Na Concentration

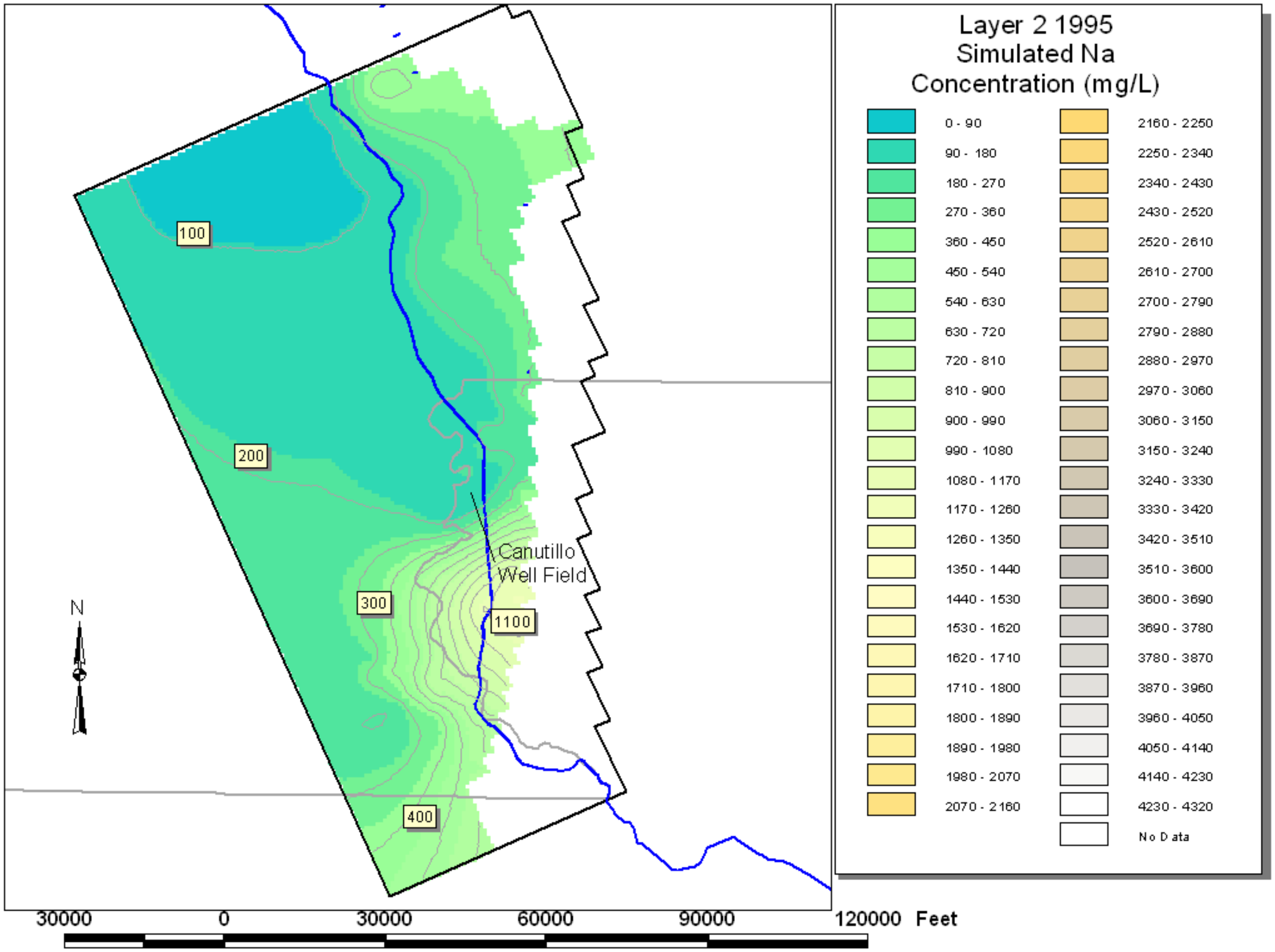

Figure 7-21. Layer 2 Simulated 1995 Na Concentration

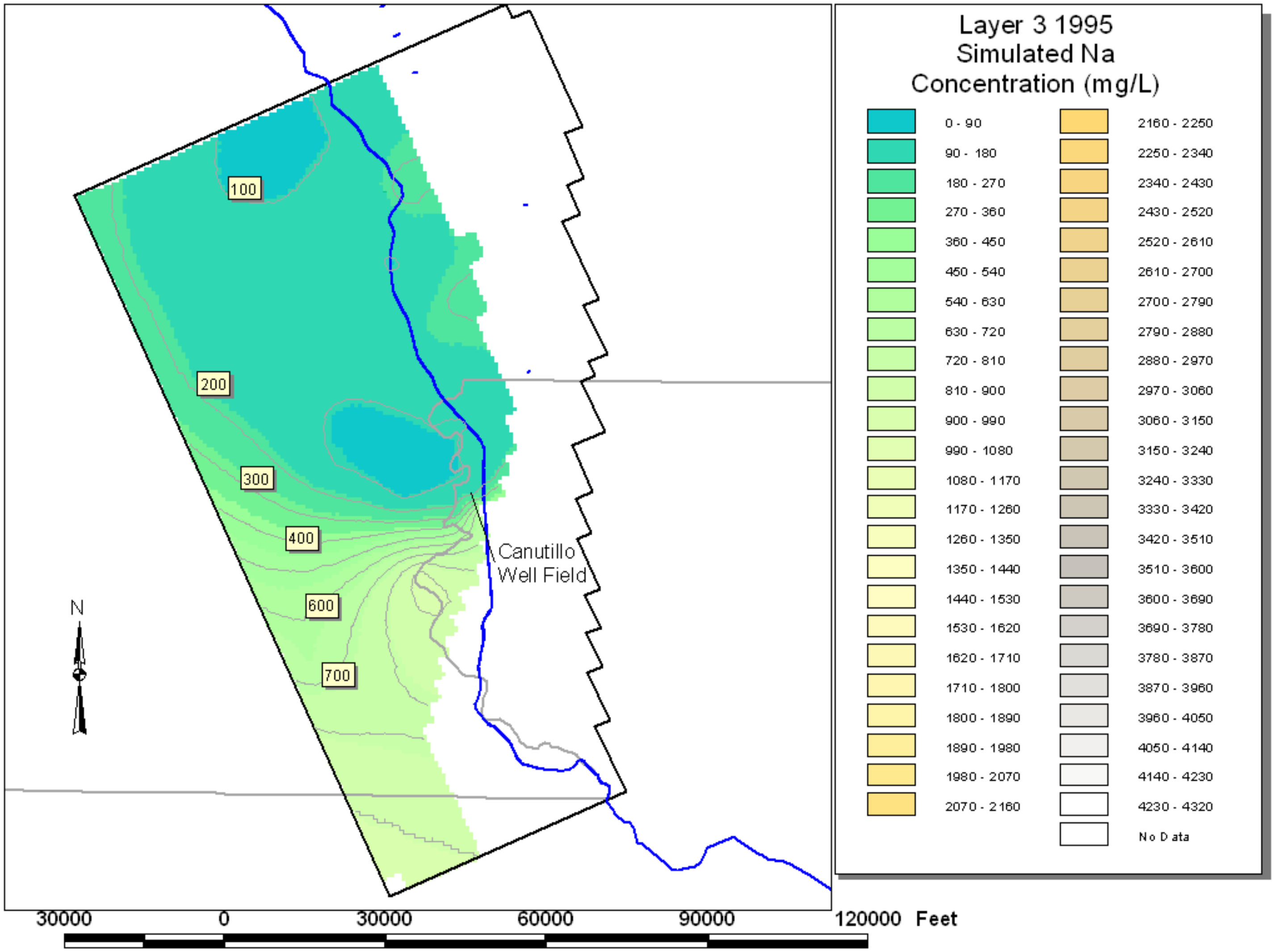

Figure 7-22. Layer 3 Simulated 1995 Na Concentration

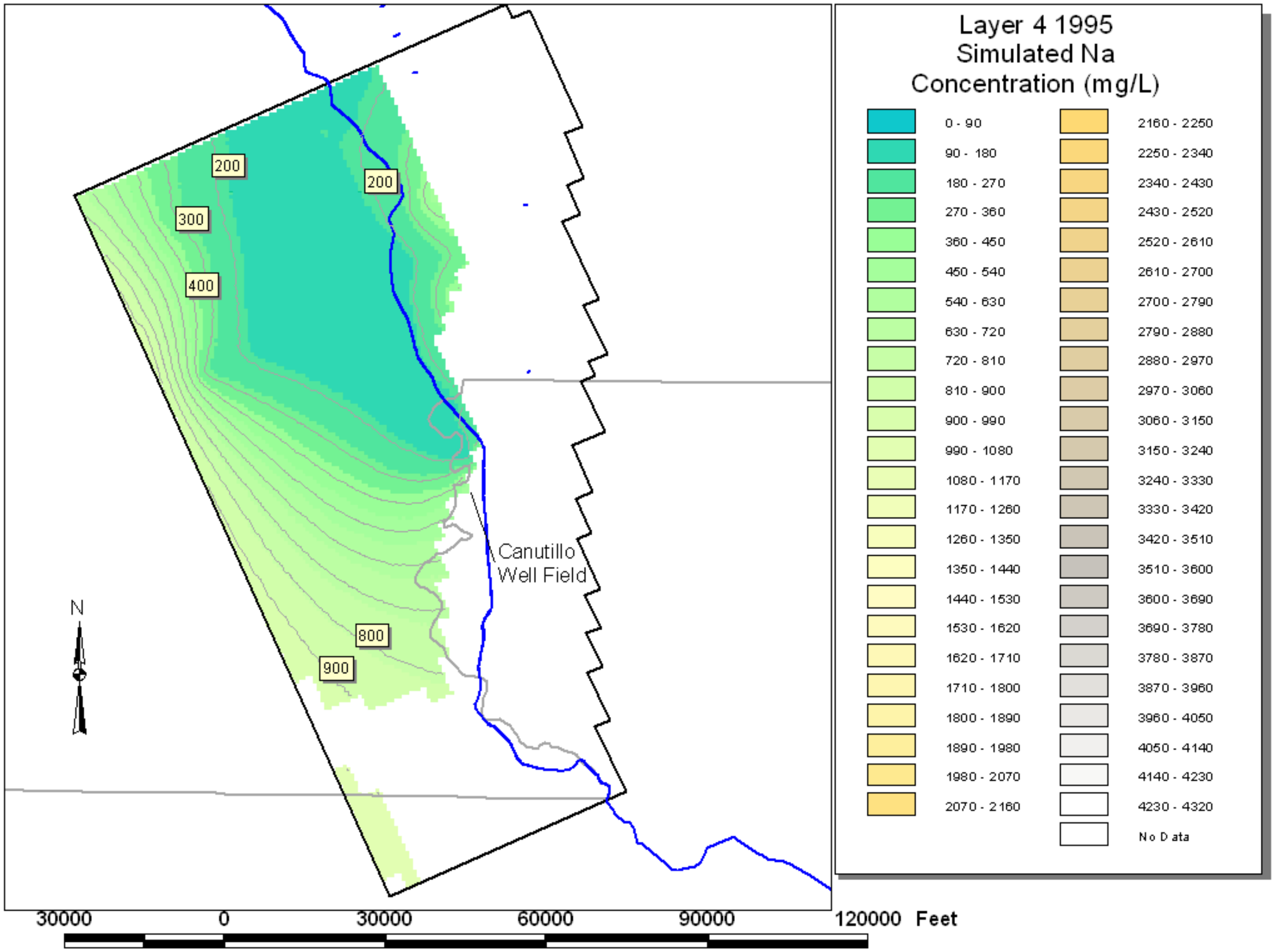

Figure 7-23. Layer 4 Simulated 1995 Na Concentration

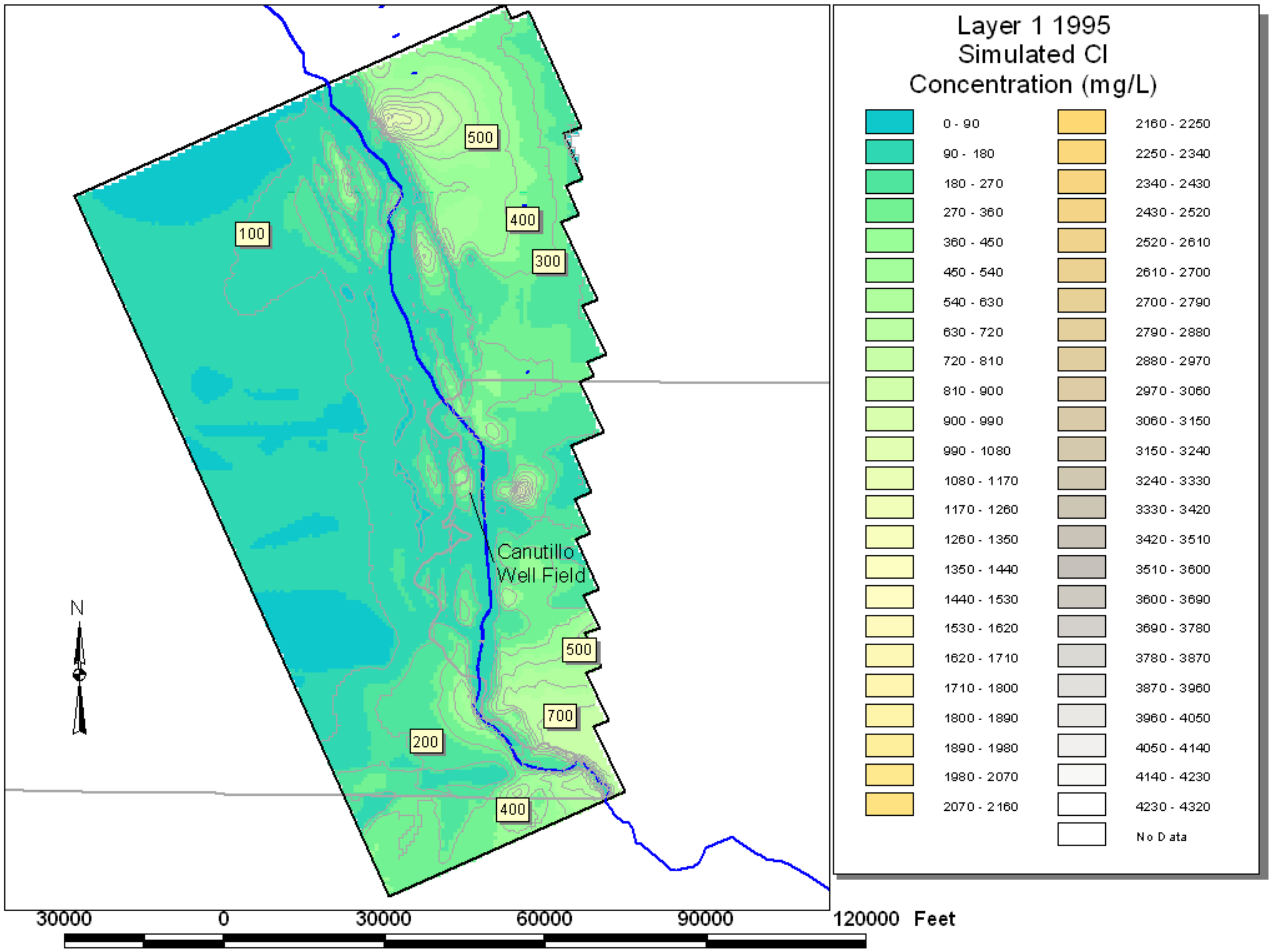

Figure 7-24. Layer 1 Simulated 1995 Cl Concentration

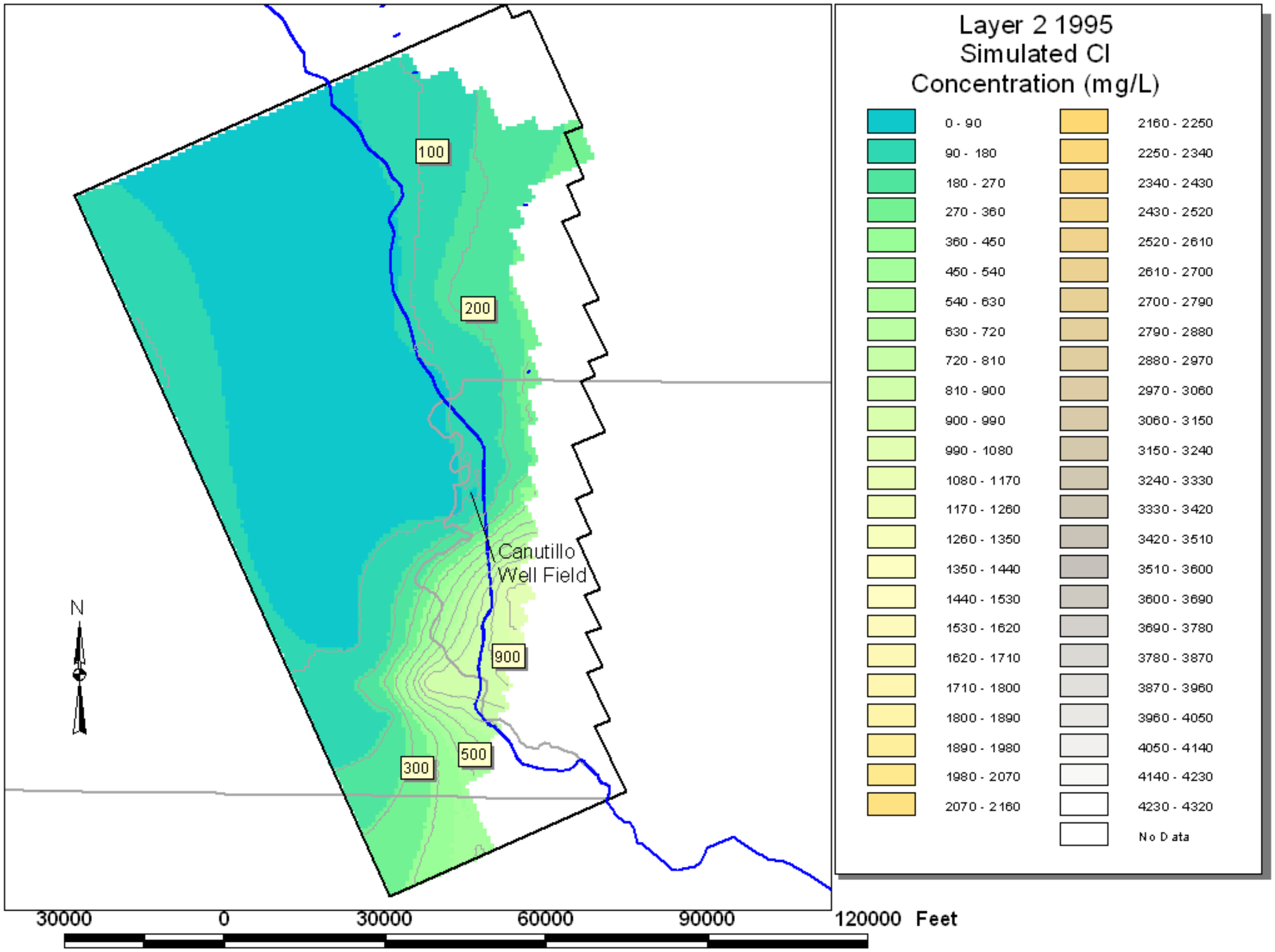

Figure 7-25. Layer 2 Simulated 1995 Cl Concentration

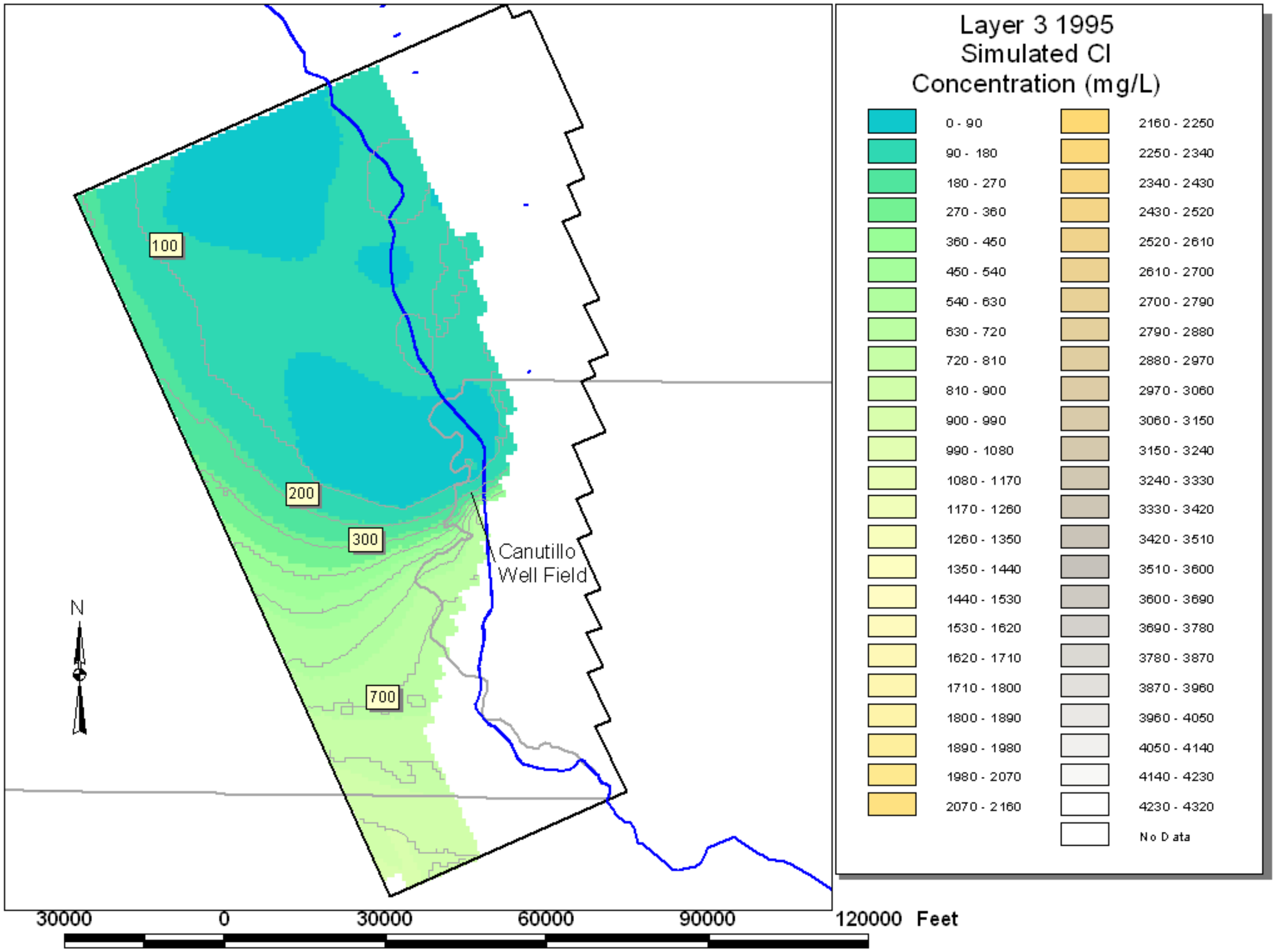

Figure 7-26. Layer 3 Simulated 1995 Cl Concentration

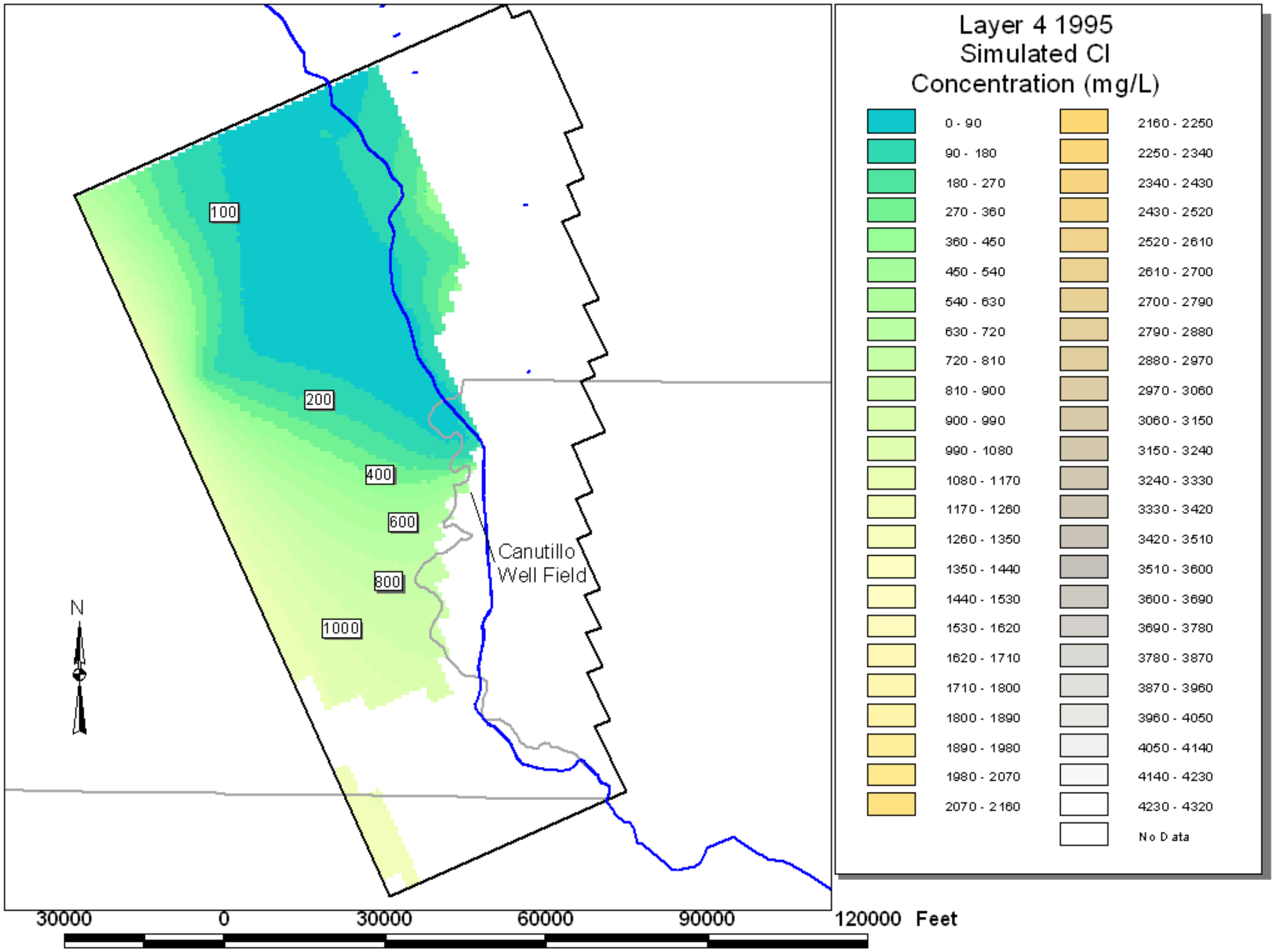

Figure 7-27. Layer 4 Simulated 1995 Cl Concentration

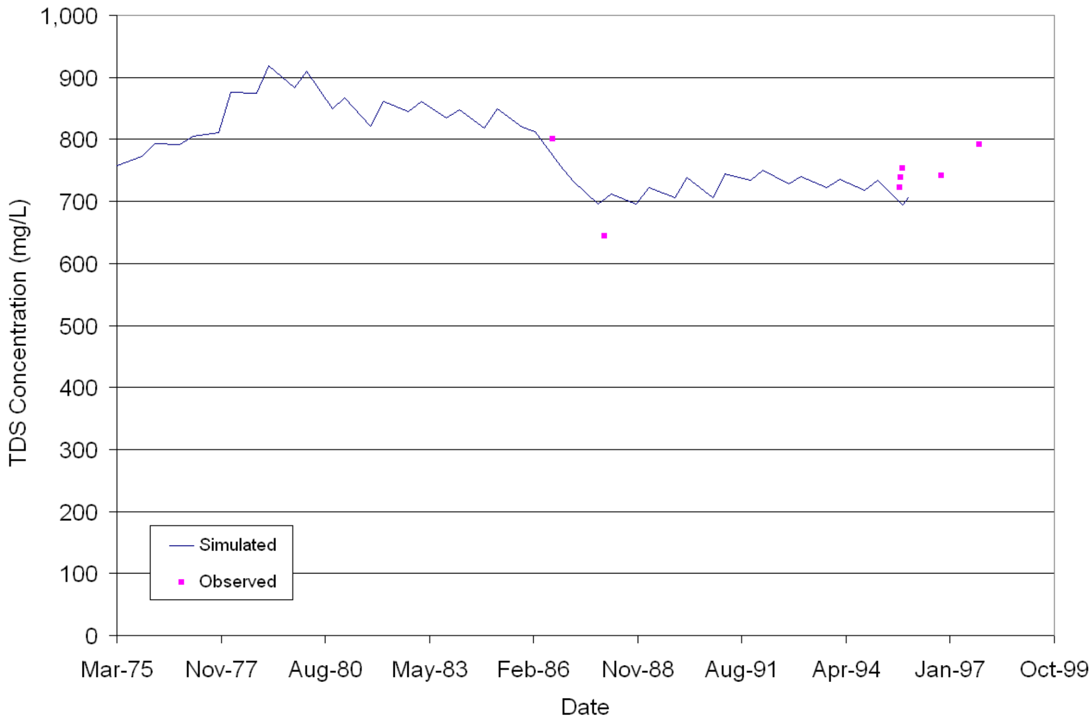

Figure 7-28. Simulated Versus Observed EPWU 101

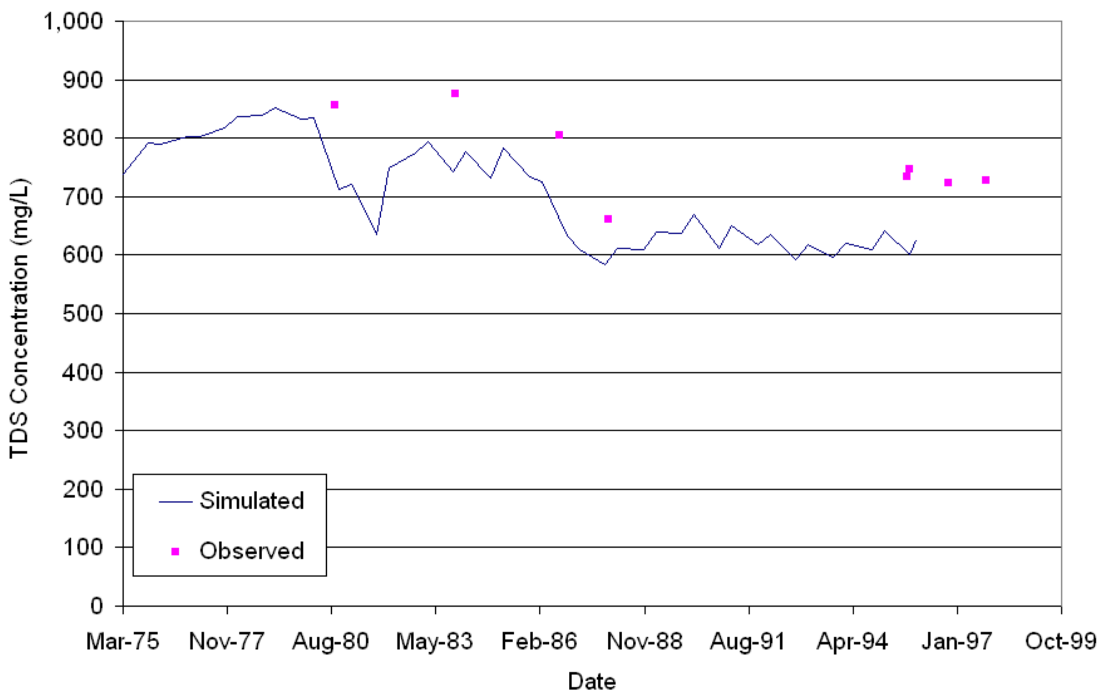

Figure 7-29. Simulated Versus Observed EPWU 102

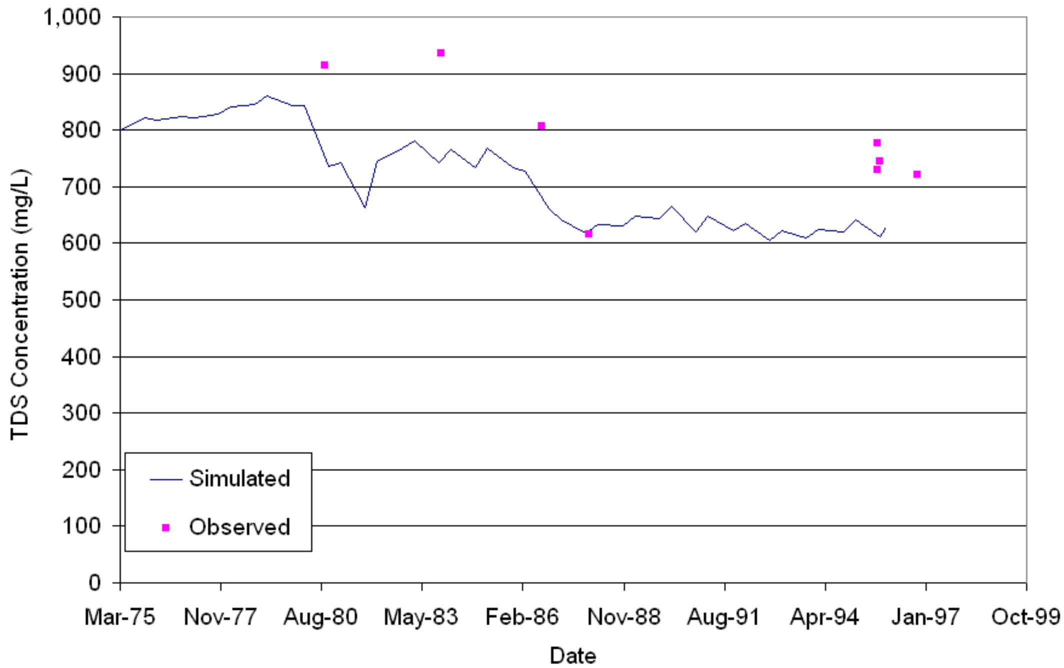

Figure 7-30. Simulated Versus Observed EPWU 103

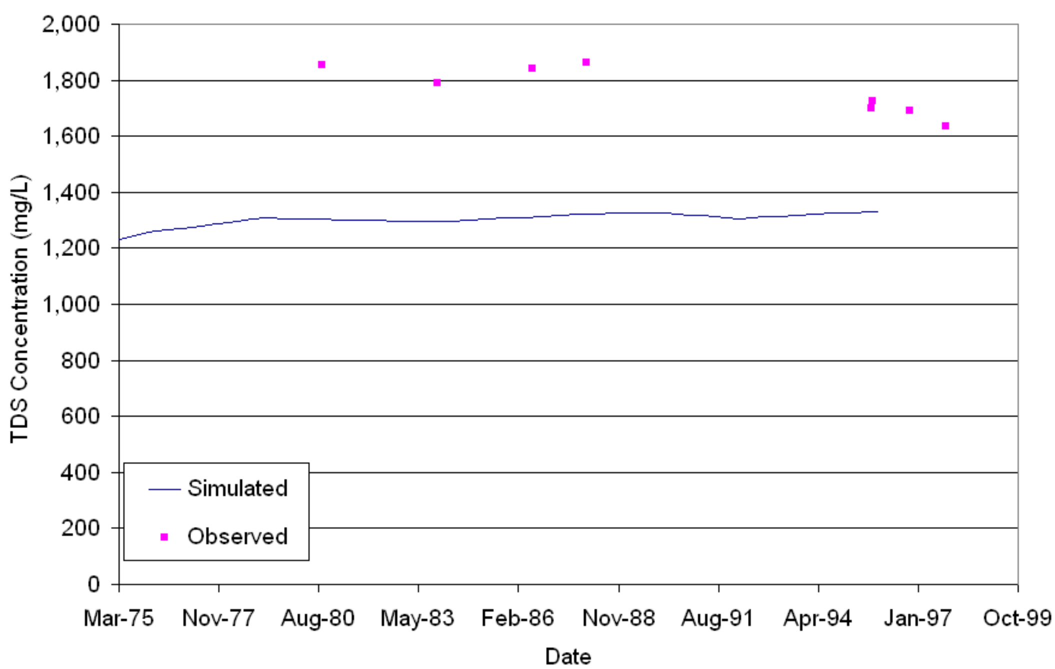

Figure 7-31. Simulated Versus Observed EPWU 104

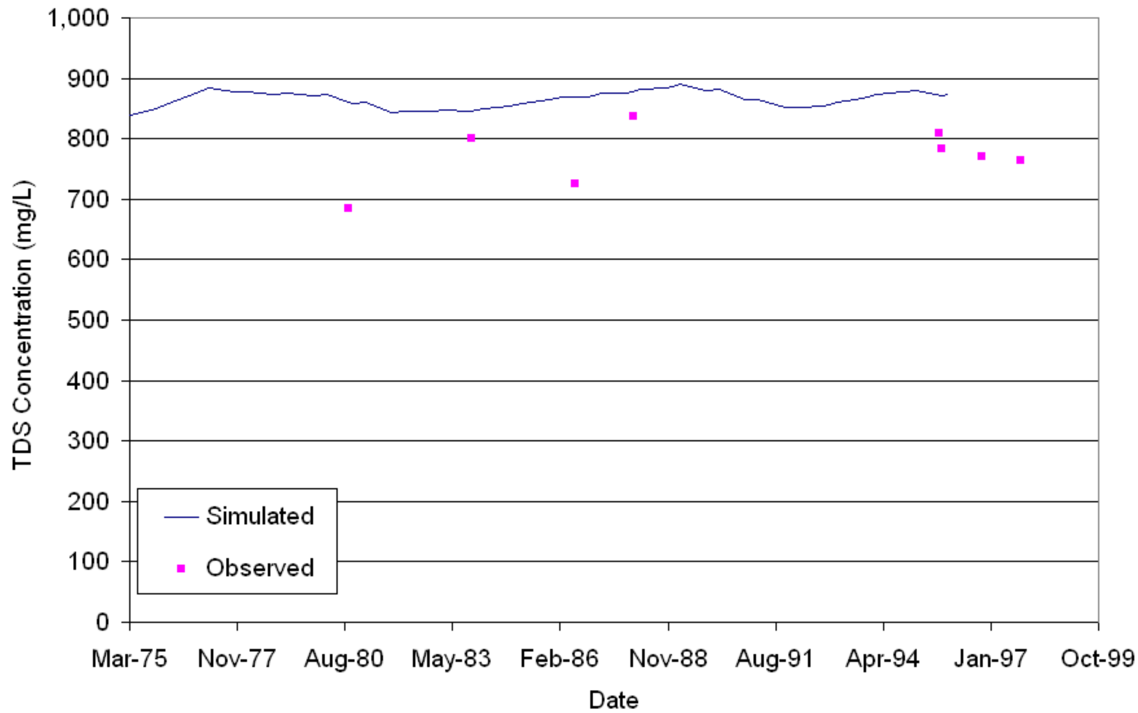

Figure 7-32. Simulated Versus Observed EPWU 105

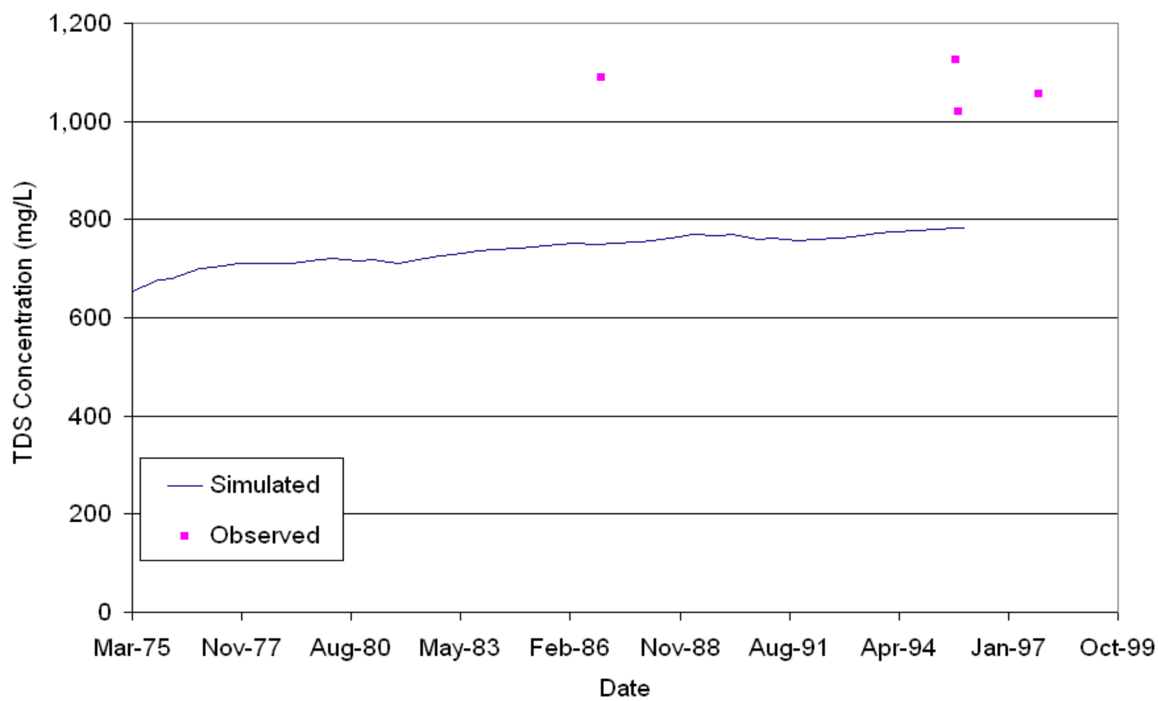

Figure 7-33. Simulated Versus Observed EPWU 106

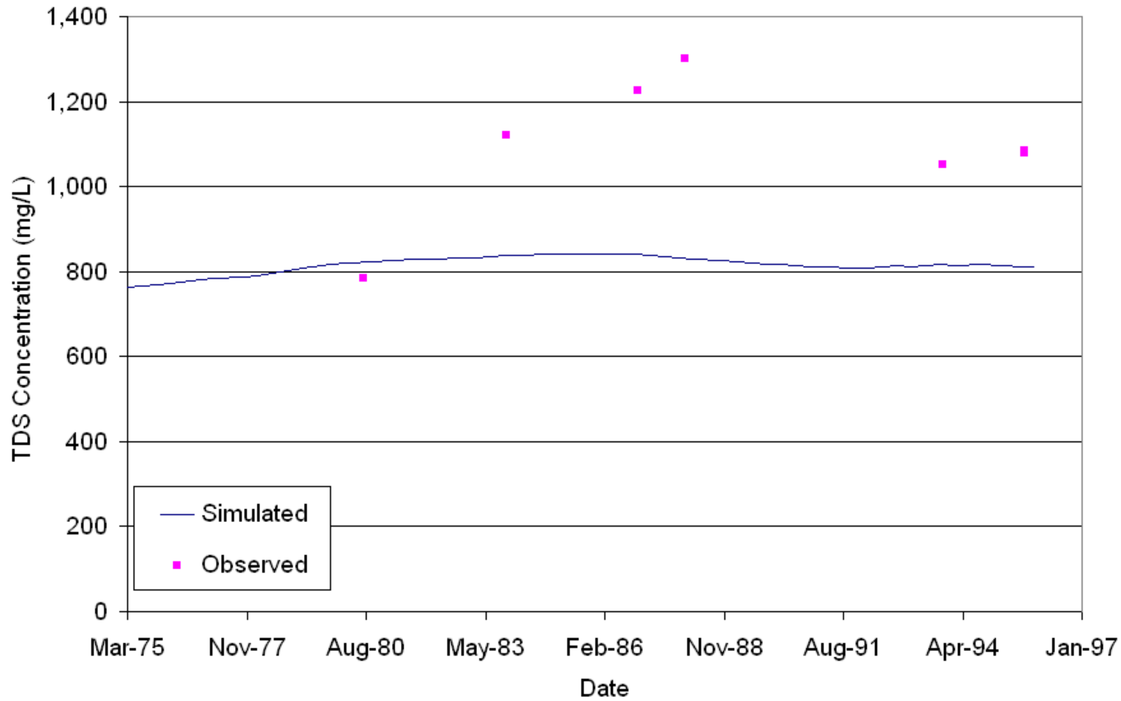

Figure 7-34. Simulated Versus Observed EPWU 107

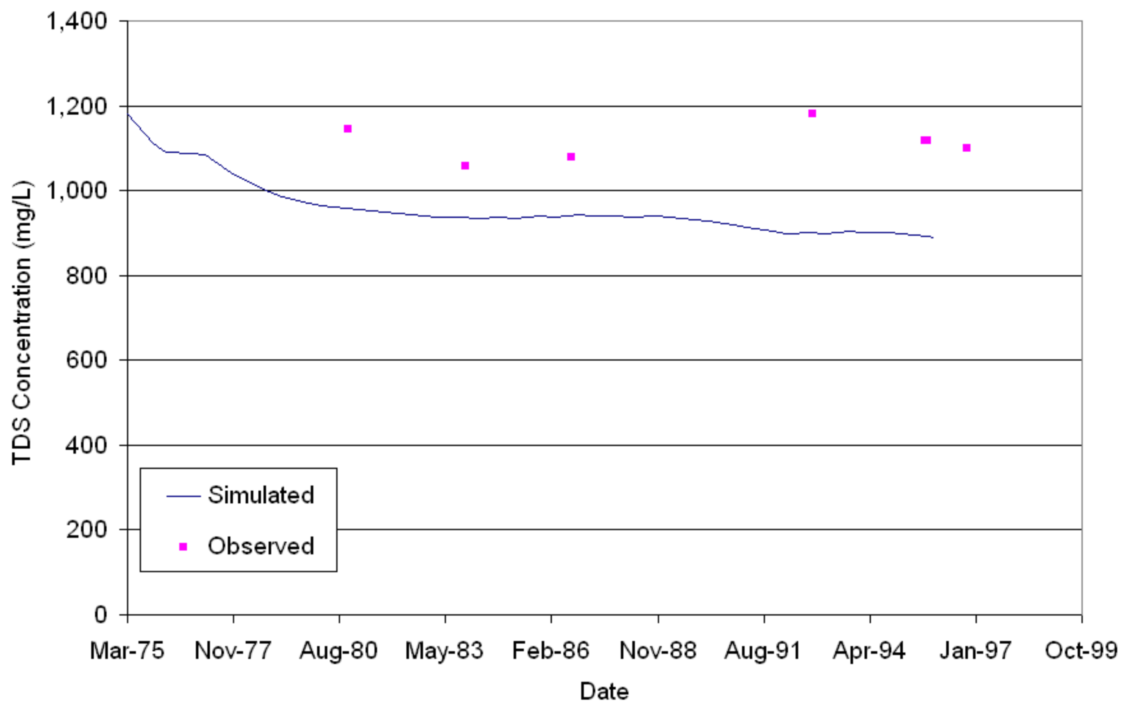

Figure 7-35. Simulated Versus Observed EPWU 108

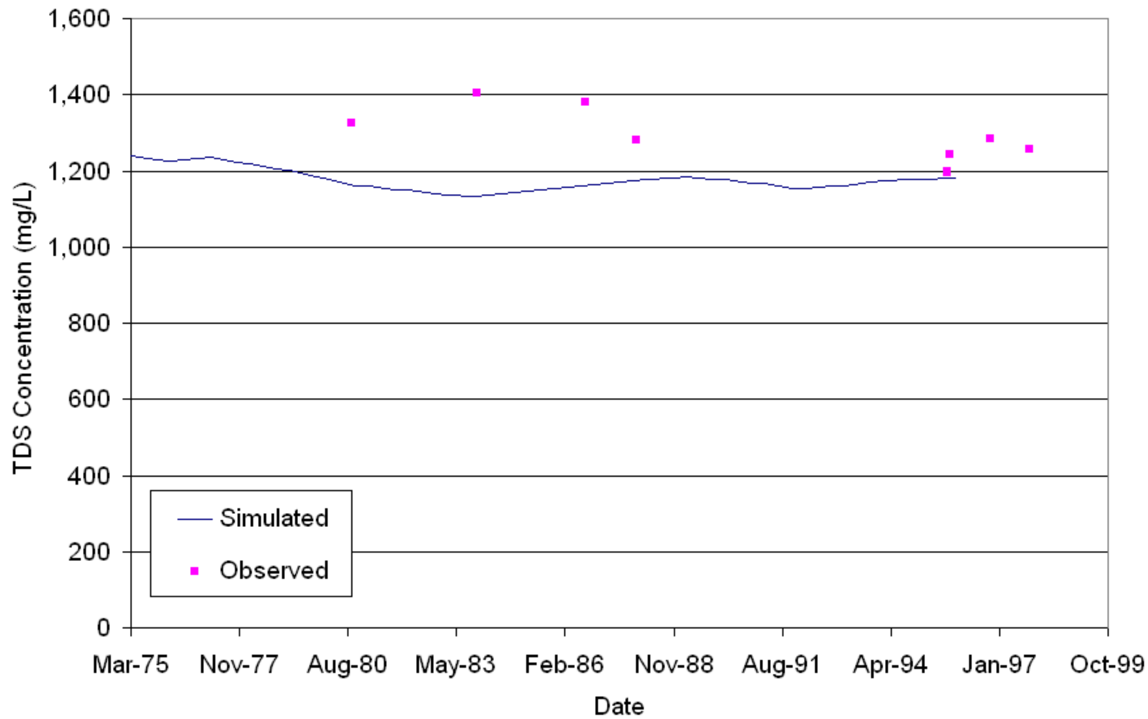

Figure 7-36. Simulated Versus Observed EPWU 109

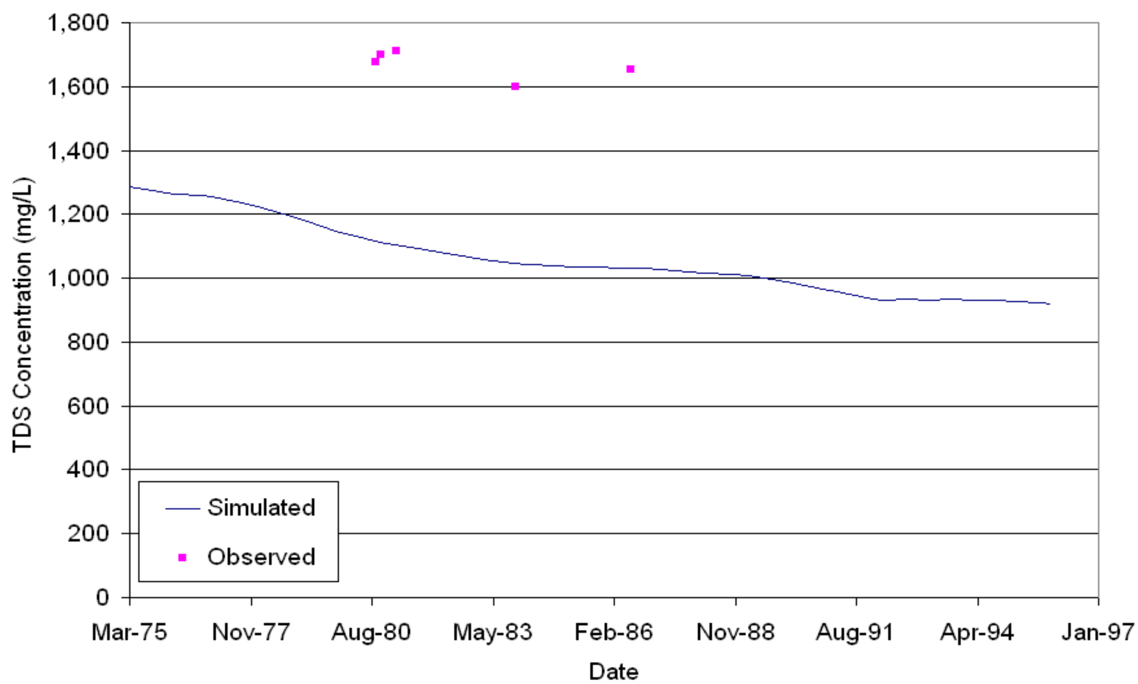

Figure 7-37. Simulated Versus Observed EPWU 110

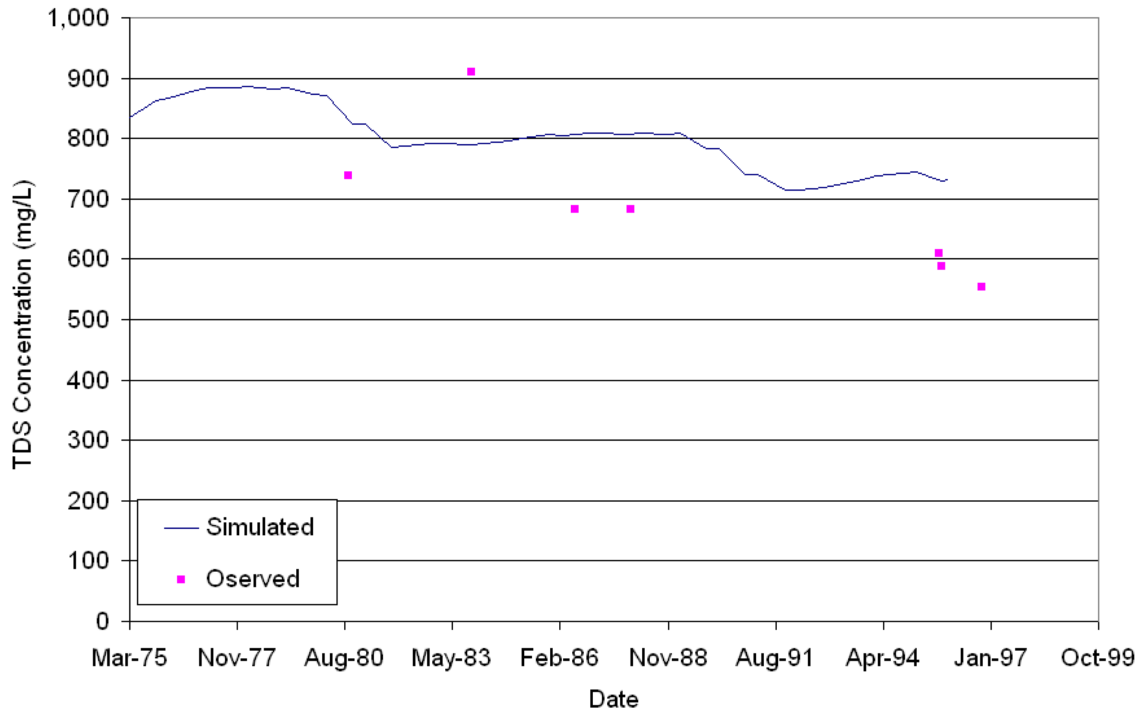

Figure 7-38. Simulated Versus Observed EPWU 111

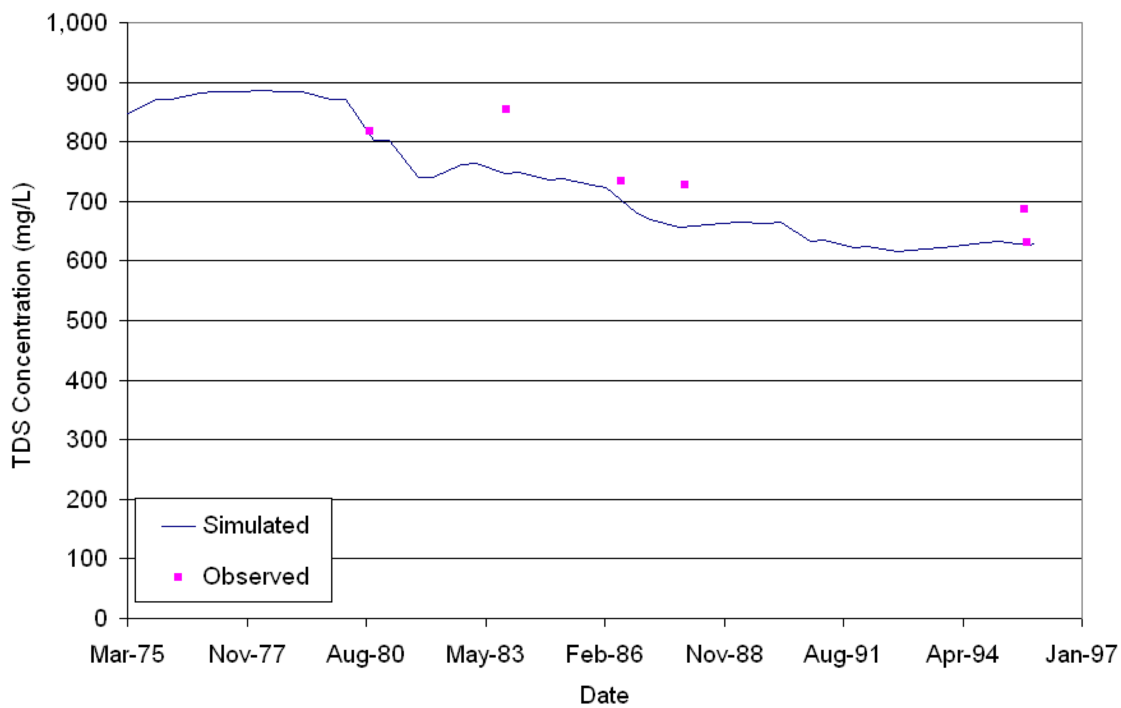

Figure 7-39. Simulated Versus Observed EPWU 112

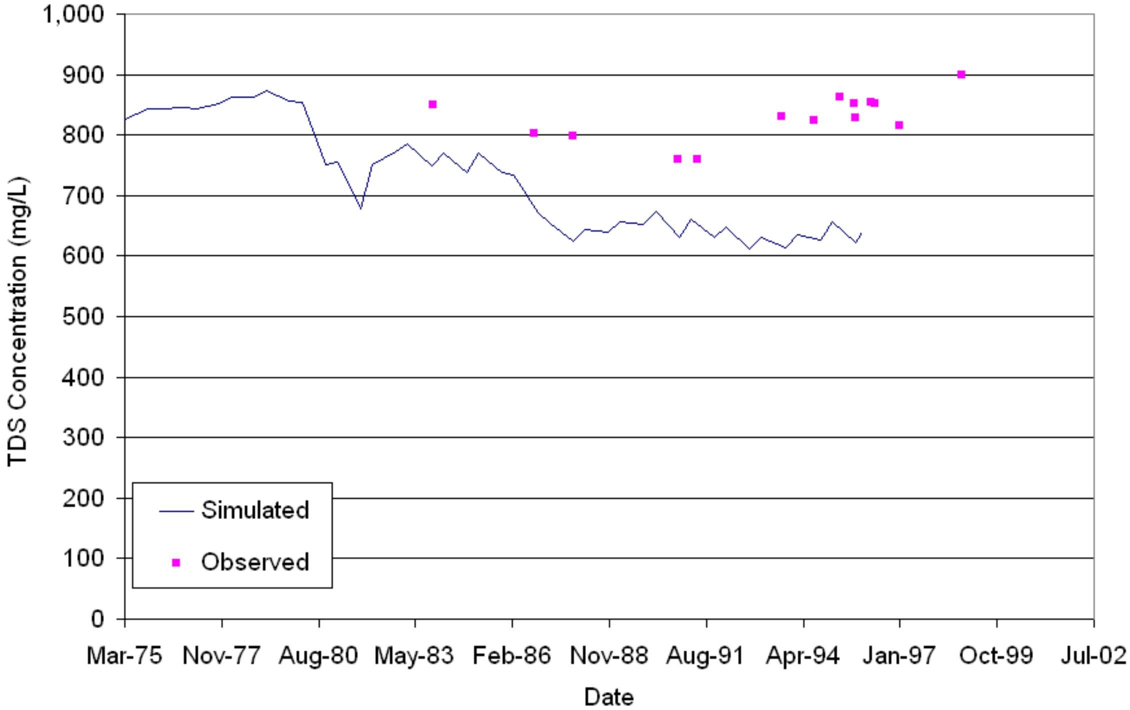

Figure 7-40. Simulated Versus Observed EPWU 115

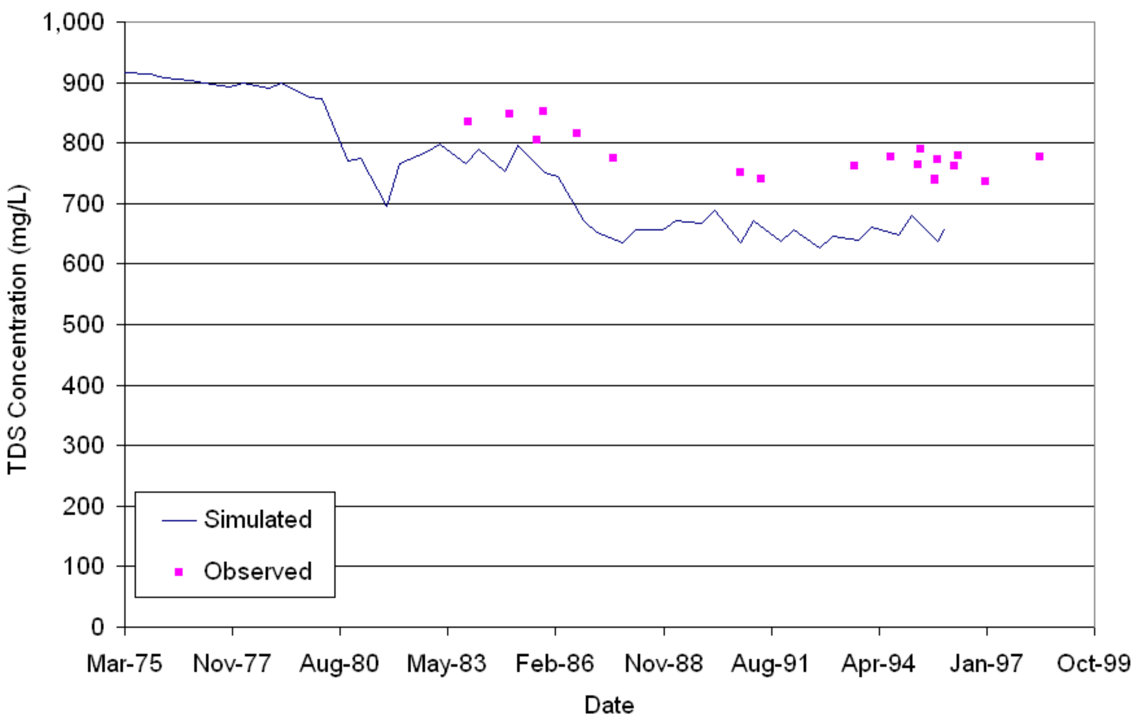

Figure 7-41. Simulated Versus Observed EPWU 116

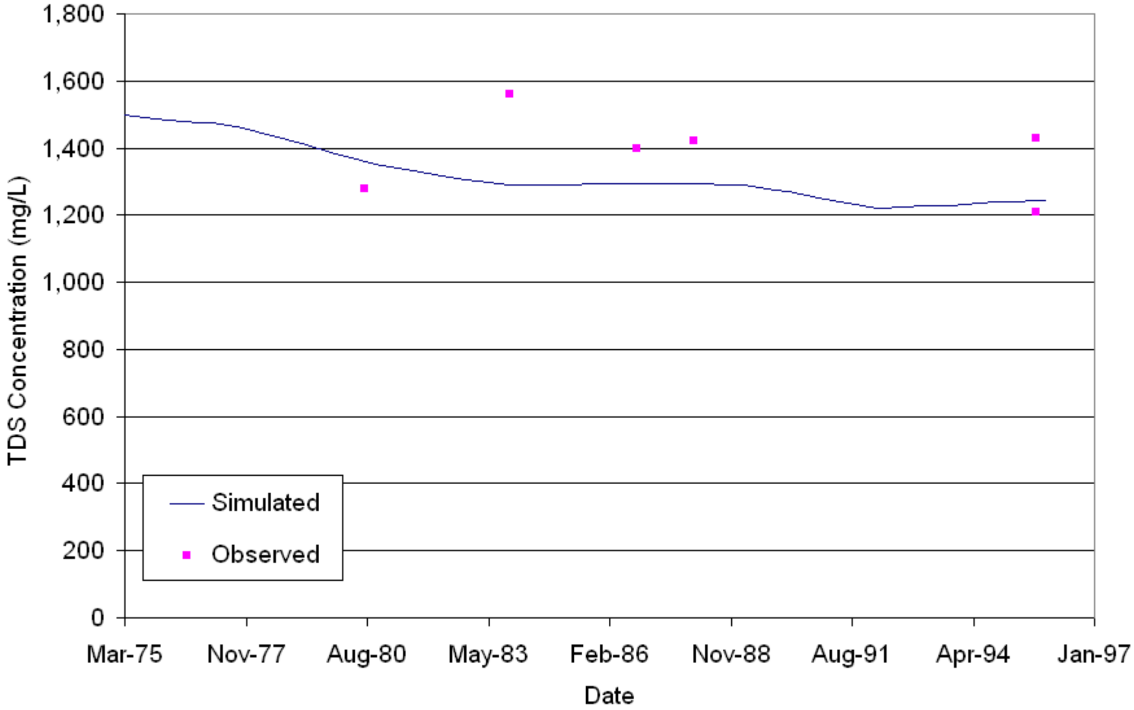

Figure 7-42. Simulated Versus Observed EPWU 117

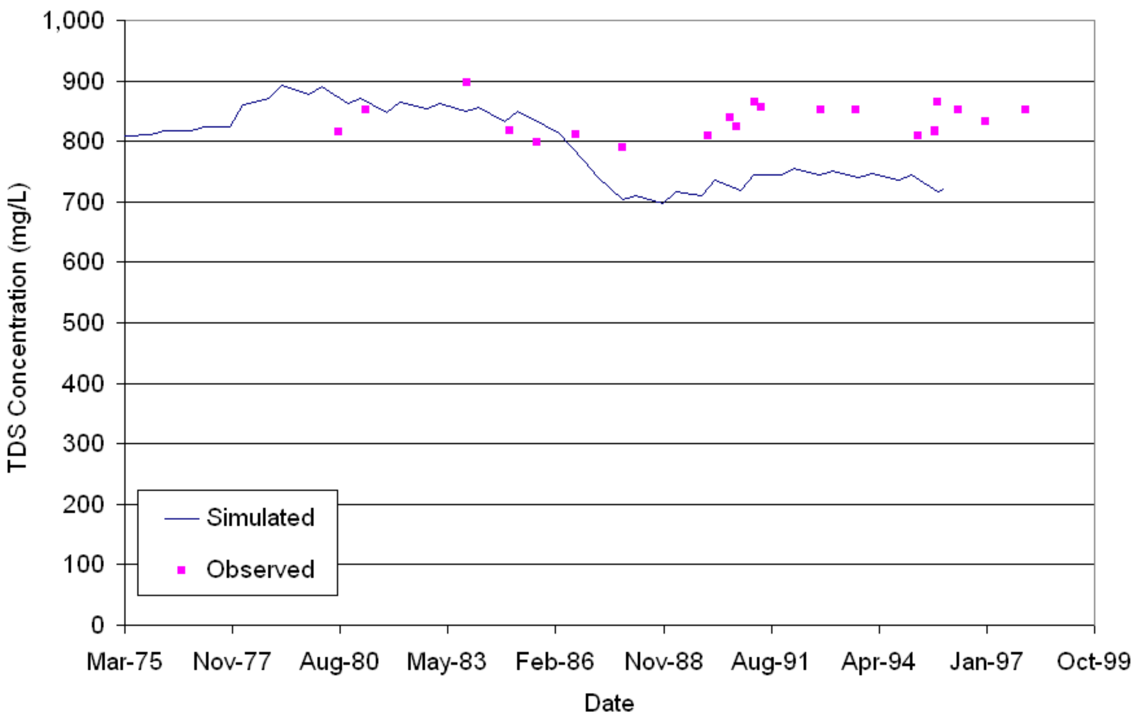

Figure 7-43. Simulated Versus Observed EPWU 118

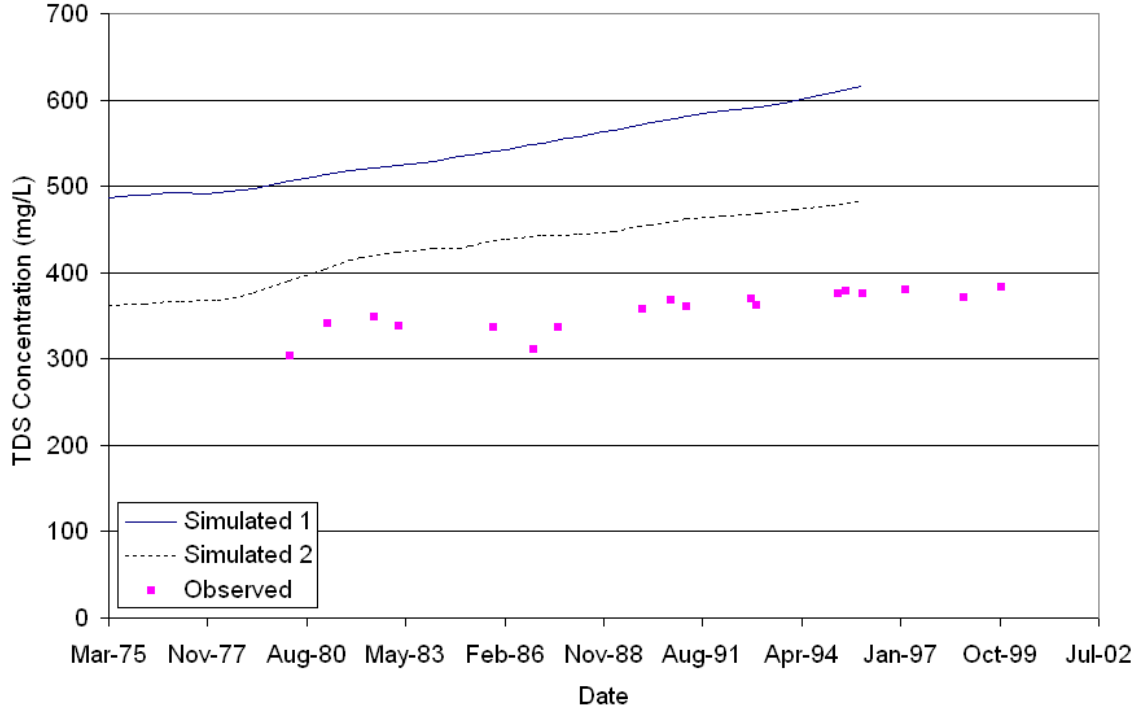

Figure 7-44. Simulated Versus Observed EPWU 201

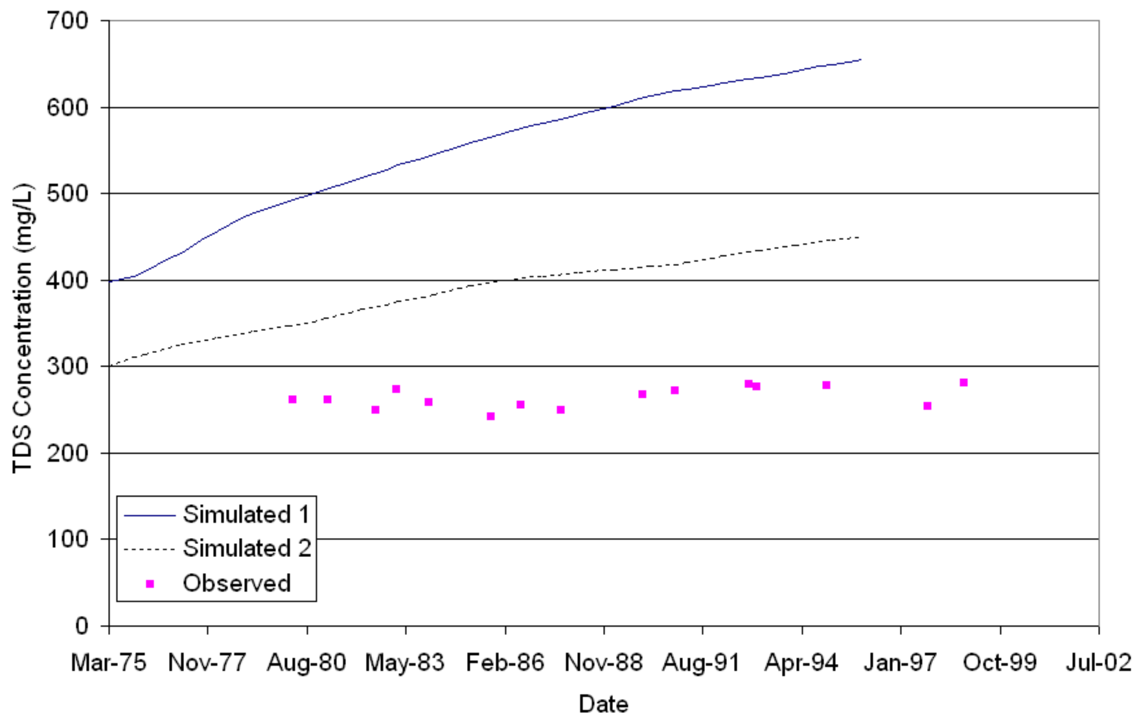

Figure 7-45. Simulated Versus Observed EPWU 202

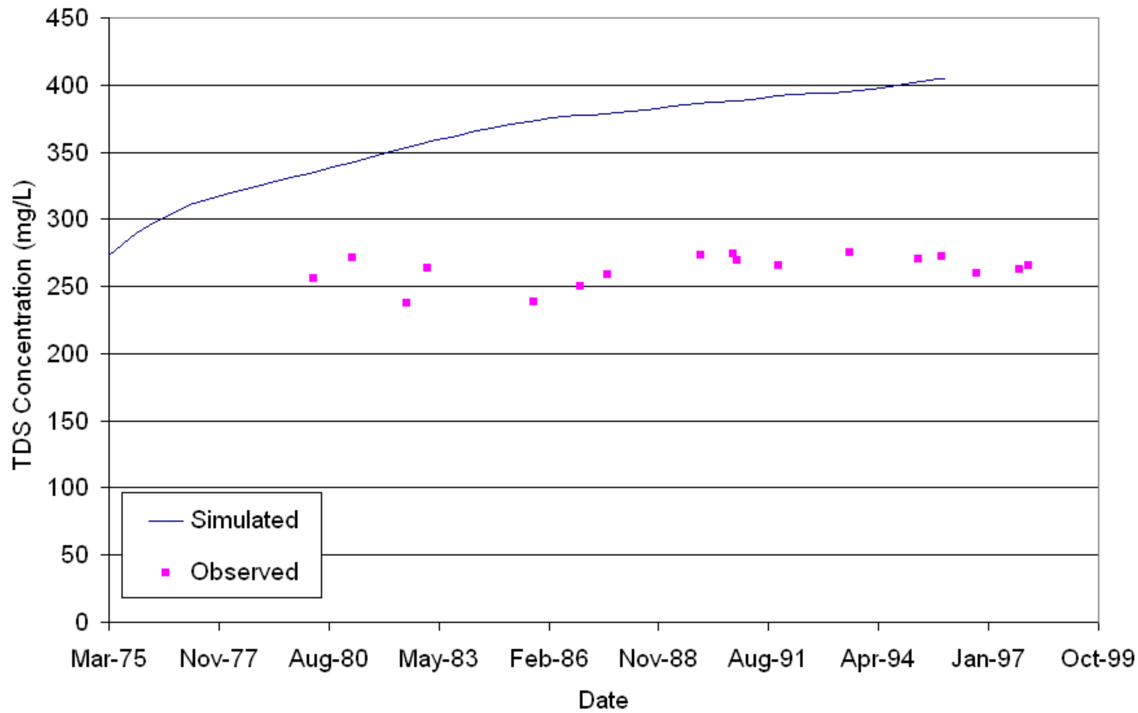

Figure 7-46. Simulated Versus Observed EPWU 203

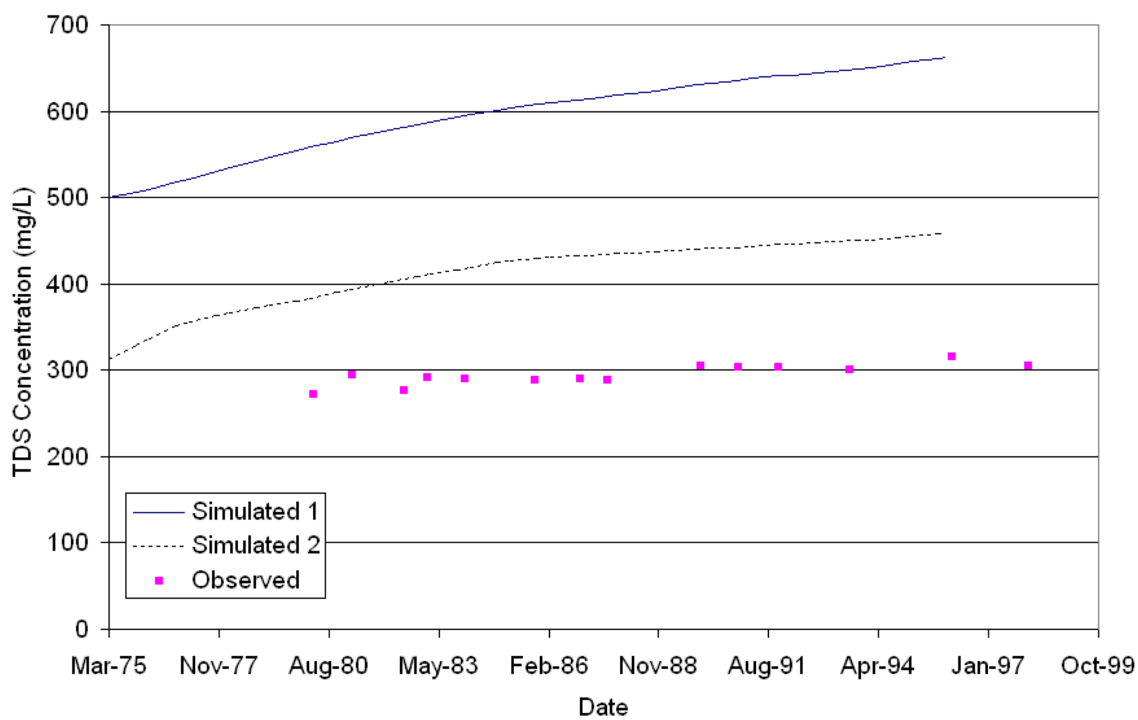

Figure 7-47. Simulated Versus Observed EPWU 204

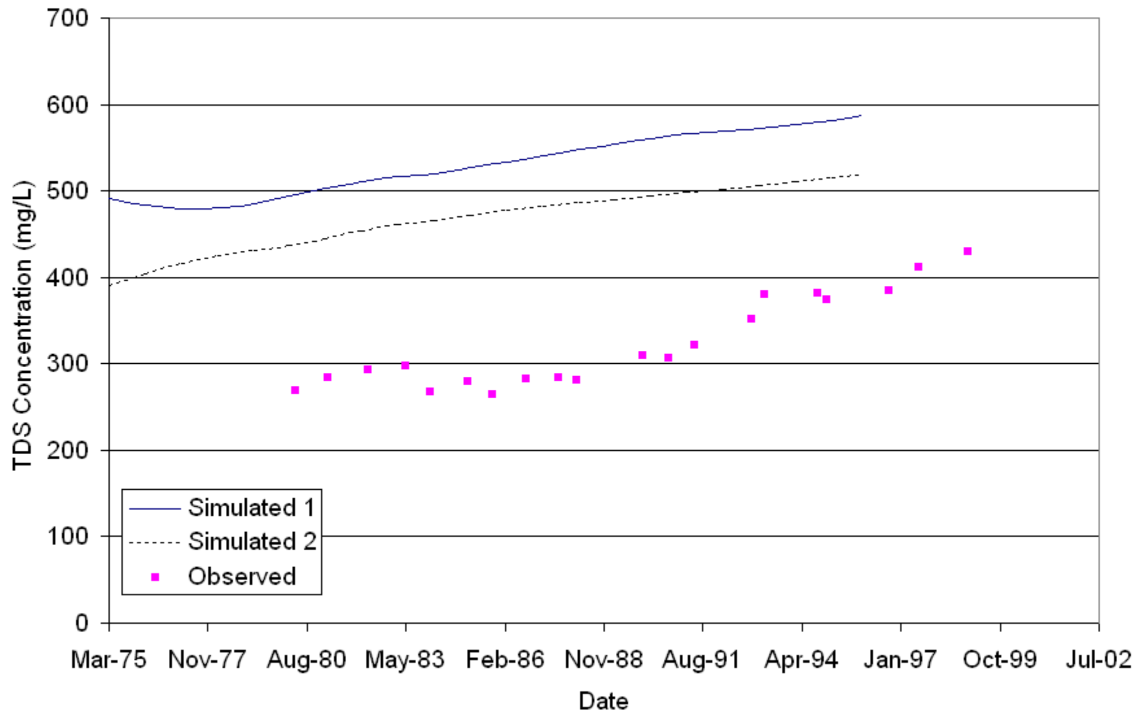

Figure 7-48. Simulated Versus Observed EPWU 205

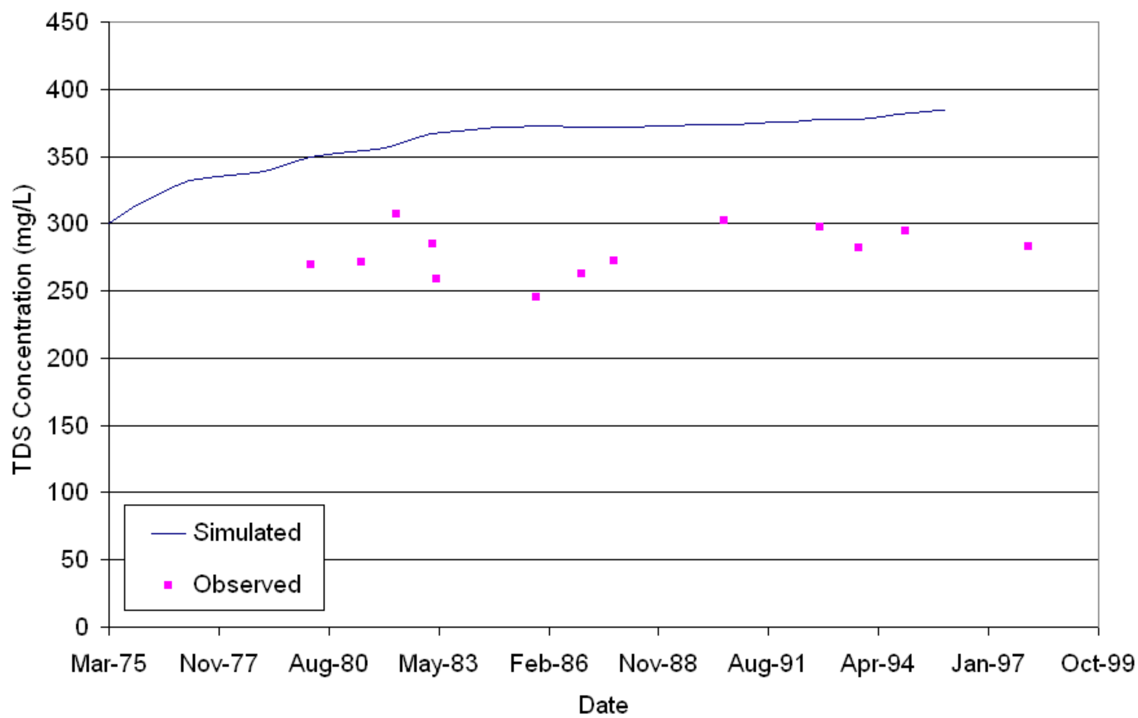

Figure 7-49. Simulated Versus Observed EPWU 206

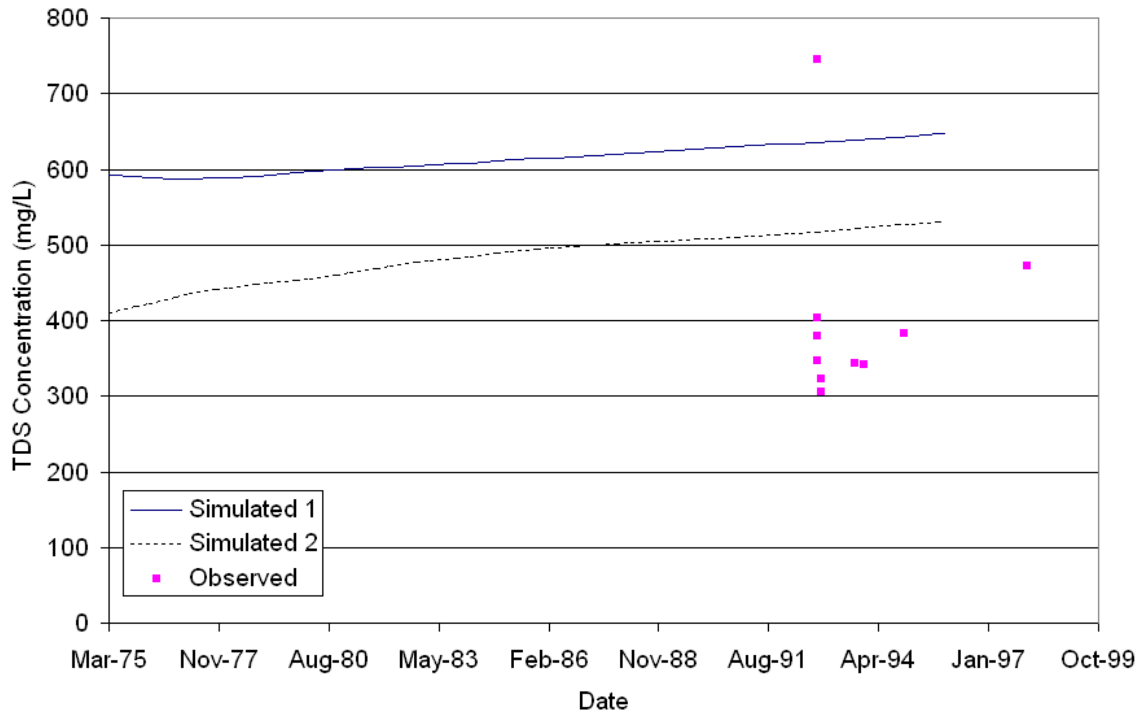

Figure 7-50. Simulated Versus Observed EPWU 207

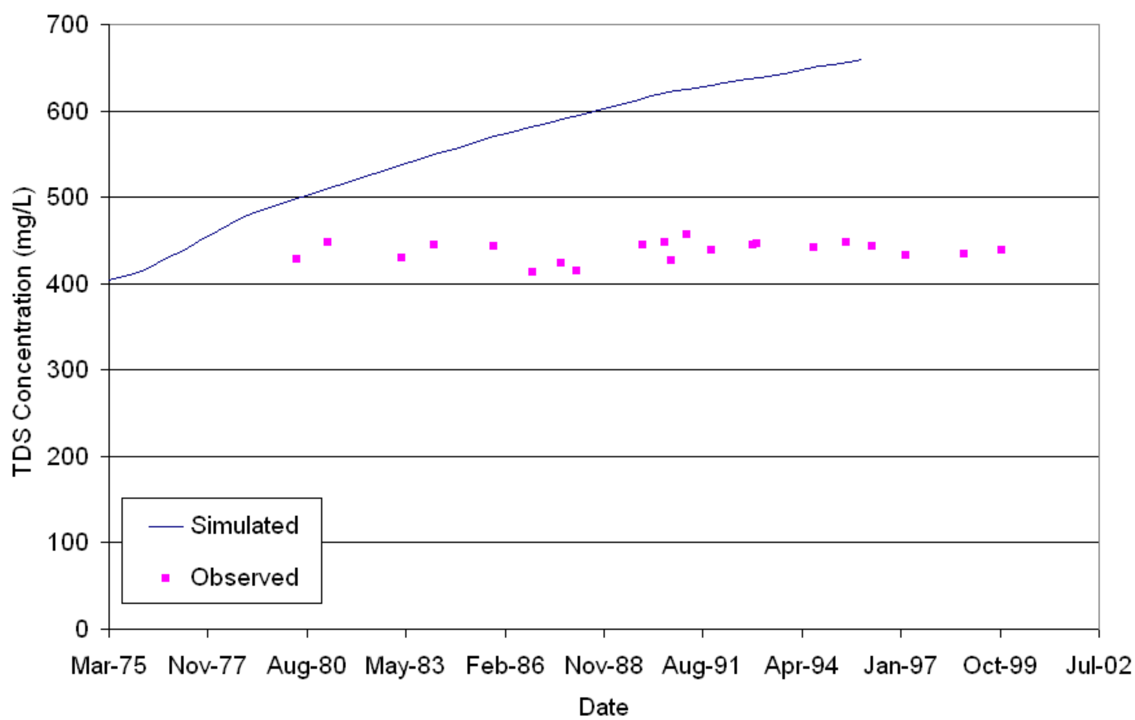

Figure 7-51. Simulated Versus Observed EPWU 301

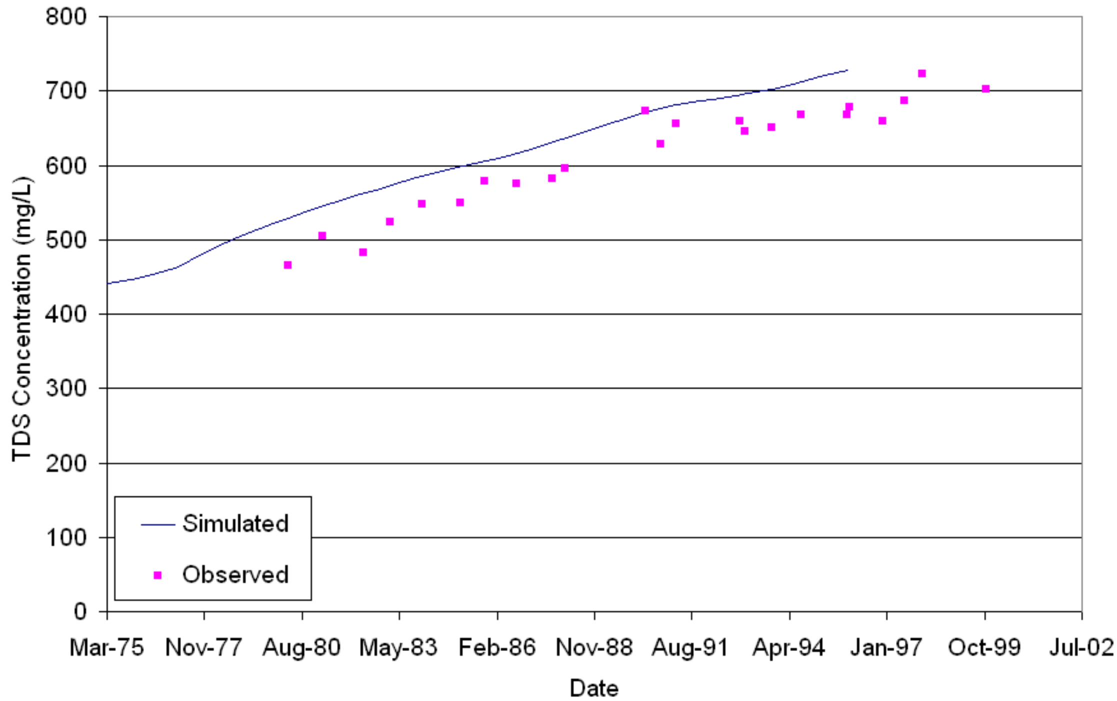

Figure 7-52. Simulated Versus Observed EPWU 302

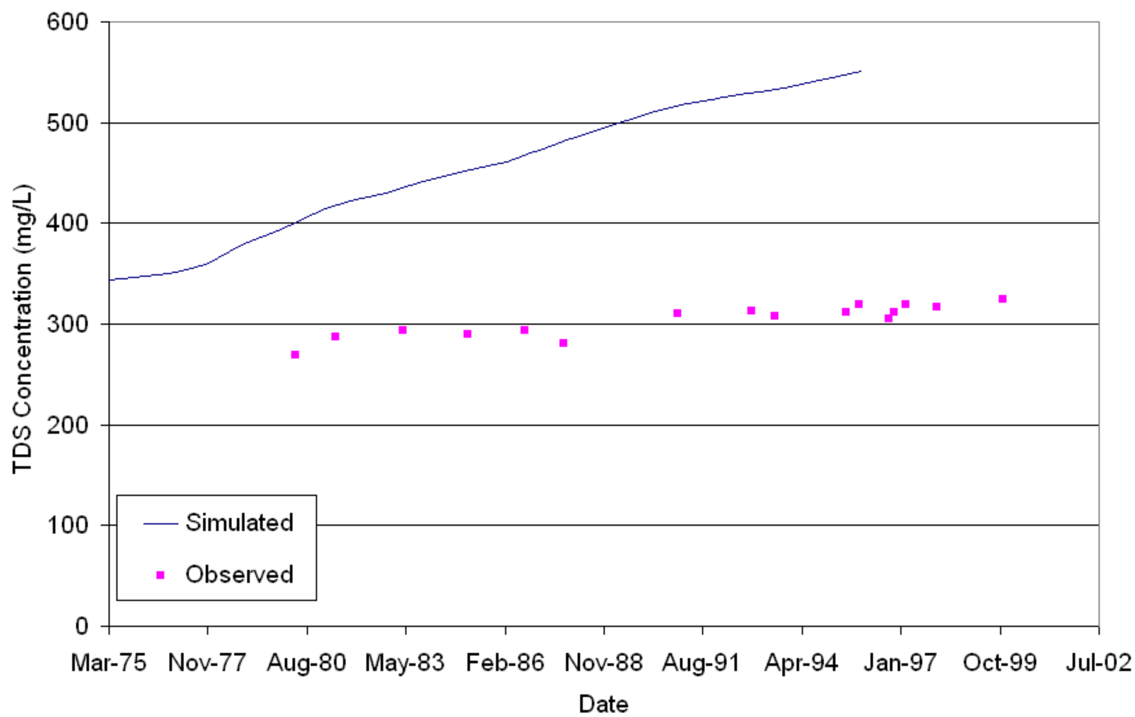

Figure 7-53. Simulated Versus Observed EPWU 303

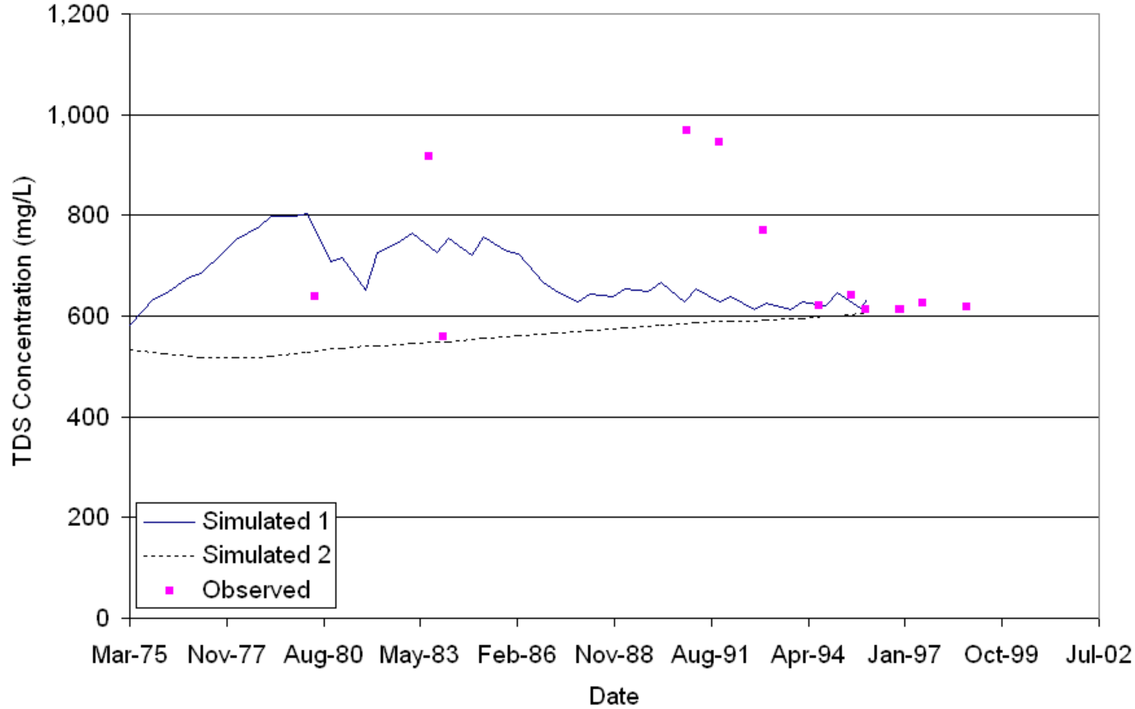

Figure 7-54. Simulated Versus Observed EPWU 304

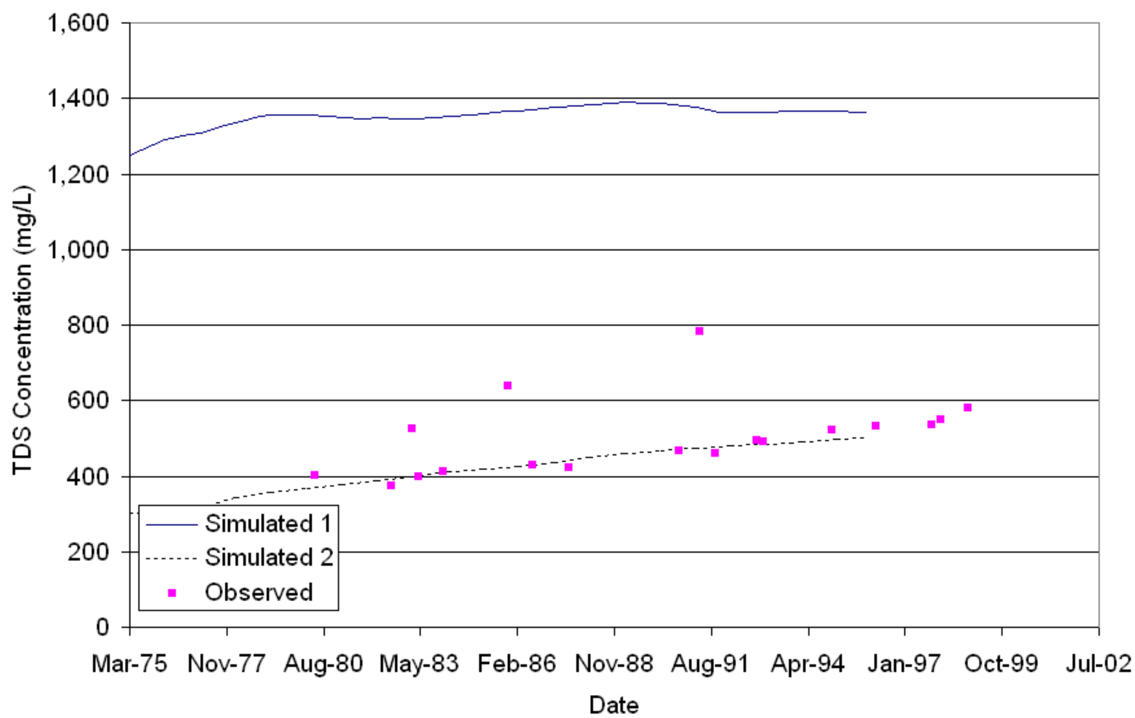

Figure 7-55. Simulated Versus Observed EPWU 305

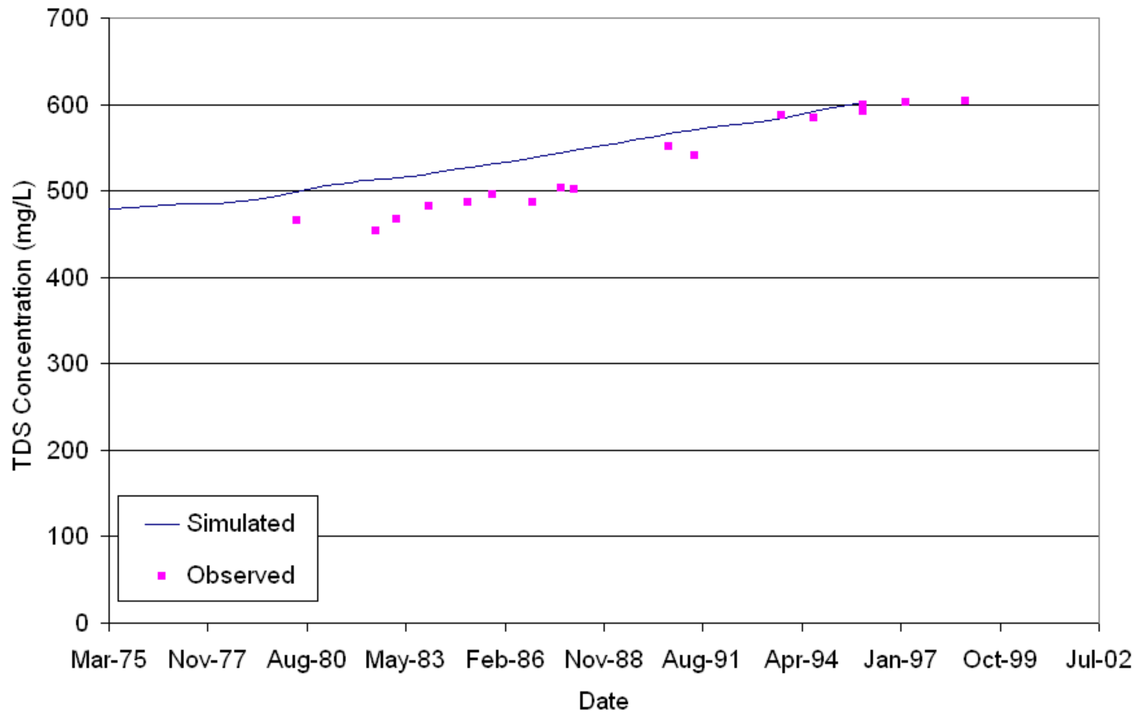

Figure 7-56. Simulated Versus Observed EPWU 306

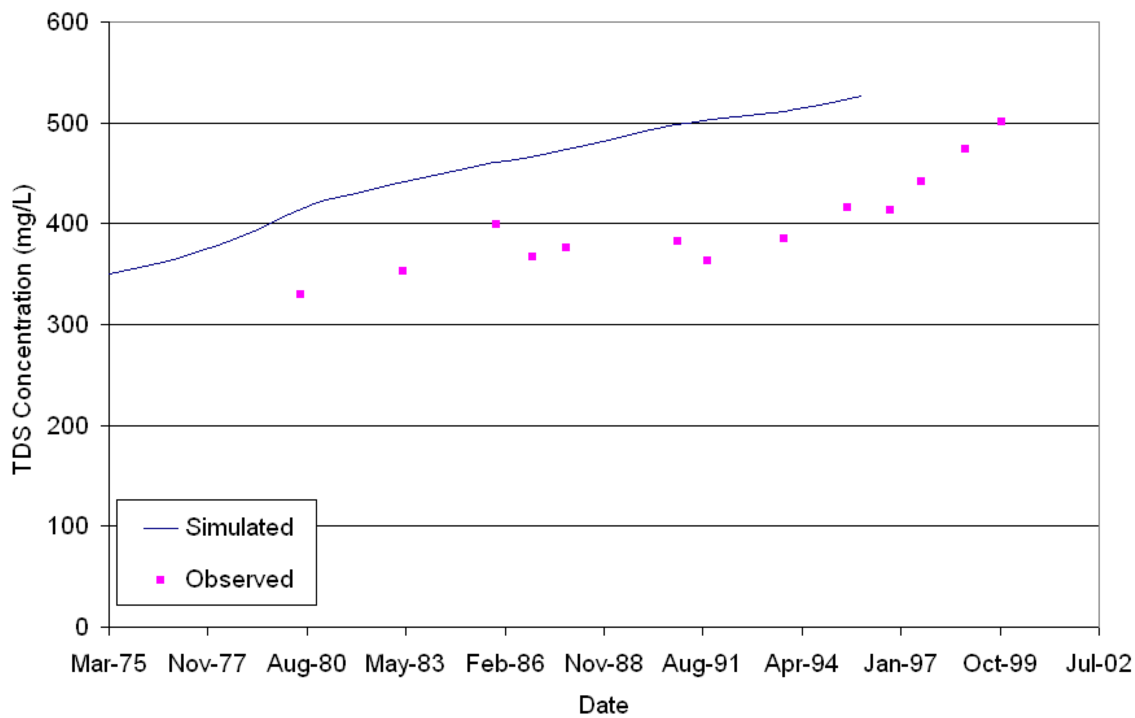

Figure 7-57. Simulated Versus Observed EPWU 307

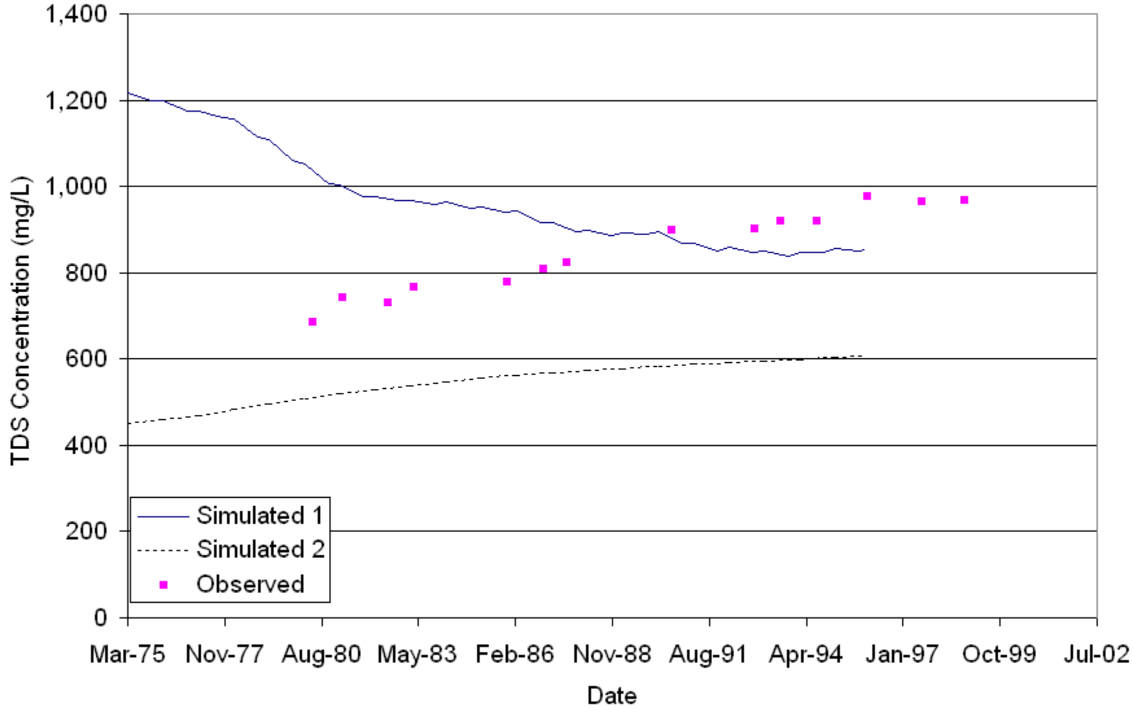

Figure 7-58. Simulated Versus Observed EPWU 308

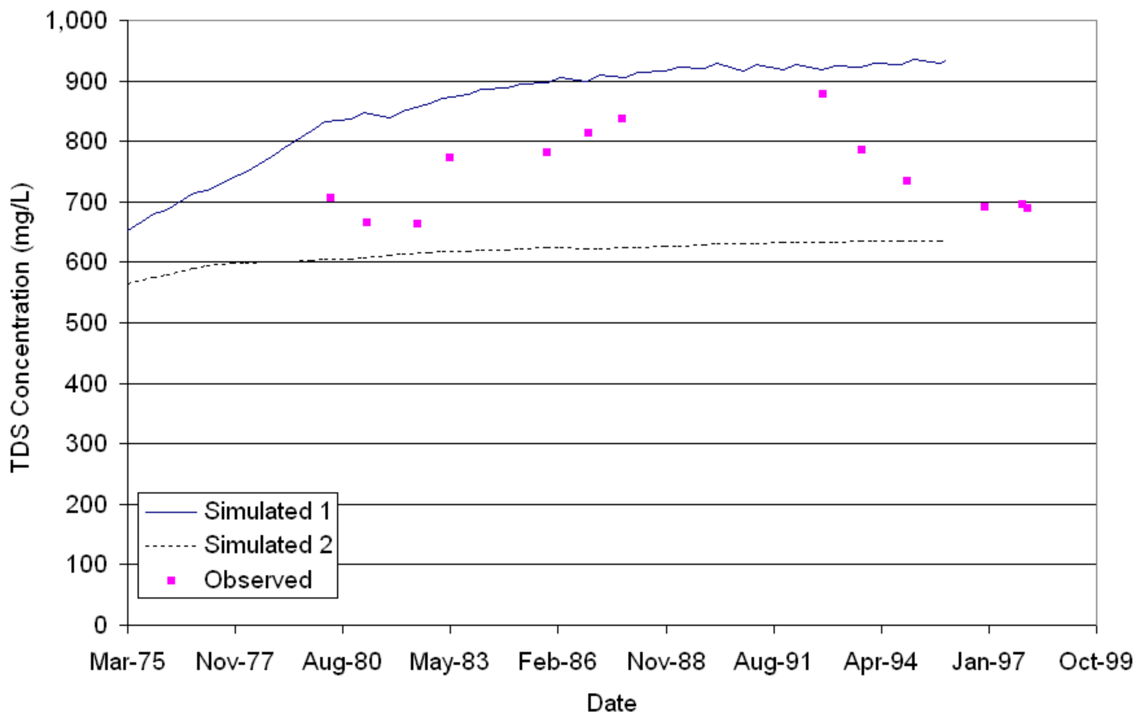

Figure 7-59. Simulated Versus Observed EPWU 309

7.5 Sensitivity Analysis

To ensure that assuming dispersion could be ignored in model development, additional simulations were completed assuming various amounts of dispersion. In addition, because the model was calibrated to a particular porosity, it is possible that similar results could be achieved with a smaller porosity when the effects of dispersion are included. Simulations were completed with smaller porosity and various amounts of dispersion. In each case the RMS error in simulated versus observed TDS was calculated for comparison. Figure 7-60 presents the change in RMS error associated with various levels of dispersion. From this figure, it can be seen that model improvement did not occur with dispersion at either the calibrated porosity or smaller porosity values. Based on results for individual layers, it appeared that some improvement to the results in layer 1 occurred with dispersion. A single simulation was completed with dispersion in layer 1 only to examine this effect. This change resulted in approximately the same model error as without any dispersion (RMS error = 104 mg/L).

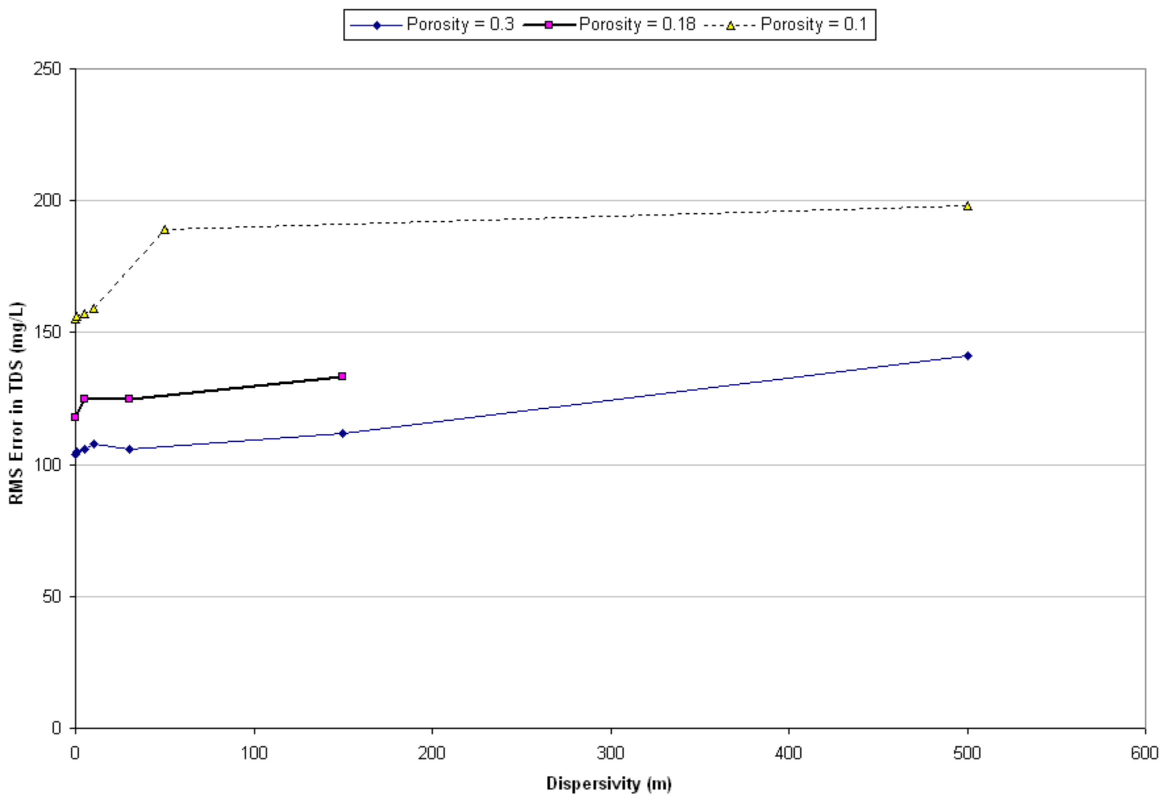

Figure 7-60. Change in RMS Error in TDS Concentration with Dispersion

7.5 Sensitivity Analysis

To ensure that assuming dispersion could be ignored in model development, additional simulations were completed assuming various amounts of dispersion. In addition, because the model was calibrated to a particular porosity, it is possible that similar results could be achieved with a smaller porosity when the effects of dispersion are included. Simulations were completed with completed with smaller a smaller porosity and various amounts of dispersion. In each case the RMS error in simulated versus observed TDS was calculated for comparison. Figure 7-60 presents the change in RMS error associated with various levels of dispersion. From this figure, it can be seen that model improvement did not occur with dispersion at either the calibrated porosity or smaller porosity values. Based on results for individual layers, it appeared that some improvement to the results in layer 1 occurred with dispersion. A single simulation was completed with dispersion in layer 1 only to examine this effect. This change resulted in approximately the same model error as without any dispersion (RMS error = 104 mg/L).

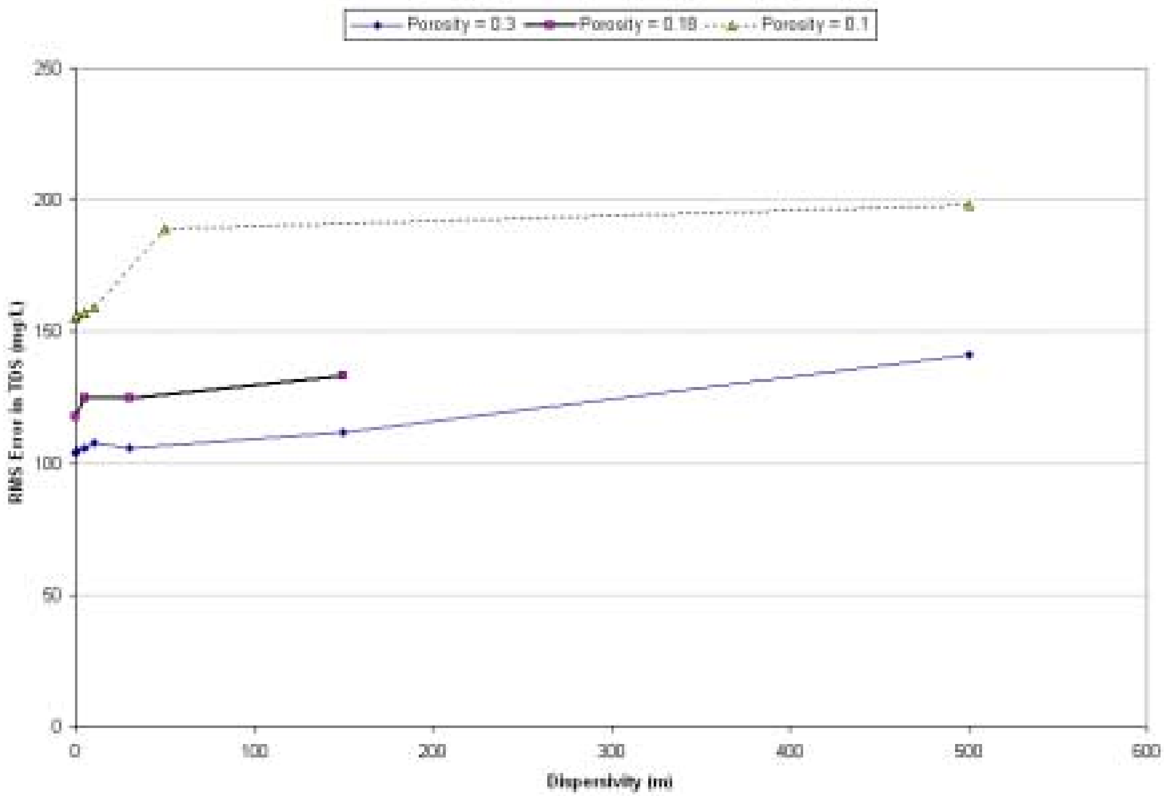

Figure 7-60. Change in RMS Error in TDS Concentration with Dispersion

8. Conclusions and Recommendations

8. Conclusions and Recommendations

Within the limitations described in this report, the Cañutillo model represents the local groundwater flow in the Cañutillo wellfield for the purpose of simulating local contaminant transport. The following bullets list conclusions with respect to the Cañutillo goundwater flow model.

- The model represents the streamflow system in the Cañutillo area well. Improvements to the model representation of streamflow would require more information on canal return flows. These data are required to determine Rio Grande leakage explicitly. These data are not presently available.
- The model represents Rio Grande seepage in the winter reasonably well and slightly better than the Weedon and Maddock (1999) model. However, observed values are of a different time scale and therefore can only act as a general guide. Likewise, Rio Grande seepage varies significantly from year to year.
- The model represents aquifer heads well, with slight improvements over Weeden and Maddock (1999).
- Based on sensitivity analysis, the model appears to be near a local optimum.

In part due to the model layering scheme used by Weedon and Maddock and in part due to spatial and temporal data gaps, some level of generalization and synthesis of data are required to represent water quality in the Cañutillo area in three dimensions. The generalizations in water quality representation increase uncertainty associated with simulation results.

Within limitations presented by the model-layering scheme used by Weedon and Maddock, the Cañutillo model represents the local groundwater flow and contaminant transport in the Cañutillo wellfield for the purpose of simulating generalized trends in local contaminant transport. Because of model limitations, model results cannot be used to accurately predict concentrations in individual wells and therefore manage the wellfield on a well-by-well basis.

The following recommendations are made to improve future model versions and reduce perceived limitations:

- Update layering to reflect hydrostratigraphic units and if possible to reflect zones where water quality is known to change significantly within individual hydrostratigraphic units.
- Segregate NIF into its components (precipitation, crop ET, etc.) and examine methodology to provide a more reliable and realistic estimate of agricultural pumping.
- Define ET based on annual estimates of ET potential coupled with land use. Segregate NIF into its components (precipitation, crop ET, etc.) and examine methodology to

provide a more reliable and realistic estimate of agricultural pumping. These will allow for better local estimates of salt buildup and removal through agricultural practices.

- Conduct a comprehensive testing program to determine hydraulic conductivity and specific capacity with emphasis on tests conducted in discrete hydrostratigraphic units to further constrain the model with respect to hydraulic conductivity.
- Continue to collect and monitor stream gaging data including canal return flow, Rio Grande flows, diversion quantities, and agricultural deliveries.
- Continue to collect municipal and industrial pumping data from the New Mexico OSE and the TWC and update the model with current data (particularly the 1991 through 1995 time period).
- Continue to collect and monitor stream concentration data from sources including canals, the Rio Grande, drains, and particularly wells.
- Complete a tracer test(s) to examine solute transport parameters empirically.
- Conduct a comprehensive testing program to monitor concentrations in the Mesilla Bolson. These data could be used to further adjust model inputs over time.
- Complete the proposed drilling and testing program to add to the concentration and hydrostratigraphy databases.

9. References

9. References

Anderson, M.P., 1979. *Using Models to Simulate the Movement of contaminants through groundwater flow systems.* CRC Crit. Rev. Environ. Control, Vol 9, pp. 97-156.

Anderson, M.P. and W.W. Woessner, 1990. *Applied Groundwater Modeling, Simulation of Flow and Advective Transport.* Academic Press Inc.

Bahr, T.G., 1979. *Water Resources and Growth of the Mesilla Valley: An Issue Paper.* Water Resources Research Institute Report No. 104.

Basler, J.A. and L.J.Alary, 1968. *Quality of the Shallow Water in the Rincon and Mesilla Valleys, New Mexico and Texas.* U.S. Geological Survey Open-file Report.

Bear, J., 1972. *Dynamics of Fluids in Porous Media.* Dover Publications, Inc.

Boyle Engineering Corporation, 1999. *Cañutillo Wellfield Master Plan.*

Boyle Engineering Corporation and Parsons Engineering Science, 1999. *El Paso-Las Cruces Regional Sustainable Water Project, Interim Draft Hydrologic Modeling Report.* April.

Boyle Engineering Corporation and Parsons Engineering Science, 1999. *El Paso-Las Cruces Regional Sustainable Water Project, Hydrologic Modeling Final Report.* April

Bromilow, F., 1956. Flow Studies in the Mesilla Valley, WR and Their Economic Importance in NM. Water Resources Research Institute, 1st Proceedings; 141: 10/31/56-11/2/56.

Carver, 2001. Riverbed Permeabilities: Information from Pooled Data. *Groundwater*, Vol. 39. No. 4 pp. 546-553

CH2M HILL, 2001a. *Draft Environmental Impact Statement.*

CH2M HILL, 2001b. *Draft Water Resources Technical Report*
.
CH2M HILL, 2000c. *Cañutillo Wellfield Expansion, Wellfield Data Review.*

CH2M HILL, 2000d. *Cañutillo Wellfield Expansion, Conceptual Well Design and Construction Program.*

Chebotarev, I.I., 1955. *Metamorphism of natural waters in the crust of weathering*. Geochemica et Cosmochima Acta, 8.

Cliett, Tom, 1995. *Report on La Tuna Federal Correctional Institution.* Tom Cliett and Associates.

Cliett, Tom, 1991. *Preliminary Report on EPWU Cañutillo Field Expansion for Westway.* Tom Cliett and Associates.

Cliett, Tom, 1990a. *Ground Water Occurrence of the Cañutillo-Anthony, Texas Area.* Tom Cliett and Associates.

Cliett, Tom, 1990b. *Cañutillo South Test Drilling Project.* Tom Cliett and Associates.

Cliett, Tom and John W. Hawley, 1995. General Geology and Groundwater Occurrence of the El Paso Area. Water Resources Research Institute 40th Proceedings; 297:51-56 10/26/95-10/27/95.

Conover, Clyde Stuart, 1954. *Ground-Water Conditions in the Rincon and Mesilla Valleys and Adjacent Areas in New Mexico.* U.S. Geological Survey, WS 1230.

Creel, B.J., 2000. Personal communication.

Creel, B.J., T.W. Sammis, J.F. Kennedy, D.O. Sitze, D. Asare, H.C. Monger, and Z.A. Samani, 1998. *Ground-Water Aquifer Sensitivity Assessment and Management Practices Evaluation for Pesticides in the Mesilla Valley of New Mexico.* Water Resources Research Institute, Report No. 305.

Croff and others, 1985. *Evaluation of Five Sedimentary Rocks Other Than Salt for High Level Waste Repository Siting Purposes.* Oak Ridge National Laboratory, ORNL/CF-85/2/V2.

Domenico, P.A. and F.W. Schwartz, 1990. *Physical and Chemical Hydrogeology*. John Wiley and Sons.

Frenzel, Peter F., 1992. *Simulation of Ground-Water Flow in the Mesilla Basin, Dona Ana County, New Mexico, and El Paso County, Texas.* U.S. Geological Survey, WRI 91-4155.

Frenzel, P.F. and C.A. Kaehler, 1990. *Geohydrology and Simulation of Ground-Water Flow in the Mesilla Basin, Doña Ana County, New Mexico, and El Paso County, Texas, With a Section on Water Quality and Geochemistry, by S.K. Anderholm.* U.S. Geological Survey; OF 88-305.

Gates, J. S., D.E. White, and E.R. Leggat, 1984. *Preliminary Study of the Aquifers of the Lower Mesilla Valley in Texas and New Mexico by Model Simulation.* U.S. Geological Survey, WRI 84-4317.

Gelhar, L.W. and S.G. McLin, 1979. *Evaluation of a Hydrosalinity Model of Irrigation Return Flow Water Quality in the Mesilla Valley, New Mexico.*

Gutierrez, Melinda, 1990. Analysis of the Sediments of Well A-3 Mesilla Valley, Texas. Student Paper.

Hamilton, S.L. and T. Maddock III, 1993. *Application of a Ground-Water Flow Model to the Mesilla Basin, New Mexico and Texas.*

Hawley, J.W., 1984. *Introduction to Hydrogeologic Features of the Mesilla Bolson Area, Doña Ana County, New Mexico.* New Mexico Bureau of Mines and Mineral Resources, OF-190.

Hawley, J.W. and R.P. Lozinski, 1992. *Hydrogeologic Framework of the Mesilla Basin in New Mexico and western Texas.* New Mexico Bureau of Mines and Mineral Resources, OF-323.

Healy, Denis F., 1995. *Water-Quality Assessment of the Rio Grande Valley, Colorado, New Mexico, and Texas - Occurrence and Distribution of Selected Pesticides and Nutrients at Selected Surface-Water Sites in the Mesilla Valley, 1994-95.* U.S. Geological Survey, WRI 96-4069.

Heywood, 2001. Personal correspondence.

Hill, 1979. *Using Models to Simulate the Movement of Contaminants through Groundwater Flow Systems*. CRC Critical Reviews in Environmental Control, Vol. 9 Issue 2 pp. 123-153.

Huff, G. F., 1998. *Water-Quality Data for the Rio Grande between Picacho Bridge near Las Cruces and Calle del Norte Bridge near Mesilla, New Mexico.* U.S. Geological Survey, OF 98-0066.

Kennedy, J.F., 2000. Personal communication.

Khaleel, R., et al., 1993. *Numerical Modeling of Ground-Water Flow in the Lower Rio Grande Basin, New Mexico.* Water Resources Research Institute.

King, W.E., J.W. Hawley, A.M. Taylor, and R.P. Wilson, 1971. *Geology and Ground-Water Resources of Central and Western Doña Ana County, New Mexico.* New Mexico Bureau of Mines and Mineral Resources.

Konikow, L.F. and J.D. Bredhoft, 1974. *Modeling Flow and Chemical Quality Changes in an Irrigated Stream-Aquifer System.* Water Resources Research Institute, Vol 10 No. 3 p. 546-562.

Lang, P.T. and T. Maddock III, 1985. *Simulation of Groundwater Flow to Assess the Effects of Pumping and Canal Lining on the Hydrologic Regime of the Mesilla Basin, Dona Ana County, New Mexico and El Paso County, Texas*.

Lansford, R.R., B.J. Creel, and C. Seipel, 1980. *Demonstration of Irrigation Return Flow Water Quality Control in the Mesilla Valley, New Mexico.*

Lee, W.T., 1907. *Water Resources of the Rio Grande Valley in New Mexico and Their Development.* USGS Water Supply Paper 188.

Lesperance, 1977. *New Mexico Climatological Data; Precipitation, Temperature, Evaporation, and Wind; Monthly and Annual Means, 1850-1975.* W.K. Summers and Associates, Socorro, New Mexico.

Maddock and Wright, 1987. *An Investigation of the Effects of Proposed Pumping in the Lower Rio Grande Declared Basin.*

Murray, C.R., 1942. *Reconnaissance Survey of Well Sites of U.S. Grazing Service in Deming-Las Cruces area, New Mexico.* U.S. Geological Survey, OF.

Myers, Robert G. and Brennon R. Orr, 1985. *Geohydrology of the Aquifer in the Santa Fe Group, Northern West Mesa of the Mesilla Basin Near Las Cruces, New Mexico.* U.S. Geological Survey, WRI 84-4190.

Nickerson, Edward L., 1999. U. S. Geological Survey Seepage Investigations of the Lower Rio Grande in the Mesilla Valley. Water Resources Research Institute 43rd Proceedings; Report 310.

Nickerson, Edward L., 1998. U.S. Geological Survey Seepage Investigations of the Lower Rio Grande in the Mesilla Valley. New Mexico Water Resources Research Institute, Proceedings of the 43rd Annual New Mexico Water Conference.

Nickerson, Edward L., 1995. *Selected Hydrologic Data for the Mesilla Ground-Water Basin, 1987 Through 1992 Water Years, Dona Ana County, New Mexico, and El Paso County, Texas.* U.S. Geological Survey, OF 95-0111.

Nickerson, E.L., 1989. *Aquifer Tests in the Flood-Plain Alluvium and Santa Fe Group at the Rio Grande Near Cañutillo, El Paso County, Texas.* U.S. Geological Survey, WRI 89-4011.

Nickerson, E.L., 1986. *Selected Geohydrologic Data for the Mesilla Basin, Dona Ana County, New Mexico, and El Paso County, Texas.* U.S. Geological Survey, OF 86-75.

Nickerson, Edward L. and Robert G. Myers, 1993. *Geohydrology of the Mesilla Ground-Water Basin, Dona Ana County, New Mexico, and El Paso County, Texas.* U.S. Geological Survey, WRI 92-4156.

NMED, 1980. *Chemical Quality of New Mexico Community Water Supplies.*

Norton and Knapp, 1977. Transport phenomena in hydrothermal systems: Nature of porosity. *American Journal of Science*, Vol. 27, pp. 913-936

Peterson, D.M., R. Khaleel, and J.W. Hawley, 1984. *Quasi Three-dimensional Modeling of Groundwater Flow in the Mesilla Bolson, New Mexico and Texas.* Water Resources Research Institute, Report No. 178.

Pinder, 1973. A Galerkin-Finite Element Simulation of Groundwater Contamination on Long Island, New York. Water Resources Research Institute, Vol. 9, No. 6, pp. 1657-1669.

Richardson, Gary L., 1972. Preliminary Groundwater Model of the Mesilla Valley. Water Resources Research Institute, 17th Proceedings, 007:44 4/6/72-4/7/72.

Richardson, Jesse U., 1956. Underground Water Problems in the Mesilla Valley. Water Resources Research Institute, 1st Proceedings, 30:10/31-11/2/56.

Sammis, T.W., 1980. *Demonstration of Irrigation Return Flow Water Quality in the Mesilla Valley, New Mexico.* Water Resources Research Institute, Report No. 117.

Slichter, 1905. *Observations on Ground-Water of Rio Grande Valley.* USGS WSP 141.

Sperka, Roger, 2000. Personal communication.

Theis, C.V., 1942. *Ground-Water Supplies Near Las Cruces, New Mexico.* U.S. Geological Survey, OF.

Turnbull, S.J., 1985. Numerical Modeling of Ground-Water Flow in the Cañutillo Wellfield, Cañutillo, Texas. Student Paper.

Updegraff, C.D. and L.W. Gelhar, 1978. *Parameter Estimation for a Lumped Parameter Groundwater Model of the Mesilla Valley, New Mexico.*

USGS, 1999. *Water Resources Data New Mexico Water Year 1998.* U.S. Geological Survey, Water Data Report Nm-99-1.

USGS, 1998. *Water Resources Data New Mexico Water Year 1998.* U.S. Geological Survey, Water Data Report Nm-98-1.

USGS, 1997. *Water Resources Data New Mexico Water Year 1998.* U.S. Geological Survey, Water Data Report Nm-97-1.

USGS, 1996. *Water Resources Data New Mexico Water Year 1998.* U.S. Geological Survey, Water Data Report Nm-96-1.

Wade, S.C. and M. Reiter, 1994. *A Hydrothermal Study to Estimate Vertical Groundwater Flow in the Cañutillo Well Field, Between Las Cruces and El Paso.* Water Resources Research Institute, Report No. 282.

Weeden, C. and T. Maddock III, 1999. *Simulation of Groundwater Flow in the Rincon Valley Area and Mesilla Basin, New Mexico and Texas.*

West, Francis, 1996. The Mesilla Valley: A Century of Water Resource Investigations. Water Resources Research Institute, 40th Proceedings, 297:21-28 10/26/95-10/27/95.

Wilson, Clyde A. and Robert R. White, 1984. *Geohydrology of the Central Mesilla Valley, Dona Ana County, New Mexico.* U.S. Geological Survey, WRI 82-0555.

Wilson, Clyde A., Robert R. White, Brennon R. Orr, and R. Gary Roybal, 1981. *Water Resources of the Rincon and Mesilla Valleys and Adjacent Areas, New Mexico.* NMSE; TR 43.

Wilson, Lee, 1989. *Projected Impacts of Expanding the Cañutillo Well Field.* Lee Wilson and Associates.

Woodward, Dennis G. and Robert G. Myers, 1997. *Seismic Investigation of the Buried Horst Between the Jornada del Muerto and Mesilla Ground-Water Basins Near Las Cruces, Dona Ana.* U.S. Geological Survey, WRI 97-4147.

Zheng, C. and P.P. Wang, 1998. *MT3DMS A Modular Three-Dimensional Multispecies Transport Model*. The University of Alabama.

Zohdy, A.R., R.J. Bisdorf, and J.S. Gates, 1976. *Schlumberger Soundings in the Lower Mesilla Valley of the Rio Grande, Texas and New Mexico.* U.S. Geological Survey, OF 76-324.